Exploiting the helminth-derived immunomodulator, ES-62 and its small molecule analogues to dissect the mechanisms underpinning the development of the pathogenic phenotype of synovial fibroblasts in autoimmune arthritis.

Marlene Corbet B Sc, M Res

A thesis submitted in fulfilment of the requirements for the degree of Doctor of Philosophy

October 2016

The Institute of Infection, Immunity and Inflammation

College of Medical, Veterinary and Life Sciences

Glasgow Biomedical Research Centre
University of Glasgow
Glasgow G128TA

Abstract

Parasitic helminths are able to survive within their hosts due to their ability to dampen immune responses by secreting molecules with anti-inflammatory and tissue repair properties. Reflecting this, there is increasing evidence of an inverse correlation between parasitic worm infection and the incidence of allergic and autoimmune disorders on a global scale. Such epidemiological evidence has led to the "hygiene hypothesis" which postulates that the recent rapid eradication of parasitic worms in developed countries has resulted in unbalanced hyper-reactive immune systems and consequently, inflammatory disease. As "worm therapy" *per se* is not ideal, this in turn triggered the idea that exploiting the ability of helminth-derived "immunomodulators" to dampen pathological host inflammation would potentially allow identification of the key pathogenic events in models of human inflammatory disease and hence provide a starting point for development of new and safer therapeutics. Consistent with this, as a serendipitous side-effect of its anti-inflammatory actions, ES-62, a phosphorylcholine (PC)-containing glycoprotein secreted by the filarial nematode, *Acanthocheilonema viteae* exhibits therapeutic potential in mouse models of inflammatory disorders such as asthma, lupus and rheumatoid arthritis (RA).

RA is a chronic autoimmune inflammatory disorder that affects 1 % of the population in industrialized countries, with no known cure. This disorder causes joint destruction and leads to reduced mobility and disability. Deregulation of T cell activation has long been considered to be a major force driving inflammation and thus to date, therapies have focused on systemic anti-inflammatory treatments, which generally leave individuals immunosuppressed and open to infection. Thus, interest has begun to focus on the role(s) that synovial fibroblasts (SF) in the joint play in the early onset of the disease, the maintenance of established inflammation and even in the spread of disease to unaffected joints. This reflects that despite not being part of the immune system, SF produce pro-inflammatory cytokines during the pathogenesis of RA and also directly mediate joint destruction by secreting matrix metalloproteinases (MMPs) that damage cartilage and bone. Indeed, there is increasing evidence that the local pro-inflammatory environment pertaining in the joints drives SF to become

imprinted pathogenic aggressors that initiate, drive and spread joint inflammation and bone resorption during development of collagen-induced arthritis (CIA), a mouse model of RA. Intriguingly, therefore, whilst it is established that protection afforded by ES-62 against joint inflammation and bone destruction in CIA is associated with reduced production of the pathogenic cytokine, IL-17 by $\gamma\delta$ and $CD4^+$ T cells, recent evidence suggested that ES-62 could also act directly to suppress the aggressive hyper-inflammatory phenotype of SF in the joint. The molecular mechanisms involved were not defined but interestingly, given that SF express the ES-62 target TLR4 and are the only cells in the joint to express the IL-22 receptor, the parasite product appeared to harness the inflammation-resolving and/or tissue repair actions of IL-22 to suppress SF responses during the established phase of disease.

Thus the core goal of this thesis was to advance our fundamental understanding of how SF become imprinted pathogenic aggressors that initiate, drive and spread joint inflammation and bone resorption in the CIA mouse model, as a surrogate for the pathogenic events in the joints in RA. In particular, the primary major aim was to investigate the impact of the local pro-inflammatory environment pertaining during disease, specifically focusing on the signalling and epigenetic mechanisms by which IL-17 and IL-22 potentially (counter)regulate the pathogenic phenotype of SF. Complementing this, another major aim was to establish whether ES-62 acted directly to modulate the phenotype of SF and thus, to identify the key mechanisms by which ES-62 could prevent SF from promoting inflammation and bone destruction and in this way render them insensitive to pro-inflammatory signals. From a therapeutic point of view, being a large immunogenic molecule, ES-62 is not suitable for use in the clinic and thus candidate small molecule analogues (SMAs) of ES-62, based around its active PC moiety have been designed, some which mimic its therapeutic potential in a variety of inflammatory disorders. Thus, it was also important to address whether ES-62 and its SMAs were similarly able to affect SF and prevent their pathogenicity.

These studies revealed that the microenvironment of the joint during induction and progression of CIA did indeed result in remodelling of the epigenetic landscape of SF and that such cell reprogramming was associated with the acquisition of a hyperinflammatory, tissue destructive phenotype. Such

reprogramming could be recapitulated *in vitro*, at least in part, by chronic exposure of normal SF to pro-inflammatory cytokines such as IL-17 and IL-1β, pathogenic mediators that are found at high levels in the arthritic joint. Such reprogramming was dependent on ERK and STAT3 signalling converging on miR-155-mediated regulation of inflammatory networks via global DNA hypomethylation. ES-62 was able to counteract this by suppressing the levels of ERK, STAT3 and miR-155 signalling but rather surprisingly, this did not result in abrogation of this hypomethylated epigenetic landscape. Rather, whereas the SMA 12b appeared to act simply by preventing/reversing global DNA demethylation to suppress the induction of genes that drive pathogenesis in CIA, ES-62 induced further global DNA hypomethylation and modulation of the epigenetic landscape by inducing HDAC1: collectively these findings suggested that ES-62 might additionally induce (homeostatic) inflammation-resolving and tissue repair genes that would have translational impact in established disease. In any case, these studies suggest that the proposal to use the global DNA methylation status of RA patients as a biomarker of disease should be treated with caution.

Author's declaration

The work presented in this thesis represents the original work carried out by the author and has not been submitted in any form to another university. Where use has been made of materials provided by others, due acknowledgement has been made.

Dr Marlene Corbet B.sc M.res

University of Glasgow

September 2016

Acknowledgements

First and foremost, I would like to thank my supervisor Margaret Harnett who shared with me her passion for biology and research and who has been an very patient and great supervisor all along my Ph.D. I would like to thank as well my co-supervisor William Harnett who with the rest of the Harnett group made me feel welcome in Glasgow. I need as well to thanks all member of the Harnett group specially Miguel Pineda and David Rodgers for positive support and valuable help at the bench.

Thank you to the Wellcome Trust program and specially Olwyn Byron and Darren Monckton for giving me this huge opportunity to work in Scotland. As well I need to thank the other Wellcome Trust PhD students (Nina, Catrina, Hussain and Kevin) for helping each other throughout this 4 year trip together. I would like to thank all everyone I had the chance to work with in the university in particular Ashok Kumawat, Anne Gaelle Besnard, Rodriguo Guabiraba, Annelie Monnier who were my second family here and provided all the moral support I needed as well as being a true source of inspiration and transmitted me their love of science.

As well a special thanks to the University of Glasgow for hosting me and all the technical assistance provided by the CRF facility and specially Tony for all the animal caring and help, and Jim for all paw sections and technical advices.

My experience in the University of Glasgow has been unique and very enriching and I won't have been able to enjoy it that much without the help of my French crew (Melanie, Florent, Marie-Anne, Juliette, Chris, Matthieu, Morgane and Olivier). As well, it is indispensable to thank my family who is my first source of motivation every day.

Table of contents

List of figures

List of tables

List of common abbreviations

ACPAs: Anti citrullinated protein antibody

Bregs: Regulatory B cell

BSA: Bovine serum albumin

CIA: Collagen-induced arthritis

CCL2: Chemokine ligand 2

DC: Dendritic cells

ELISA: Enzyme linked immunosorbance assay

ES: Excretory secretory

FBS: Fetal bovine serum

H & E: Haematoxylin and eosin

HDAC: Histone deacetylase

HLA: Human Leukocyte antigen

IFN: Interferon

Ig: Immunoglobulin

IL-: Interleukine

i.p: Intra-peritoneal

i.v: Intra-venous

kDa: Kilo Daltons

MMP: Matrix metalloproteinase

OASF: Osteoarthritic synovial fibroblasts

OVA: Ovalbumin

PBS: Phosphate buffered saline

PC: Phosphorylcholine

PTN22: Protein tyrosine phosphatase non receptor type 22

RA: Rheumatoid arthritis

RASF: Rheumatoid arthritis synovial fibroblasts

SCID: Severe combined immunodeficiency

SF: Synovial fibroblasts

SLE: Systemic lupus erythematosus

SMAs: Small molecule analogues

TLR: Toll like receptor

TNF: Tumor necrotic factor

VEGF: Vascular endothelial growth factor

1. General introduction

1.1 Rheumatoid arthritis

Rheumatoid arthritis (RA) is a chronic autoimmune disease characterized by symmetrical polyarticular inflammation of the synovium that causes pain, swelling and stiffness in the joints, usually the small joints of the hands, wrists and feet. However, it is increasingly recognised that various co-morbidities are associated with RA such as cardiovascular defects and increased risk of cancer as well as osteoporosis. RA affects nearly 1 % of the global population, mainly women between 40 and 50, but disease is evident in either sex at any age[1]. Currently, there is no cure for RA, but the recent increase in our knowledge of disease pathogenesis has enabled the development of earlier diagnostic methods[1] and a variety of treatments that can slow the disease process. However, such therapies still give rise to long-term treatment challenges, such as notable side effects, loss of efficiency or the need for combination with multiple treatments. Therefore, there is still an unmet need for the development of more specific, safe and efficient therapies as well to the improvement of the early diagnosis tools to facilitate efficient treatment.

Current therapies for RA aim either to relieve pain or slow/stop disease progression[2]. To relieve pain, patients are generally given a combination of paracetamol and codeine, but such painkillers do not treat the joint inflammation. Thus, Non-steroidal Anti-Inflammatory Drugs (NSAIDs) such as ibuprofen are also used to reduce the inflammation in the joints. However, none of these drugs will prevent the arthritis from getting worse over time. To prevent disease progression many drugs are available and are often divided into two categories, namely Disease Modifying Anti-Rheumatic Drugs (DMARDs) and Biologics. Typical DMARDs are steroids, such as methotrexate, which by suppressing immune responses, either alone or in combination with other drugs, can diminish inflammation and the joint destruction process. Even when these drugs are effective for many patients they can exhibit some serious side-effects including tiredness, stomach and liver issues and induction of birth defects. Biologics are newer treatments than DMARDs that can target specific immune

responses that are responsible for the inflammation as well as bone and cartilage destruction: however, these therapies can also immunosuppress patients and leave them at higher risk of potentially catastrophic infection. Although the use of these therapies can be effective when all are used in combination, some, 60% of patients seem to have some kind of persistent disease and a substantial number of patients remain completely unresponsive to the various treatments available to block disease progression[3]. There is therefore still a strong need for further understanding of pathogenesis and consequent development of new alternative therapies to suppress disease activity in a safe way.

RA occurs as a result of both genetic and environmental factors, as identical twin studies[3], showing that only 15% of both twins have RA, have highlighted the importance of environmental factors. Nevertheless, for non-identical twins, only 4% of both twins will develop RA underlining the significant role that genetic factors can play. Certainly, a number of disease-associated genes have been identified so far, with two clearly implicated in the development of RA. Indeed, the HLA-DRB1 gene is the strongest risk factor associated with disease, with some of its many variants acting as severe risk factors. Likewise, the protein tyrosine phosphatase 22 gene (PTPN22) is strongly associated with the development of RA, despite not much being known about its pathogenic actions. Potential environmental factors that have been well-investigated are smoking, obesity, stress, insecticides and, since 70% of patients are women, female hormones. Indeed, the best known environmental contribution to RA is smoking, and this can increase patient susceptibility by up to 20-40 fold[4].

Although some susceptibility factors have been discovered, the molecular and cellular events underpinning initiation of RA pathogenesis are still far from being fully understood: it is absolutely necessary to delineate these in order to enable early diagnosis and thereby increase the chance of remission and avoid irreversible joint damage. Nevertheless, the most accepted hypothesis is that initiation of RA relies on repeated, aberrant activation of the immune system, which somehow at some point tips the balance towards the clinical form of the disease. Some elements have been identified as being characteristic of the pre-clinical phase, such as the high production of two types of autoantibodies, namely rheumatoid factor and anti-citrullinated peptide antibodies (ACPA)[5].

Rheumatoid factor comprises autoantibodies against the Fc portion of IgGs (fragment crystallisable of immunoglobulin G), that result in the formation of immune complexes which drive inflammation and hence presumably contribute to initiation of RA. Certainly high levels of rheumatoid factor are found in patients and these are associated with the severity of symptoms and the development of destructive articular arthritis. ACPAs are not properly autoantibodies since they target a protein modification, rather than the protein itself, that is found in many matrix proteins like fibrinogen, keratin enolase or vimentin, which are all highly expressed in the joint. Indeed, half of all patients appear to exhibit antibodies against anti-citrullinated alpha enolase, and intriguingly, this citrullination (conversion of the amino acid arginine in a protein into the amino acid citrulline) is associated with PTPN22 (Protein Tyrosine Phosphatase, Non-Receptor Type 22) and HLA-DRB1 (Major Histocompatibility Complex, Class II, DR Beta 1) variants. Moreover, smoking can increase citrullination in lung tissue leading to the production of ACPAs. Rheumatoid factor and ACPA autoantibodies are now used for diagnosis especially since they can develop more than 10 years before the clinical onset of disease. However, even if they contribute to the initiation or enhancement of synovitis they are probably not the leading cause of RA, and more investigations are still necessary[6].

Once autoimmunity is initiated, T cells become activated and invade the joint, where they constitute 30 to 50% of invading cells. Such T cells are induced to differentiate to Th17 and Th22 cells, to produce the cytokines IL-17 and IL-22 that are particularly implicated in promoting joint inflammation and bone destruction[7,8]. In addition, depending of the particular stimuli, T cells can secrete TNFα and IL-4 within the joint and these cytokines have also been reported to be crucial in RA pathogenesis[9-12]. B cells become activated after being in contact with such T cells and cytokine stimulation. B cells not only differentiate into plasma cells to produce auto-antibodies and rheumatoid factor, but also contribute to cytokine production. Moreover, macrophages produce IL-1 and TNFα, cytokines that activate chondrocytes to promote bone resorption in patients[13,14]. Therefore many of the therapies developed selectively target the cytokines, TNFα, IL-1β, IL-17 or IL-6. However, such

cytokines are involved in many processes and inhibiting them can cause many side effects and immunosuppression. This is the reason why there is a need to understand better joint biology to develop more specific and targeted therapies.

1.2 Inflammation and destruction of the synovial joint

1.2.1 Synovial joint biology

The main site affected in RA is the joint, where inflammation and bone destruction occurs. In addition to providing mechanical support, joints are the connectors of the skeletal system that allow movement, those found in hands and feet having a large capacity of movement and are called diarthrodial or synovial joints. Synovial joints, relative to cartilaginous and fibrous joints[15], are the most complicated structure (

Figure 1-1A) being characterized by the presence of a synovial cavity filled by synovial fluid; a fibrous joint capsule, composed of collagen and fibronectin that provides structural support and a synovial membrane that connects the articular cartilages. The synovial fluid, produced by the synovial membrane, has both a lubricating and nourishing function whilst the synovial membrane is involved in the absorption of joint cavity debris and blood synovial fluid exchanges[16,17].The synovial membrane is composed of two different layers of cells, the intimal and subintimal layers (

Figure 1-1B). The intima is a continuous layer of cells, one or two cells thick, that is in contact with the intra-articular cavity and produces the synovial fluid important for the lubrication process. The subintimal layer comprises the loose fatty connective tissue underneath the intima and although it is still relatively acellular and mainly composed of extracellular matrix, it contains a variety of cell types, mainly resident fibroblasts and macrophages but some infiltrating immune cells, adipocytes and blood vessels as well[18].

Normal synoviocytes comprise two different cell types called type A and type B synoviocytes: type A are macrophage-like whilst type B are fibroblast-like synoviocytes[18]. Macrophage-like synoviocytes are present mainly in the intimal

layer and are derived from bone marrow via circulating monocytes that migrate to the synovium where they differentiate and become resident[19]. They strongly express the same markers as other resident macrophages populations such as Major Histocompatibility Complex (MHC) Class II, CD68, CD163 and FcRɣ and, to a lesser extent, CD14[16]. They actively phagocytose debris and waste from the joint cavity as well as exhibiting an antigen-presenting capacity. By contrast, fibroblast-like synoviocytes (FLS) are present in both layers of the synovial membrane and whilst their origin is still controversial, they are considered to be derived from mesenchymal cells[16] and exhibit most of the characteristics of other fibroblast populations. Thus, they express markers such as type IV and V collagens, vimentin and CD90, as well as adhesion molecules such as ICAM-1 (intracellular adhesion molecule), CD44, ß1 and ß3 integrins (albeit these last three molecules are expressed at higher level than in other fibroblasts populations), and VCAM-1 (vascular cell adhesion molecule 1), which is absent in most fibroblast populations[20-23]. They are also characterized by the presence of an abundant and rough endoplasmic reticulum, reflecting their important role in the production of matrix and specialised synovial fluid components like hyaluronan, collagens or fibronectin. Perhaps unexpectedly, in normal synovium, FLS are found to produce pro-inflammatory cytokines but at lower levels than during inflammation. Indeed, IL-1, IL-6 and TNFα (interleukine 1,6 and tumor necrosis factor alpha) can be observed in normal synovium in addition to anti-inflammatory cytokines such as IL-1 receptor antagonist. Similarly, FLS also secrete a low level of the osteoclastogenesis inducer RANKL (receptor activator of nuclear factor kappa-B ligand) but, in the absence of inflammation, the effects of this appear to be compensated by the production of osteoprotegerin[21] and such expression presumably reflects homeostatic mechanisms of tissue repair and homeostasis.

1.2.2 The synovial joint in RA

During RA, joint inflammation (synovitis), cartilage and bone destruction occur (

Figure 1-1C). Synovitis is characterized by the hyperplasia of the synovial membrane resulting from hyperproliferation of synovial fibroblasts (SF) as well as the massive invasion of cells to the site of inflammation. In addition,

angiogenesis occurs in the subintimal layer as a consequence of angiogenic factors produced in response to the local hypoxic environment further facilitating the inflammatory cell invasion. In the intimal layer, the fibroblast and macrophages proliferate leading to the expansion of this structure from 1-2 cells up to 10-20 cells thick[16]. In terms of the inflammatory cell infiltrate, up to approximately half of the cells found in the inflamed synovium have been reported to be $CD4^+CD45RO^+$ memory T cells although a smaller proportion of $CD8^+$ T cells are found as well[24]. However, B cells, dendritic cells, macrophages and neutrophils are also observed.

Activation of both the SF and the infiltrating cells leads to the accumulation of proinflammatory cytokines responsible for inducing and maintaining the inflammation in the RA joint. The cytokines proposed to be particularly involved in the pathogenesis of RA are TNFα, IL-1β, IL-6 and IL-17[25]. The key role of TNFα in RA is well known now and is highlighted by the development of anti-TNF therapies that are effective for many for RA patients[26]. The more recent emergence of an important role for IL-17 (and Th17 cells) in RA was first indicated by the increased levels of IL-17 found in patient sera and synovial fluids[27]. Moreover, and directly indicative of a pathogenic role, IL-17 deficient mice were found to be protected against collagen-induced arthritis (CIA). In addition, overproduction of Th17 cells was found to enhance the pathogenicity of arthritis[28,29] presumably reflecting, at least in part, that via their production of IL-17, Th17 cells are involved in regulating osteoclast differentiation and matrix metalloproteinases (MMPs) secretion[30-32]. IL-1β is also highly abundant in the joint of patients and has been identified as one of the susceptibility genes for RA[13]. Consistent with this, whilst overexpression of IL-1β in rabbit knee joints causes arthritis with clinical features of RA, IL-1β blockade significantly reduces arthritis score[33]. Similarly, IL-6 is another pleiotropic cytokine of major importance in RA that is abundantly found in the synovial fluid and serum of patients and for which, expressions levels correlate with disease score. Indeed, IL-6 has been shown to promote synovial inflammation and joint destruction by stimulating osteoclast maturation, pannus proliferation and migration of neutrophils[34]. Interestingly, therefore, both Type A and B synoviocytes can produce these cytokines.

1.2.3 Pannus formation

Interestingly, during RA pathogenesis, leukocytes appear to infiltrate the synovium before proliferation of the synovial membrane occurs suggesting that this leukocyte invasion induces a reorganization of the synovial architecture and a change in the SF phenotype. Such formation of this new fibrovascular tissue or granulation tissue at the joint surface commonly called pannus. However, the precise mechanisms underpinning pannus development remain unsolved. Nevertheless, pannus tissue in RA patients has been described as an invasive granulation tissue covering the articular cartilage[35] and it appears that at the beginning of inflammation, the synovial membrane starts thickening to form this tissue called pannus, which drives inflammation and invades cartilage and bones. Due to these characteristics, the pannus is sometimes thought of as being a tumor-like tissue although mitotic figures are rare and metastasis does not occur. Closer analysis of this tissue revealed that it is composed of macrophages and fibroblasts-like mesenchymal cells, macrophage-like cells, other inflammatory cells and osteoclast precursors[36]. Moreover, those pre-osteoclasts were found to be induced in response to proinflammatory mediators such as M-CSF and RANK ligand, produced by the interactions of fibroblasts and T lymphocytes. Once stimulated, such osteoclast-precursors migrate and attach to the bone surface where they differentiate into active osteoclasts and mediate bone resorption by producing tissue destructive enzymes able to destroy cartilage and bone and thereby perpetuate the inflammation[37]. Indeed, in RA the macrophage-like synoviocytes display a strongly activated phenotype, producing a wide range of pro-inflammatory cytokines, chemokines and growth factors that participate in the activation and “transformation” of SF to an aggressive pathogenic phenotype.

1.3 Synovial fibroblasts in rheumatoid arthritis (RASF)

1.3.1 Tumor-like characteristics of RASF

Pathogenesis in RA is driven by the concerted action of different cell types: thus, whilst it is clear that autoimmunity and resultant aberrant inflammation is

central to RA, it is increasingly evident that in addition to T cells and macrophages driving such inflammation in the joint that the activated aggressive SF play a key pathogenic role.

In RA, activated SF display new characteristics that are reminiscent of tumor-like mesenchymal cells: indeed, the proliferative pannus appears to behave like a locally invasive tumour, with the SF exhibiting the capacity to migrate and then attach to, and invade, bone and cartilage[38], functional responses not observed with other fibroblasts. Reflecting these characteristics, they upregulate proto-oncogenes involved in cell cycle regulation, like c-Fos, Ras, Raf, Myc, and Myb whilst displaying low levels of expression of tumor suppressor genes, such as p53 and PTEN[39-41]. Thereby, the cells become resistant to apoptosis and lose the property of contact inhibition and have been shown not only to migrate within the joint, but also to be able to migrate and spread the inflammation to other sites. Such "transformed" fibroblasts were first observed by Fassbender in the 1980s when he noticed the presence of “immature-looking synovial cells” that attached to the cartilage and were responsible for its degradation in articular tissue from patients[42]. Consistent with their functional phenotype, these cells display large and pale nuclei and abundant cytoplasm containing numerous lysosomes. He hypothesized that these “transformed fibroblasts” are immature mesenchymal cells that can return to the synovial membrane and re-differentiate into fibroblasts once they have resorbed bone (Figure 1-2).

What makes fibroblasts change their behaviour to an aggressive pathogenic phenotype during RA? Whilst it has been suggested that they are simply passive responders to the pro-inflammatory milieu, it has also been proposed that they act as active drivers of pathogenesis[43]. These suggestions are not necessarily mutually exclusive, as fibroblasts appear to directly respond to the extracellular signals found in the synovial fluid (such as pro-inflammatory cytokines or TLR ligands), before quickly returning to a quiescent non-aggressive state if not further stimulated. Increasing data however suggest that some fibroblasts retain phenotypic features consistent with their “transformation” to an active pathogenic form, as SF extracted from patients' synovium and cultured *in vitro*

appear to be "imprinted", being aggressive hyper-responders to pro-inflammatory stimuli [20].

1.3.2 Characteristics of the aggressive SF phenotype

SF are highly differentiated and specialised cells, therefore their role in the joint is very precise and their functions limited. These comprise producing the synovial fluid, regulating the leukocyte movement within the joint and maintaining the joint capsule. Once “transformed” the SF acquire functions driven by the production of a wide range of new factors summarized in Figure 1-3 and developed here, below.

1.3.2.1 Adhesion molecules: anchorage and migration

One of the most important features of the aggressive phenotype of RASF is their capacity to express a wide number of adhesion molecules that allow them to acquire motility and facilitate their anchorage to cartilage. Amongst these, integrin α5ß1, VCAM-1, ICAM-1 and cadherin-11 are particularly highly expressed[44-47]. Integrins by interacting with fibronectin, collagen or cartilage matrix proteins not only promote the anchorage of RASF to the cartilage extracellular matrix (ECM) but also, the signalling resulting from the interactions between integrins and fibronectin induces the expression of MMPs and of pro-inflammatory cytokines such as IL-6, IL-8 as well as chemokines CCL2 and CXCL1[48-50] that by remodelling the ECM will further facilitate migration to, and tissue damage at, the site of erosion. The importance of these properties is reflected by reports of the ability of RASF to migrate and spread inflammation: indeed, Lefèvre *et al*. have demonstrated, by transferring "transformed" fibroblasts into an immunodeficient mouse, that active RASF can migrate *in vivo* to sites of implanted healthy human cartilage and actively degrade it and hence spread disease[38].

1.3.2.2 Tissue destruction

Bone and cartilage destruction is the effector end-stage consequence of autoimmune pathogenesis in RA and RASF have been shown to promote cartilage degradation, even in absence of T cells and monocytes in a SCID mouse (severe combined immunodeficiency mouse) engrafted with human cartilage[51]. Firstly, they act directly to erode bone and cartilage by secreting cathepsins and MMPs, specifically the two collagenases, MMP-1 and MMP-13 as well as the stromelysin, MMP3 and the gelatinases, MMP-2 and MMP-9[52]. However, such production of MMPs appears to be strongly increased by interactions of RASF with T cells[53] whilst RASF can also act indirectly to induce bone and cartilage damage by stimulating osteoclastogenesis via their secretion of RANK ligand (RANKL) as wells as vascular endothelial growth factor (VEGF), that can substitute for M-CSF for such differentiation during pathogenesis[54].

1.3.2.3 Secretion of a large panel of growth and chemotactic factors

RASF are also involved in perpetuating inflammation by driving cell infiltration and survival, angiogenesis and cell activation by their responses to the pro-inflammatory milieu of the joint. Thus, many important pro-angiogenic cytokines and growth factors have been shown to be released by SF, such as transforming growth factor-ß, interleukin (IL)-8, platelet derived growth factor (PDGF), granulocyte-macrophage colony stimulating factor (G-MCSF), epidermal growth factor (EGF), fibroblast growth factor (FGF) and one of the most potent angiogenic factors, VEGF (Vascular endothelial growth factor)[55], the constitutive secretion of which is augmented by hypoxia and IL-1 stimulation[56]. Angiogenesis is accompanied by vasculature leakage that facilitates the immune cell infiltration that perpetuates the inflammation of the joint. SF impact on the attraction of leucocytes into the joint by producing a variety of chemoattractant molecules following their exposure to pro-inflammatory cytokines or via CD40-mediated contact with T cells[3,57]. Specifically recruitment of monocytes to the synovium is due to the secretion of CCL2 (macrophage chemotactic protein [MCP]-1) and CCL3 (macrophage inflammatory protein [MIP]-1α) whilst the release of IL-16, CCL5 (Rantes) and CXCL8 (IL-8) is responsible for the infiltration by T cells, eosinophils and neutrophils[58]. Interactions amongst these cells result

in their (further) activation and the maintenance of inflammation, for example, with the release of IL-1ß, IL-6 and TNF-α acting to maintain the activated phenotype of inflammatory cells via induction of pathogenic cytokines[14]. Amongst these, IL-15 and IL-7 drive (auto-reactive) T cell activation whilst GM-CSF promotes the survival and differentiation of hematopoietic cells and their precursors[59].

1.4 Inducing cell transformation and dedifferentiation

It is increasingly clear that the aggressive SF found in the inflamed joint display features distinct from those in healthy synovium and these are maintained even when the cells are isolated from their pro-inflammatory environment[43]. The acquisition of this aggressive pathogenic phenotype appears to be enabled by mutations and/or epigenetic modifications resulting in their "imprinting" by permanent modification of their gene expression.

1.4.1 Somatic mutations

Fibroblasts like synoviocytes (FLS) from RA patients have been shown to contain somatic mutations of genes regulating cell cycle, proliferation and apoptosis, characteristic of transition mutations resulting from damage caused by high levels of reactive oxygen species (ROS) or reactive nitrogen oxide (RNS)[60]. A key example is the inactivation mutation of the tumor suppressor, p53[61,62], but not PTEN, gene although Ras and HPRT genes have also often been reported to be affected in patients[63,64]. Although the precise mechanisms leading to such somatic mutations have not been fully defined, it appears that the presence of ROS and RNS in the inflamed joint leads to the inhibition of the MSH6 gene (methyl-directed mismatch repair protein homolog 6), involved in the repair of transition mutations and perhaps explains the high rate of microsatellite instability displayed by some patients[65]. Interestingly, mitochondrial DNA damage is suspected to be particularly involved in RA pathogenesis: thus, as many mitochondrial proteins have a bacterial homologue, it has been proposed that during their presentation by MHC complexes, mutated peptides might appear as bacterial peptides and thereby act to induce aberrant immune reactions[66].

1.4.2 Epigenetic modifications

Some cellular events other than of somatic mutation can be responsible for a stable and heritable transcriptome modification. Such events are named epigenetic modifications and involve modifications of the DNA structure that do not involve the nucleotide sequence. Humans have 46 molecules of DNA (chromosomes) that have been predicted to measure approximately 2 m long. Such a large amount of DNA is tightly packed in the nucleus, that measures on average 6 mm in diameter, thanks to the nucleosome structure. Indeed, in DNA, approximately 147 base pairs are coiled in 1.67 left-handed superhelical turns around an 8 histones core (pairs of the histones H2A, H2B H3 and H4) to comprise the nucleosome unit[67]. All nucleosomes are then folded through different levels of higher structures to ultimately form the chromosome. Therefore, modifications in such nucleosomes (affecting the histones or the DNA) can affect the position of the nucleosome within its structure: in turn, this can lead, in part through a change in the electrostatic charge of the nucleosome, to either a tightening-up of the structure resulting in the formation of closed untranscriptable 'heterochromatin' or its loosening to a 'euchromatin' form which enables the DNA to be more accessible to transcription factors.

It is well established that such epigenetic modifications play important roles in cell differentiation and transformation in cancer and other disorders[68,69]. This reflects that, for example, post-translational modifications of histone proteins impact on the interactions between the DNA and histone complexes to regulate the transitions between euchromatin and heterochromatin, or recruit various factors important for the control of gene expression. Such modifications usually occur in the N-terminus flexible tail of the histone that is exposed while the globular part of the protein is compacted in the nucleosome. Various post-translational modification can occur, amongst them acetylation, methylation and sumoylation, all of which have been shown to be important in the regulation of RASF responses.

Histone acetylation is a modification that targets specific lysine residues present on histones, H3 and H4: this is usually associated with transcriptional activation probably due to the change in the electrostatic charge of the histone tail

resulting in a change of structural conformation that loosens the chromatin structure and facilitates the formation of euchromatin. Perhaps counter-intuitively, therefore, given the upregulation of pro-inflammatory genes in RA, histone deacetylase (HDAC) inhibitors have been reported to display beneficial effects *in vivo* in a diverse range of animal models of RA[70-72]. Moreover, when such inhibitors have been exploited to unravel the importance of dysregulated histone acetylation in RA, they indicated that HDACs may exert positive and negative effects in RA. For instance, in a recent study, the class I deacetylase inhibitor, Largazole, suppressed some pathogenic mediators like MMP2 but enhanced TNF-α induced ICAM-1 and VCAM-1 expression in RASF. Furthermore, it is difficult to assess the role of specific classes of HDACs in RA pathogenesis since most of the drugs available so far are not sufficiently specific. However, and perhaps consistent with the *in vivo* inhibitor data, expression of HDAC1 and HDAC2 was found to be increased in RASF compared to that in osteoarthritic SF (OASF) and silencing of these two enzymes affected the RASF gene expression profile resulting in a reduction of their proliferative capacity and increased susceptibility to apoptosis[73,74]. Nevertheless, the situation is complex as even though deacetylation seems to play an important role in the RA process, aberrant acetylation of some promoters has been found as well. Indeed, the MMP-1 gene is found to be hyperacetylated in RASF and the stimulation *in vitro* of RASF by TNFα and IL-1ß leads to high acetylation levels of the promoter of the p21 gene involved in cell cycle regulation[75,76].

Collectively, therefore, these findings may suggest that HDAC-I may act to prevent downregulation of homeostatic induction of anti-inflammatory genes to effect resolution of inflammation. Nevertheless, in the absence of information regarding the selectivity of different HDAC for particular promoters, these studies do not explain how the potential stabilisation of gene induction of pro-inflammatory genes may be protective. Perhaps of relevance, RASF also seem to display high levels of small ubiquitin-like modifier (SUMO) 1 that is associated with a decrease in the SUMO-specific protease SENP1. Interestingly, therefore, overexpression of SENP1 in RASF leads to the decrease in histone H4 acetylation in the MMP-1 promoter and this is associated with a decreased invasiveness of the cells. These data are suggestive of an active sumoylation post-translational modification of histone proteins process in RASF, but the targeted proteins have

yet to be identified[75] Moreover, and by contrast to the focus on histone acetylation/deacetylation generated by HDAC-I, little is known regarding the consequences for RA of histone methylation, a modification that affects the lysine and arginine residues mainly on H3 and H4 histones. For example, although it has been shown recently that the histone methyl transferase (HMT) enhancer of zeste homologue 2 (EZH2) is overexpressed in RASF, compared to OASF, the consequences of this for RA pathogenesis remain unknown[77]. Collectively, therefore, given the conflicting data relating to the role of HDACs in RA, it is plausible that the differential and combinatorial profiles (acetylation, methylation and sumoylation) of histone modification at particular promoters, as well as the specific classes of HDACs and HMT involved will dictate pathological outcome.

By contrast, DNA methylation is an epigenetic modification controlling gene expression that is generally associated with gene silencing. It occurs by the direct addition of a methyl group (predominantly) to cytosine, resulting in the formation of 5-methylcytosine. In humans, 5-methylcytosines constitute about 1.5% of the whole genome and are almost always found in CpG islands[78]. Such DNA methylation appears to repress gene induction by directly interfering with the binding of transcription factors as well as by the recruitment of proteins, containing methylated-DNA binding domains (MBD) notably such as HDAC, that promote transition to the heterochromatin structure[79]. Addition of methyl groups to cytosine is catalysed by DNA methyltransferases (DNMTs)[80]. DNMTs constitute a highly conserved family of proteins with the three, DNMT1 DNMT3a and DNMT3b found in mammals being essential for development and the maintenance of genome stability. Indeed, DNA methylation is the most studied epigenetic modification as a consequence of its importance in many biological processes such as embryonic development, chromosome stability and genomic imprinting[79]. In adults, DNMT1 is the most abundant DNA methylase, which as a 'maintenance DNMT', binds to the hemi-methylated DNA found after DNA replication to add methyl groups to the newly synthetized strand to maintain the DNA methylation pattern through cell division. By contrast, DNMT3a and DNMT3b are '*de novo* DNA methylases' that add methyl groups to new cytosine sites in response to specific stimuli. Consistent with these key cellular roles, aberrant expression of DNMTs and consequent disruption of normal DNA methylation

profiles has been implicated in many disease states, especially that of cancer[81,82].

Thus although a number of epigenetic mechanisms are in place to control gene expression, DNA methylation appears to be the easiest way to silence genes as high levels of methylcytosine promotes the formation of heterochromatin structure[67,81]. The DNA methylation status is therefore of importance to stem cell differentiation, the process by which cells lose pluripotentiality and acquire specialisation and cell identity[83]. Thus, DNA methylation is strongly associated with potency as stem/progenitor cells (low genome methylation) are typically able to activate a larger set of genes than a terminally differentiated cell (high global DNA methylation) that can only accomplished a specialised set of functions due to silencing of genes irrelevant to its differentiated cell function[84]. Thus, cell reprogramming is generally associated with changes in DNA methylation patterns and serves to explain why carcinogenesis is often associated with a global loss of DNA methylation and acquisition of a dedifferentiated or pluripotent state.

Cells, particularly FLS, from RA patients have been reported to exhibit DNA that is hypomethylated compared to that from OA patients and healthy individiuals[85]: this global hypomethylation of DNA appears to be due to an increased polyamine metabolism in RASF that causes a decrease in S-adenosyl-L-methionine levels[86]. Following on from this, a more complex picture has emerged as DNA methylome studies revealed that whilst genes involved in migration, adhesion or matrix-degradation are hypomethylated in RASF, certain promoters such as that of the death receptor 3 gene (DR3; a member of the pro-apoptotic Fas gene family) are hypermethylated in some RA patients[87]. Neverthless, more direct evidence supporting the importance of hypomethylation in mediating fibroblast transformation to an aggressive phenotype was provided studies demonstrating that normal FLS cultured under conditions inducing global hypomethylation of DNA acquired a hyper-activated phenotype similar to that observed in RASF[85].

1.5 The therapeutic potential of helminth-based immunomodulators

1.5.1 Hygiene hypothesis

In developed countries, RA affects 1-2% of the population and the prevalence is increasing every year. Although the reasons for this increase in incidence of RA and other autoimmune disorders have not been fully defined, it is clear that it has coincided with the rapid eradication of infections by pathogens, through improved hygiene, vaccines and antibiotics. The 'hygiene hypothesis' was originally formulated by Strachan in 1989 after noticing the rise of childhood immune related disorders such as asthma and eczema during the post industrial revolution[88]. He observed a link in hay fever epidemiology and family size, concluding that unhygienic contact amongst siblings is an important protective factor and hence, the dramatically increased incidence of immune-mediated diseases may reflect, the great improvement in general hygiene, over the past century. Consistent with this, there is increasing evidence that in developing countries, where parasitic helminth infection is endemic, such inflammatory disorders are infrequent. From these observations it has been hypothesized that infection with helminth parasites might protect against development of autoimmune disorders[89]. There has indeed been increasing evidence showing that infection by parasitic worms can be protective in a number of animal model for immunopathological diseases[90,91]. Moreover, some preliminary clinical trials exploiting "worm therapy" in patients were promising for inflammatory bowel diseases like Crohn's disease[92,93], coeliac disease[94] or ulcerative colitis[95] as well as for other inflammatory disorders such as severe asthma[96] and rhinitis[97].

1.5.2 Immunomodulators produced by helminths

The word "helminth" is derived from the Greek "helmins" for worm and a third of the world population is infected by parasitic helminths. Their eggs contaminate food, water, air and faeces, maintaining life cycles mediated by intermediate invertebrate hosts like blackflies. Although many of these parasitic worms reside

in the gut, others reside in other body sites like blood (*schistosome*) and lymph (*Wuchereria bancrofti*, *Brugia malayi*, and *Brugia timori*)[98]. Over millenia of co-evolution, these parasites have developed numerous strategies both to evade the host immune system by dampening inflammation and create a favourable environment to enhance their survival, without leaving the host immunosuppressed and hence vulnerable to other infections. A key strategy appears to be the secretion of immunomodulatory molecules that are able to silence or selectively modulate immune responses and promote tissue repair[98]. From a therapeutic point of view, these anti-inflammatory, tissue repair-promoting molecules are very interesting since their actions may identify more selective and hence safer therapeutic targets for treatment of disorders associated with aberrant inflammation like RA[99]. Certainly their potential, unlike most of the current immunosuppressive drugs such as glucocorticoids used in treating autoimmune disorders, to target only "harmful", leaving "safe"-infection-fighting inflammation, represents a potential starting point in a novel therapeutic approach[100]

1.5.3 ES-62 a helminth-derived immunomodulator

Amongst the increasing number of parasite-derived products identified with therapeutic potential, ES-62, the major secreted glycoprotein of the rodent filarial nematode *Acanthocheilonema vitae* with homologues found in human filarial nematodes, is one of the most well-characterized helminth immunomodulators. it is a 62kDa phosphorylcholine (PC)-containing glycoprotein secreted as tetramer that exhibits various immunomodulatory activities, suppressing inflammation and pathology in a range of models of allergic or autoimmune disorders such as asthma, lupus or RA[101-104]. ES-62 appears to sense and modulate aberrant inflammation, mainly through the disruption of TLR4 signalling. For example, in the CIA mouse model of RA, ES-62 is protective through its inhibition of pathogenic IL-17 production[104]. Indeed, ES-62 acts in a TLR4-dependent manner to downregulate MyD88 expression in dendritic cells (DC), macrophages and T cells to prevent pathogenic inflammatory responses, in particular by regulating DC priming of Th17 lymphocyte and IL-17-producing $\gamma\delta$ T cell differentiation. Since IL-17 is a major effector cytokine driving arthritis in animal models, as well as being over-produced in the joints of RA patients, IL-17

was therefore considered to be one of the most promising targets for the development of new therapies[105]. Various IL-17 blockers, such as the monoclonal anti-IL-17A (secukinumab and ixekizumab) and anti-IL-17 receptor sub-unit A (brodalumab) antibodies have been successfully evaluated in phase II clinical trials and secukinumab is even in phase III clinical trials for patients unresponsive to methotrexate, a TNFα inhibitor[106]. However, such treatments can immunosuppress the patients and are not always efficacious[107]. By contrast, although ES-62 reduces the levels of IL-17-producing Th17 and γδT cells it does not induce immunosuppression[104] as it does not target NK and NK T cells that can still produce IL-17 allowing the host to fight the common opportunistic infections that are proving to be a problem with current IL-17-blockers[108]. Thus, the ability to selectively modulate distinct cellular pools of IL-17 potentially makes ES-62, or drugs that mimic its action, a safer therapeutic for IL-17-based inflammatory diseases[109].

1.5.4 Small molecule analogues (SMAs) of ES-62

ES-62 is secreted as a tretrameric molecule of approximately 240 kDa and as it is generally immunogenic, it is therefore likely not suitable for therapeutic use. However, the Harnett group has identified the PC moiety of ES-62 as being responsible for the most of the immunomodulatory effects of the parasite product[110], with indeed PC-conjugated to BSA (or ovalbumin [OVA]) being sufficient for protection against CIA[111]. Thus, a library of low molecular weight, non-immunogenic SMAs based on the PC moiety are being developed for drug discovery, with candidates selected by a primary *in vitro* screen in macrophages aimed to identify compounds able to downregulate the production of pro-inflammatory cytokines promoting Th1 (IFNɣ)/Th17 (IL-17) responses that are elicited in response to pathogen associated molecular patterns (PAMPS)[112]. Two SMAs, 11a and 12b were especially effective and were selected for further investigation of their anti-inflammatory potential, in vivo. Both proved to be protective in the CIA model with 11a mimicking the actions of ES-62 in decreasing IFNɣ and IL-17 production[113], as well as in its mechanism of action by downregulating MyD88 expression. Surprisingly, although 12b also downregulated MyD88 and inhibited IL-12p40 production in response to PAMPS, it did not

suppress Th1/Th17 responses: rather analysis of the genes modulated by 12b in macrophages revealed its capacity to downregulate a number of genes involved in inflammasome signalling, especially IL-1ß and it did so in an manner involving NRF2[114], a transcription factor that is a master regulator of cytoprotective anti-oxidant genes and is well established not only to counteract the inflammasome but also to protect against CIA[115].

1.6 Conclusions and discussion

It is now well established that ES-62, and its SMAs 11a and 12b, afford protection in the CIA model. Consistent with deregulation of T cell activation being considered to be a major force driving inflammation, the protection afforded by ES-62 (and 11a) is associated with downregulation of Th1/Th17-type responses. Moreover, 12b (and to a lesser degree ES-62 and 11a) antagonises IL-1β responses, which in addition to driving pathogenic inflammation is also critical to Il-17 responses[114]. However, further studies examining the IL-23/IL-17 inflammatory axis demonstrated that ES-62 not only suppressed the pathogenic actions of the related cytokine, IL-22 during initiation of disease but also harnessed the tissue repair ability of IL-22 to promote resolution of established inflammation in the joint. These dual activities focused on SF, the major cell population in the joint[116].

These findings were timely as increasingly, many studies were strongly suggesting that such fibroblasts play key roles in the early onset of the disease, the maintenance of inflammation and even in the spread of the disease to the unaffected joints, as well as mediating joint destruction, directly by secreting MMPs that damage the cartilage and bone and indirectly, by promoting osteoclastogenesis. Interestingly, despite the fact that SF are not part of the immune system, they appear to act as a bridge perpetuating inflammatory effector cells responses as they are known to produce pro-inflammatory cytokines during the pathogenesis of RA and they express TLR4, a well-characterised target of ES-62 and are the only cell in the joint that expresses the IL-22 receptor.

Hence, from a therapeutic point of view it became important to address whether the protection afforded by ES-62 and its SMAs, 11a and 12b reflected their ability to affect SF and prevent their pathogenicity. Indeed, if this were to be the case, it opens the door for targeted topical joint therapies that could circumvent many problems associated with those blocking inflammation, systemically. Thus, as the microenvironment of the joint during induction and progression of arthritis exposes SF to many different cytokines and interactions with inflammatory cells that results in their pathogenic transformation to an aggressive phenotype, it was imperative to investigate whether ES-62 could prevent this by changing the joint microenvironment in CIA in vivo. Specifically, therefore, the aims of this thesis were to:

- Further characterise the therapeutic potential of ES-62 and its SMAs in a mouse model of RA, in particular to understand whether they can directly target joint-specific cells such as SF
- Delineate how ES-62 can desensitize such SF from the external pro-inflammatory environment, specifically by regulating ERK and STAT pathways implicated in their “transformation”
- Understand whether CIA SF are intrinsically different from naïve SF and undergo epigenetic modifications, especially DNA methylation, downstream of their transformative signalling pathways. Relating to this it was also planned to determine whether ES-62 impacts on the epigenetic landscape to prevent such cell transformation?

Collectively in this way the inter-related aims were designed to inform not only on the capacity of ES-62 to modulate immune cells but also stromal cells. In particular, the aim was for this new approach to uncover how ES-62 might condition the cells such that they either do not initiate and/or maintain inflammatory responses, central events to the development of RA. This process should also allow for the identification of the key mechanisms responsible for the establishment and maintenance of the aggressive phenotype of SF during CIA.

Figure 1-1 Synovial joints in health and RA

A: Synovial joints allow the maintenance of the mobility between linked bones: their special characteristics comprise a joint capsule that maintains the joint architecture, a synovial cavity containing the lubricant synovial fluid and a synovial membrane that produces the synovial fluid and cleans it.

B: The synovial membrane is composed of intimal and subintimal layers defined by their indicated differential cell constituents. The intimal lining is composed of intimal fibroblasts and macrophages and is 1 to 2 cells thickness. The subintimal lining is a looser tissue composed of a variety of cell types: SF, resident macrophages and adipocytes, surrounded by extracellular matrix. Capillaries present in the subintimal lining allow the infiltration of immune cells within the synovial membrane.

C: During RA, and CIA mice, three events are responsible for the observed pathogenesis, namely joint inflammation and synovial membrane hyperproliferation resulting in the pannus formation that leads to bone and cartilage destruction.

A

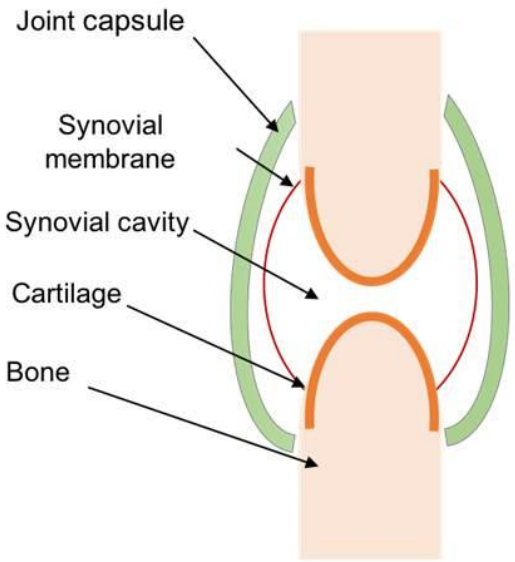
Joint capsule
Synovial membrane
Synovial cavity
Cartilage
Bone

B

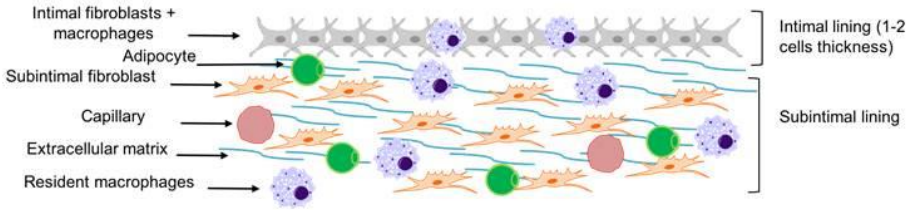
Intimal fibroblasts + macrophages
Adipocyte
Subintimal fibroblast
Capillary
Extracellular matrix
Resident macrophages
Intimal lining (1-2 cells thickness)
Subintimal lining

C

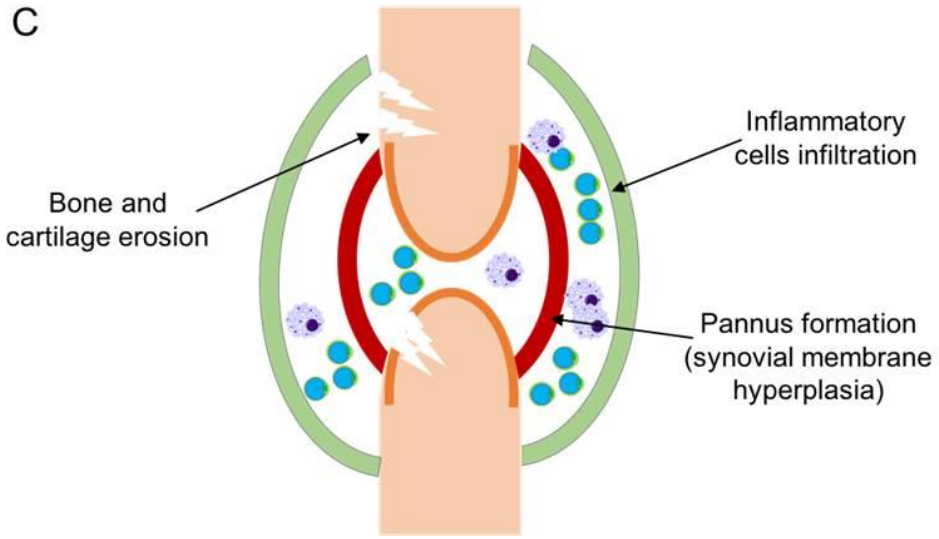
Bone and cartilage erosion
Inflammatory cells infiltration
Pannus formation (synovial membrane hyperplasia)

Figure 1-2 Fassbender model of SF dedifferentiation into mesenchymal stem cells inducing bone and cartilage resorption degradation

Fassbender hypothesized that SF from the intimal layer become activated and undergo dedifferentiation into mesenchymal stem cells to acquire properties such as cell proliferation and loss of contact inhibition to allow them to initiate pannus formation, motility and tissue invasion and attach to the bone to induce its degradation. Once bone resorption has occurred the dedifferentiated cell has the capacity to return to the intimal layer and redifferentiate into a SF.

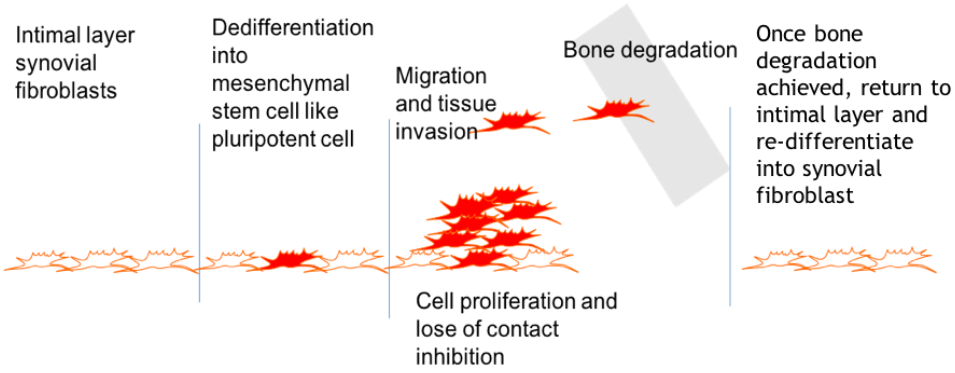
Intimal layer synovial fibroblasts
Dedifferentiation into mesenchymal stem cell like pluripotent cell
Migration and tissue invasion
Bone degradation
Once bone degradation achieved, return to intimal layer and re-differentiate into synovial fibroblast
Cell proliferation and lose of contact inhibition

Figure 1-3 Scheme summarizing the major functions of SF in the joint and their tumor-like capacities acquired during inflammatory arthritis.

SF exhibit diverse characteristics depending on their local environment. Thus, in healthy joints they are specialised producers of the lubricating synovial fluids, particularly hyaluronic acid and lubricin, as well as acting to maintain capsule strength by the generation of collagen and fibronectin, and regulating leukocyte infiltration of the joint through their surface expression ICAM and VCAM. By contrast, during RA or CIA, the apoptosis-resistant, hyper-proliferative phenotype of SF drives synovial membrane hyperplasia and contributes to the inflammation by producing a wide range of pro-inflammatory cytokines, stimulating angiogenesis and as well contributing to bone destruction directly by secreting MMPs and by inducing osteoclastogenesis with RANKL.

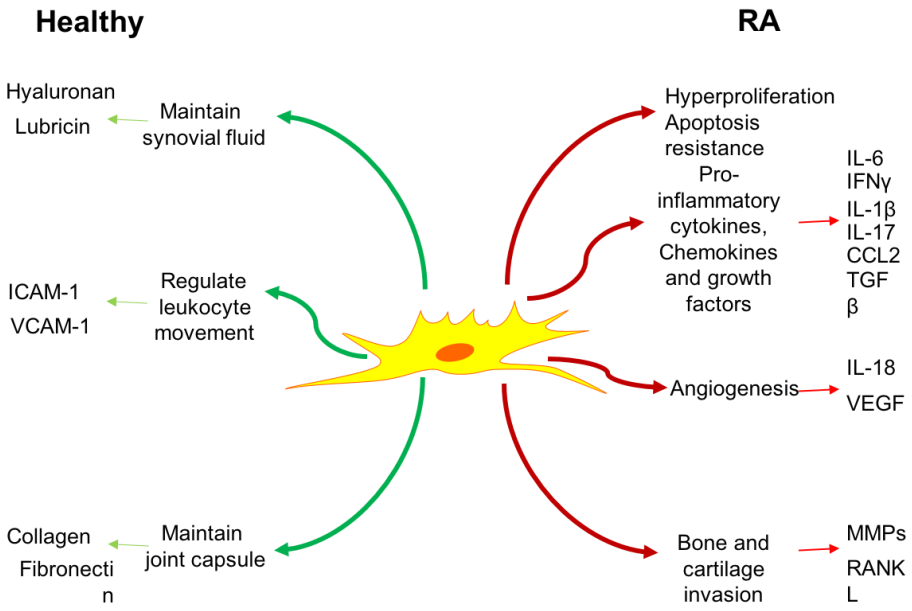
Healthy
RA
Hyaluronan
Lubricin
Maintain synovial fluid
ICAM-1
VCAM-1
Regulate leukocyte movement
Collagen
Fibronectin
Maintain joint capsule
Hyperproliferation
Apoptosis resistance
Pro-inflammatory cytokines, Chemokines and growth factors
IL-6
IFNγ
IL-1β
IL-17
CCL2
TGF β
Angiogenesis
IL-18
VEGF
Bone and cartilage invasion
MMPs
RANKL

2. Material and Methods

2.1 Mice

DBA/1 and BALB/c (Harlan Laboratories) animals were maintained in the Biological Services Unit of the University of Glasgow in accordance to the Home Office UK Licence PPL60/26532 and PIL70/26532 and the Ethics Review Board of the University of Glasgow.

2.2 Purification of the filarial nematode product ES-62

ES-62 was purified as previously described[117]. ES-62 is secreted by the adult filarial nematode, *Acanthocheilonema viteae* and was purified at the University of Strathclyde by Drs Lamyaa Al-Riyami, Justyna Rzepecka and Felicity Lumb. Briefly, adult parasites were recovered from the jird, *Meriones libycus* and transferred to Petri dishes and cultured in RPMI medium (endotoxin free RPMI 1640 (Life Technology) with added glutamine (2 mM), penicillin (100 U/ml), streptomycin (100 µg/ml)). Larval forms were removed by filtering the conditioned medium with a 0.22 µm filter (Sigma). The ES-62-containing medium was then concentrated by ultracentrifugation (Millipore) units containing a YM10 membrane (Amicon) before purifying ES-62 using a sepharose column fitted to an isocratic fast protein liquid chromatography system (Pharmacia). The purity and identity of each batch were assessed by SDS-PAGE and the absence of endotoxins was confirmed using the Endosafe Kit (Charles River Laboratories).

2.3 CIA mouse model of RA

Male DBA/1 mice (8-weeks old) were used in the CIA model. Each mouse received on day 0, 100 µg of 2 mg/ml Bovine Type II collagen (CII; MD biosciences) emulsified with equal amount of complete Freunds adjuvant (CFA) containing 4 mg/ml of *Mycobacterium tuberculosis* (MD biosciences) injected intra-dermally just above the tail base. On Day 21, mice were administered 200

µg of type II collagen in PBS via intra-peritoneal injection[117]. Mice were monitored every two days for signs of arthritis, which was determined according to the following articular scores: 0 = normal; 1 = digit(s) involvement; 2 = erythema; 3 = erythema and swelling; 4 = extension/loss of function. For each mouse the total score was recorded, representing the sum of the severity scores of the 4 limbs. In addition, hind paw swelling was measured by callipers (POCO 2T, Kroeplin Längenmesstechnik).

For prophylactic regime treatment, ES-62 (2 µg) or the SMAs 11a and 12b (1 µg) in PBS were administered subcutaneously in the scruff on days -2, 0 and 21. Moreover, on a therapeutic regime injections of ES-62 (2 µg) and SMAs (1 µg) where injected subcutaneously every 3 days from the apparition of the first symptoms. Mice were sacrificed using CO_2. Paws were harvested and used for analysis of pathology or for SF and infiltrating inflammatory cell extraction and analysis.

All CIA models were managed and monitored in collaboration with Dr M.A. Pineda.

2.3.1 Hypoxia analysis

Ex vivo analysis of *in vivo* hypoxia status was realised by following the Hypoxyprobe^{TM}–1 plus kit protocols. Briefly, Pimonidazole HCl was dissolved in PBS at a concentration of 20 mg/ml and a dose of 60 mg/kg mouse body weight was injected intra-peritoneally (e.g. 1.5 mg/25 g mouse). The mouse was sacrificed 24 hours after the injection[118]. Paws were dissected and joint cells were extracted then fixed in chilled 70% ethanol and stored at -20ºC for 24 hours. Cells were then resuspended in PST (PBS with 4% serum and 0.1 % Triton) and stained in PST using the FITC-conjugated Mab1 (diluted 1:1000) antibody for 2 hours at 37ºC prior to analysis by flow cytometry.

2.3.2 Vasculature permeability analysis

To analyse vasculature permeability occurring *in vivo,* Evans blue dye (Sigma; 0.5% in PBS) was prepared and filter sterilized. Evans Blue solution (200 µl) was

injected intravenously in the mouse lateral tail. After 30 minutes the mouse was sacrificed and paws were collected[119]. Once the skin was removed from the paws, pictures were taken. Inflamed paws with vasculature permeability are stained blue by the dye while the healthy paws remain clear since the dye does not leak out of the vasculature (Figure 2-1).

2.3.3 Isolation and culture of SF

Isolation and culture of murine SF was performed according to the protocol of Armaka *et al*[120]. To summarize, once hind and front paws were recovered from the mice, skin was peeled and paws were washed using 100% ethanol and then in DMEM medium containing antibiotics (penicillin and streptavidin at 50 units/ml) before dissection and crushing of the joints. Fresh and filtered collagenase IV from *Clostridium histolyticum* (Sigma) was prepared (2 mg/ml) and an equal volume of collagenase was added to the ground joints to generate a final concentration of 1 mg/ml and incubated in a shaking waterbath at 37ºC for 1 hour. Following completion of the digestion incubation time, cells were released by vigorously vortexing the tissue samples. Cells were then resuspended in DMEM medium (Lonza), supplemented with 10% FBS, 2mM L-glutamine, 50 units/ml penicillin and 50 µg/ml streptomycin (denoted 10% FCS DMEM), and plated in 100 mm dishes. After 24 hours, non-adherent cells were removed and used for infiltrating cell phenotype analysis by flow cytometry. The medium was replaced twice weekly and once the cells reached 90% confluence, they were trypsinized and passaged. SF were expanded for 3 to 4 weeks before analysis. The phenotype of the explant fibroblasts was confirmed by flow cytometry as being $CD54^+$ $CD11b^+$ $CD90.2^+$ (Figure 2-2).

2.3.4 Histology

Paws harvested were fixed with 10% formalin, changing the fixative every day for one week. Bone decalcification, paraffin sectioning and staining with H&E or Trichrome solutions was realized with the assistance of Mr Jim Reilly of the Institute Histology Service. Briefly, bones were decalcified in hydrochloric

acid/formic solution (8% each) for a couple of days. Once decalcification was complete, acids were neutralized using an ammonia solution for 30 minutes. Bones were then washed under running tap water for 24 hours and were then ready for routine paraffin embedding and sectioning. In the H&E staining, hematoxylin is a violet stain that binds to basophilic substances such as DNA, therefore it is used to reveal nuclei in purple. Eosin is a red stain that binds to acidophilic substances such as positively charged amino acid side chains (e.g. lysine, arginine). It colours collagen in pale pink, cytoplasm in red, erythrocytes in cherry red and muscles in dark red. The trichrome staining reveals muscle fibres in red, collagen in green/blue and erythrocytes in orange.

2.4 Flow cytometry

Cells were seeded at a concentration of 0.5 x 10^6 cells per well in round bottom 96-well plates. Cells were washed three times with PBS at 400 x g for 5 minutes at 4ºC and then stained with the fixable viability dye eFluor®780 (eBioscience) at 1 µl/ml for 30 minutes at 4 ºC and protected from light. Cells were then washed three times with FACS buffer (PBS + 0.5% FCS 2mM EDTA) and Fcɣ receptors were blocked using 100 µl of hybridoma 2.4G2-conditioned supernatant containing CD16/CD32-specific antibody for 10 minutes at room temperature. Primary antibodies or their relevant isotype controls (Table 2-1) were added to the wells and incubated for 30 minutes at 4ºC, again protected from light. The cells were then washed 3 times with FACS buffer before incubation with the relevant secondary antibody or streptavidin-conjugated fluorophores where necessary. Cells were washed another 3 times with FACS buffer then passed through a nitex gauze into FACS tubes.

For intracellular cytokine staining, cells were first stimulated with 50 ng/ml PMA plus 500 ng/mg ionomycin (both Sigma-Aldrich) and after 30 minutes incubation at 37ºC, 10 µl/ml of Brefeldin A (Sigma-Aldrich) was added for a further 5 hours incubation at 37ºC with 5% CO_2. Then after staining for surface antigens, 100 µl of Fixation buffer (Biolegend) was added to the cells for 20 minutes at room temperature. Cells were then washed in permeabilization buffer (eBioscience) 3 times. Intracellular staining was realised by incubation with appropriate

antibodies in permeabilization buffer in the dark at room temperature for 20 minutes. Then cells were washed 3 times with FACS buffer and passed through a nitex gauze into FACS tubes.

All samples were acquired using the BD LSR II and analysed by FlowJo. In the flow Jo analysis program when result graphs are presented as overlays, the Y-axis is presented as percentage of maximum (% of Max) as opposed to cell number. This is useful if the two experiments overlaid have different cell counts as it allows normalization and direct comparison of the data.

2.5 ELISAs

Cytokine secretion was measured using the relevant ELISA kits as instructed by the manufacturers. Cells were plated in 96-well plates or in 6-well plates (Corning) at respectively 1 x 10^4 and 0.3x10^6 cells per well. After an overnight incubation in DMEM medium containing 1% FCS (1% FCS DMEM) to synchronize the cells, the FCS was increased to 10% (10% FC DMEM) and the cells were stimulated for 24 hours with LPS (1 µg/ml, Sigma-Aldrich), BLP (Pam_3Cys-Ser-$(Lys)_4$; 0.5 µg/ml, Enzo), IL-1ß (10 ng/ml, Immunotools), IL-17 (25 ng/ml, Immunotools), IL-22 (25 ng/ml, Immunotools) or IFNß (10 ng/ml R&D systems). Supernatant was collected and analysed using ELISA kits detecting IL-6, CCL-2 and IL-1ß (Ready-SET-Go!® from eBioscience). Briefly, 96-well plates were coated overnight with the relevant capture antibody. Wells were then blocked for an hour, and samples and standards were added to the plate for incubation overnight at 4ºC or 2 hours at room temperature. Samples were washed and incubated with detection antibody for a further 1 hour and then streptavidin conjugated horseradish peroxidase was added for 30 minutes. Plates were then washed a final time prior to being incubated with TMB substrate and then once colour developed, stop solution (1M H_2SO_4) added. Absorbance was read at 450nm using a Tecan Sunrise plate reader.

2.6 FACE assays

Fast-activated cell-based (FACE) ELISA assays were performed as developed and described previously by Versteeg *et al*[121] Cells were plated and synchronised by 1% FCS DMEM overnight in 96-wells plate at 1 x 10^4 cells per well. Cells were then stimulated for the indicated time points (from 0 to 120 minutes) before being treated with fixative buffer (Biolegend) according to the manufacturer recommendations. Once the cells are permeabilized, an ELISA-like protocol is followed e.g. using as detection antibodies, antibodies specific both for ERK and the dually phosphorylated active form of ERK (P-ERK) (Cell Signalling Technology) for 1 hour before addition of streptavidin-conjugated horseradish peroxidase for 30 minutes (anti-rabbit HRP, Cell Signalling Technology). Plates were then washed a final time and incubated with TMB substrate for approximately 15 minutes before addition of stop solution (1M H_2SO_4). Absorbance was read at 450 nm using a Tecan Sunrise plate reader.

2.7 Western blots

Cells were plated at 1x10^6 cells per well in 6-well plates and synchronised overnight in 1% FCS DMEM before being treated for 24 hours (or the indicated time) with various inflammatory stimuli: LPS (1 µg/ml, Sigma-Aldrich), IL-1ß (10 ng/ml, Immunotools), IL-17 (25 ng/ml, Immunotools), IL-22 (25 ng/ml, Immunotools) or IFNß (10 ng/ml R&D systems). After stimulation, cells were washed twice with cold PBS, and cells pelleted. Cells were lysed by addition of 100 µl of RIPA buffer (50 nM Tris buffer (pH 7.4) containing 150 mM sodium chloride, 2% (v/v) NP40, 0.25% (w/v) sodium deoxycholate, 1 mM EGTA, 1x Halt™ protease inhibitor and 1x Halt™ phosphatase inhibitor (Pierce)) and incubation for 30 minutes on ice. Lysed cells were then centrifuged at 16,000 x g for 15 minutes at 4ºC and the supernatant containing the solubilised proteins kept with protein concentration measured by the BCA protein assay kit (Pierce). Proteins (20 µg) were mixed with 4 x loading buffer (Novex, life technologies) and 10 x reducing agent (Novex, life technologies) then incubated for 10 minute at 70ºC to denature the proteins. Proteins were separated by gel electrophoresis, on 4-

12% Bis-Tris gradient gels, using the NuPAGE Novex system (Invitrogen). Gels were run in NuPAGE MOPS buffer, with addition of antioxidant, at 180V until the protein bands reach the bottom of the gel. Proteins were then transferred onto nitrocellulose membranes (GE) using the wet transfer NuPAGE system. Quality of the transfer was assessed using Ponseau red staining (Thermo scientific). The membrane containing the proteins was then washed with TBS-T (0.5 mM sodium chloride, 20 mM Tris-HCl (pH7.4) and 0.1% (v/v) Tween-20). Membranes were blocked for 1 hour in 5% non-fat milk protein in TBS-T and then incubated with the primary antibody in 5% BSA TBS-T overnight at 4ºC. The list of primary antibodies used in this study is presented in Table 2-2. After washing 3 times with TBS-T, the relevant secondary antibody conjugated with HRP was added in 5% milk for 1 hour at room temperature. After a final 3 washes in TBS-T, ECL Western blotting substrate (Thermo Fisher Scientific) was added for 1 minute then exposed to X-ray film (Kodak). Membranes were stripped using Restore Western Blot stripping buffer (Thermo Fisher Scientific) for 1 hour for further reuse and conserved in TBS-T.

2.8 mRNA and miRNA analysis

Total RNA and miRNA were isolated and separated using the miRNeasy kit (Qiagen) following the manufacturer's instruction. For miRNAs, the miScript Reverse Transcription Kit (Qiagen) was used for cDNA preparation. miScript SYBR green qPCR kit (Qiagen) and miScript primer assay (Qiagen) were used for semi-quantitative determination of the expression of mouse miR-19b-1 (MS00005915), miR19b-1* (MS00024493), miR-19b-2* (MS00024500), miR-23b-2 (MS00032606), miR-24-1* (MS00011543), miR-34a (MS00001428), miR-124*(MS00011081), miR-125a (MS00001533) miR-146 (MS00001638), miR-155 (MS00001701), miR-203 (MS00001848), miR-203* (MS00011452) and miR-346_2 (MS00032753). The expression of Hs-RNU6-2_11 (MS00033740) was used as endogenous control[122].

For mRNAs, retrotranscription was realized using the high capacity cDNA reverse transcription kit (Invitrogen) and qPCRs were performed using Taqman® gene expression assay kits, with all primers obtained from Life Technologies. The following genes were studied CCL2 (Mm00441242_m1), DNMT1 (Mm01151063_m1), DNMT3a (Mm00432881_m1), GAPDH (Mm03302249_g1), IL-6

(Mm00446190_m1), IFNβ (Mm00439552_s1), MMP9 (Mm00442991_m1) and MMP13 (Mm00439491_m1).

2.9 DNA methylation analysis and induction of DNA demethylation

2.9.1 Measurement of global DNA methylation

Global DNA methylation levels can be determined via the measurement of methyl cytosine levels using specific antibodies. Briefly, genomic DNA was extracted from cells (PureLink Genomic DNA Mini Kit, Invitrogen) and methyl cytosine levels assessed following the manufacturer's instructions (Imprint® Methylated DNA Quantification Kit-Sigma). Thus, genomic DNA was added to the wells and left to adhere for 2 hours before methyl cytosine was detected by the primary antibody (mouse anti-methyl cytosine antibody), and revealed by a secondary HRP-conjugated antibody and its tetramethylbenzidine (TMB) Substrate Solution. Reactions were stopped and Absorbance values read at optical density (OD). Those OD values were used to compare levels of global methyl cytosine in the various samples.

2.9.2 Inducing DNA demethylation with the DNMT1 inhibitor 5-azacytidine

First synthesized about 40 years ago, 5-azacytidine is a commonly used drug that exhibits many anti-metabolic activities and in particular is used as chemotherapy for cancers such as myelogenous leukemia[123]. Mechanistically, 5-azacytidine is a commonly used DNMT1 inhibitor that induces global DNA demethylation. SF treatment with 5-azacytidine was realised according to previous publications[124,125]. Fibroblasts were first synchronized overnight in 1% FCS DMEM and then cultured for 7 days with DMEM - 10% FCS and 5-azacytidine (1 μM, Sigma-Aldrich). The media was changed everyday. After one week, global methyl cytosine was substantially reduced (Figure 2-3).

2.9.3 *In vitro* treatment with cytokines for the induction of global DNA demethylation

SF were first synchronized overnight in 1% FCS DMEM and then cultured for 14 days in 10% FCS DMEM and stimulated daily with the following cytokines. IL-1ß was used at 1 ng/ml, IL-17 at 2.5 ng/ml and IL-22 at 2.5 ng/ml (all Invitrogen) (these chronic exposure studies used concentrations of stimuli10 times less than those typically used for acute functional inflammatory response assays over 24 hours stimulation). This protocol follows that published for SF from RA patients using IL-1ß *in vitro* to induce global DNA demethylation[126].

2.10 Statistical analysis

All statistical analyses were performed using Prism software (GraphPad Software). For data sets with two groups: parametric data were analysed using the one-tailed Student's t-test; for the analysis of non-parametric data, the Mann-Whitney test was used. For data sets with more than 2 groups, one-way ANOVA analysis with Tukey's post-test was used and in experiments where two variables were measured, the two-way ANOVA test was used with the Tukey's post-test. Statistical significance is shown as *=$p<0.05$, **=$p<0.01$ and ***=$p<0.001$.

Figure 2-1 Vasculature permeability assay using Evans Blue dye reveals vasculature leakage in the joint during CIA induced inflammation.

Evans Blue dye binds to albumin: thus, healthy vasculature, which is impermeable to albumin, will retain the dye. However, once vasculature permeability is induced during pathological conditions such as inflammation, proteins such as albumin leak into the local tissue. Therefore, the Evans blue dye allows clear visualisation of the location of leakage *in vivo*. Here, it is clear that the inflammation induced during CIA drives vasculature leakage in the joint, as revealed by the blue staining of the tissue in the paw with CIA (score 4) relative to the healthy control (score 0).

Healthy Vasculature leakage

Score 0 Score 4

Figure 2-2 Strategy for phenotyping SF according to Armaka *et al*[120]

After extraction from the paws and expansion in culture, SF were confirmed as being positive for CD54 (ICAM-1), CD106 (VCAM-1) and CD90.2 (Thy1.2). Positive staining (black) is shown by reference to the relevant isotype control represented in grey.

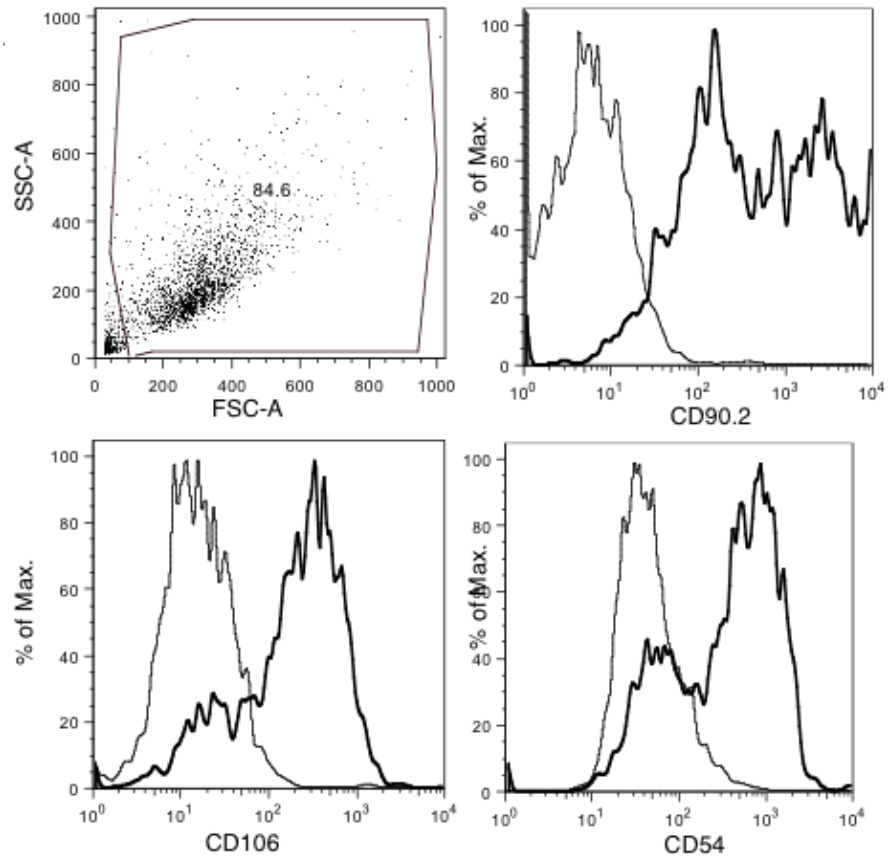
SSC-A
FSC-A
84.6
% of Max.
CD90.2
% of Max.
CD106
% of Max.
CD54

Table 2-1 List of FACS antibodies used in this study

Antigen	Fluorophores	Clone	Source	Concentration used (µg/ml)
CD11b	FITC	M1/70	eBioscience	5
CD11b	PerCP	M1/70	Biolegend	2
CD3	Pacific Blue	UCHT1	Biolegend	5
CD4	Biotin	H129.19	BD biosciences	5
CD54	PE	YN1/1.7.4	Biolegend	2
CD8	APC	53-6.7	Biolegend	2
CD8	FITC	53-6.7	BD biosciences	5
CD90.2	PerCP	30 H12	Biolegend	2
GR1	biotin	RB6-8CR	Biolegend	5
IFNγ	PeCy7	XMG1.2	BD biosciences	2
IL-17	APC	TC11-18H10.1	Biolegend	2
IL-22	PE	1H8PWSR	eBioscience	2
Mab-1	FITC/HRP	4.3.11.3	Hydroxyprobe	5
methyl-cytosine	none	polyclonal	Novux biologicals	30

Table 2-2 List of Western blot primary antibodies used in this study

Antigen	Source	Concentration used (µg/ml)
DNMT1	Cell signaling	1:1000
DNMT3a	Cell signaling	1:1000
SOCS1	Abcam	1:5000
SOCS3	Abcam	1:1000
ERK	Cell signaling	1:2000
P-ERK	Cell signaling	1:2000
STAT1	Cell signaling	1:1000
P-STAT1	Cell signaling	1:1000
STAT3	Cell signaling	1:1000
P-STAT3	Cell signaling	1:1000

Figure 2-3 5-azacytidine treatment efficiently induces global DNA demethylation.

The DNMT1 inhibitor, 5-azacytidine, was added (at 1 µM daily for 7 days) to bone marrow derived macrophages. Since DNMT1 is inhibited, the cells dividing are no longer able to maintain their global DNA methylation status leading in the = long term to global DNA hypomethylation. Here, the level of methyl-cytosine expression was revealed by staining with a anti-methylcytosine antibody (Novus Biologicals) and counter-staining of the nucleus revealed by DAPI staining. After 7 days treatment with 5-azacytidine, a strong global DNA demethylation is observed. Data are represented as merged for DAPI (red) and methyl cytosine (green) and individual staining for methyl cytosine is as well represented in grey scale for more clarity.

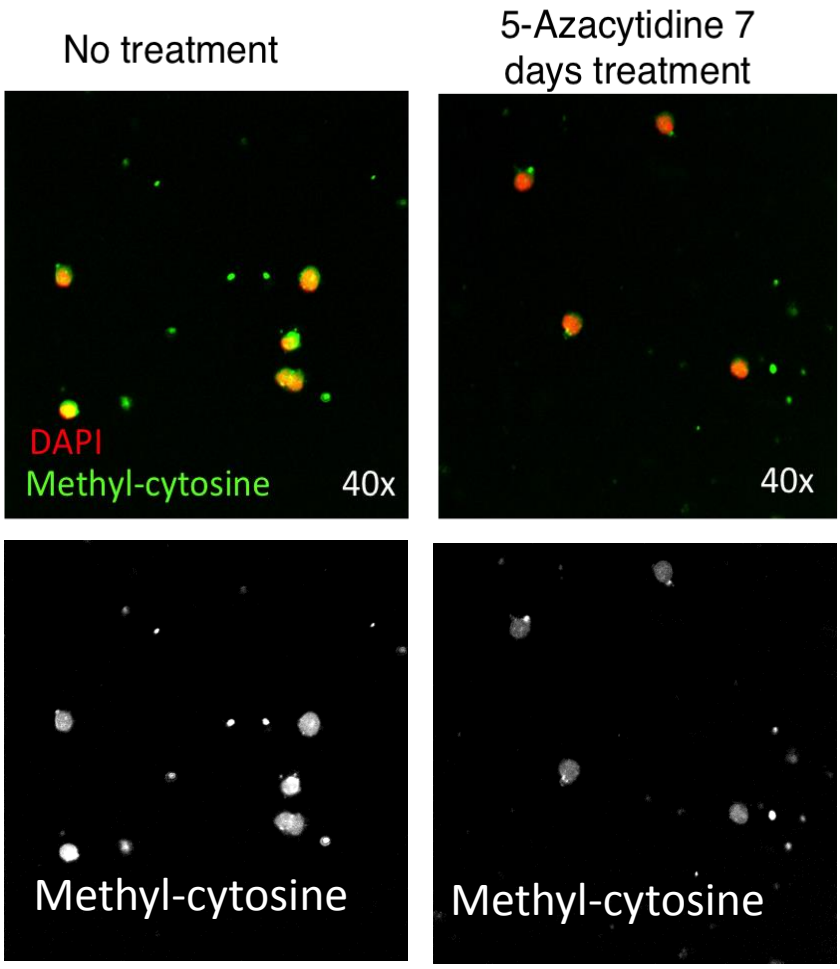
No treatment
5-Azacytidine 7 days treatment
DAPI
Methyl-cytosine
40x
40x
Methyl-cytosine
Methyl-cytosine

3. ES-62 and its SMAs prevent the development of CIA

3.1 Introduction

Research investigating the host-parasite relationship has revealed the potential of immunomodulators produced by helminths to modulate the host immune system. Such molecules are the result of long co-evolution that has enabled the parasite to safely downregulate inflammation to avoid being attacked without inducing immunosuppression, therefore maintaining the host's ability to react against other infections. Those molecules are particularly interesting in terms of their potential as therapeutics in autoimmune disease since on the one hand there is a close relationship between the absence of parasite and the rise of autoimmune disorders as explained by the Hygiene Hypothesis[98,127,128], whilst on the other hand, most therapies for autoimmune disorders, like RA, are strongly immunosuppressive, placing patients at risk[129]. ES-62 is a helminth immunomodulator produced by the filarial nematode *Acanthocheilonema viteae,* that is the best-characterized helminth immunomodulator to date[98]. It has already provided proof of concept of the therapeutic potential of such molecules as indeed, ES-62 protects against the development of CIA, OVA-induced airway hypersensitivity and lupus development in mice[101,104,113]. ES-62 protects against CIA development through modulating Th17/Th1 priming and effector responses[104]. Importantly, as ES-62 is itself unsuitable as therapy not only because of its size, ES-62 is a 62 kDa protein secreted as a tetramer, but as well because of its phosphoryl choline moiety found in various peptides such as bacterial peptides. Therefore, the SMAs of ES-62, 11a and 12b have been shown to be protective in various model of autoimmune disease and allergies and as well as displaying therapeutic potential in CIA[103,113,114,130-132]. Moreover, investigation of the mechanisms by which ES-62 and its SMAs protect against CIA has brought new insight to our understanding of RA disease pathogenesis, particularly in terms of the importance of IL-22, IL-17 and IL-1β[104,114,133].

Nevertheless, the pathway(s) to pathogenesis is still not fully understood and therefore in this chapter, the therapeutic potential of ES-62 and its SMAs, especially 12b, is further explored in the mouse CIA model to reveal new characteristics of the protective mechanisms of ES-62 and 12b, in particular in reducing the aggressive phenotype of SF.

The SF is the major cell population found in the joint and over the last decade the importance of this cell type in the development, spread and maintenance of pathogenicity has been proven[134,135]. Once activated, SF seem to play a key role not only in the perpetuation of inflammation but also in driving the bone and cartilage damage. Therefore, they represent an excellent therapeutic target since controlling their aggressiveness would enable modulation of the two main clinical symptoms of RA, namely joint inflammation and bone destruction. Such a target might provide new therapies for patients not responding to the usual treatment of systemic suppression of immune responses[3] as well as, and more importantly, safer and cleaner strategies since this cell population is specific to the joint avoiding bone marrow suppression, which at present is a major cause of mortality associated with current therapies.

The specific aims of this chapter are therefore to confirm and extend the initial observations[104,133] that ES-62 can act to dampen down the aggressive phenotype of SF, In particular, the objectives were to:

- Characterise the protection afforded by ES-62 and 12b in the CIA model, particularly in terms of reducing joint infiltration by pro-inflammatory cells and consequent bone degradation.
- Investigate whether the protection provided by ES-62 and 12b treatment is associated with modulation of the pathogenic features of SF, namely the capacity to produce mediators of inflammation and bone destruction.

3.2 Characteristics of CIA joint pathology

Understanding the pre-clinical onset of the disease is key to diagnosing and treating patients to prevent disease. However, it is not possible to understand the mechanisms resulting in the increase in ACPAs (Anti Citrullinated protein antibody) and rheumatoid factor and consequent pathogenesis in patients with established disease, retrospectively. Thus relevant experimental animal models are essential and necessary in order to understand the various mechanisms, pathways and kinetics that need to be further explored to reveal potential therapeutic and diagnosis targets in RA. Moreover, even when human tissues are useful in defining important ongoing pathways their use remains limited, as relevant tissue such as bone marrow, spleen or lymph nodes are not generally and ethically obtainable, and even for synovial tissue, the targeted lesion is not always available. Various animal models have therefore been developed to recapitulate different aspects of the disease and include both induction or spontaneous, genetically-modified arthritis models that offer different advantages[136,137]. Nevertheless in this thesis, the focus has been on CIA as it is not only one of the most commonly used animal models but also because it is considered the gold standard, since it recapitulates many aspects of RA[138]. CIA in mice relies on an induced break in self-tolerance which is dependent on both B and T cell responses and produces collagen-specific autoantibodies and inflammation such that the animals develop an acute asymmetric polyarthritis characterized by synovial infiltration, synovial hyperplasia, cartilage and bone erosion. CIA initiation is associated with the production of anti-type II collagen IgG, reflecting that in patients disease is associated with the production of autoantibodies against self type II collagen as well as citrullinated proteins (inducing ACPAs) and IgG (inducing the rheumatoid factor). Indeed, serum transfer from a CIA mouse is able to induce arthritis in naive mice, revealing the importance of humoral immunity for the initiation of pathogenesis and confirms the hypothesis that type II collagen might be an important autoantigen[138,139]. The most common mouse strain used for CIA is DBA/1, although to allow easier assessment of the effect of genetic modification on disease development, C57BL/6 mice can also be used.

In this thesis, CIA mouse model was used to assess the prophylactic and therapeutic potential of ES-62 and its SMA. Under our animal house conditions, the first joint symptoms begin to appear after challenging the mice at day 21 (with collagen type II) such that by day 30 mice will typically have an average clinical score of 4.7 ± 1.48 (SEM) with, approximately 60 % of mice displaying affected joints and amongst these, 50 % will be characterized as exhibiting a serious clinical score, as indicated by a total articular score ≥4 (Figure 3-1). This model recapitulates various key features of RA such as joint infiltration by polymorphonuclear and mononuclear cells, synovitis and pannus formation leading to bone and cartilage degradation as revealed by immunohistochemistry of joint sections using H&E and trichrome staining (respectively Figure 3-2A and

Figure 3-2B). Here, immune cell infiltration and pannus formation is clearly visualised by H&E and trichrome staining as well as some cartilage and bone degradation being clearly visible in the trichrome stained sections. One of the main contributors to this influx of hyperactive immune cells is the local loss of vasculature integrity, which facilitates cell infiltration. To measure such potential vasculature permeability, mice were injected with Evans Blue, a non-toxic dye commonly used to inspect vasculature leakage (

Figure 3-2C). It is injected into the tail vein prior to cull and vasculature leakages are immediately detected by a blue coloration of the tissue. Here a preliminary study was performed to evaluate the relationship of this experimental protocol to articular score. The inflamed paws were clearly stained in blue indicating localized vasculature leakage and the importance of the vasculature leakage and the multiplication of leakage sites correlated with the clinical score.

3.3 Aggressiveness of SF during CIA

SF from naïve (naive fibroblasts) and CIA (CIA fibroblasts) mice can be extracted and cultured *ex vivo* for up to 4-5 weeks. As such cells are therefore isolated from their pro-inflammatory environment; this enables assessment of whether the cells are intrinsically rewired or simply responding to the pro-inflammatory milieu. This approach has suggested that it appears that CIA fibroblasts are intrinsically different to naïve cells, since over this time in culture they retain at least some of their aggressive features in terms of maintaining hyper-production of mediators of inflammation and bone degradation[43]. Indeed, their capacity to produce pro-inflammatory cytokines, such as IL-6, or chemokines, such as CCL2, remains significantly higher compared to that of cells from naive mice even after 4 weeks *ex vivo,* even in the absence of external stimuli (Figure 3-3A and Figure 3-3B, respectively). Moreover, it seems that the hyper-secretion of such molecules in the absence of external stimulation is directly regulated at the gene expression level since the mRNA levels of IL-6 and CCL2 are similarly significantly increased in CIA fibroblasts compared to the naïve cells (Figure 3-3C and Figure 3-3D respectively). Furthermore, CIA fibroblasts, even once isolated *ex vivo,* still exhibit an enhanced capacity to induce tissue and bone destruction as they display a significantly higher expression of MMP9 mRNA in the absence of stimulation and more MMP9 and MMP13 mRNA in response to IL-17 (Figure 3-3E, Figure 3-3F respectively), a key pathogenic mediator in the joint[105].

3.4 ES-62 and 12b prevent development of CIA

3.4.1 Prophylactic treatment with ES-62 protects against CIA in DBA/1 mice

ES-62 is a homotetramer, comprising 62 kDa PC-containing glycoprotein subunits, that exhibits various immunomodulatory properties on a number of cell types, resulting in anti-inflammatory activities conferring its therapeutic potential in models of allergic or autoimmune disorders such as asthma or RA[104,140,141]. It has been previously shown that in the CIA model of RA, treatment with ES-62, both prophylactically and therapeutically, significantly reduces CIA disease severity[104,117]. ES-62-mediated protection is associated with the downregulation of IL-17 responses achieved by targeting dendritic cells and the IL-17-producing Th17 and γδ T cells resulting in decreased level of the pro-inflammatory cytokine IL-17 in the joint[104]. Complementing this action, more recently it has been demonstrated that ES-62 upregulates the levels of IL-22 in the joints during established disease, and this appears to be crucial for the protective effect of the parasite molecule[142]. At the time, this was a rather surprising finding as IL-22 had previously been shown to be pathogenic in the early stages of the disease[133]: however, as ES-62 acted to dampen IL-22 responses during the initiation phase, these studies were amongst the first to identify that IL-22 plays a dual role during CIA, also being involved in the normal homeostatic inflammation resolution and tissue repair process once disease has been established. ES-62 is therefore protective in CIA by both downregulating pathogenic IL-17 responses and promoting the inflammation resolution potential of IL-22.

Corroborating the published findings that prophylactic treatment with ES-62 reduces joint inflammation and prevents development of CIA, here exposure to the parasite product reduces both articular score (Figure 3-4A) as well as disease incidence (Figure 3-4B), with about half of PBS-treated disease control CIA mice (CIA) presenting with severe arthritis (articular score ≥4) (Figure 3-4C) whilst most of the mice undergoing CIA but treated with ES-62

(≥80%) exhibited low or no disease scores. Reflecting the low clinical scores of ES-62-treated CIA mice, joint sections stained with H&E and trichrome reveal suppression of pro-inflammatory cells infiltration and bone degradation (Figure 3-2). As the inflammation and tissue damage occurring in CIA mice induces hypoxia that can create a pro-arthritogenic environment and perpetuates pathology in the joint[143], preliminary experiments were carried out to assess the joint microenvironment pertaining in naive, CIA and ES-62 mice *in vivo*. To this end, hypoxia levels in cells from the joints were assessed using a hypoxia-sensing probe, the drug pimonidazole that had been injected intraperitoneally 24 hours before culling the mice. Once activated in an oxygen-dependent manner *in vivo*, pimonidazole will bind covalently to thiol-containing proteins specifically in hypoxic cells. Thus, following isolation *ex vivo*, cells containing pimonidazole can be detected by flow cytometry using a FITC-conjugated monoclonal antibody specific for the probe (M & M section 2.3.1). Joint cells extracted from CIA, ES-62 and naïve mice were pooled by treatment group and analysed for pimonidazole staining (Figure 3-5A). It revealed two clear populations, with some cells displaying low levels of pimonidazole yet others displaying stronger staining indicative of a higher hypoxic state. Focusing on the cells exhibiting higher levels of hypoxia, it appears than there are more "high hypoxic" cells derived from CIA, compared to ES-62 mice (Figure 3-4E), consistent with the ES-62-mediated suppression of pro-inflammatory cells infiltrating the joint contributing to this decrease in local hypoxia.

During arthritis many inflammatory cell types are found infiltrating the joint, including B and T lymphocytes as well dendritic cells, macrophages or granulocytes, particularly neutrophils. Once in the joint they participate in the maintenance of the pro-inflammatory environment by secreting cytokines and chemokines contributing to joint swelling and inflammation and also to bone and cartilage damage. It has previously been shown that exposure to ES-62 reduces the levels of plasma cells as well as neutrophils infiltrating the joint[144]. Further analyses of these joint cells now shows that ES-62-treated mice with CIA also demonstrate a lower infiltration (Figure 3-5B) of the two major T cell subpopulations, CD8+ cytotoxic CT cells and CD4+ helper T cells,

data pertinent to the previous studies showing that ES-62 protects from CIA by inhibiting both the Th1 and Th17 subsets of CD4 T cells[104].

3.4.2 Therapeutic potential of the SMAs

ES-62, as a potentially immunogenic protein, is probably unsuitable for use as a therapeutic treatment as explained earlier due to its PC moiety and the large protein size and therefore as the PC moiety of ES-62 is responsible for the protective effect of the parasite product in CIA, a library of drug-like SMAs modelled on the PC moiety has been designed and synthesised as the first step in the development of a novel class of anti-inflammatory drugs. A primary *in vitro* screen of macrophage cytokine production identified two SMAs, 11a and 12b that are able to recapitulate ES-62 protection in various models of autoimmune (CIA[114,132] and the MRL/Lpr model of SLE[113]) and allergic (the OVA-induced model of asthma[103] and the oxazalone-model of skin contact dermatitis[130]) inflammatory disease. Rather surprisingly, our recent data showed that whilst both SMAs protect against CIA, they do so by targeting different mechanisms associated with ES-62-mediated immunomodulation, with 11a mimicking its ability to suppresses pathogenic IL-17/IFNγ responses whilst 12b downregulates the inflammasome and IL-1β production in the joints of mice with CIA by inducing NRF2-regulated anti-oxidant cytoprotective pathways[114]. Since IL-17 and hypoxia/ROS have been reported to act on SF to promote chronic inflammation in the arthritic joint, it was thus decided to investigate whether the SMAs acted like ES-62 to effect resolution of inflammation in the joint and investigate their effect on SF during CIA.

Importantly, given that one of the main interests of the Harnett labs is to determine whether the SMAs 11a and 12b can be developed as potential therapeutics for inflammatory arthritis, the effects of the SMAs on mice with established arthritis were tested, with reference to the steroid methotrexate (MTX), a common treatment for patients with RA (Figure 3-6). Like ES-62[117] and MTX[145], even when administered therapeutically after onset of disease,

11a and 12b act to suppress further disease progression[114] (Figure 3-6 A-B). The parasite-derived immunomodulators are therefore efficient at both preventing development of inflammation and also suppressing further progression once disease is established[114,132]. Importantly, this study now shows that such protection is also associated with desensitisation of pro-inflammatory SF responses. Indeed, SF derived from CIA mice treated therapeutically with SMAs showed a lower basal production of IL-6 as well as that in response to BLP but not LPS or IL-1ß, relative to those from PBS-treated CIA mice (Figure 3-6C). Reflecting its immunosuppressive nature, exposure to MTX inhibited responses to all stimuli, whereas the SMAs act to dampen MyD88 and inflammasome signalling which might render them less able to antagonise LPS (but not BLP) responses as these may be compensated by the MyD88-independent pathway of TLR4 signalling whilst IL-1ß could potentially acutely overcome 11a and 12b protection.

3.4.3 IL-1β overcomes the protection afforded by ES-62 and 12b in CIA mice

In order to address validating that 12b confers protection by suppression of IL-1β responses, it was investigated whether administration of IL-1ß was able to overcome the protective effects of prophylactic administration of 12b (Figure 3-7A). This study confirmed our previous findings[114] with the clinical articular score and paw swelling of mice treated with 12b being significantly decreased (Figure 3-7B and Figure 3-7C, respectively). Moreover, whilst a 50% incidence of disease in the CIA cohort of mice was reached by day 23, none of the CIA-12b mice exhibited pathology at this stage with a level of 28.5 % incidence only being reached for this group at cull on day 29 (Figure 3-7D). Administration of recombinant murine IL-1ß *in vivo* was found not only to abolish 12b-mediated protection, but even to enhance disease clinical score, paw width (Figure 3-7B and Figure 3-7C, respectively) with disease incidence up to 66.7% in the CIA + IL-1ß and 75 % in the 12b + IL-1ß groups (Figure 3-7D). Such findings are corroborated by histopathological examination demonstrating reduced cell infiltration and bone degradation associated with

12b protection (Figure 3-8), which is completely abrogated by co-administration of IL-1ß, as this drives a massive cell infiltration and stimulates bone destruction in such 12b-treated mice. There is however no evidence of enhanced bone destruction or cell infiltration induced in the joints of IL-1ß CIA mice compared to those of CIA mice with equivalent articular scores of 4 suggesting that the administration of IL-1β is not simply creating damage *per se*. Likewise, the visible increase in infiltrating cells observed in 12b+ IL-1β mice do not reflect an increase in cytotoxic T cells (CD3+ CD8+) or helper T cells (CD3+ CD4+), since the reduction of such cell populations within the joint induced by 12b was further enhanced by the presence of IL-1ß. Although this may simply reflect that other cell populations such as neutrophils are greatly expanded under these conditions, administration of IL-1ß did increase the proportions of those T cells populations in the CIA mice (Figure 3-9). Thus as IL-1β is important for the differentiation and maintenance of Th17 cells, this apparent decrease in the T cell population may reflect disruption of homeostatic networks since the change in the IL-1ß levels are likely to be more pronounced in 12b than in the CIA mice. It may therefore, reflect the IL-1β-mediated induction of Bregs (regulatory B cells) and consequent inhibition of pathogenic Th responses observed recently in the antigen-induced model of arthritis following perturbation of the gut microbiome[146,147]. Thus it would be important to establish whether the increased cellular infiltration observed in the joint sections more likely reflects other cell type known to infiltrate the joint like Bregs or neutrophils [148,149].

Even though ES-62 has not been shown to strongly inhibit IL-1ß production, but rather mainly act through inhibition of IL-17 and rewiring of IL-22 responses[133,134,150], it was interesting to assess whether IL-1ß could also overcome the protection afforded by ES-62 *in vivo*. This revealed that IL-1ß can indeed overcome ES-62 protection and, as observed above in the 12b study, co-administration resulted in the induction of even higher articular scores as well as increased levels of paw swelling and disease incidence than observed in the CIA + IL-1ß cohorts of mice (Figure 3-7). Again, these findings were supported by the histopathological analysis, as the exposure to IL-1ß totally abrogated the absence of cell infiltration and bone destruction

exhibited in sections derived from CIA mice afforded protection by ES-62 (Figure 3-8). Moreover, like with 12b, T cell infiltration induced by IL-1ß in the joint was as well supressed in an ES-62 context and such reduction of T cell infiltration was even stronger than for ES-62 treated mice alone (Figure 3-9).

3.5 ES-62 and 12b modify the aggressiveness of SF during CIA

During RA, or in the murine CIA model surrogate, a cocktail of pro-inflammatory signals, such as IL-17, IL-6, CCL2 and TNF-α, perpetuate inflammation in the joint. Although these mediators will be produced predominantly by the lymphocytes, neutrophils and monocytes invading the joint, some of these will also be generated by SF as these cells are able to sense the pro-inflammatory environment and can be activated via TLRs or cytokine receptors[134,150]. Thus, in turn, they produce a wide range of pro-inflammatory factors and chemokines that maintain the pro-inflammatory environment and recruit more immune cells to the joints. Consistent with this, exposure of mice undergoing CIA to ES-62 *in vivo* has previously been reported to suppress pro-inflammatory (IL-6) responses of SF[104].

These findings were confirmed and extended here by analysis of the functional responses of SF derived from naive, CIA or ES-62-treated CIA mice (Figure 3-10). Thus, measurement of their capacity to generate pro-inflammatory mediators *ex vivo* again confirmed that SF from mice with CIA exhibit a hyperactive phenotype (Figure 3-10). However, it revealed a significant decrease in spontaneous IL-6, but not CCL2, release by SF from ES-62 (ES-62) relative to PBS (CIA) treated mice undergoing CIA: indeed, exposure to ES-62 resulted in SF that exhibit responses comparable to those of SF derived from naive mice. This cytokine and chemokine release by all three groups of SF was strongly stimulated by subsequent exposure *in vitro* to IL-1β, LPS and particularly, BLP (bacterial lipoprotein), the latter likely reflecting the proposed key pathogenic role for TLR2 signalling in the joint in

RA[150]. Nevertheless, the SF derived from CIA mice still showed enhanced IL-6 (to all 3 stimuli) and CCL2 (IL-1β and LPS) responses relative to SF from naive mice, whilst those from CIA mice exposed to ES-62 *in vivo* were no different to those from healthy mice. These data suggested that exposure to ES-62 in vivo can suppress development and/or maintenance of an aggressive SF phenotype in mice undergoing CIA.

Exposure to 12b in vivo seems to be if anything even more efficient at suppressing the aggressive phenotype of SF as cells from such mice showed significantly decreased ability to produce, spontaneously or after stimulation with LPS or IL-17, either IL-6 and CCL2 relative to those from CIA mice (

Figure 3-11). Moreover, such dampening of SF aggressiveness occurs at the level of gene expression as the decreased release of IL-6 and CCL2 resulting from exposure to either ES-62 or 12b is mirrored by significant reductions in the mRNA levels of both IL-6 and CCL2 (Figure 3-12). Likewise, SF extracted from CIA mice treated with ES-62 displayed a significant decrease in the expression of both MMP9 and MMP13, gene products responsible for bone and cartilage degradation (

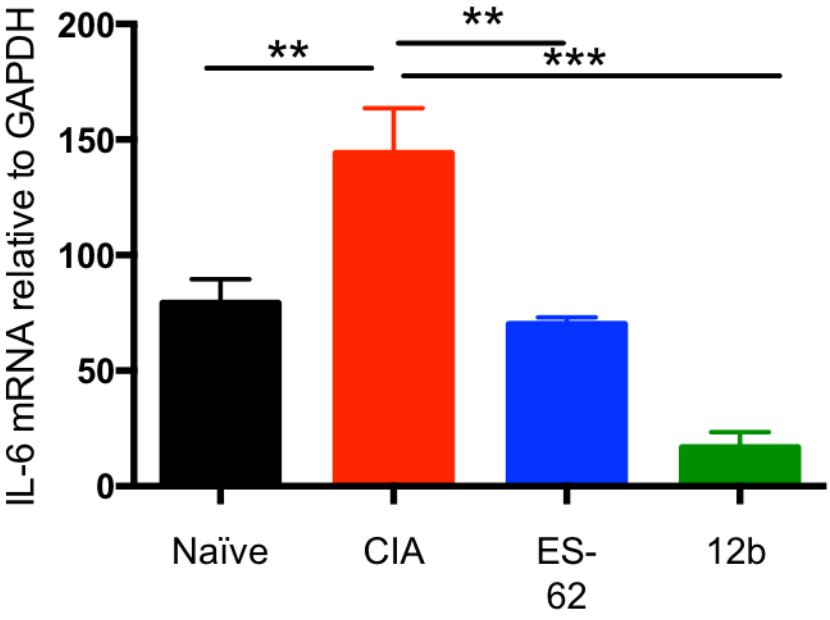
IL-6 mRNA relative to GAPDH
200
150
100
50
0
**
**
***
Naïve
CIA
ES-62
12b

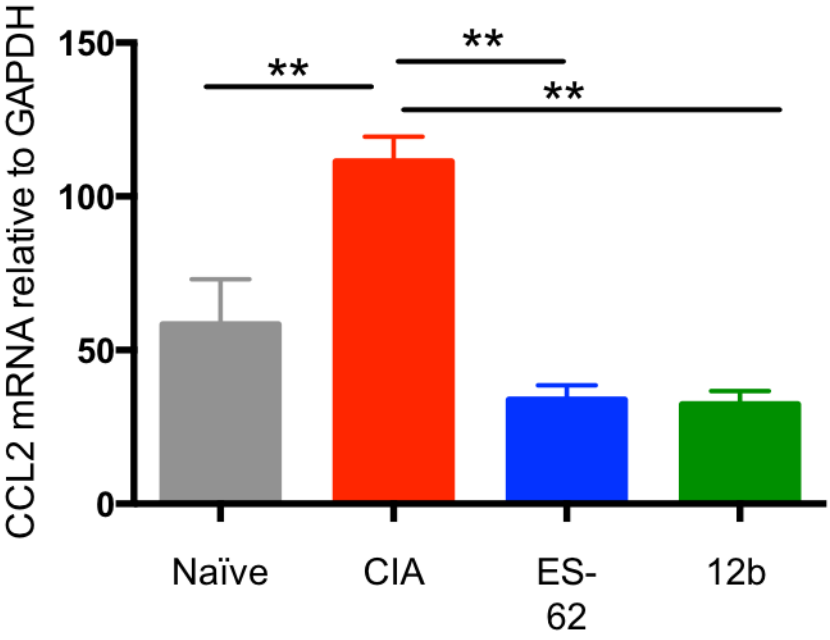
CCL2 mRNA relative to GAPDH
150
100
50
0
**
**
**
Naïve
CIA
ES-62
12b

Figure 3-13): indeed, the cells from ES-62-treated mice are completely refractory to the increase in MMP13 mRNA observed following stimulation with IL-17 in both the naive and CIA groups. Similarly, in further independent experiments, whilst SF from CIA mice again showed elevated levels of MMP9 and MMP13 mRNA relative to those from naive mice, this was not the case for SF from mice treated with 12b and indeed the levels of MMP13 were significantly decreased compared to the naïve levels (

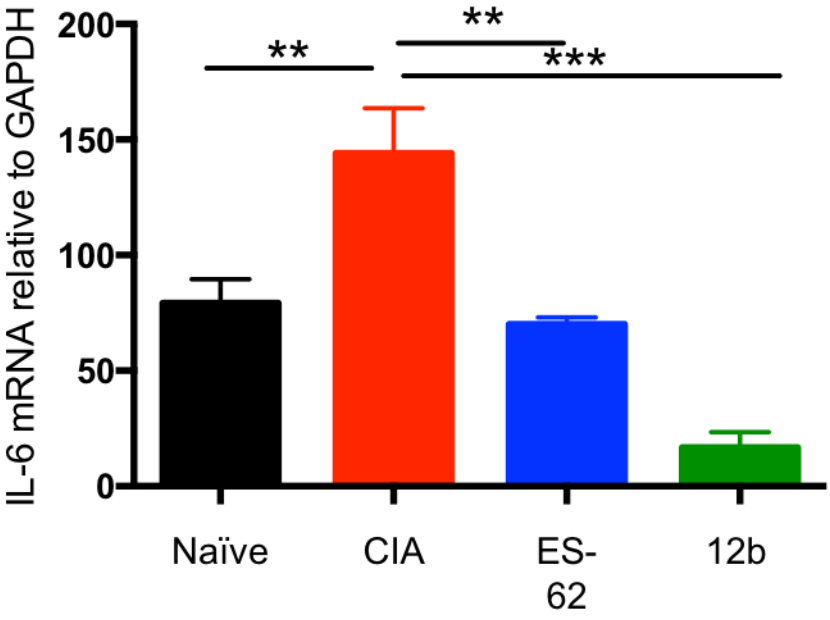
IL-6 mRNA relative to GAPDH
200
150
100
50
0
**
**
***
Naïve
CIA
ES-62
12b

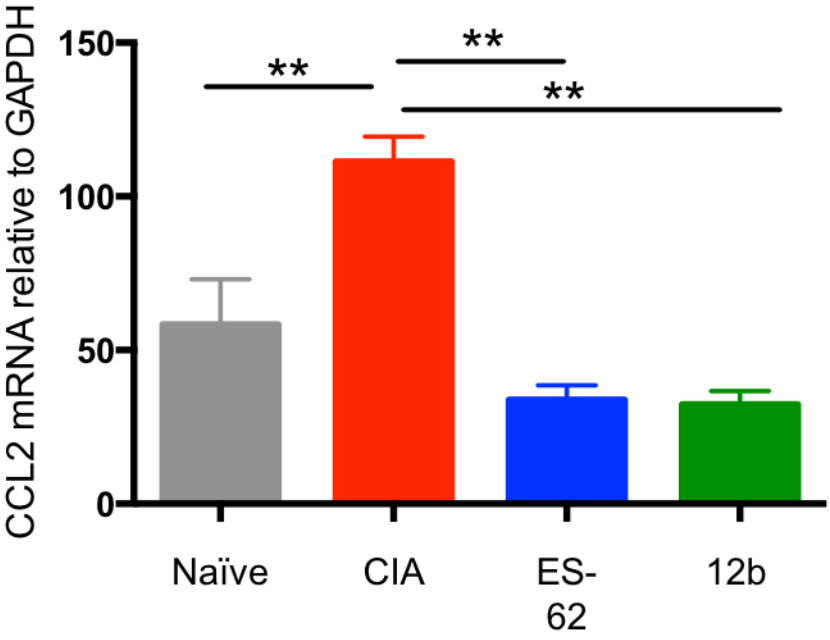
CCL2 mRNA relative to GAPDH
150
100
50
0
**
**
**
Naïve
CIA
ES-62
12b

Figure 3-13). Interestingly administration of IL-1β *in vivo* strongly enhanced the mRNA levels of both MMP9 and MMP13 in SF from CIA mice: however, whilst exposure to 12b is able to prevent this IL-1β-driven increase in MMP9 expression, there is a substantial increase in MMP13 mRNA in cells from 12b plus IL-1β-, relative to 12b- and even the PBS-treated CIA mice, even if these expression levels remain significantly lower than those in CIA plus IL-1β group, perhaps explaining, at least in part, the enhanced severity of disease in these mice.

3.6 Conclusions & Discussion

The data presented in this chapter confirm the potential of ES-62, 11a and 12b to reduce pathology in CIA. Moreover, administration of IL-1β was able to overcome 12b- (and ES-62) mediated protection providing supporting evidence that its production is a target of 12b in CIA[133] and providing further support for the further development of such ES-62 SMA-based therapies in RA. Importantly, these new findings suggest that, like ES-62, 12b can act to functionally modulate SF aggressiveness both in terms of the perpetuation of inflammation and the bone and cartilage destruction that contributes to CIA progression. This perhaps suggests that further development of 12b in terms of targeting SF may avoid the immunosuppression associated with current immunomodulatory therapies and, for the reasons developed below, provide effective control of RA.

SF have been proposed to play a key role in the perpetuation and even the spread of inflammation: although it is not clear whether SF are involved in the initiation process of RA, once inflammation is established, SF are able to sense the pro-inflammatory environment and respond by secreting multiple factors that drive the inflammation and pathology that generates the arthritic joint[151]. For example, during RA, the synovial cavity pressure increases and leads to the collapse of blood vessels, with consequent episodes of hypoxic reperfusion injury. This results in the generation of reactive oxygen species (ROS) that are proposed to induce modification of joint proteins that, by

allowing breaking of tolerance, leads to the formation of autoantibodies[152]. In addition, the localised conditions of hypoxia within the joint contribute to the activation and maintenance of inflammatory cell responses[118,153]. This altered pro-inflammatory microenvironment in the arthritic synovium reflects the hyper-proliferative and metabolically active status of cells such as SF within, and lymphocytes, monocytes and neutrophils invading, the joint: thus the ability of ES-62 to target not only DC polarization, Th17 differentiation and IL-17 production by Th17 γδ T cells[104] but also the hypoxic status, affects the local environment, making the joint less pro-arthritogenic which in turn may modulate fibroblast aggressiveness.

Moreover, since SF express TLR4[150] at their surface this suggests that they might also be directly targeted by ES-62 (and its SMAs), to inhibit the expression, and therefore the production, of pro-inflammatory factors such as IL-6, CCL2 or MMPs even within an established pro-inflammatory environment (Figure 3-14). This may be particularly important in the light of the evidence[43] that SF in both CIA and RA are intrinsically modified cells and not only passive responders to their local environment. Thus, if SF can be directly targeted by ES-62 and 12b, such molecules may have the capacity to interfere with this transformation process and prevent them from acquiring, or even reverse, an aggressive CIA-like phenotype, allowing the development of effective therapies acting in the joint in established disease.

Figure 3-1 Scoring the pathogenic development of the CIA mouse model

DBA/1 mice were immunized on day 0 with type II bovine collagen (CII) and CFA (Freund's adjuvant) and on day 21 with CII in PBS. Clinical articular score (A) and paw width (B) were monitored every other day for each mouse (n=6), with clinical score assessed as described in the Materials and Methods (section 2.1 and 2.3) Data are presented as mean score ± SEM. Mann-Whitney tests were performed to assess statistical significance between the first and last days of disease model where *** $p<0.001$. Incidence of arthritis (C) was calculated by the percentage of mice with diagnosed pathology (designating a mouse as exhibiting arthritis once it reaches an articular score of 2). Incidence of diagnosed severe disease on the culling day at day 29 (D) was categorised as the percentage of mice with a total articular score ≥ 4.

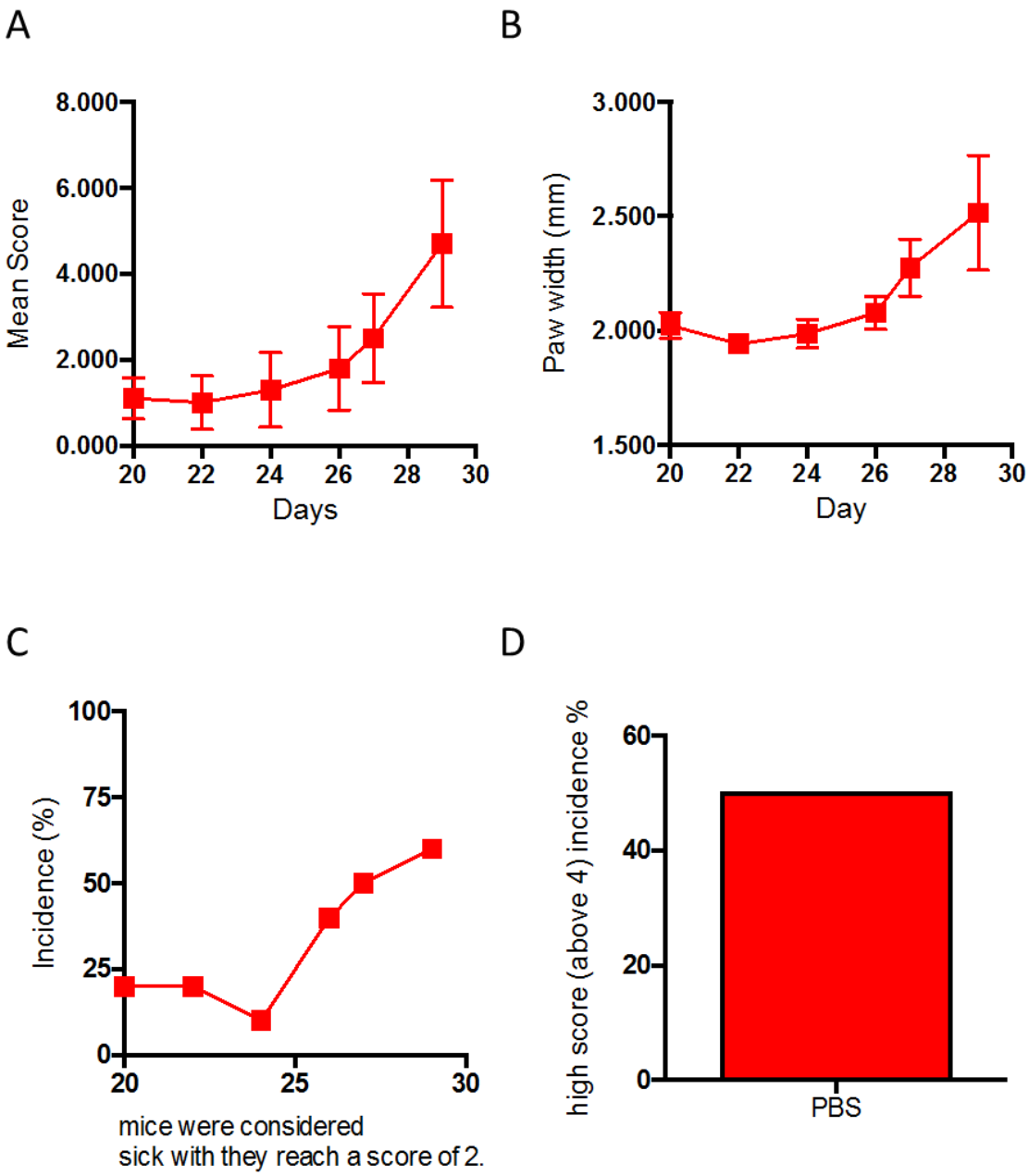
A
8.000
6.000
4.000
2.000
0.000
Mean Score
20
22
24
26
28
30
Days
B
3.000
2.500
2.000
1.500
Paw width (mm)
20
22
24
26
28
30
Day
C
100
75
50
25
0
Incidence (%)
20
25
30
mice were considered
sick with they reach a score of 2.
D
60
40
20
0
high score (above 4) incidence %
PBS

Figure 3-2 Differential phenotypes between naïve and CIA joints specially in term of cell infiltration and vasculature leakage

A-B: Paws from naïve (local score of 0) and CIA (local score of 3 total score of 9), mice were collected for decalcification, sectioning and histopathology H & E (A) and trichrome (B) staining. In H & E (A) staining, Haematoxylin is a violet stain that binds to basophilic substances such as DNA, therefore it is used to reveal cell nuclei (purple). Eosin is a red stain that binds to acidophilic substances such as positively charged amino acid side chains (e.g. lysine, arginine) and is used to visualise collagen (pale pink). In the trichrome staining (B) staining reveals collagen deposition (green/blue) and erythrocytes (red). Black arrows are used to point out either inflammatory cell infiltration (CI) or bone destruction (BD). The presented pathology sections are from a CIA model not presented in this thesis where for the CIA mice average score = 2.5 ± 0.8, n=12.

C. CIA mice (average score 4.67 ± 2, n=6) were injected intravenously with the Evans blue dye and individual paws with local articular scores ranging from 0 to 3 are presented, revealing the vasculature leakage associated with pathology. A paw with a score of 4 from an independent experiment is shown in Figure 2-1). Black arrows point out the local Evans blue leakage and therefore tissue staining. Paws with a local score of 0 exhibit little or no staining, whilst those with a local score of 1 only display leakage in the toes or ankle. With scores of 2 and above multiple leakage points are revealed in both toes and ankle with leakage becoming more severe and correlating with the local articular score.

A

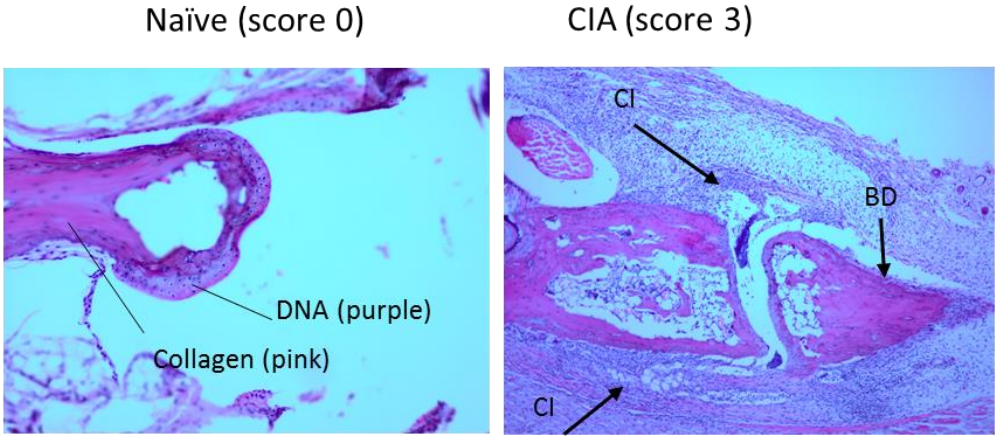
Naïve (score 0)
CIA (score 3)
DNA (purple)
Collagen (pink)
CI
BD
CI

B

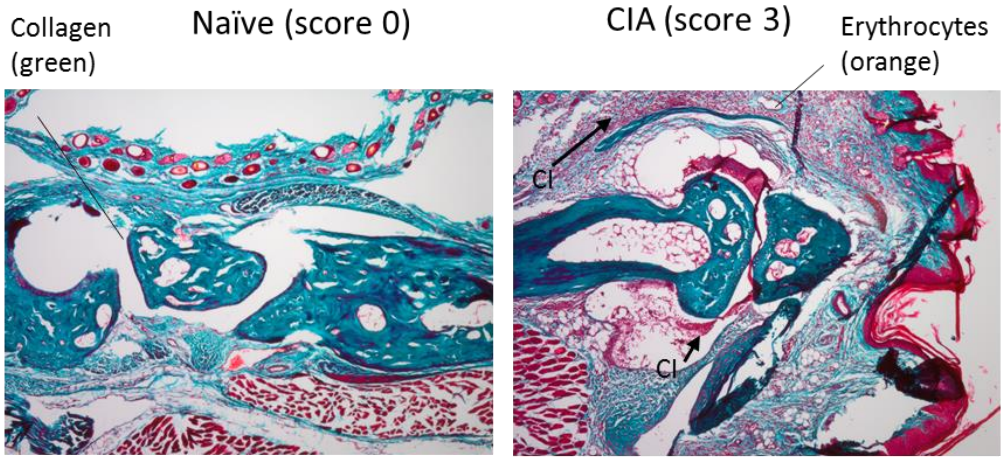
Collagen (green)
Naïve (score 0)
CIA (score 3)
Erythrocytes (orange)
CI
CI

C

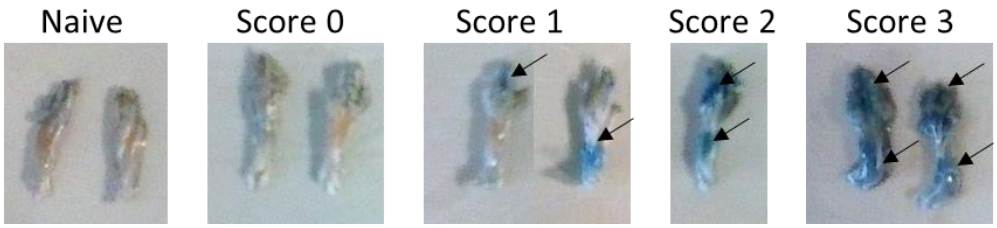
Naive
Score 0
Score 1
Score 2
Score 3

Figure 3-3 SF from CIA mice display properties consistent with aggressive inflammatory responses and bone destruction in the joint

A-B: SF from naïve or CIA mice from 4 independent CIA models were pooled prior to expansion *ex vivo*. For each CIA model SF were cultured as 3 independent cultures and IL-6 or CCL2 levels produced in 24 hours in the supernatant was assessed by ELISA as described in the M&M section 2.5. Here it is represented the mean value of each of the 4 CIA models (assayed as triplicate) normalised to their respective naïve fibroblast population for IL-6 (A) and CCL2 (B) production. Mann-Whitney tests were performed to assess statistical significance where ** $p < 0.01$, *** $p<0.001$.

C-D: SF from naïve and CIA mice (average score 3.17 ± 1.38, n=6) were extracted and plated as 3 independent cultures. Their level of IL-6 and CCL2 mRNA levels was assessed by RT-qPCR as described in section 2.8). Results are expressed as the mean ± SEM of messenger RNA level relative to GAPDH and for statistical analysis Mann-Whitney tests were performed where ** $p < 0.01$

E-F: SF from naïve or CIA mice from two independent CIA model (mean score 3.67 ± 1.5, n=6 and mean score 4.5 ± 1.2, n=10) were pooled and cultured *ex vivo*. Independent cultures (3 for each CIA model) of SF were stimulated for 6 hours with IL-17 (50 ng/ml) or DMEM as control. After stimulation cells were harvested and total RNA was extracted. Levels of MMP9 and MMP13 were assessed by RT-qPCR and the data are presented as mRNA levels (means of triplicate estimations) normalized to those of GAPDH and expressed as fold change. Symbols represent the values from individual cell cultures of both CIA models. Mann-Whitney tests were performed for each condition where, for statistical analysis * $p < 0.05$; ** $p < 0.01$, *** $p<0.001$.

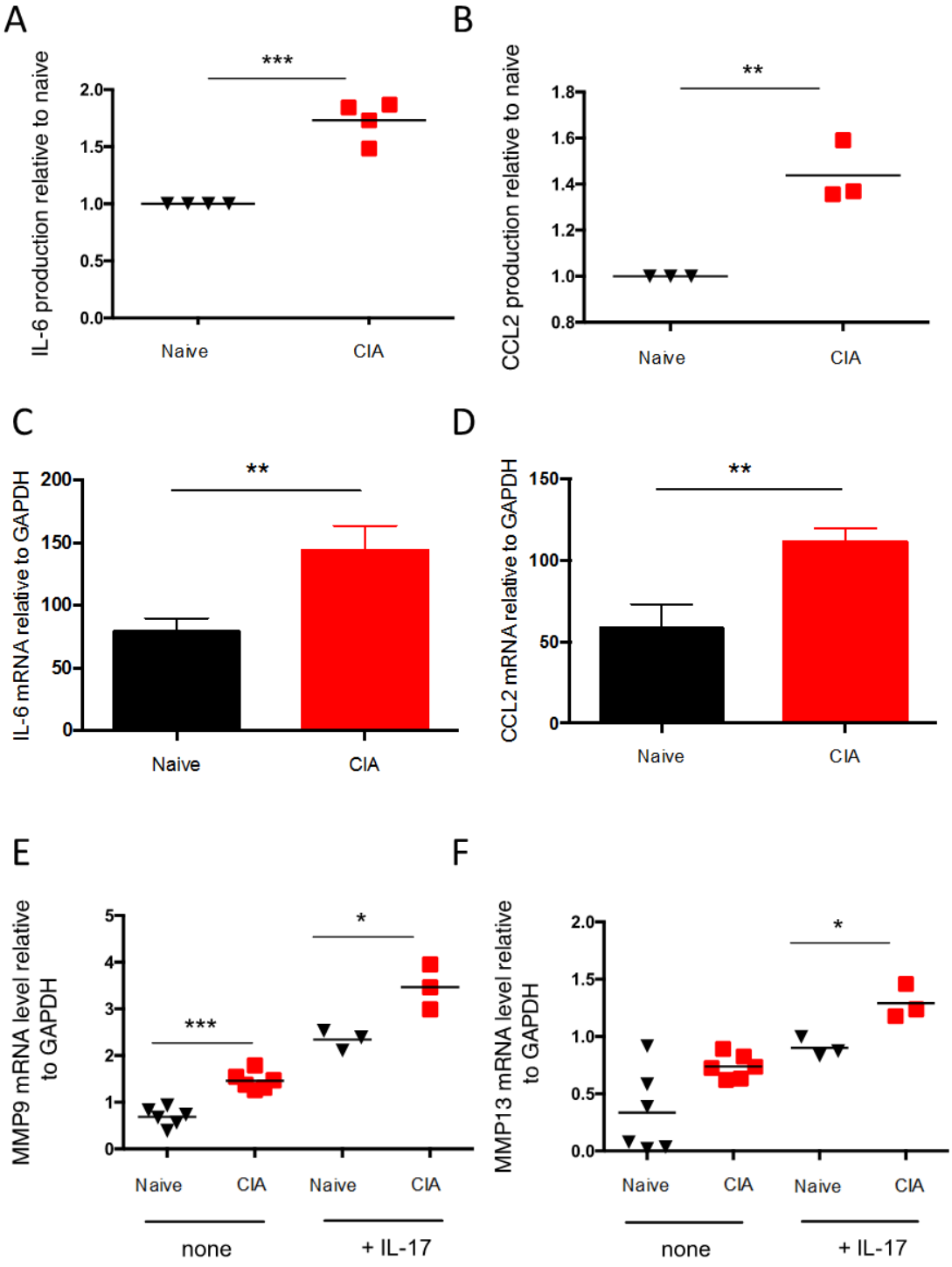
A
IL-6 production relative to naive
***
2.0
1.5
1.0
0.5
0.0
Naive
CIA
B
CCL2 production relative to naive
**
1.8
1.6
1.4
1.2
1.0
0.8
Naive
CIA
C
IL-6 mRNA relative to GAPDH
**
200
150
100
50
0
Naive
CIA
D
CCL2 mRNA relative to GAPDH
**
150
100
50
0
Naive
CIA
E
MMP9 mRNA level relative to GAPDH
***
*
5
4
3
2
1
0
Naive
CIA
Naive
CIA
none
+ IL-17
F
MMP13 mRNA level relative to GAPDH
*
2.0
1.5
1.0
0.5
0.0
Naive
CIA
Naive
CIA
none
+ IL-17

Figure 3-4 Prophylactic administration of ES-62 reduces CIA clinical score as well as cell infiltration and bone destruction observed in joint sections.

DBA/1 mice were immunized on day 0 with type II bovine collagen (CII) in CFA and on day 21 with CII in PBS. Mice were treated with ES-62 (2 μg each dose) on days -2, 0 and 21 or injected with PBS as a control (CIA mice). Clinical articular score (A) was monitored every other day for each mouse (n= 6 each group). Data are presented as mean score ± SEM. Incidence of arthritis (B) was calculated by the percentage of mice with pathology, with mice considered arthritic once a clinical score of 2 is reached. Incidence was also categorized as of severe disease (C) as indicated by the percentage of mice with a score above 4.

A

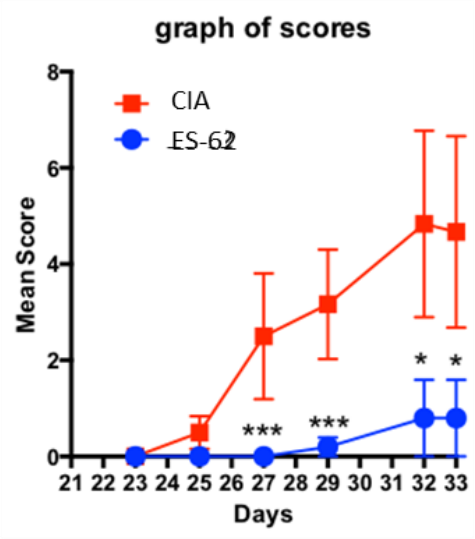
graph of scores
CIA
ES-62
Mean Score
Days
0
2
4
6
8
21 22 23 24 25 26 27 28 29 30 31 32 33
***
***
*
*

B

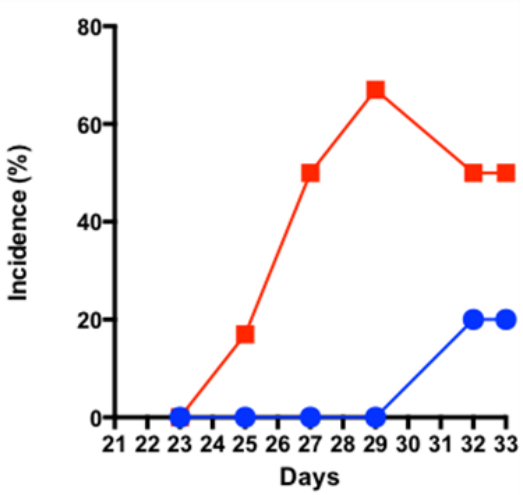
Incidence (%)
Days
0
20
40
60
80
21 22 23 24 25 26 27 28 29 30 31 32 33

C

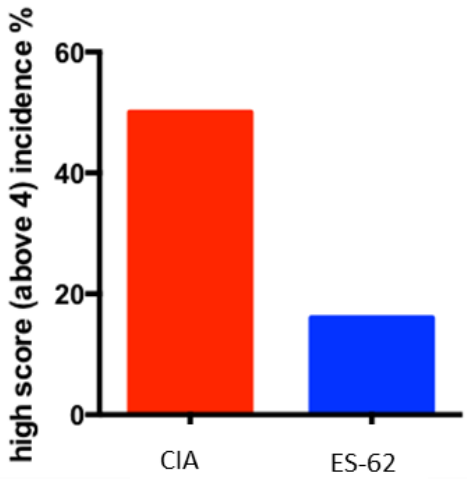
high score (above 4) incidence %
0
20
40
60
CIA
ES-62

Figure 3-5 Prophylactic administration of ES-62 reduces local hypoxia and T cell infiltration in the joint

A: Mice from CIA model and prophylactic treatment with ES-62 (respectively CIA: mean score = 4.667 ± 1.99, n=6 and ES-62 mean scores = 0.800 ± 0.800, n=5) were injected intra-peritoneally 24 hours before culling with pimonidazole (60 mg/kg) to address assessing the levels of hypoxia present in the joint under these differential conditions as described in the M&M section 2.3.1. Paws were harvested and isolated joint cells from the Naive, CIA and ES-62 groups were pooled together. "Hypoxic" cells containing pimonidazole-conjugates were detected using a specific FITC-conjugated monoclonal antibody by flow-cytometry. The data are also shown as the percentage of highly pimonidazole positive cells present in the joints of naïve CIA or ES-62 treated mice.

B-C: Paw tissue from CIA mice treated prophylactically with ES-62 (mean score 1.5 ± 1.145, n=6) or PBS as control (CIA mice, mean score = 3.667 ± 1.498, n=6) were digested with collagenase and after an over-night incubation, non-adherent joint cells were harvested. Cells were stainind for flow cytometry as described in the M&M section 2.6, gated as single, live cells were analysed for the T cell marker CD3 and for more specific markers CD8 (A) and CD4 (B) to distinguish respectively cytotoxic T cells and helper T cells by flow cytometry and the percentage of these cell population is represented in the double positive (CD3+CD8+ or CD3+CD4+) gates. Data are representative of a single experiment.

A

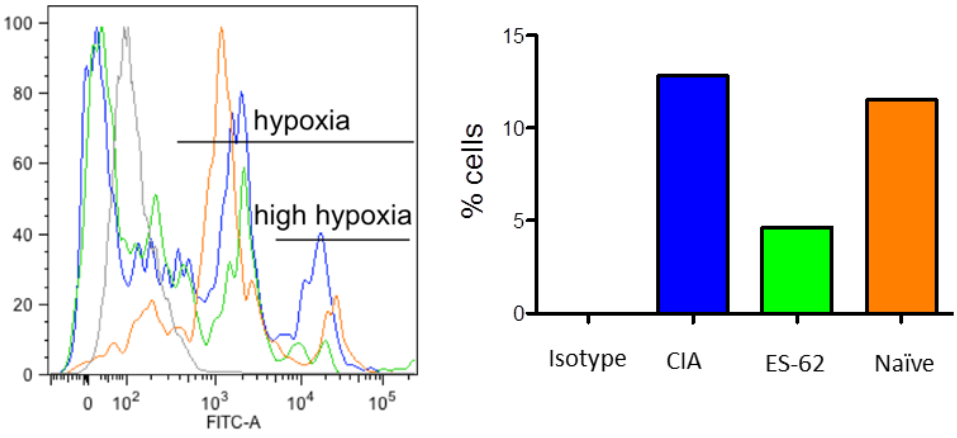
hypoxia
high hypoxia
FITC-A
% cells
Isotype
CIA
ES-62
Naïve

B

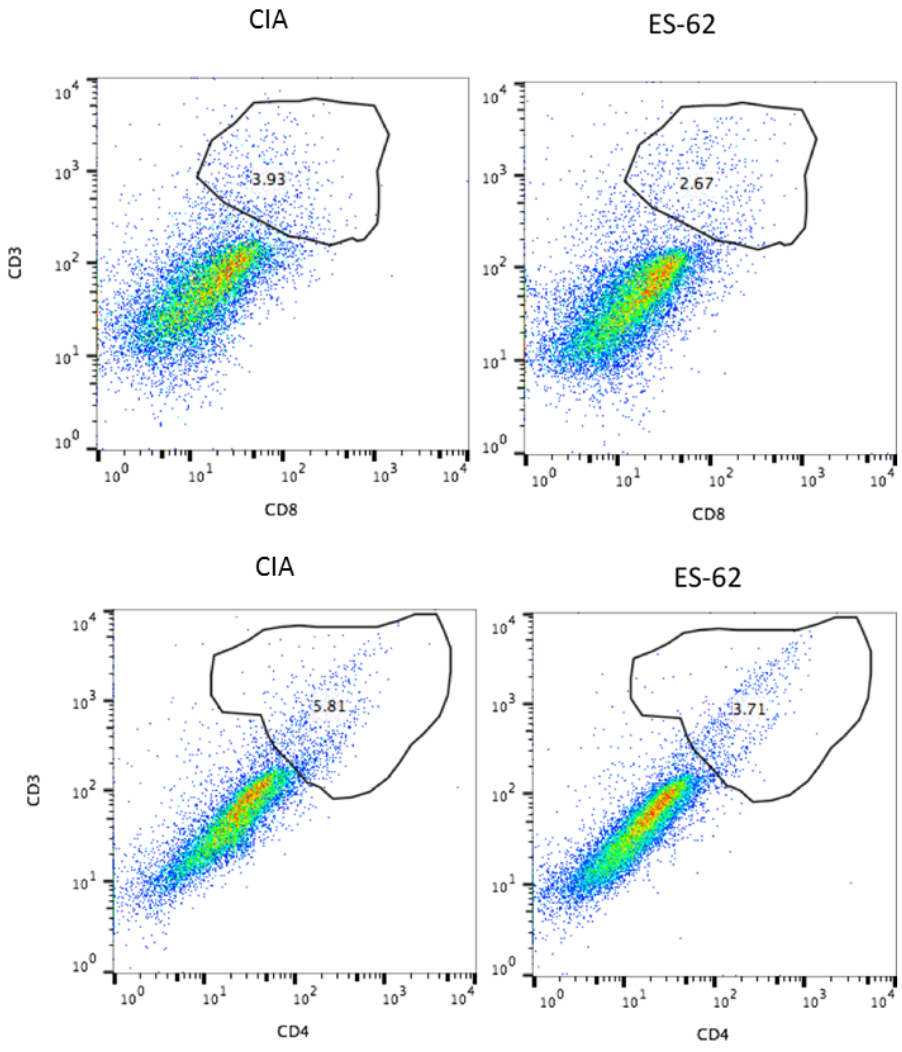
CIA
ES-62
3.93
2.67
CD3
CD8
CIA
ES-62
5.81
3.71
CD3
CD4

Figure 3-6 Therapeutic potential of the SMAs of ES-62

A: The timeline of the therapeutic CIA model is presented. DBA/1 mice were immunized on day 0 with type II bovine collagen (CII) and CFA and on day 21 with CII in PBS. From the first appearance of clinical inflammatory symptoms, mice were sequentially randomly allocated to blinded treatments and the code broken at the end of the experiment. Mice were injected s/c either with 11a (1 μg per dose), 12b (1 μg per dose), methotrexate (50 μg per dose) or PBS as control (CIA mice) every three days (n=6 for each treatments).

B: Therapeutic treatment of individual mice commenced at different times and initial clinical scores: thus, disease progression was normalised to the score on the first day of intervention for each condition. ANOVA followed by Tukey multiple comparison tests were performed for time points (days post first symptoms) and results are expressed as the mean ± SEM. For statistical analysis * $p < 0.05$; ** $p < 0.01$, *** $p<0.001$

C: SF from the therapeutic model presented in B were extracted and pooled by treatment group. Following expansion ex vivo, three independent cultures were performed for each group treatment in which cells were stimulated *in vitro* for 24 hours with the following stimuli: DMEM as control, BLP (0.5 μg/ml), LPS (1 μg/ml) or IL-1β (10 ng/ml) and IL-6 release measured. by ELISA. Results are presented as the mean values of the independent cultures (each assayed in triplicate) and analysed by ANOVA followed by the Tukey multiple comparison test where * $p < 0.05$; ** $p < 0.01$, *** $p<0.001$

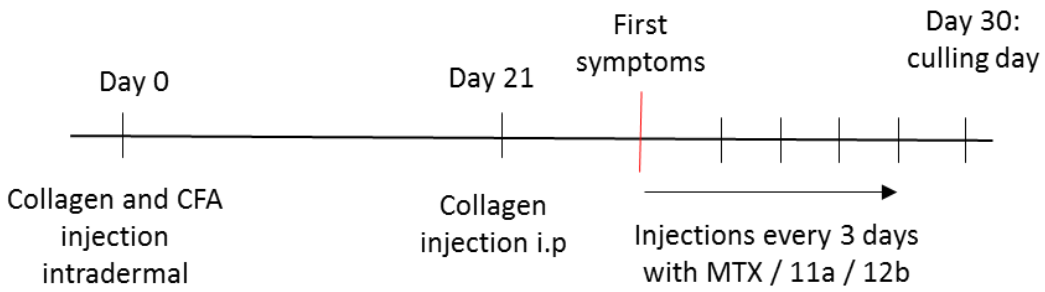
Day 0
Day 21
First symptoms
Day 30: culling day
Collagen and CFA injection intradermal
Collagen injection i.p
Injections every 3 days with MTX / 11a / 12b

B

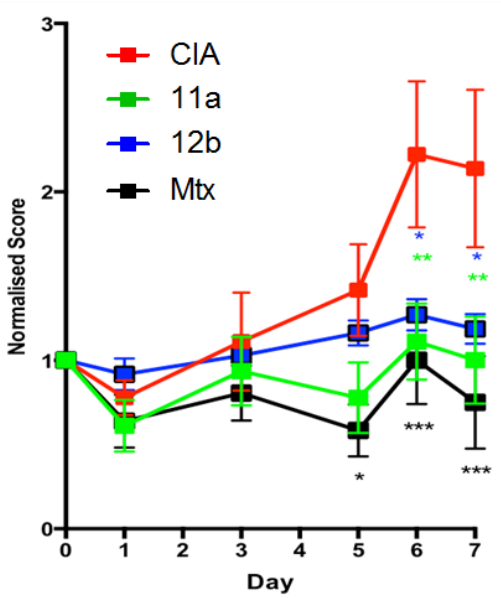
CIA
11a
12b
Mtx
Normalised Score
Day

C

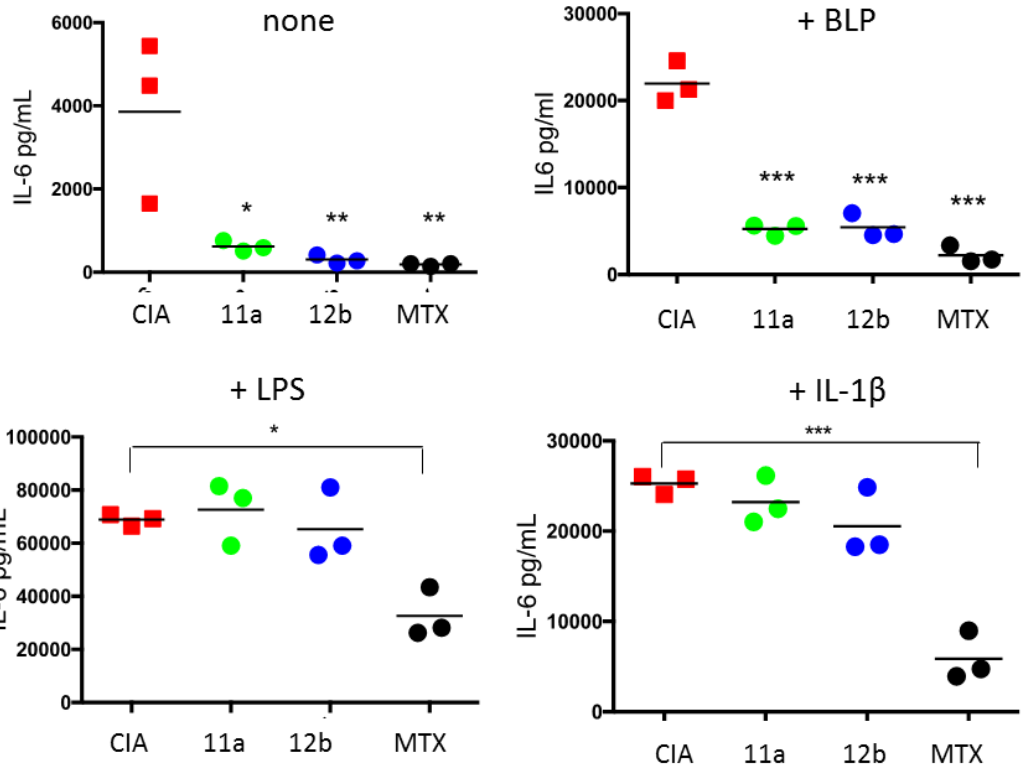
none
+ BLP
+ LPS
+ IL-1β
IL-6 pg/mL
IL6 pg/ml
CIA
11a
12b
MTX

Figure 3-7 12b and ES-62 prophylactic treatment protects against CIA development which is overcome by IL-1ß

CIA was induced in DBA/1 mice as described previously in Figure 3-4. However, in this independent model, cohorts of mice were injected prophylactically with 12b (1 µg per dose, dark green line, n=7) or ES-62 (2 µg, dark blue line, n=6) on days -2, 0 and 21 or with PBS as a control (CIA, red line, n=6). Additional cohorts were injected with recombinant murine IL-1ß (1 µg per dose) twice-weekly from day 21 (CIA + IL-1ß, pink line n=6 and 12b + IL-1ß, light green line n=8) as represented in the scheme (A). Clinical scores (B) and paw width (C) were monitored every other day for each mouse. Data are presented as mean score ± SEM. Incidence of arthritis (D) was calculated by the percentage of mice diagnosed with CIA (with clinical score above 2). For more clarity the results are splited in 2 graphs, showing separately 12b and ES-62 data both compared to the same CIA + IL-1ß.

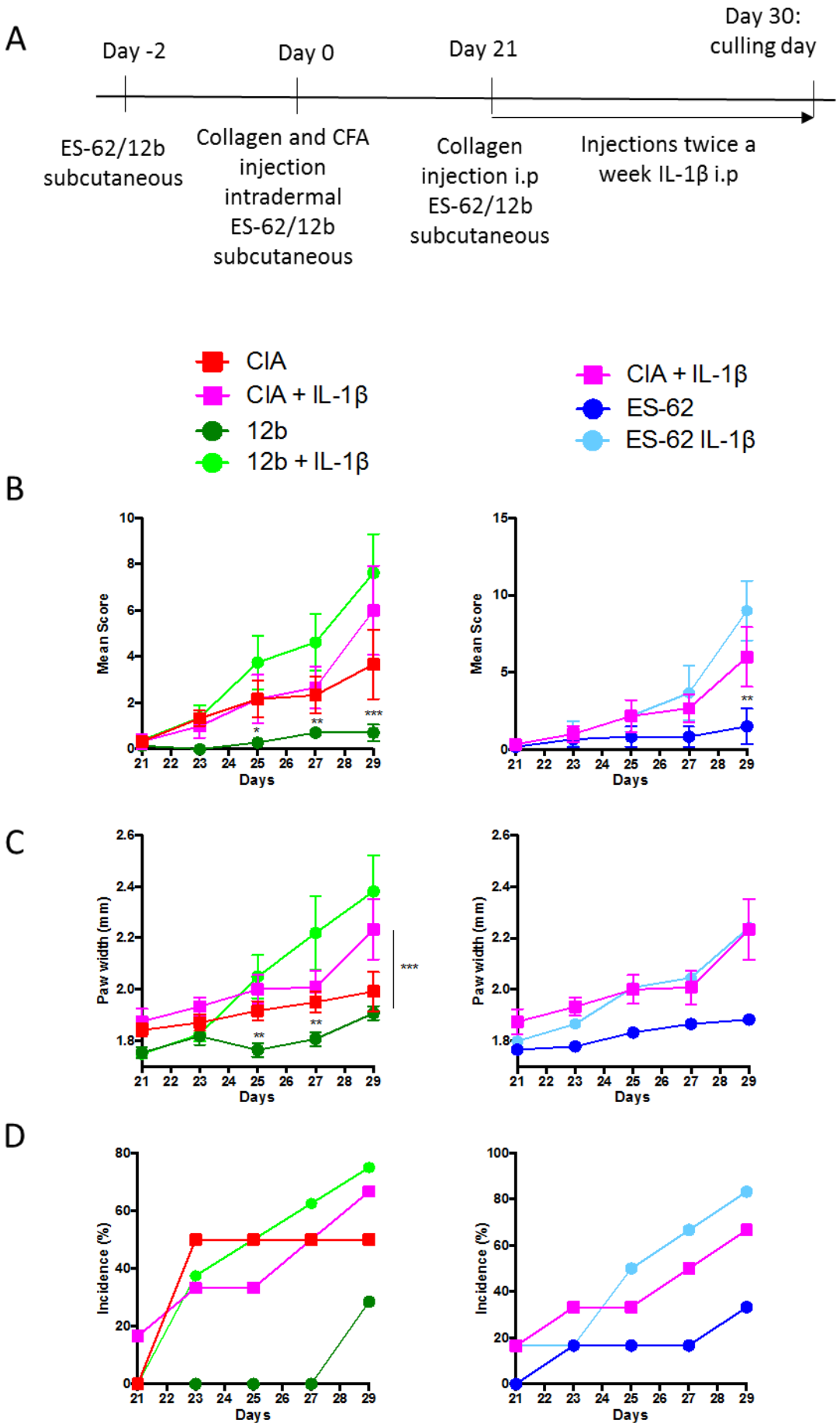
A
Day -2
Day 0
Day 21
Day 30: culling day
ES-62/12b subcutaneous
Collagen and CFA injection intradermal ES-62/12b subcutaneous
Collagen injection i.p ES-62/12b subcutaneous
Injections twice a week IL-1β i.p
CIA
CIA + IL-1β
12b
12b + IL-1β
ES-62
ES-62 IL-1β
B
Mean Score
Days
C
Paw width (mm)
Days
D
Incidence (%)
Days

Figure 3-8 12b and ES-62 prophylactic treatments reduce cell infiltration and bone destruction in the joint, whose effect is abrogated by IL-1ß.

Paws relevant of each treatments presented in Figure 3-7: CIA (paw score 4 [mouse total score 9]); CIA + IL-1ß (paw score 4 [mouse total score 11]); 12b (paw score 0 [mouse total score 0]), 12b + IL-1ß: (paw score 4 [mouse total score 11]), ES-62 (paw score 0 [mouse total score 0]) and ES-62 + IL-1ß (paw score 4 [mouse total score 11]). Such paws were collected for decalcification sectioning and histopathology H & E (on the left) and trichrome (on the right) staining Haematoxylin is a violet stain that binds to basophilic substances such as DNA, therefore it is used to reveal cell nuclei (purple). Eosin is a red stain that binds to acidophilic substances such as positively charged amino acid side chains (e.g. lysine, arginine) and is used to visualise collagen (pale pink). In the trichrome staining (on the right) staining reveals collagen deposition (green/blue) and erythrocytes (orange). Black arrows are used to point out either inflammatory cell infiltration (CI) or bone destruction (BD). For more visibility the data have been splited into PBS, ES-62, and 12b treatment groups.

CIA (score 4)

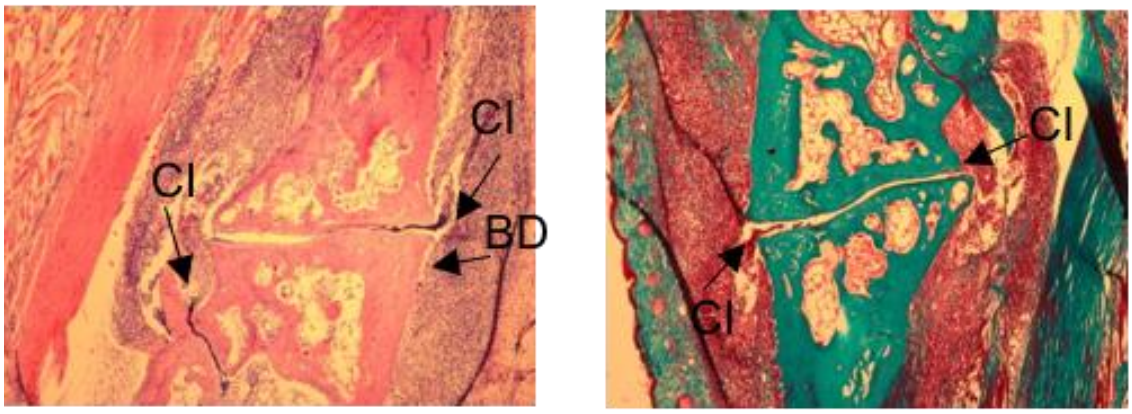

CIA + IL-1β (score 4)

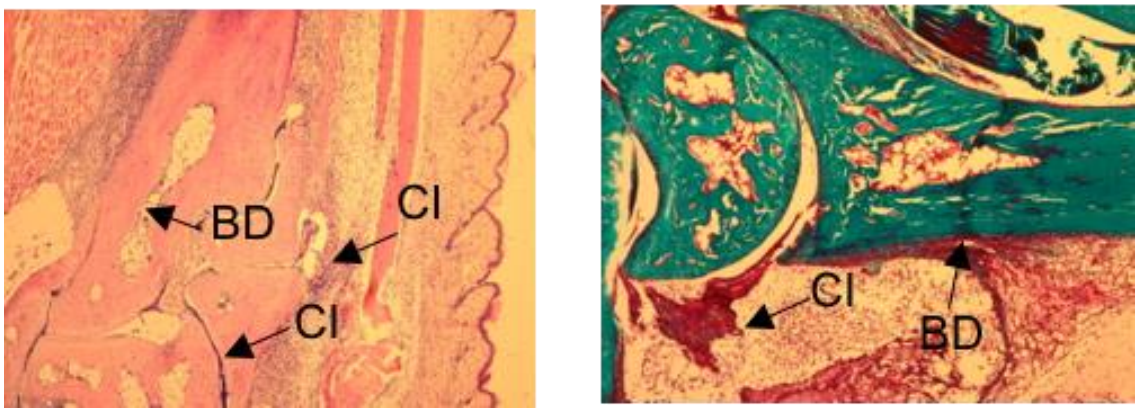

12b (score 0)

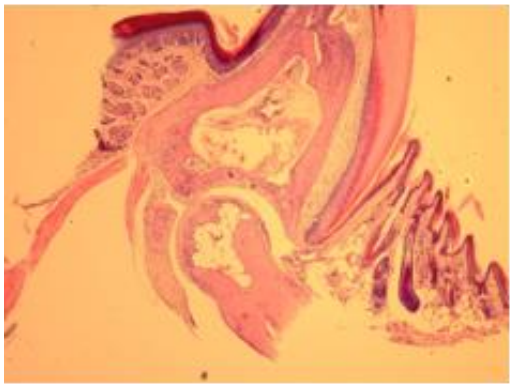

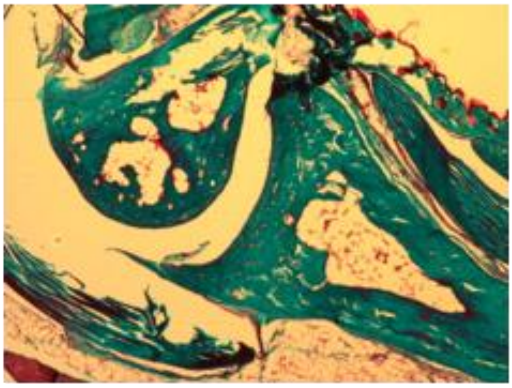

12b + IL-1β (score 4)

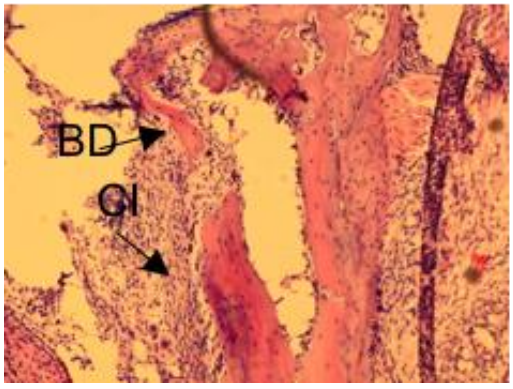

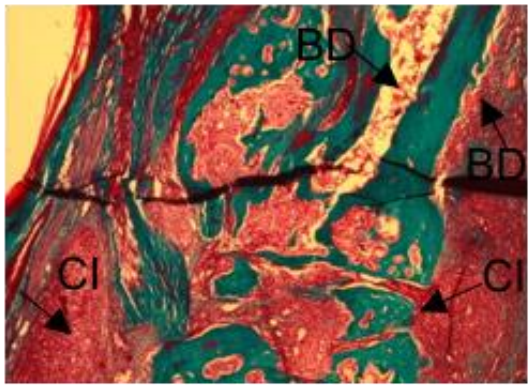

ES-62 (score 0)

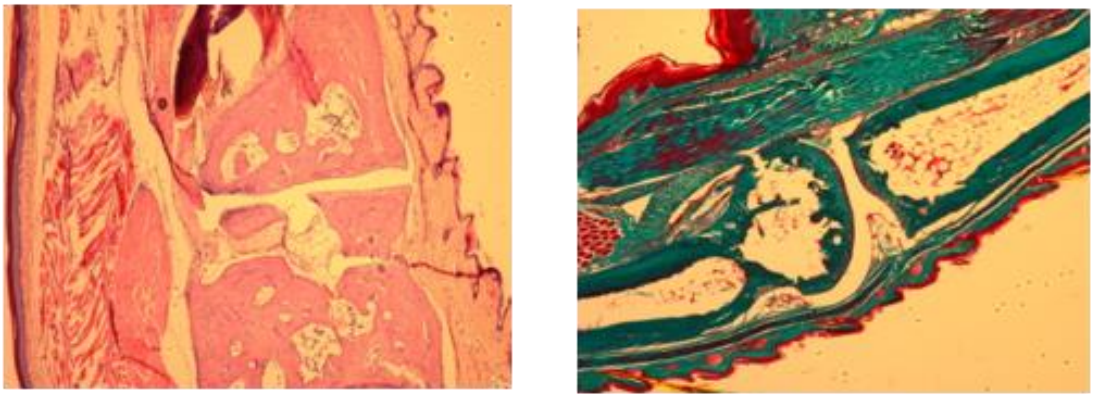

ES-62 + IL-1β (score 4)

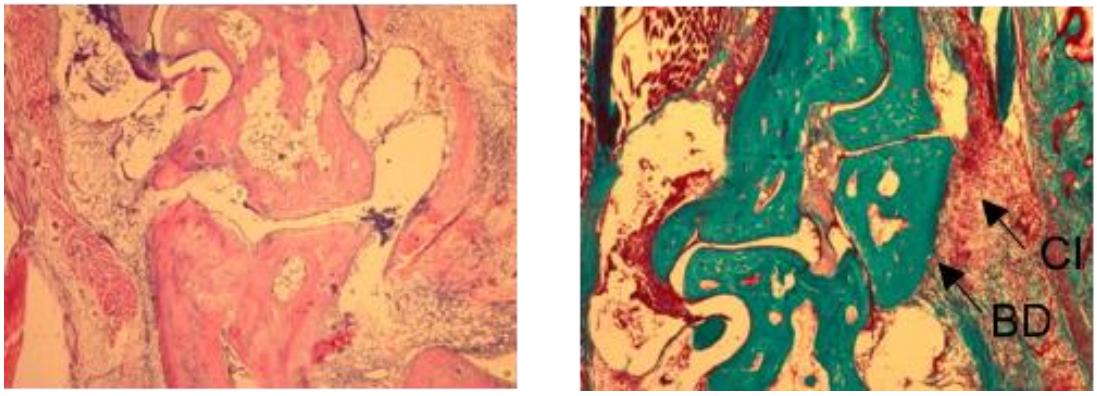

Figure 3-9 IL-1β increases T cell infiltration in the joint alone but decreases it in presence of 12b and ES-62

Joints from the CIA mice presented in Figure 3-7 were digested with collagenase, cultured overnight and non-adherent joint cells pooled in their treatment groups: CIA mice (mean score 3.66 ± 1.5, n=6), CIA + IL-1β (mean score 6 ± 1.93, n=6) 12b mice (mean score 0.71 ± 0.36, n=7) and 12b + IL-1β mice (mean score 7.62 ± 1.67, n=8), ES-62 (mean score 1.5 ± 1.14, n=6) and ES-62 + IL-1β (mean score 9 ± 1.93, n=6). Cells, gated as single, live cells were analysed for the T cell marker CD3 and for more specific markers CD8 (A) and CD4 (B) to distinguish respectively cytotoxic T cells and helper T cells by flow cytometry and the percentage of these cell population is represented in the double positive (CD3+CD8+ or CD3+CD4+) gates. For more clarity results are summarized in a table below. Data are representative of a single experiment.

A

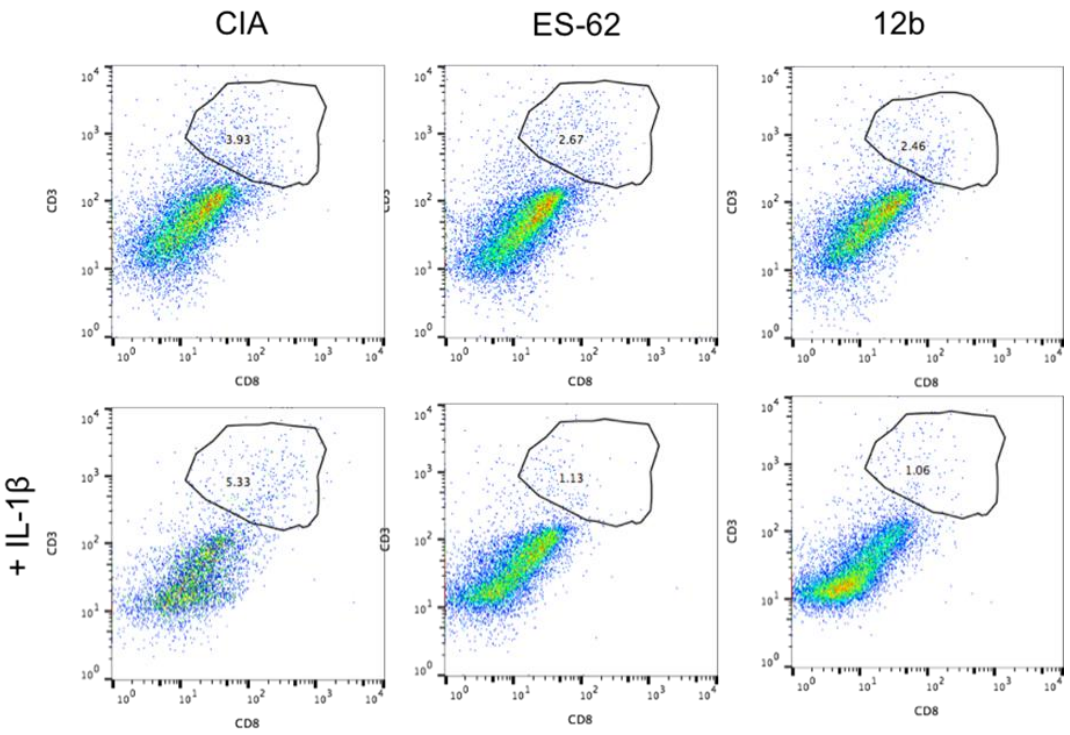

	CIA	ES-62	12b
none	3.93	2.67	2.46
+ IL-1β	5.33	1.13	1.06

B

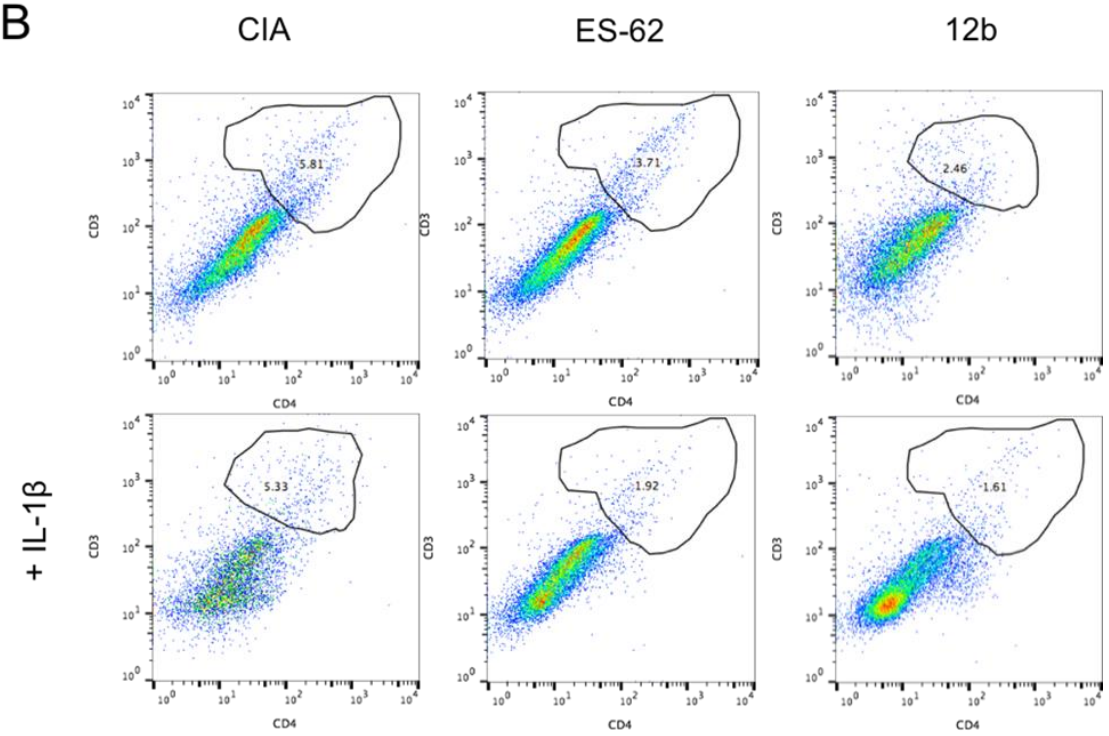

	CIA	ES-62	12b
none	5.81	3.71	2.46
+ IL-1β	5.33	1.92	1.61

Figure 3-10 Prophylactic treatment with ES-62 reduces SF pro-inflammatory cytokines, IL-6 and CCL2, production.

SF from Naive mice or mice with CIA, prophylactically treated with ES-62 (2 μg each dose, mean score 0.5 ± 0.22, n=6) or PBS (CIA mice : mean score 3.17 ± 1.38, n=6) were pooled by treatment group and expanded *ex vivo*. Three independent cultures were set up for each treatment group. Levels of spontaneous (A and B) or IL-1β (10 ng/ml)-, LPS (1 μg/ml)- or BLP (0.5 μg/ml)-stimulated (C and D) IL-6 and CCL2 release at 24 h were measured by ELISA. All results are expressed as the symbols representing the mean values for the independent cultures (each assayed in technical triplicate) with analysis by ANOVA followed by the Tukey multiple comparison test. For statistical analysis * $p < 0.05$; ** $p < 0.01$, *** $p<0.001$. The data for the spontaneous release of cytokine as well as under LPS stimulation, has been repeated successfully with another two independent animal models and has not been repeated for IL-1β and BLP.

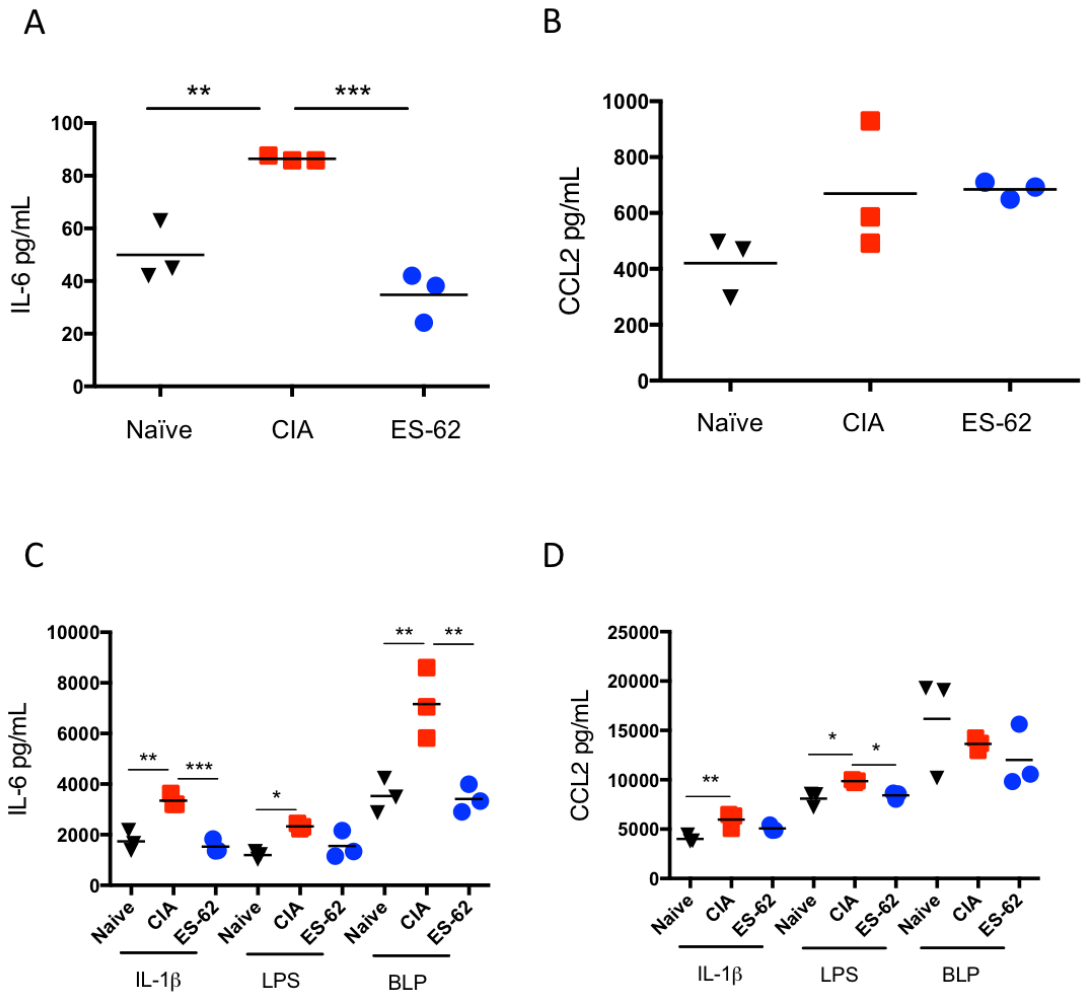
A
B
C
D
IL-6 pg/mL
CCL2 pg/mL
Naïve
CIA
ES-62
IL-1β
LPS
BLP

Figure 3-11 Prophylactic treatment with ES-62 reduces SF pro-inflammatory cytokines, IL-6 and 12b, production.

DBA/1 mice were used for CIA and were prophylactically treated with 12b (1 µg each dose, mean score 0.71 ± 0.36, n=7) or PBS as control (mean score 3.66 ± 1.5, n=6). SF from those mice were extracted and pooled down by treatment group. After 3 weeks of *ex vivo* culture cells were plated as three independent culture for each group treatment at 0.3x10^6 cells per well. After stimulation with DMEM (as control, A-B), IL-17 (25 ng/ml) (C-D) and LPS (1 µg/ml) (E-F), supernatants were collected and IL-6 (A-C-E) and CCL2 (B-D-F) concentrations were measured by ELISA as described in the M&M section (section 2.5). Data are plotted as the mean of each independent culture assay triplicate. ANOVA test followed by Tukey multiple comparison test was performed for each experiment and results are expressed as the mean ± SEM. For statistical analysis * $p < 0.05$; ** $p < 0.01$, *** $p<0.001$. This experiment has been repeated successfully with another animal model.

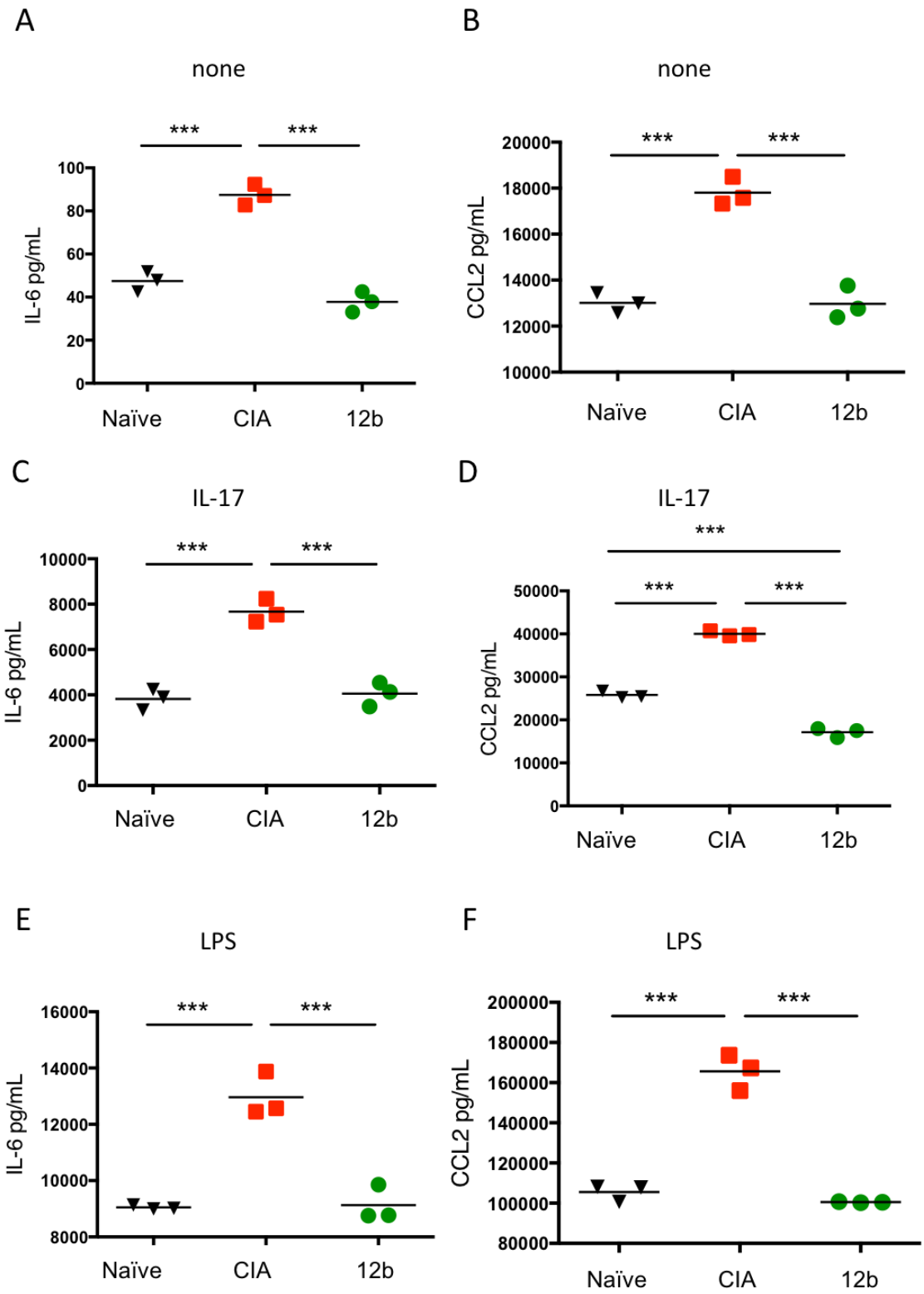
A
none
IL-6 pg/mL
100
80
60
40
20
0
***
***
Naïve
CIA
12b
B
none
CCL2 pg/mL
20000
18000
16000
14000
12000
10000
***
***
Naïve
CIA
12b
C
IL-17
IL-6 pg/mL
10000
8000
6000
4000
2000
0
***
***
Naïve
CIA
12b
D
IL-17
CCL2 pg/mL
50000
40000
30000
20000
10000
0
***
***
***
Naïve
CIA
12b
E
LPS
IL-6 pg/mL
16000
14000
12000
10000
8000
***
***
Naïve
CIA
12b
F
LPS
CCL2 pg/mL
200000
180000
160000
140000
120000
100000
80000
***
***
Naïve
CIA
12b

Figure 3-12 Inhibition of IL-6 and CCL2 mRNA expression by ES-62 and 12b

SF from naïve, CIA (mean score 3.66 ± 1.5, n=6), ES-62 (mean score 1.5 ± 1.15, n=6) or 12b (mean score 0.71 ± 0.36, n=7) treated mice were pooled and cultured *ex vivo* for 3 weeks. Parallel cultures from this model were used for RNA extraction and measurement of mRNA level of IL-6 and CCL2 by RT-qPCR as described in the M&M section 2.8. Levels of IL-6 and CCL2 were normalized to GAPDH and then expressed as a fold change. Results are expressed as the mean values (of triplicate analyses) from the independent cultures ± SEM. Data were analysed by ANOVA followed by Tukey multiple comparison test where * $p < 0.05$; ** $p < 0.01$, *** $p<0.001$. This experiment has been done only once.

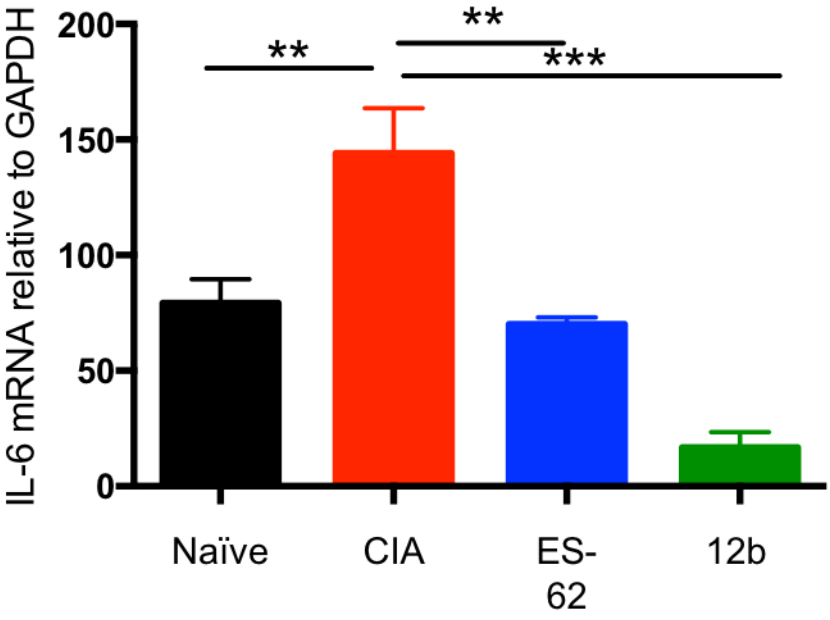
IL-6 mRNA relative to GAPDH
200
150
100
50
0
**
**
***
Naïve
CIA
ES-62
12b

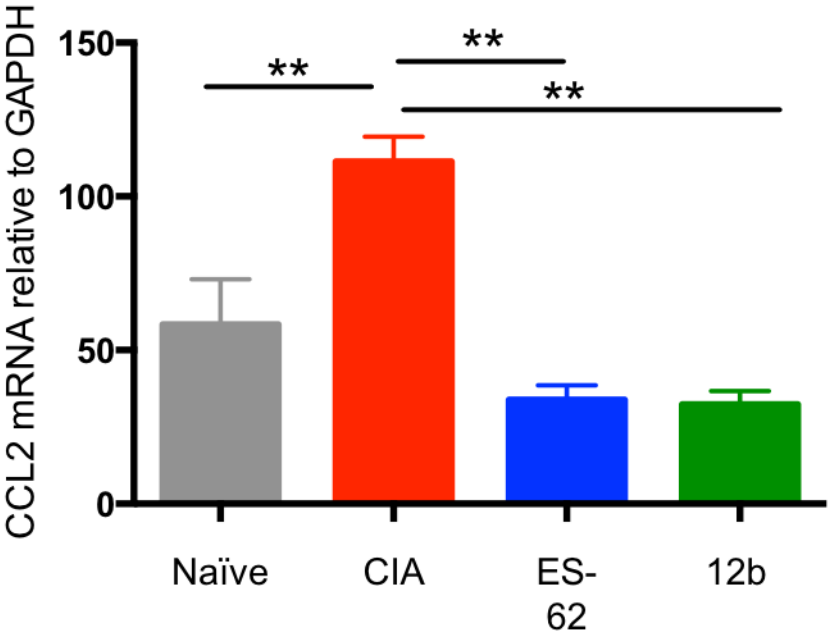
CCL2 mRNA relative to GAPDH
150
100
50
0
**
**
**
Naïve
CIA
ES-62
12b

Figure 3-13 ES-62 and 12b reduces SF MMP expression

A-D: SF from naïve mice, CIA mice (mean score 3.66 ± 1.5, n=6) and ES-62 mice (mean score 1.5 ± 1.15, n=6) were extracted, expanded for 3 weeks *ex vivo* and plated as triplicate cultures for each treatment at 0.3 10^6 cells per well. After stimulation with IL-17 (25ng/ml) for 24 hours after which cells were harvested RNA was extracted and mRNA level of MMP9 (A and C) and MMP13 (B and D) RNA messenger level were analysed by RT-qPCR as described in the M&M section 2.8. Levels of MMP9 and MMP13 were normalized to GAPDH and then expressed as a fold change. A Mann-Whitney t-test were performed for each experiment and results are expressed as the mean ± SEM. For statistical analysis * $p < 0.05$, ** $p < 0.01$, *** $p<0.001$

E-F: SF from naïve mice, CIA mice (mean score 3.66 ± 1.5, n=6), 12b mice (mean score 0.71 ± 0.36, n=7) and as well CIA + IL-1β (mean score 6 ± 1.93, n=6) and 12b + IL-1β mice (mean score 7.62 ± 1.67, n=8) were extracted, expanded for 3 weeks *ex vivo* and plated as triplicate cultures for each treatment at 0.3 10^6 cells per well. Cells were synchronised in 1% FCS DMEM then left in 10% FCS DMEM for 24 hours after which cells were harvested RNA was extracted and mRNA level of MMP9 (A and C) and MMP13 (B and D) RNA messenger level were analysed by RT-qPCR. Levels of MMP9 and MMP13 were normalized to GAPDH and then expressed as a fold change. A Mann-Whitney t-test were performed for each experiment and results are expressed as the mean ± SEM. For statistical analysis * $p < 0.05$, ** $p < 0.01$, *** $p<0.001$

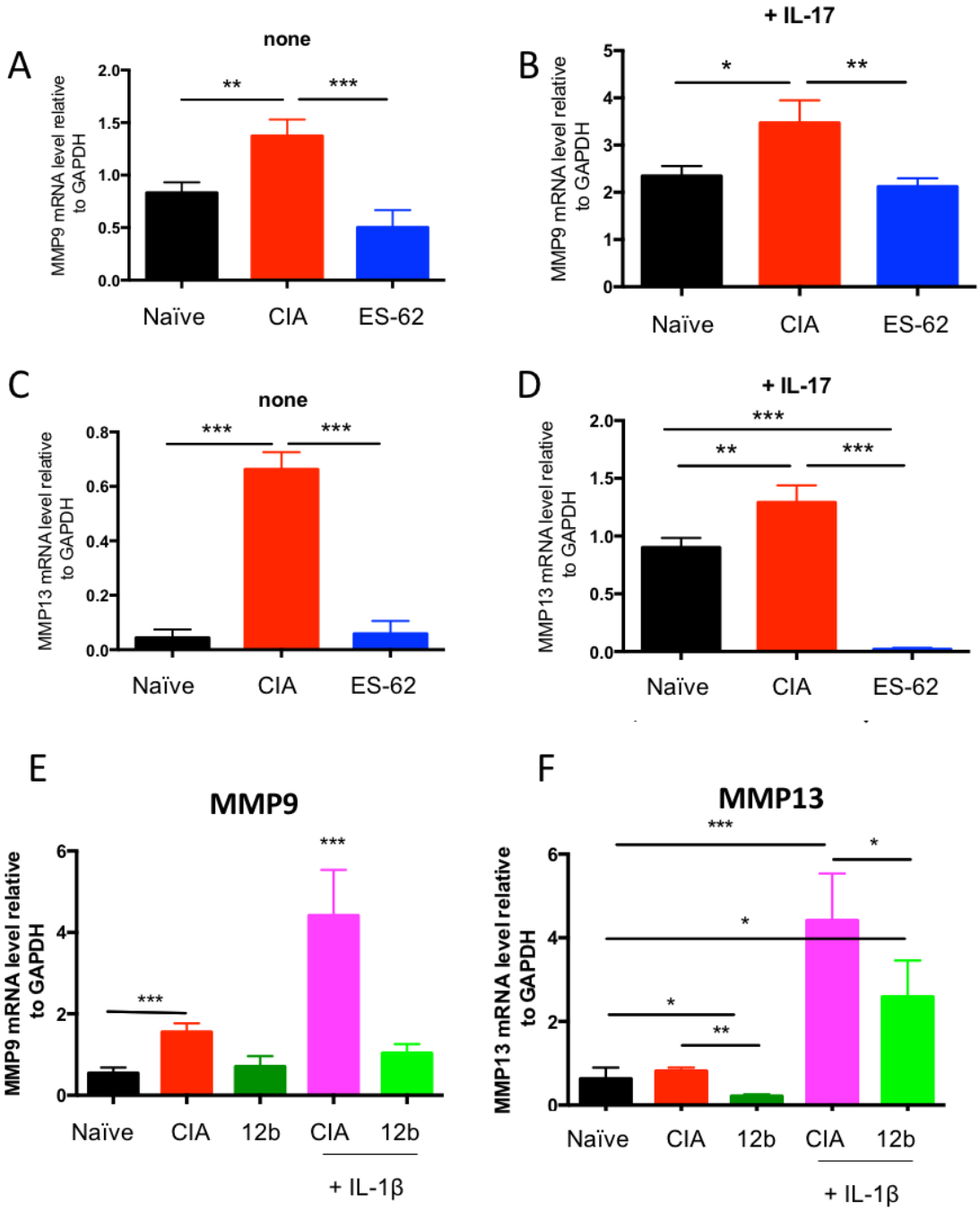
A
none
MMP9 mRNA level relative to GAPDH
2.0
1.5
1.0
0.5
0.0
**
***
Naïve
CIA
ES-62
B
+ IL-17
MMP9 mRNA level relative to GAPDH
5
4
3
2
1
0
*
**
Naïve
CIA
ES-62
C
none
MMP13 mRNA level relative to GAPDH
0.8
0.6
0.4
0.2
0.0
***
***
Naïve
CIA
ES-62
D
+ IL-17
MMP13 mRNA level relative to GAPDH
2.0
1.5
1.0
0.5
0.0
***
**
***
Naïve
CIA
ES-62
E
MMP9
MMP9 mRNA level relative to GAPDH
6
4
2
0
***
***
Naïve
CIA
12b
CIA
12b
+ IL-1β
F
MMP13
MMP13 mRNA level relative to GAPDH
6
4
2
0
***
*
*
*
**
Naïve
CIA
12b
CIA
12b
+ IL-1β

Figure 3-14 Primary model of ES-62 and 12b action on SF

During CIA, chronic hyper-production of pro-inflammatory cytokines such as IL-17, IL-1β and endogenous TLR ligands stimulate SF to induce expression and secretion of pro-inflammatory cytokines (e.g. IL-6), chemokines (CCL2) and tissue- and bone-destructive mediators such as MMP9 and MMP13 in the joint. ES-62 and 12b are both protective in CIA and act to reduce pro-inflammatory cytokines and MMPs at the gene expression level in SF.

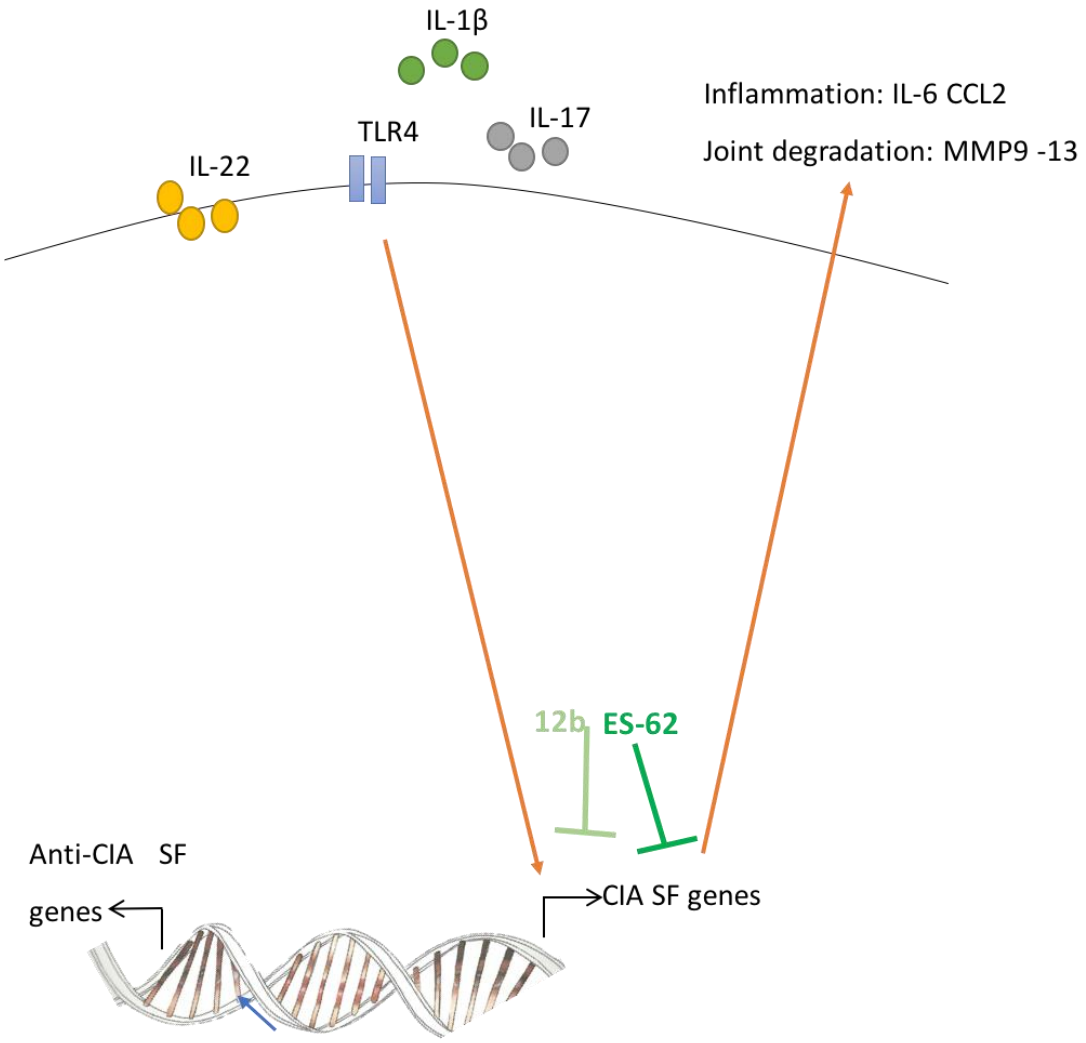
IL-1β
IL-17
TLR4
IL-22
Inflammation: IL-6 CCL2
Joint degradation: MMP9 -13
12b
ES-62
Anti-CIA SF genes
CIA SF genes

4. ES-62 modulates the SF responses to pro-inflammatory cytokines.

4.1 Introduction

SF are key cells in the development of joint pathology in RA as they are involved in promoting both inflammation and bone resorption. They therefore present a perfect therapeutic target since any such therapy would be joint specific and not leave the patient open to systemic immunosuppression, as many current drugs do[154]. It is therefore crucial to understand the mechanisms by which these cells become activated, and maintain their hyperactivated pathogenic phenotype. T cell invasion of the joint seem to be an early event in the establishment of disease, as it occurs even before pannus formation[155] and results in their secretion of a wide range of pro-inflammatory mediators that shape the pathogenic environment that contributes to the activation and "transformation" of SF. Indeed, several cytokines such as IL-17, IL-6 and IL-1ß have already been identified as being able to induce a pathogenic phenotype of SF[156]. Since exposure to ES-62 during CIA appears to suppress the development of hyperesponsive SF[104], it is important to understand whether this reflects an ability to rewire fibroblasts such that they lose the capacity to respond to these cytokines in a pathogenic manner. As such cytokines are in themselves targets of ES-62[104], this would effectively disrupt amplification/perpetuation of pathogenic inflammation. Relating to this, the pleiotropic cytokine, IL-22 plays key dual roles in regulating inflammation during RA: thus, it has been elegantly demonstrated that whilst IL-22 mediates pro-inflammatory functions early in CIA, once inflammation has been established it is involved in the resolution of joint inflammation[133]. Moreover, ES-62 appears to suppress CIA joint pathology, at least in part, by promoting rewiring the responses of SF towards the resolution and tissue repair functions of IL-22[133] to counteract the potential inflammatory actions of this cytokine. Understanding the (ES-62-targeted) mechanism(s) by which the responses of SF to pleiotropic cytokines such as IL-

22 can switch from pathogenic to tissue repair functions potentially offers a good therapeutic strategy. It is therefore necessary to dissect the downstream signalling responses elicited by such pleiotropic cytokines during these distinct functional outcomes in order to understand how ES-62 achieves such desensitisation of the pathogenic responses of SF. Potential targets are provided by evidence that IL-22, like IL-10, may be able to differentially induce STAT1 or STAT3 activation and IL-6 can activate either ERK or STAT3 signalling depending on the context[157]. Thus, depending on the signalling pathway induced by the cytokine, different genes will be induced to drive differential effects: coupling to a particular signalling pathway is regulated environmental co-signals, for example, in RASF, ERK signalling activation by IL-6 is enhanced by the presence of IL-1ß[158].

Mitogen-activated protein kinases (MAPKs) comprise a family of serine/threonine protein kinases that are activated in response to a broad range of extracellular stimuli (mitogens, growth factors, cytokines or stress) acting via a variety of receptor, (cytokine and chemokine receptors, integrins, TLRs, Growth Factor Receptors (intrinsic receptor tyrosine kinases) and Antigen and Fc Receptors) types[159] (Figure 4-1). Once activated MAPKs can translocate to the nucleus to modulate target gene expression, via transactivation of transcription factors. In humans, there are currently 7 families of MAPK divided into the classical MAPKs (ERK 1/2, p38, JNK proteins and ERK5) and the atypical MAPKs (ERK3, ERK4, ERK7 and NLK)[160]. Dysregulation of classical MAPKs has been proposed to be central to the pathophysiology of RA[161], these being found to be hyper-activated in the RA synovium[162]: reflecting this, the ERK MAPK signalling cascade (Figure 4-1) is generally considered to be a key regulator of cell proliferation, survival and differentiation and indeed, its over-activation is often observed in cancer cells[163]. In RASF, the ERK pathway seems to play a major role in the downstream signalling of pro-inflammatory cytokines such as IL-17, TNFα, IL-1 and IL-6, as well as perpetuating their production[164]. Moreover, other events promoting joint destruction also seem to be dependent on this signalling pathway. For instance, IL-1ß upregulates ICAM-1 expression in an ERK-dependent manner to enhance leukocyte adhesion[165], whilst Cadherin-11

signals through ERK to produce MMPs[166]. Indeed, inhibition of ERK signalling can prevent the development of pathology, in the CIA mouse model of RA[167].

Likewise, JAK/STAT signalling (

Figure 4-2) is critical for many cytokine receptors, particularly type I and II cytokines, providing rapid gene induction regulating cell proliferation, survival, differentiation as well as pathogen resistance via the induction of pro-inflammatory responses[168]. Dysregulation of JAK/STAT signalling has been implicated in a number of aberrant inflammatory disorders such as irritable bowel disease, dermatitis and RA[169] as well as cancers[170]. Indeed the key roles for JAK/STAT signalling in RA[171] has generated interest in the therapeutic potential of inhibitors of JAKs (Jakinibs) and more recently, STATs[172]. For example, focusing on the synovium, in RA patients, STAT1 expression and activation (generally associated with IFN signalling) has been reported to be at a high level, particularly in T cells, B cells and fibroblasts isolated from the intimal lining[173]: perhaps consistent with this, STAT4, that is required for Th1 and consequent IFNγ-mediated responses, is also highly expressed in the synovium and also appears necessary for the development of proteoglycan-induced inflammatory arthritis in mice [174]. Likewise, a role for STAT5 has been implicated in RA pathogenesis: this follows demonstrations that CCL13, which acts as an attractant for inflammatory cells and can exhibit immunomodulatory actions on stromal cells, is produced by RASF in response to IL-6 in a STAT-5, ERK and P38 MAPK dependent manner. However, In RASF STAT3 signalling has been shown to be particularly important as indeed, the survival of RASF is dependent on STAT3 activation[175] and it is well established that STAT3 is activated in response to TNFα, IL-6 and IL-1ß[176]. Moreover, and pertinently to this project, STAT3 signalling has been reported to be responsible for the rewiring of RASF, generation of Th17 responses as well as the production of MMPs and RANKL, the latter mediators resulting in osteoclast differentiation[177]. STAT molecules are fine tuners of downstream signaling and can target a wide range of genes in a context-dependent manner. Therefore, it is important to analyse how STAT3 is activated in SF although the balance between STAT3 and STAT1, which can be modulated by

IFNs, will be of particular interest here since IL-22 may exhibit its pleiotropic effects in CIA by differentially inducing proliferative STAT3- or apoptosis-inducing STAT1 signalling. Such tight regulation of STAT3/STAT1 balance could potentially explain the rewiring by ES-62 of IL-22 responses from pathogenic towards those promoting resolution of inflammation and tissue repair.

In this chapter the main aim is to understand how ES-62 regulates the capacity of SF to respond to the various pro-inflammatory cytokines present in the joint during inflammation, and more precisely, determining whether:

- ES-62 affects SF directly rather than as a result of downregulation of the local pro-inflammatory environment, *in vivo*?
- ES-62 inhibits pathogenic activation of ERK pathways?
- ES-62 downregulates STAT3 and/or upregulates STAT1 signalling?
- ES-62 resets the STAT3/STAT1 balance by inducing IFNs or SOCS proteins to induce STAT1 and inhibit STAT3 activation, respectively?

Answering these questions will inform on the mechanism by which ES-62 can render the aggressive phenotype of SF hyporesponsive to the pro-inflammatory environment and/or induce a protective phenotype during the development of CIA.

4.2 ES-62, and its SMAs, directly modulate the capacity of SF to respond to pro-inflammatory cytokines and TLR ligands.

In the previous chapter it was established that *in vivo* treatment with ES-62 reduced the aggressiveness of SF responses when compared to those from the disease untreated mice (CIA SF). Although this could be explained by ES-62 acting to reduce inflammation in the joint, it was important to determine whether ES-62 could act directly on SF. ES-62 can act directly on a number of cells, including T cells and dendritic cells and this action is TLR4 dependent, since TLR4 KO cells do not respond to ES-62[178], and results in the downregulation of MyD88 and consequent inhibition of downstream functional responses[104,179]. Likewise, its SMAs, 11a and 12b, but not the inactive 19o compound, also act to downregulate MyD88[132]. Interestingly, therefore, as SF express TLR4 at their surface[180], hypothetically they can be directly targeted by ES-62 (and potentially by extension its SMAs), acting intrinsically to prevent SF activation. *In vitro* treatment of SF, expanded from mice with CIA *ex vivo*, with ES-62 and the SMAS 11a and 12b revealed that these molecules could directly modulate cell activity. Thus, *in vitro*, ES-62 (≥ 0.25 μg/ml) is able to reduce the ability of SF derived from mice undergoing CIA (CIA), to produce IL-6 in the presence or absence of LPS, a surrogate for endogeneous TLR4 ligands (Figure 4-3A). The SMAs 11a and 12b both also directly modulated LPS-induced IL-6 production by the SF although only 11a significantly reduced basal IL-6 production (Figure 4-3B). It was therefore decided to investigate whether ES-62 modulated MAPK and/or STAT signalling to intrinsically prevent the SF activation during inflammatory arthritis.

4.3 ES-62 suppression of the capacity of SF to respond to external pro-inflammatory molecules is associated with inhibition of the ERK signaling pathway.

As MAPKs play central roles in driving the production of cytokines and MMPs in RAs, they have been presented as good candidate targets for therapeutics[161]. Pertinently, in SF, ERK signalling is crucial for IL-6 secretion[164,181]: thus, in terms of ES-62 therapeutically rewiring these cells it was important to determine which pathogenic stimuli could activate this pathway. Interestingly, therefore, given their disease initiating potential, whilst IL-17 can stimulate ERK activation in SF, as evidenced by the dual (thr/tyr) ERK phosphorylation, this did not appear to be the case for IL-22, or indeed the TLR4 ligand, LPS either at 20 min post-stimulation (Figure 4-4), or over a 0-120 min time course for naïve and CIA SF (results not shown). Moreover, and consistent with the idea of ERK driving SF pathogenicity, inhibition of IL-17-mediated ERK activation using the MEK PD98059 inhibitor (Figure 4-5A) resulted in a significant decrease of IL-6 production by SF from CIA mice in response to either IL-17 or IL-17 combined with IL-22 (Figure 4-5B). Similarly, the level of MMP9 and MMP13 was significantly reduced with the inhibitor in response to IL-17 stimulation (Figure 4-5C). Consistent with the proposal that SF are desensitised to IL-22 pro-inflammatory signalling during established disease, such *in vitro* stimulation with IL-22 alone did not significantly induce IL-6 production and if anything, tended to suppress the IL-17-mediated response.

In addition, it appears that SF from mice with CIA display higher levels of ERK activation than SF from naïve mice (Figure 4-6) and this may be consistent with the idea that CIA SF are tumor-like cells and display a deregulated intracellular signalling network compared to naïve SF. As seen previously with the BALB/c SF (Figure 4-4), IL-17 is able to induce strong ERK activation in SF from both naive and CIA mice on the DBA/1 background (Figure 4-6) Interestingly IL-22 displays a different activity depending on the disease

status of the derived SF. Thus, in naïve SF, IL-22 by itself does not really modulate ERK activation, but can efficiently inhibit ERK activation otherwise induced by IL-17: however in cells from CIA mice, consistent with its inflammation-resolving activity in established disease, IL-22 strongly reduces the elevated basal ERK activation and tends to weakly antagonise the limited further hyperactivation observed in response to IL-17, the latter perhaps reflecting its marginal suppression of IL-6 production under these conditions of acute exposure to IL-22 (Figure 4-6A). In addition, ES-62 was extremely efficient in inhibiting ERK signaling induced by IL-17 stimulation in SF from naive mice, however this capacity to inhibit such responses was largely revoked in CIA SF (Figure 4-6): collectively, these data may suggest that ES-62 could act on healthy SF to prevent their pathogenic activation but once the aggressive phenotype is established, such acute *in vitro* exposure to ES-62 is not sufficient to dramatically suppress the elevated ERK signalling observed in SF derived from mice with CIA.

Importantly, therefore, SF from CIA mice treated with ES-62 *in vivo* exhibited levels of basal ERK activation comparable than those seen in SF from naive mice and profoundly lower levels than those observed with CIA SF fibroblasts stimulated with IL-17, which demonstrated strong hyperactivation of ERK 30-60 min post-stimulation in vitro. Moreover, SF obtained from CIA mice in which the administration of recombinant IL-22 *in vivo* resolved joint inflammation (SF derived from the relevant mice in Pineda *et al.*[133]), likewise exhibited IL-17-resistant profile comparable to that observed with SF from naive mice or ES-62-treated mice (Figure 4-7A). As well, such effect of ES-62 on ERK activation is observed after 24 hours stimulation with IL-17 (Figure 4-7B). Moreover, 24 hours stimulation reveals to be enough to bring naïve SF to a level of ERK activation even higher than CIA SF. These findings therefore perhaps provide further support for ES-62 acting to harness the inflammation-resolving activities of IL-22 in the joint[133] to intrinsically desensistise SF responses, as well as suppressing the production of IL-17 that promotes the aggressive SF phenotype[133].

4.4 ES-62 modulates the capacity of SF to respond to pro-inflammatory cytokines by targeting STAT pathways

As described in section 4.1, STATs, particularly STAT3, are activated downstream of many cytokines implicated in RA pathogenesis, such as IL-17, IL-6 and IL-1β[182,183]. Moreover, IL-22 exhibits pleiotropic functions reflecting its ability to differentially activate either proliferative STAT3[175] or apoptosis - inducing STAT1[184] signalling. Thus, it was of interest to investigate whether ES-62 achieved its desensitisation of SF responses to IL-17 by targeting STAT3 and/or STAT1 in addition to its modulation of ERK activation in CIA SF.

4.4.1 IL-17 drives CIA SF aggressiveness through STAT3 activation, which can be reduced by ES-62

Perhaps reflecting the role of IL-17-driven STAT3 in SF pathogenicity[175], a pilot study in BALB/c fibroblasts (Figure 4-8) showed that IL-17, but not LPS or IL-22 acutely induces STAT3 phosphorylation in such healthy cells, despite IL-22 promoting pathogenic SF rewiring during initiation of CIA[133] and RA[185]. However, IL-22, a member of the IL-10 family has previously been shown to have the capacity to signal via STAT3 and STAT1, depending on the micro-environmental context[186] and thus, a further study was realised in SF from naïve DBA/1, which are prone to CIA to determine whether this lack of IL-22-STAT3 signalling suggested that STAT3 was not important for this cytokine's effects or alternatively, SF from healthy BALB/c were not suitably "conditioned" to respond to this pro-inflammatory mediator Figure 4-9.

Perhaps reflecting this, on this mouse (inflammatory) genetic background, treatment with IL-22 alone also appears to induce STAT3 phosphorylation in these SF from naive mice (Figure 4-9A-B). As well once combined to IL-17, IL-22 reduced IL-17 potential to induce STAT3, which again highlights the

protective role of IL-22 in pro-inflammatory environment. Interestingly, therefore, pre-treatment of naïve SF *in vitro* with ES-62 efficiently reduced IL-17-mediated STAT3 activation by suppressing STAT3 phosphorylation.

In addition analysis of STAT3 phosphorylation in resting SF from ES-62-treated mice revealed that such cells exhibited reduced levels of phosphorylated STAT3 compared to those from CIA SF or naïve SF (Figure 4-9C).

Thus, the role of STAT3 in driving IL-17 and/or IL-22 –mediated rewiring of SF, was assessed by investigating the effect of 5.15 DPP, a STAT3 inhibitor, on the levels of IL-6 produced by CIA SF exposed to these stimuli **Figure 4-10**). After validating the efficacy of this inhibitor (at 50 μM, 5.15 DPP should inhibit in theory at least 50% of STAT3 activity (**Figure 4-10**A-B). Such inhibition of STAT3 activation prevented the production of IL-6 induced by IL-17, or IL-17 plus IL-22 supporting the idea that Il-17-stimulated STAT3 promotes and maintains the pathogenic SF phenotype (Figure 4-10C). By contrast, the little or no IL-6 production resulting from exposure of pathogenic CIA SF to IL-22 is not modulated by the inhibitor, findings consistent with the apparent inability of IL-22 to stimulate any of ERK, STAT3, or IL-6 production in SF from CIA in the established phase of disease, where this cytokine rather seems to play a role in inflammation resolution. Interestingly, whilst 5.15 DPP also significantly induced a decrease in the MMP9 expression induced by IL-17 (Figure 4-10D), there was no significant effect on MMP13 expression, perhaps indicating some differential regulation of these effector proteases. In any case, STAT3, like ERK, indeed seems to be a pathogenic driver of IL-17-, but not IL-22 mediated CIA SF responses.

4.4.2 ES-62 promotes STAT1 activation

ES-62 has been shown to protect against CIA not only by reducing the production of IL-17 and SF sensitivity to IL-17[104], but also by increasing IL-22 production in the joint and resetting its signaling towards desensitisation of SF responses[133]. As mentioned previously IL-22 is a member of the IL-10 family that is able to activate either STAT3 or STAT1, depending on the

inflammatory context[186]. Consistent with its pathogenic role in (IL-17-mediated) SF transformation, STAT3 has previously been shown to induce SF survival and proliferation[175] and here, IL-6 and MMP9 expression. By contrast, STAT1 induces a set of pro-apoptotic genes[173]. Therefore, since ES-62 can suppress STAT3 activation, it is of interest to understand whether this is accompanied by an upregulation of counter-regulatory STAT1 signalling. Pertinently, STAT1 is usually activated by IFNs (IFNɣ or IFNα and IFNß[187]) and IFNß has found to be protective in the joint during the established phase of disease in the CIA model[188]. It was therefore investigated whether ES-62 can induce IFNß production and consequently STAT1 activation (Figure 4-11).

Acute treatment of SF from naive mice with IFNß (but not IL-6 which has been shown rather to drive pathogenic STAT3 activation[177]), was found to stimulate STAT1 activation (Figure 4-11A), whilst more chronic treatment (24 h) induced an increase in the expression of STAT1 protein (Figure 4-11B). Interestingly, as this was not recapitulated by ES-62 directly, the finding that ES-62 SF constitutively displayed phosphorylated STAT1 (Figure 4-11C-D), suggested that this may be as a result of ES-62 promoting IFNß production by SF in response to inflammation in the joint. Consistent with this, analysis of SF from naive, CIA or ES-CIA mice showed that when such cells were subsequently exposed to IL-17 *in vitro*, those exposed to ES-62 *in vivo* were able to significantly upregulate IFNß expression at the mRNA level (Figure 4-11E). Collectively, therefore, these data may suggest that as a result of the high levels of IL-17 signalling in the joint, ES-62 induces IFNß expression that can facilitate the induction and activation of STAT1, whilst downregulating STAT3 signalling to reset IL-22 towards inflammation resolution during CIA.

4.5 ES-62 and 12b mediated modulation of SF sensitivity to cytokines is associated with induction of suppressors of cytokine signaling (SOCS)

The SOCS protein family are involved in the inhibition of the JAK-STAT signaling pathways and hence have frequently been implicated as being dysfunctional in autoimmune dysregulation[189]. SOCS1, cloned in 1997 by Starr et al[190] despite being able to inhibit IFNɣ signaling has been shown to be highly expressed in RA patients[191] and proposed to act by promoting SF motility[192]. However, another well studied SOCS family member is SOCS3 that is widely-established suppressor of STAT3 signaling[189]. Therefore, as ES-62 targets both IFNγ and IL-17 in CIA, to further understand how ES-62 regulates JAK/STAT responses to cytokines in SF, it was decided to next investigate its effect on SOCS1 and SOCS3 expression (Figure 4-12). First of all, consistent with the pathogenic effector role of IFNγ, it appears that CIA SF express less SOCS1 mRNA than SF from naive mice. Rather counter intuitively therefore, SF from CIA mice express more SOCS3 mRNA than those from naïve SF: however, this may be evidence of a homeostatic negative feedback loop to limit inflammation, as exposure to either ES-62 or 12b *in vivo* induced significant increases in the expression of both SOCS1 and SOCS3 at the mRNA level. Such upregulation of SOCS1 by 12b is was well seen at protein level (Figure 4-13A) and abrogated by IL-1ß but even more interestingly mice treated therapeutically with 12b, where disease progression is stopped by 12b, display a strong SOCS1 production in their SF potentially acting as a negative feedback loop and allowing the resolution of inflammation (Figure 3-13B).

4.6 Discussion and conclusions

The proposal that IL-17 is important in driving SF pathogenicity[7,28,105] is further supported by the data presented in this chapter. In addition, they also

provide more evidence that activation of both the ERK and STAT3 signaling pathways is required for the induction of pathogenic response genes, namely mediators of inflammation (IL-6) and tissue and bone destruction (MMP9 & MMP13). By contrast, the role of IL-22 appears to be more complicated, as, despite its pro-inflammatory role in the initiation phase of CIA, it did not appear to activate either ERK or STAT3 signalling. Rather, and consistent with its inflammation-resolving role in established disease, it reduces the activation of both ERK and STAT3, but not to the same extent as ES-62. These data are therefore perhaps consistent with ES-62 mediating its effects on SF, at least in part, by promoting IL-22 production, as indicated by previous studies that showed that blocking of IL-22 during the established phase of CIA abolishes protection afforded by ES-62[133].

Nevertheless, these new data also suggest that both ES-62 and its SMAs can prevent the acquisition of a pro-inflammatory, bone destroying phenotype of SF by directly targeting SF, presumably at least in the case of ES-62 through subversion of TLR4 signalling, which has previously shown to be necessary to perpetuate Th1 and Th17 response in RA[150]. Thus, in addition to suppressing the aggressive phenotype of SF in CIA by ES-62 acting to reduce the levels of IL-17 in the joint[104], it appears that the more recent data suggesting that it also acts to modulate the phenotype of SF such that they will no longer efficiently respond to IL-17 may reflect these new findings that ES-62 efficiently prevents IL-17 from stimulating both ERK and STAT3 activation in SF during CIA.

The molecular mechanisms involved in this desensitisation are not clear but appear to involve ES-62 inducing STAT1 signalling that likely acts to counteract STAT3 signalling, perhaps by inducing apoptosis of the aggressive SF. Moreover, this rebalancing of STAT1/STAT3 signalling provides a potential mechanism for the hypothesis that ES-62 promotes rewiring of IL-22 signalling in SF to an anti-proliferative/anti-inflammatory phenotype as this cytokine has the capacity to differentially couple to STAT1/STAT3 depending on the context[193]. Nevertheless, the data presented here suggest that ES-62 may not directly induce STAT1 expression but rather that this effect may be secondary

to its induction of IFNß, a cytokine which has been shown to be protective in CIA. Indeed, mice lacking IFNß display more severe disease in the CIA model not only in terms of SF phenotype, but also with respect to the development of pathogenic osteoclasts and macrophages, but not T cell, responses [194]. Thus, we can hypothesize that ES-62 resets IL-22 towards inflammation resolution by switching the balance of the downstream signaling towards STAT1, thanks to the production of IFNß, and as well as the reduction of IL-17-mediated activation of STAT3 (Figure 4-14).

The mechanisms involved have not been fully dissected, but there are various ways to desensitise cells, such as for instance reducing the level of cytokine receptors at the surface, or as shown here by inhibiting their downstream signaling pathways and/or promoting feedback loops involving negative regulators like the SOCS family members. Indeed, this preliminary investigation of the mechanisms underpinning the modulation of STAT3 signaling revealed that both ES-62 and 12b promoted the expression of SOCS1 and 3, molecules that negatively regulate JAKSTAT signalling. These findings are consistent with ES-62 desensitising SF to both Th1 (IFNγ STAT1 signalling is inhibited by SOCS1[195]) and TH17- (IL-1β, IL-6 and IL-17 STAT3 signalling is inhibited by SOCS3[189]) driven inflammatory responses in the joint, in addition to reducing the absolute levels of these pathogenic cytokines. Certainly, directly targeting the downstream effectors potentially allows ES-62 to control the actions of many cytokines that exhibit convergent signalling and some of the potential mechanisms for regulating these are investigated in chapters 5 and 6.

Figure 4-1 An introduction to the ERK signalling pathway

This is a generic model of the ERK signalling pathway utilised by a range of receptors including cytokine and chemokine (GPCR) receptors or integrins, TLRs, Growth Factor Receptors (intrinsic receptor tyrosine kinases) and Antigen and Fc Receptors. For example, with tyrosine kinase receptors, once the ligand binds it causes receptor dimerization and consequent phosphorylation of its cytoplasmic domain. This phosphorylation enables adaptors (Shc, GRB2, Crk, etc.) to bind the receptor attracting the relevant guanine nucleotide exchange factors (SOS, C3G, etc.) required to transduce the signal to small GTP-binding proteins (Ras, Rap1), which in turn activate the core unit of the cascade composed of a MAPKKK (Raf), a MAPKK (MEK1/2), and MAPK (ERK). Once activated, ERK can translocate to the nucleus, where it can phosphorylate a variety of transcription factors regulating gene expression, as well as having some cytosolic functions where it phosphorylates multiple substrates such as $cPLA_2$, SOS, EGFR, PDEs, Mnk or RSKs to activate the subsequent downstream pathways[196].

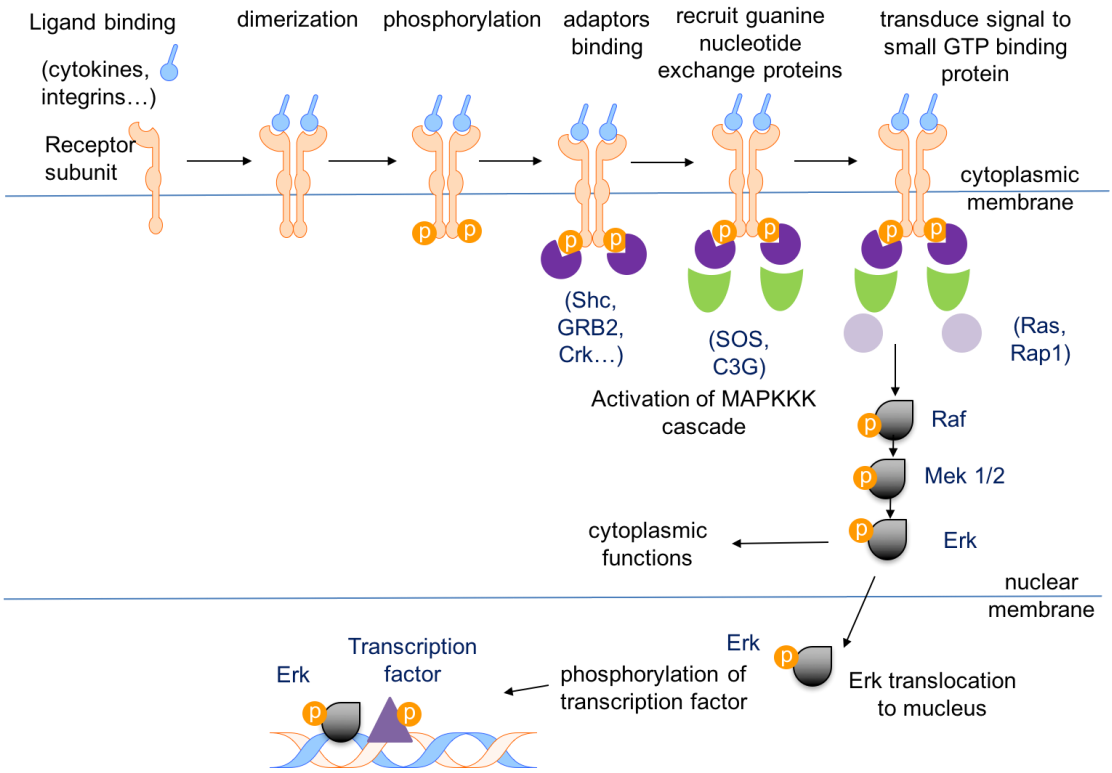
Ligand binding
(cytokines, integrins…)
Receptor subunit
dimerization
phosphorylation
adaptors binding
recruit guanine nucleotide exchange proteins
transduce signal to small GTP binding protein
cytoplasmic membrane
(Shc, GRB2, Crk…)
(SOS, C3G)
(Ras, Rap1)
Activation of MAPKKK cascade
Raf
Mek 1/2
Erk
cytoplasmic functions
nuclear membrane
Erk
Erk translocation to mucleus
phosphorylation of transcription factor
Transcription factor
Erk

Figure 4-2 An introduction to the STAT signalling pathway

This model provides a generic overview of STAT signalling, where cytokine, binding to its receptor induces its oligomerization, resulting in activation of relevant JAK kinases. JAK-mediated phosphorylation (on tyrosine) of the receptor provides binding sites for STATs, which contain phosphotyrosine recognising SH2 domains. Once bound, the STATs also become phosphorylated and dimerize allowing them to translocate to the nucleus to regulate target gene expression. Such STAT signalling is usually transitory since their target genes include the SOCS (suppressor of cytokine signaling) family that act, amongst the various functions of SOCS proteins, directly or indirectly to inhibit JAK/STAT activation. Other signalling elements that contribute to negative feedback are the protein tyrosine phosphatases (PTPs) that can also inhibit JAK activity and/or dephosphorylate the cytokine receptor as well as the PIAS family that target STATS. The functional outcome of JAK STAT signalling depends on the particular STAT recruited and its specific set of target genes.

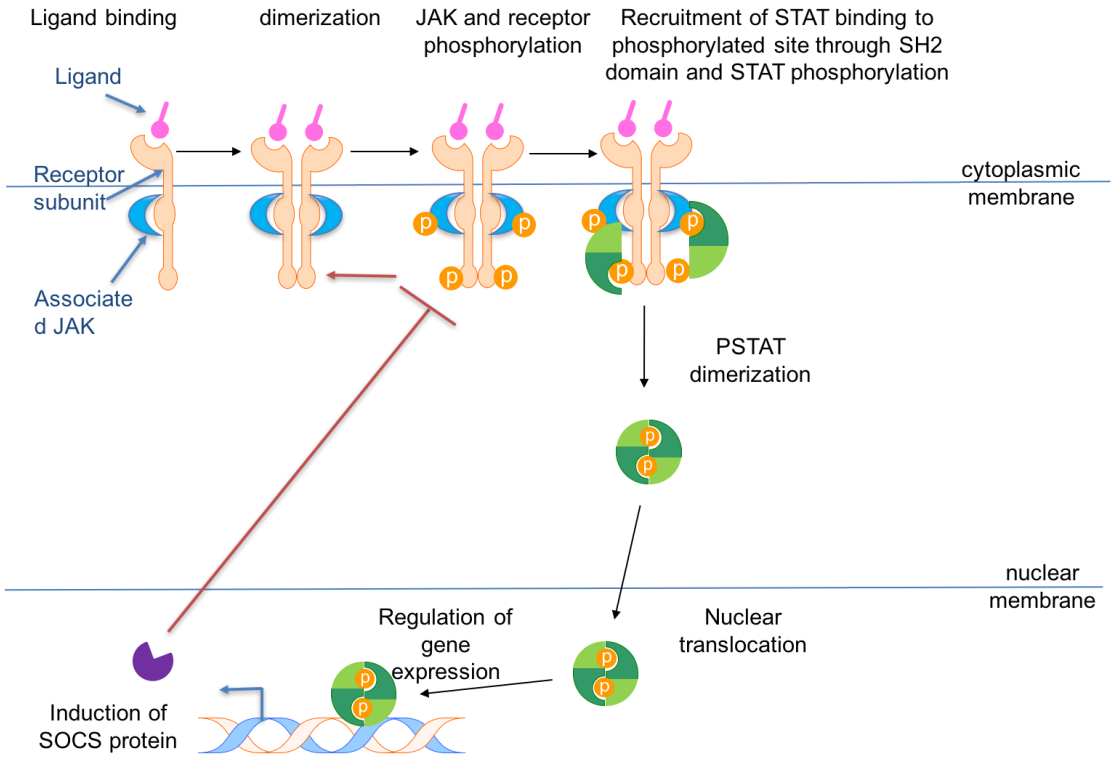
Ligand binding
dimerization
JAK and receptor phosphorylation
Recruitment of STAT binding to phosphorylated site through SH2 domain and STAT phosphorylation
Ligand
Receptor subunit
Associate d JAK
cytoplasmic membrane
PSTAT dimerization
nuclear membrane
Regulation of gene expression
Nuclear translocation
Induction of SOCS protein

Figure 4-3 ES-62, and its SMAs 11a and 12b modulate *in vitro* SF production of pro-inflammatory cytokines in response to pro-inflammatory stimuli.

(A). SF from CIA mice were pooled (mean score 2.43 ± 0.84, n=7) and expanded *ex vivo*. Three independent cultures from this mouse model were plated at 10^4 cells per well in a 96 wells-plate and once synchronised overnight in 1% DMEM were treated *in vitro* for 2 hours with various concentrations of ES-62 (none, 0.25 μg/ml, 0.5 μg/ml and 1 μg/ml) prior to 24 hours stimulation with LPS (1 μg/ml) or DMEM (as control) 10% FCS. Supernatants were collected and IL-6 release measured by ELISA. Data are plotted as the mean values of each of the independent cultures, with each culture being assayed in triplicate. Statistical analysis was by one-way ANOVA with the Tukey multiple comparison post-test where* $p < 0.05$; ** $p < 0.01$, *** $p<0.001$.

(B) SF from naïve or CIA (mean score 4.7 ± 1.5, n=10) mice were pooled and expanded *ex vivo*. From this animal model cells were plated at 10^4 cells per well in order to have 3 independent culture for each *in vitro* treatment. Once synchronised overnight in 1% DMEM, SF were treated *in vitro* for 2 hours with the SMAs 11a and 12b prior to 24 hours stimulation with LPS (1 μg/ml), or as control, in DMEM 10% FCS. Supernatants were collected and IL-6 release measured by ELISA. Data are plotted as the mean values obtained from each independent culture, assayed in triplicated. Statistical analysis was by one-way ANOVA with the Tukey multiple comparison post-test where* $p < 0.05$; ** $p < 0.01$, *** $p<0.001$.

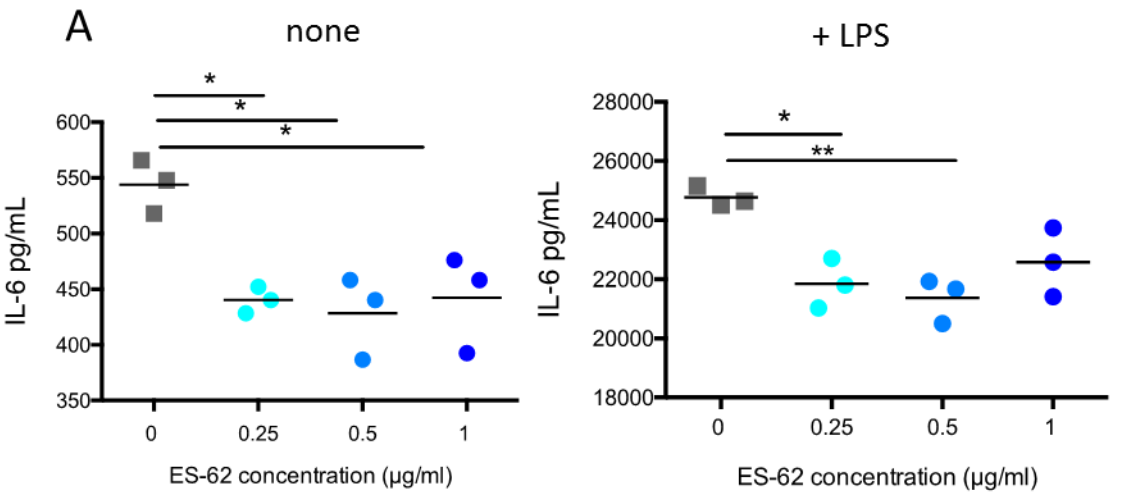
A
none
+ LPS
IL-6 pg/mL
ES-62 concentration (µg/ml)
0
0.25
0.5
1

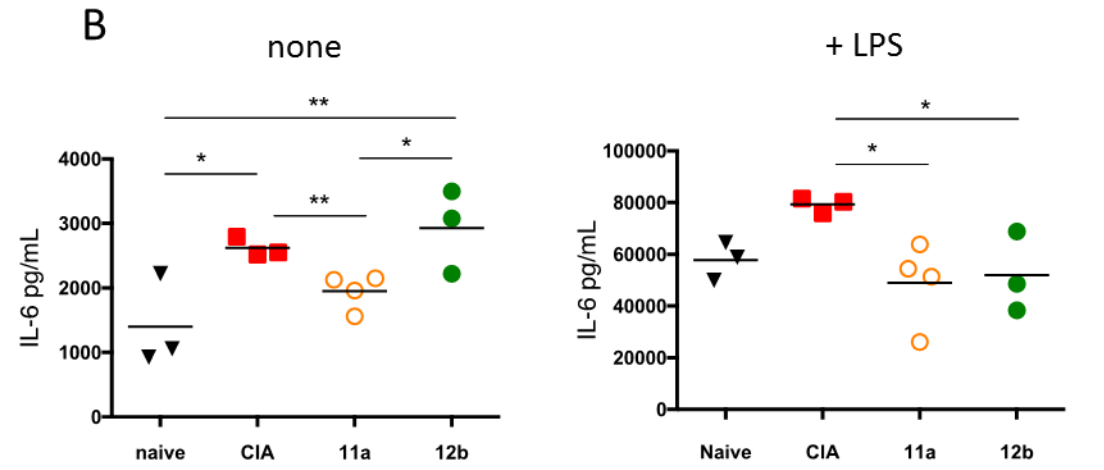
B
none
+ LPS
IL-6 pg/mL
naive
CIA
11a
12b
Naive

Figure 4-4 IL-17 stimulates ERK signaling in SF from naive BALB/c mice

SF were extracted from BALB/c mice and expanded *ex vivo*. After stimulation with LPS (1 µg/ml), IL-17 (25 ng/ml), IL-22 (25 ng/ml), or DMEM (as control) for 20 minutes, cells were then analysed for phosphorylated ERK (pERK, red line) and total ERK (tERK, blue line) expression identified by staining using specific antibodies (relative to an isotype control antibody, black line) and flow cytometry as described in the M&M section (section 2.4). Data are presented as percentage of max on the Y axis and fluorescence intensity of pERK or tERK expression on the X axis.

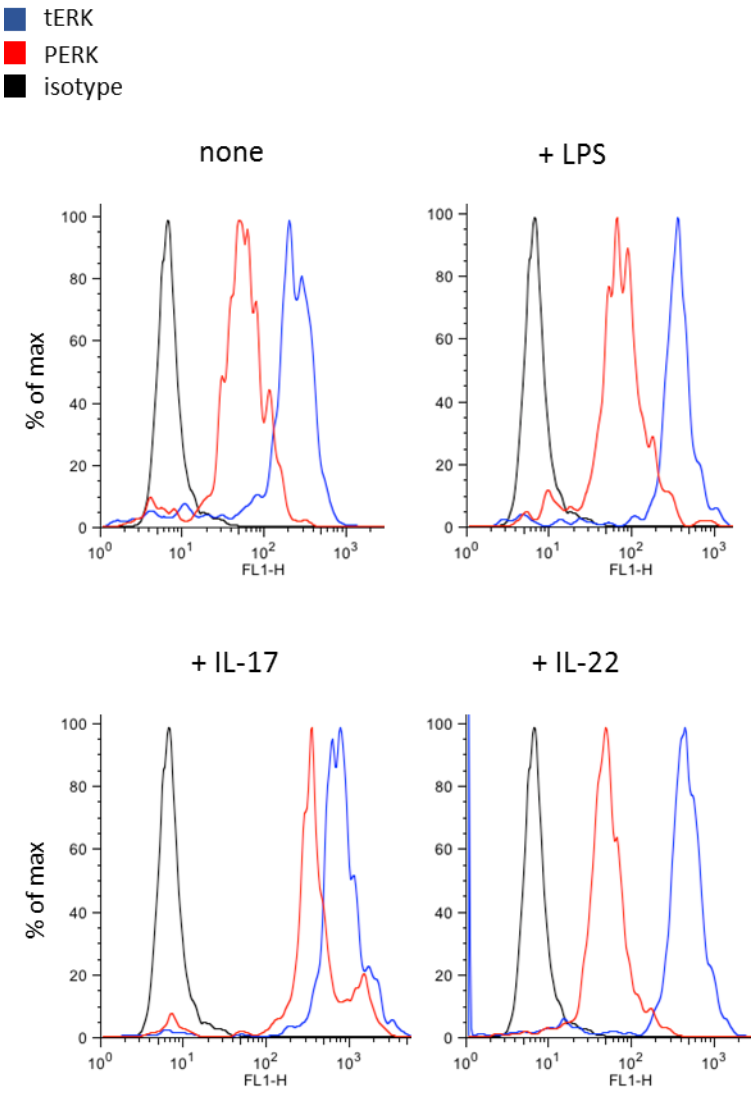
tERK
PERK
isotype
none
+ LPS
+ IL-17
+ IL-22
% of max
FL1-H

Figure 4-5 pd98059 MEK inhibitor suppresses IL-17-stimulated IL-6, MMP9 and MMP13 production by CIA SF

A: SF were extracted and pooled from naïve or CIA (mean score 4.5 ± 1.24, n=10) cohorts of mice and expanded *ex vivo*. Cells from this animal model were plated as independent triplicate for each *in vitro* treatment group at a concentration of 10^4 cells per well. Before being analysed for ERK activation by the FACE assay (as described in the M&M section 2.6), cells were treated for 2 hours with DMEM or the MEK inhibitor, pd98059 (IE, 25 μM[197]) before being stimulated for 20 minutes with IL-17 (25 ng/ml) or with DMEM (as control) and then analysed for ERK activation. ERK activation is represented as the ratio of OD values of pERK/tERK expression and data are expressed as the mean ± SEM of statistical analysis was by 1-way ANOVA with the Tukey post test where * $p < 0.05$.

B-C: SF were extracted and pooled from naïve or CIA (mean score 4.5 ± 1.24, n=10) cohorts of mice and expanded *ex vivo*. Cells from this animal model were plated as independent triplicates for each *in vitro* treatment group at a concentration of 0.3 10^6 cells per well in a 6 well-plate. Before being analysed for cytokine secretion by the ELISA, or mRNA expression by RT-qPCR assays (as respectively described in the M&M section 2.5 and 2.8), cells were treated for 2 hours ± pd98059 (iE, at 25 μM[197]) and then stimulated with IL-17, IL-22 both (at 25 ng/ml), or medium (none) for 24 hours. Supernatants were collected and IL-6 release was measured by ELISA (B) Results are expressed as the mean ± SEM of culture triplicates each assayed in technical triplicate. Statistical significance was shown using Mann-Whitney T-test where * $p < 0.05$; ** $p < 0.01$, *** $p<0.001$. Moreover, total RNA was extracted to measure MMP9 and MMP13 mRNA levels relative to GAPDH by qRT-PCR (C). Results are expressed as the mean ± SEM of culture triplicates each assayed in technical triplicate. They are represented as well relative to the house keeping gene mRNA level, GAPDH. Statistical significance was shown using the 1-way ANOVA with the Tukey post test, where * $p < 0.05$; ** $p < 0.01$, *** $p<0.001$.

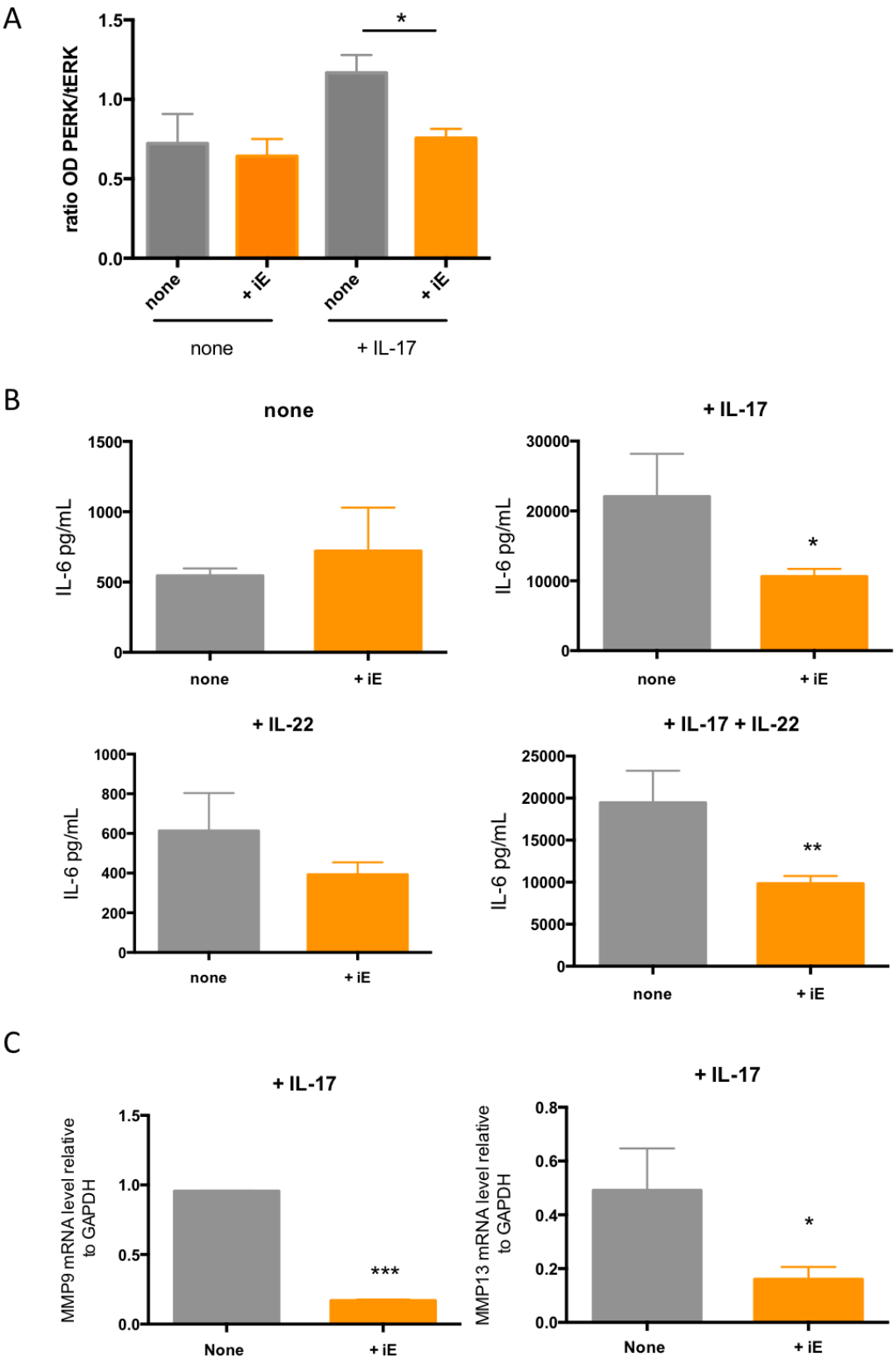
A
ratio OD PERK/tERK
1.5
1.0
0.5
0.0
*
none
+ iE
none
+ iE
none
+ IL-17
B
none
+ IL-17
IL-6 pg/mL
1500
1000
500
0
30000
20000
10000
*
+ IL-22
+ IL-17 + IL-22
800
600
400
200
25000
20000
15000
5000
**
C
+ IL-17
+ IL-17
MMP9 mRNA level relative to GAPDH
MMP13 mRNA level relative to GAPDH
0.8
0.6
0.4
0.2
***
None
+ iE

Figure 4-6 IL-17 induces ERK activation, while IL-22 and ES-62 reduces it in CIA SF

A: SF were extracted from naïve and CIA mice (mean score 2.42 ± 0.84, n=7) and expanded *ex vivo*. After pre-treatment with ES-62 (1 µg/ml) for 24 hours stimulation and stimulation with IL-17 (25 ng/ml), IL-22 (25 ng/ml) for 20 minutes, cells were analysed for phosphorylated ERK (pERK, red line) and total ERK (tERK, blue line) expression identified by staining using specific antibodies (relative to an isotype control antibody, black line) and flow cytometry as described in the M&M (section 2.4). Data are presented as percentage of max on the Y axis and fluorescence intensity of pERK or tERK expression on the X axis.

B: Quantification of the % of Max (representing the normalised cell number) is realised and the ratio of the % of max pERK/tERK is represented in a graph (n=1). No stimulation is in grey, IL-17 in red, IL-22 in purple, IL-17 + IL-22 in bright green and IL-17 + ES-62 in dark blue.

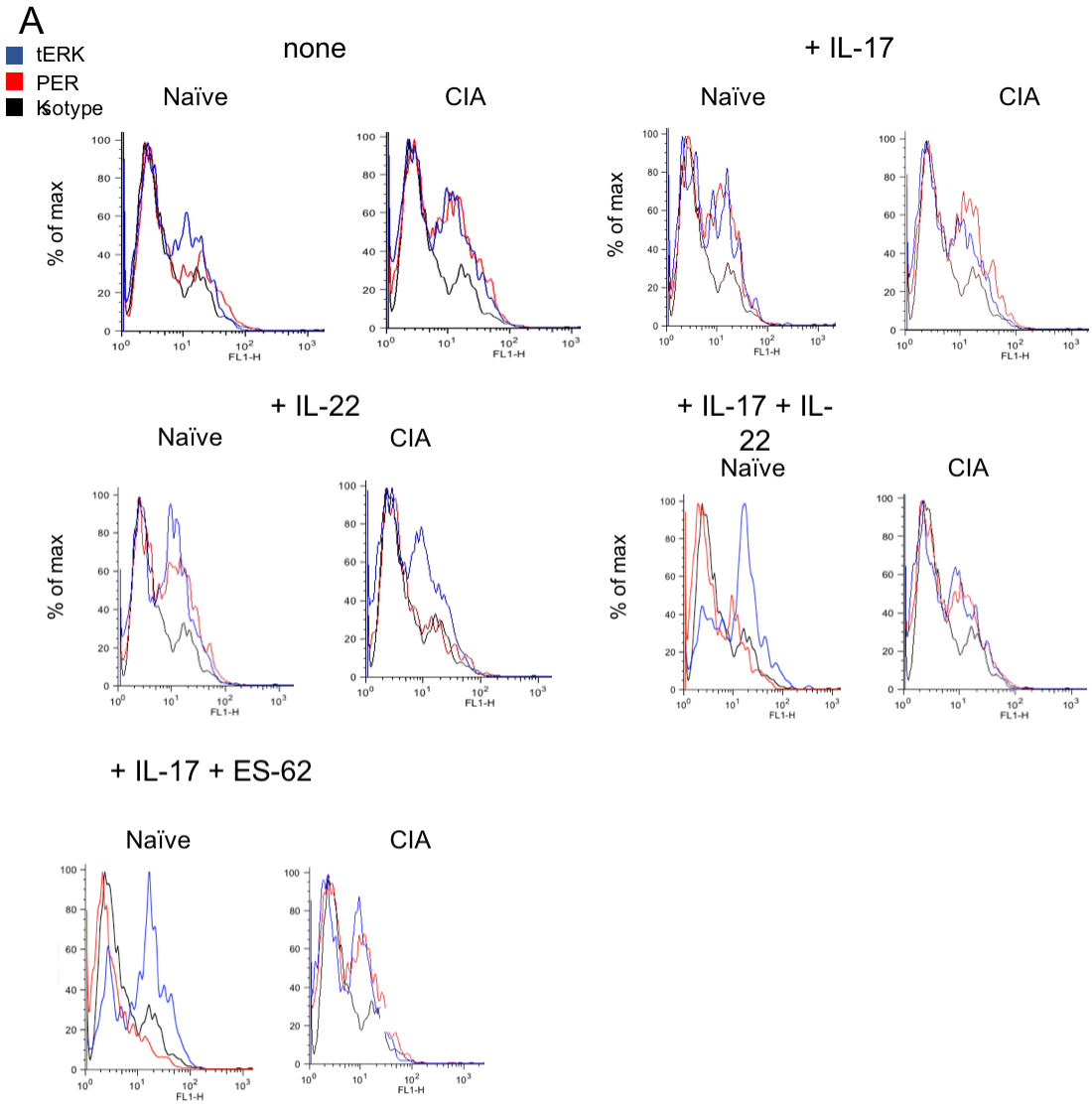
A
tERK
PER
Isotype
none
+ IL-17
+ IL-22
+ IL-17 + IL-22
+ IL-17 + ES-62
Naïve
CIA
% of max
FL1-H

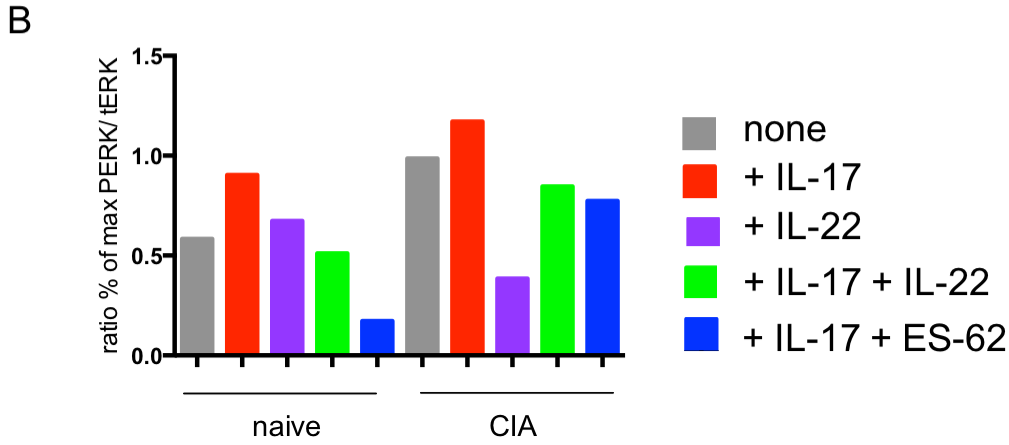
B
ratio % of max PERK/ tERK
1.5
1.0
0.5
0.0
naive
CIA
none
+ IL-17
+ IL-22
+ IL-17 + IL-22
+ IL-17 + ES-62

Figure 4-7 ES-62 and IL-22 *in vivo* reduce as well ERK activation induced by IL-17

A: SF were extracted from naïve, CIA (mean score 2.8 ± 1, n=7), CIA ES-62 treated mice (mean score 0.8 ± 0.8, n=5), as well as those treated therapeutically with rIL-22 *in vivo* (from the previously published animal model by Pineda *et al*[133]. mean score 3.14 ± 0.8, n=4) and were expanded *ex vivo* as plated as three independent cultures for each group treatment. Cells were stimulated with IL-17 (25 ng/ml) for up to 120 minutes, with time points every 20 minutes. To assess levels of phosphorylated ERK, cells were permeabilised and stained for phosphorylated ERK (pERK) and total ERK (tERK) expression by the FACE assay and the data are presented as the OD ratio of pERK/tERK expression and results are expressed as the mean values of the independent cultures (each assayed in triplicate) ± SEM. This experiment is representative of two sets of independent cultures from two different animal model except of the rIL-22 data which were not repeated.

B: SF were extracted from naïve, CIA (mean score 4.5 ± 1.241, n=10) and ES-62 treated mice (mean score 1.714 ± 1.063, n=7) and expanded *in vivo*. Cells from each treatment were plated at the concentration of 0.3 10^6 cells per wells in a 6 wells-plate as independent cultures for each treatment group. After stimulating the cells for 24 hours with IL-17 (25 ng/ml), total proteins were extracted used for pseudo-quantification of pERK and GAPDH by Western blot as described in the M&M section 2.7. Semi quantification by ImageJ of the pERK (both bands together) is presented as relative to GAPDH protein level. Data are represented as the mean + SEM. Statistical significance was shown using the 1-way ANOVA with the Tukey post test, where * $p < 0.05$ and ** $p < 0.01$

A

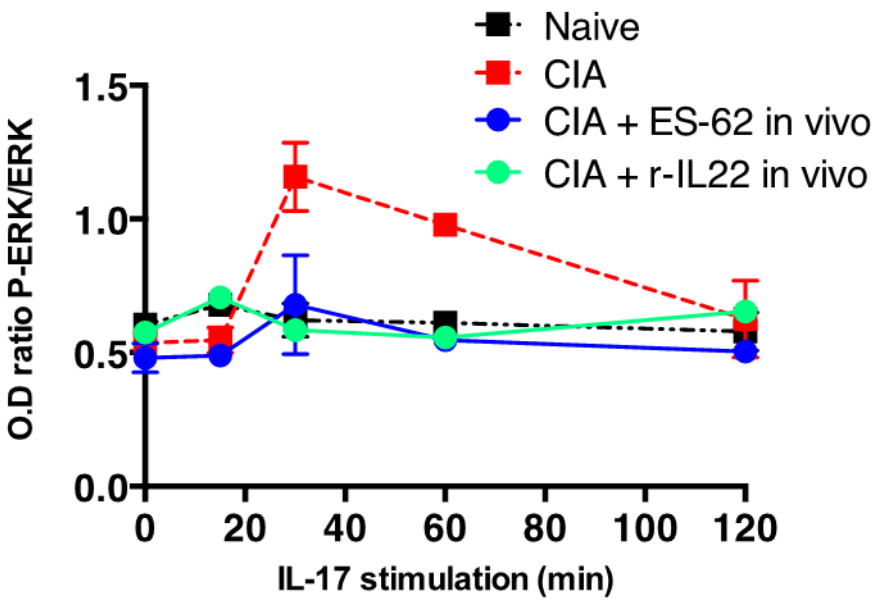
Naive
CIA
CIA + ES-62 in vivo
CIA + r-IL22 in vivo
O.D ratio P-ERK/ERK
1.5
1.0
0.5
0.0
0
20
40
60
80
100
120
IL-17 stimulation (min)

B

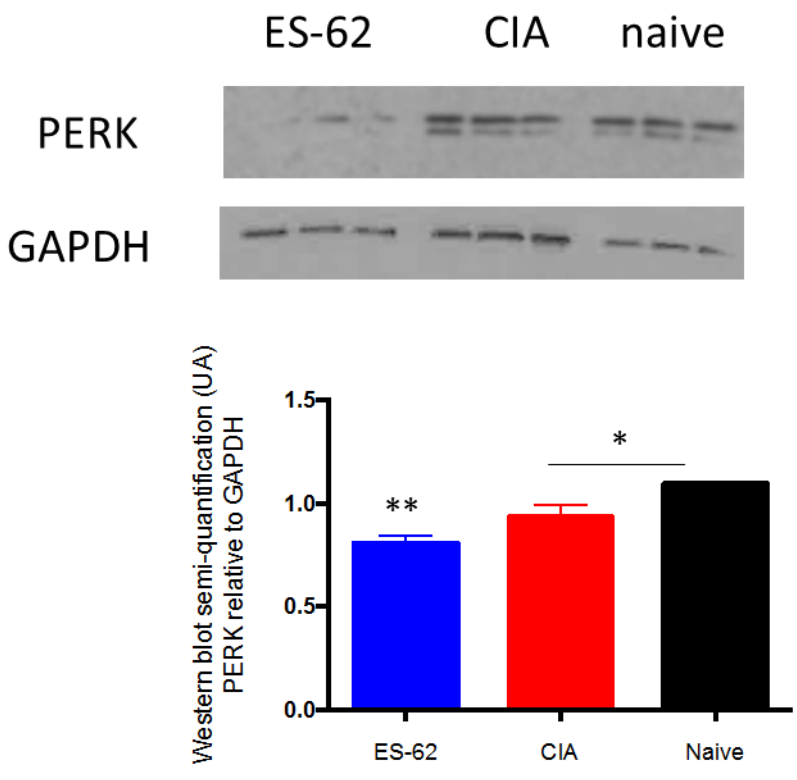
ES-62
CIA
naive
PERK
GAPDH
Western blot semi-quantification (UA)
PERK relative to GAPDH
1.5
1.0
0.5
0.0
**
*
ES-62
CIA
Naive

Figure 4-8 STAT3 phosphorylation is induced by IL-17 in SF from BALB/c mice

SF were extracted from BALB/c mice and expanded *ex vivo*. After stimulation with LPS (1 μg/ml), IL-17 (25 ng/ml), IL-22 (25 ng/ml) or DMEM (as control) for 20 minutes, cells were analysed for expression of phosphorylated STAT3 (PSTAT, red line) and total STAT3 (tSTAT3, blue line) by staining with specific antibodies relative to their isotype control (black line) by flow cytometry as described in the M&M section. Data are present as a percentage of max response on the Y axis (normalized cell count) and fluorescence intensity of pSTAT3/tSTAT3 expression on the X axis.

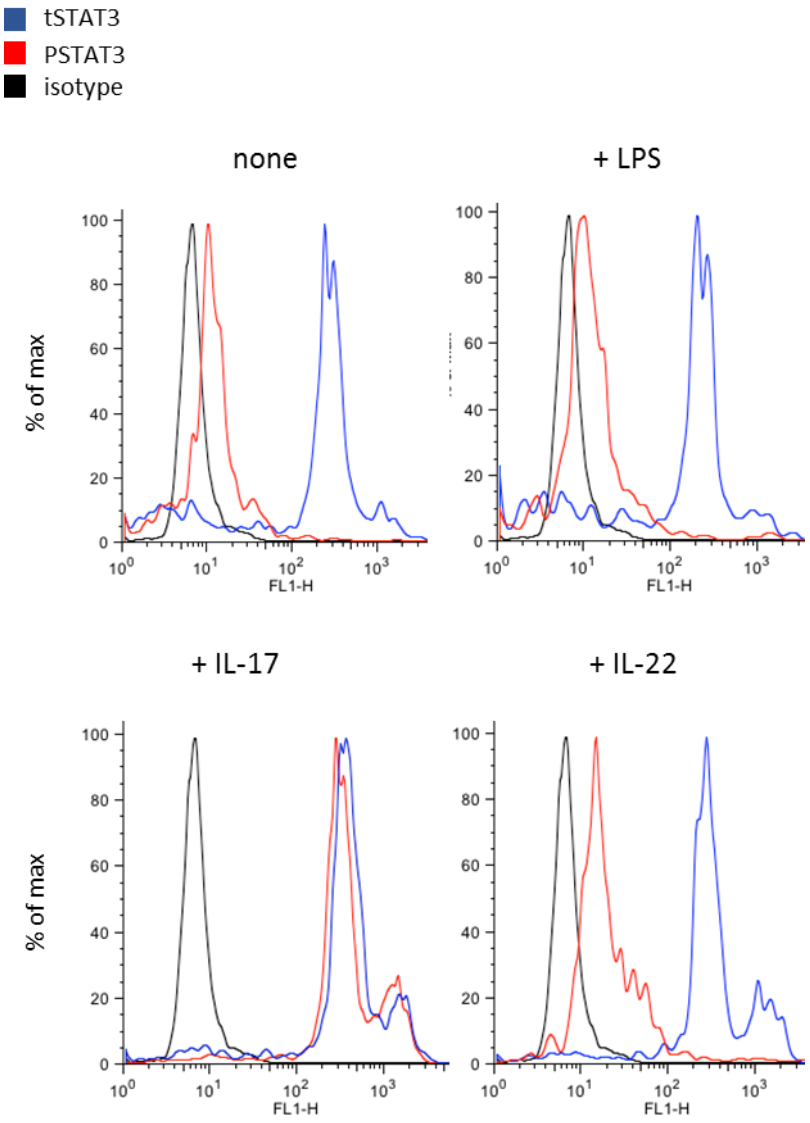
tSTAT3
PSTAT3
isotype
none
+ LPS
+ IL-17
+ IL-22
% of max
FL1-H

Figure 4-9 ES-62 reduces STAT3 activation by IL-17 in naive SF

A: SF were extracted from naïve mice and expanded *ex vivo* for 3 weeks. After synchronizing them overnight in 1 % DMEM, some cells were pre-treated with ES-62 (1 µg/ml) for 24 hours before stimulating all cells with IL-17 (25 ng/ml), IL-22 (25 ng/ml), both cytokines, or DMEM as control for 20 minutes. Cells were thereafter harvested permeabilised and stained intracellularly for phosphorylated STAT3 (pSTAT3, red line), total STAT3 protein (tSTAT3, blue line) and isotype (black line) as described more precisely in the M&M section. Cells were analysed then by flow cytometry. Data are represented as % of max in the Y axis as explained in the M&M and the fluorescence intensity in the X axis

B: Quantification of the mean fluorescence intensity (MFI) is realised and the ratio of the MFI pSTAT3/ MFI tSTAT3 is represented in the graph where DMEM control is in black, IL-17 is in red, IL-22 in purple, IL-17 + IL-22 in bright green and IL-17 + ES-62 in dark blue.

C: SF were extracted from naïve, CIA (mean score 3.17 ±, n=6) or ES-62 (mean score 0.5 ± 0.22, n=6) treated mice and expanded *ex vivo* for 3 weeks and were plated at 1 10^6 cells per well and synchronised overnight in DMEM 1 % FCS. Total proteins were extracted from unstimulated cells in triplicates and pSTAT3 protein was revealed by Western blot. Semi-quantification by ImageJ of pSTAT3 level relative to the constitutive tERK is represented as well. This experiment is representative of 2 independent experiments.

A

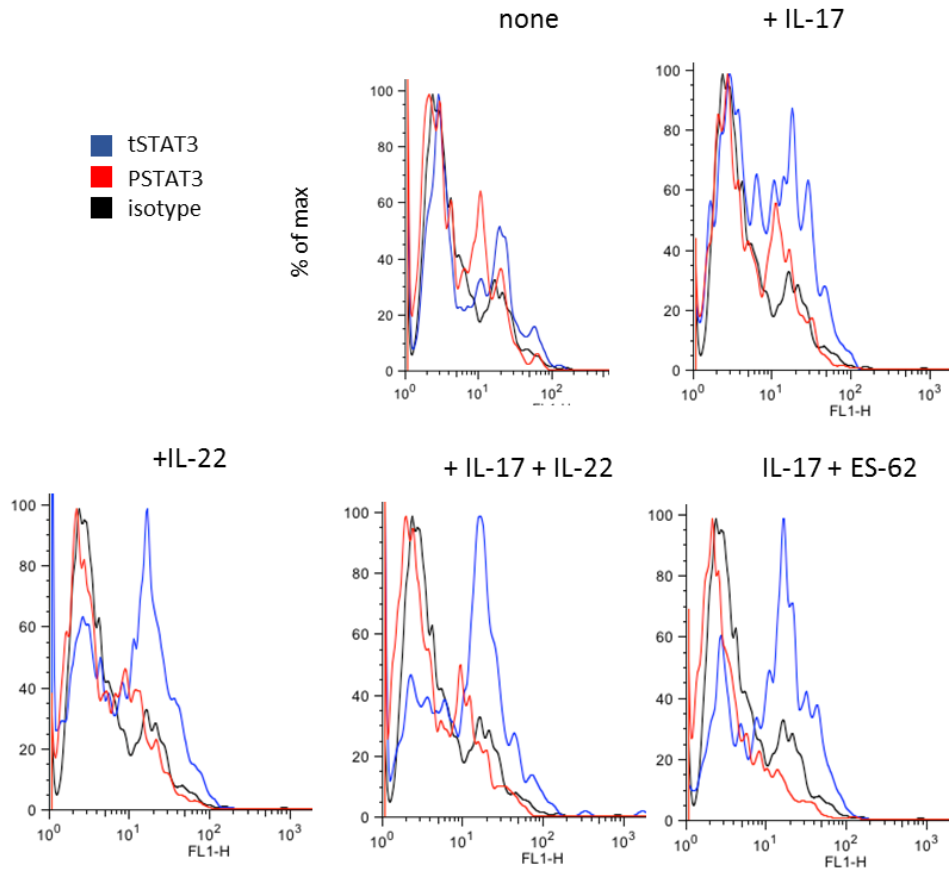
none
+ IL-17
tSTAT3
PSTAT3
isotype
% of max
+IL-22
+ IL-17 + IL-22
IL-17 + ES-62
FL1-H

B

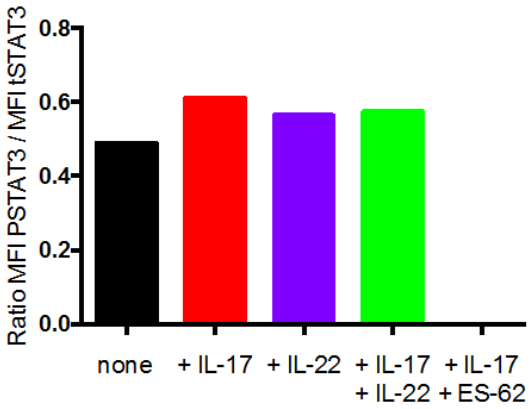
Ratio MFI PSTAT3 / MFI tSTAT3
none
+ IL-17
+ IL-22
+ IL-17 + IL-22
+ IL-17 + ES-62

C

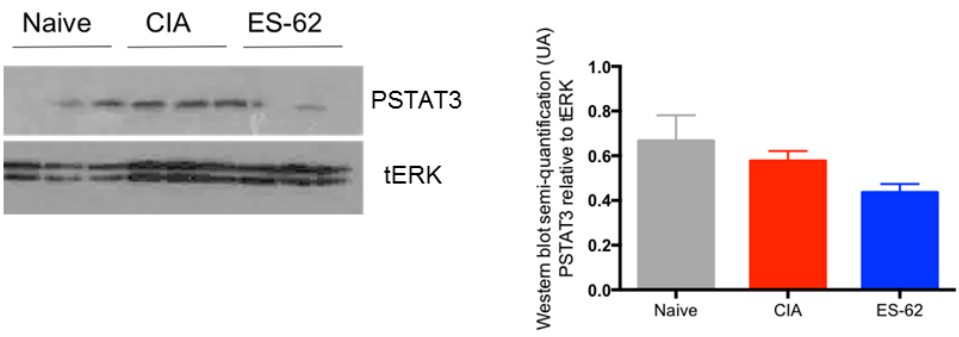
Naive
CIA
ES-62
PSTAT3
tERK
Western blot semi-quantification (UA)
PSTAT3 relative to tERK
Naive
CIA
ES-62

Figure 4-10 Inhibition of STAT3 activation reduces IL-17-stimulated production of IL-6 production and MMP9 by CIA SF

A- (A) SF extracted from CIA mice (mean score 4.5 ± 1.24, n=10) were pulled down and grown *ex vivo* for 3 weeks. The STAT3 inhibitor 5.15 DPP potentiality was assessed on those cells. Cells were plated at 1 10^6 cells per well in a 6 wells plate. After a pre-treatment for two hours with 5.15.DPP (50 μM[198]) and stimulation for 20 minutes with IL-17 (25ng/ml) or with DMEM as control, total protein was extracted and phosphorylated STAT3 (pSTAT3) as well as total STAT3 (tSTAT3) proteins were revealed by Western blot, as described in the M&M section 2.7. (B) Semi-quantification using ImageJ was done and data are presented as a ratio of tSTAT3/tSTAT3 and relative to tERK levels (B). This experiment has been done only once.

C-D: SF extracted and pooled from CIA (mean score 4.5 ± 1.24, n=10) cohorts of mice and expanded ex vivo. Cells from this animal model are the same than the one used in the Figure 4-5B-C (unstimulated control is the same). SF were plated as independent triplicate for each in vitro treatment group at a concentration of 0.3 10^6 cells per well in a 6 wells-plate. Before being analysed for cytokine secretion by the ELISA or mRNA expression by RT-qPCR assays (as respectively described in the M&M section 2.5 and 2.8). Cells were treated with 5.15.DPP (iST, at 50 μM) and stimulated with IL-17 and/or IL-22 both (at 25 ng/ml) or DMEM as control for 24 hours. Supernatants were collected and IL-6 release was measured by ELISA (C) Results are expressed as the mean ± SEM of culture triplicates each assayed in technical triplicate. Statistical significance was shown using Mann-Whitney T-test where * $p < 0.05$; ** $p < 0.01$, *** $p<0.001$. Moreover, total RNA was extracted to measure MMP9 and MMP13 mRNA levels relative to GAPDH by qRT-PCR (D). Results are expressed as the mean ± SEM of culture triplicates each assayed in technical triplicate. They are represented as well relative to the house keeping gene mRNA level, GAPDH. Statistical significance was shown using the 1-way ANOVA with the Tukey post test, where * $p < 0.05$; ** $p < 0.01$, *** $p<0.001$.

A

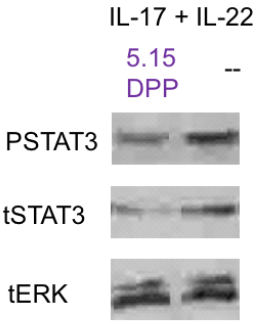
IL-17 + IL-22
5.15 DPP
--
PSTAT3
tSTAT3
tERK

B

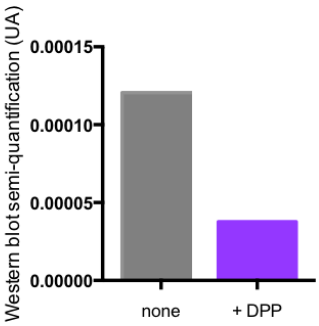
Western blot semi-quantification (UA)
0.00015
0.00010
0.00005
0.00000
none
+ DPP

C

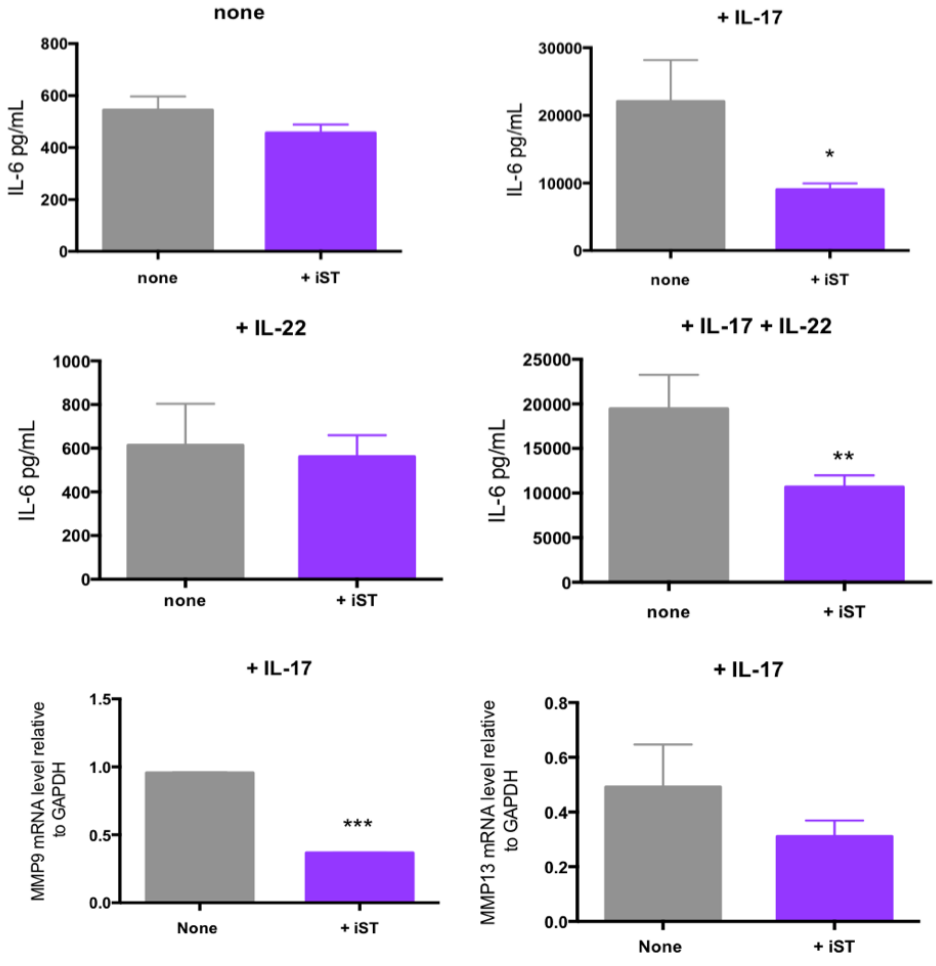
none
IL-6 pg/mL
800
600
400
200
0
none
+ iST
+ IL-17
30000
20000
10000
0
*
+ IL-22
1000
800
600
400
200
0
+ IL-17 + IL-22
25000
20000
15000
10000
5000
**

D

+ IL-17
MMP9 mRNA level relative to GAPDH
1.5
1.0
0.5
0.0
***
None
+ iST
MMP13 mRNA level relative to GAPDH
0.8
0.6
0.4
0.2
0.0

Figure 4-11 ES-62 promotes upregulation of IFNß expression in presence of IL-17 under inflammatory conditions and induces STAT1 activation.

A: SF were extracted and pooled from naïve DBA mice and expanded *ex vivo*. Cells were plated as three independent cultures for each treatment group of this animal model. After stimulation for 20 minutes with IFNß (10ng/ml) and IL-6 (10 ng/ml), or DMEM as control, total protein was extracted and phosphorylated or total STAT1 protein (respectively pSTAT1 and tSTAT1) and the constitutive ERK protein (tERK) were revealed by Western blot, as described in the M&M section 2.7. This experiment has been realised only once.

B: SF were extracted and pooled from naïve DBA/1 mice and expanded for 3 weeks *ex vivo*. Cells were plated at a concentration of 10^4 cells per well, as triplicates for each treatment group. After treatment for 24 hours with ES-62 (1 µg/ml) and IFNß (10 ng/ml) cells were fixed and permeabilised for FACE assay as described in the M&M section 2.6. Total STAT1 protein level was revealed and data are represented as the OD value measured by the assay. All Results are expressed as the mean ± SEM. Statistical significance was shown using the 1-way ANOVA with the Tukey post test where *** $p<0.001$

C-D: SF were extracted from naïve, CIA (mean score 3.167 ± 1.376, n=6) and ES-62 (mean score 0.5 ± 0.22, n=6) treated mice and expanded for 3 weeks *ex vivo*. Cells were plated in a 6 wells plate at a concentration of 1.10^6 cells per well as independent triplicate cultures for each treatment group. Total protein was extracted and phosphorylated STAT1 protein and the house keeping GAPDH protein were revealed by Western blot as described in the M&M section 2.7 (D). The semi quantification by ImageJ of pSTAT1 relative to GAPDH is represented as well (E). All Results are expressed as the mean ± SEM. Statistical significance was shown using the 1-way ANOVA with the Tukey post test.

E: SF were extracted from from naïve, CIA (mean score 4.5 ± 1.24, n=10) and ES-62 (mean score 1.71 ± 1.06, n=10) treated mice and expanded for 3 weeks *ex vivo*. Cells were plated in a 6 wells plate at a concentration of 1.10^6 cells per well in independent triplicate culture for each conditions. After

stimulation with IL-17 (25 ng/ml) for 6 hours or DMEM as control, total RNA was extracted and level of IFNß messenger RNA was quantified using RT-qPCR as described in the M&M section 2.8. All Results are expressed as the mean ± SEM. Statistical significance was shown using the 1-way ANOVA with the Tukey post test where *** $p<0.001$. Such experiment has been successfully reproduced with another independent animal model.

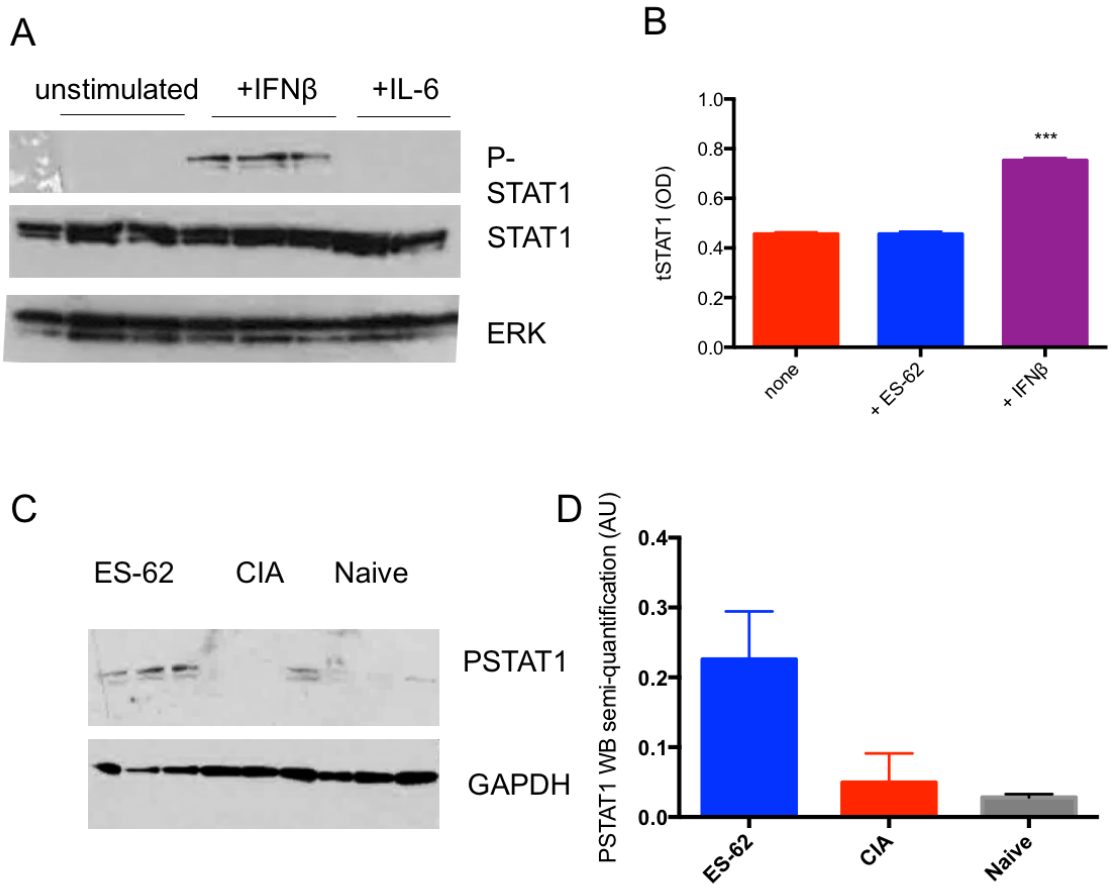
A
unstimulated
+IFNβ
+IL-6
P-STAT1
STAT1
ERK
B
tSTAT1 (OD)
1.0
0.8
0.6
0.4
0.2
0.0
***
none
+ ES-62
+ IFNβ
C
ES-62
CIA
Naive
PSTAT1
GAPDH
D
PSTAT1 WB semi-quantification (AU)
0.4
0.3
0.2
0.1
0.0
ES-62
CIA
Naive
E
IFNβ expression relative to GAPDH
1.0
0.8
0.6
0.4
0.2
0.0
***
Naive
CIA
ES-62
Naive
CIA
ES 62
none
+ IL-17

Figure 4-12 ES-62 and 12b upregulate SOCS expression in SF.

SF were extracted from naïve, CIA (mean score 3.67 ± 1.5, n=6), ES-62 (mean score 1.5 ± 1.15, n=6) and 12b (mean score 0.71 ± 0.36, n=7) treated mice and expanded for 3 weeks *ex vivo*. Cells of each treatment group were plated as triplicate cultures. Total RNA was recovered from biological triplicates of each cell type and messenger level of SOCS1 and SOCS3 was measured relative to the house keeping gene GAPDH by RT-qPCR as described in the M&M section 2.8. All results were expressed as the mean ± SEM. Statistical significance was shown using the 1-way ANOVA with the Tukey post test, where * $p < 0.05$; ** $p < 0.01$, *** $p<0.001$. This experiment has been done only once.

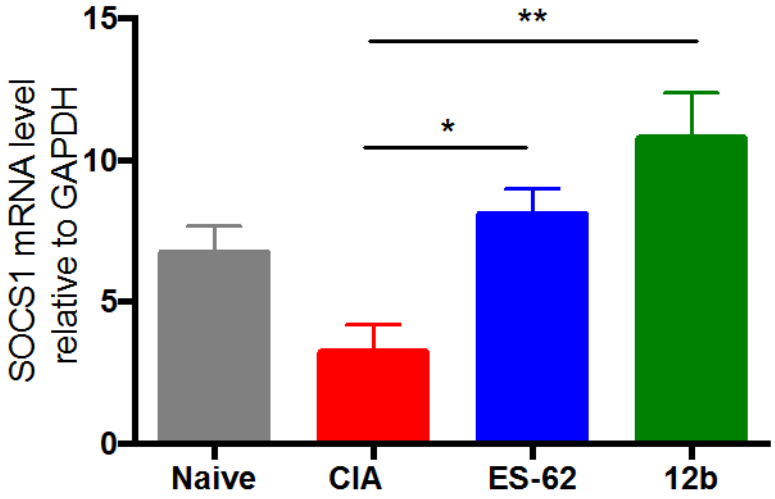
SOCS1 mRNA level
relative to GAPDH
15
10
5
0
**
*
Naive
CIA
ES-62
12b

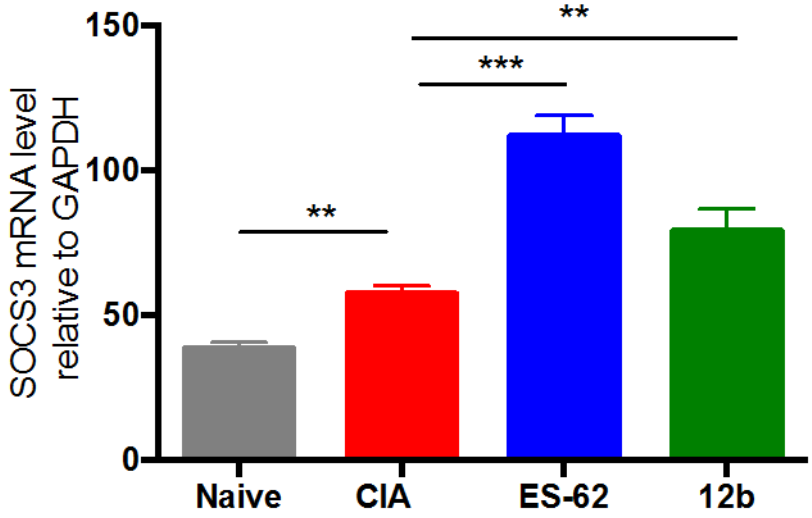
SOCS3 mRNA level
relative to GAPDH
150
100
50
0
**
***
**
Naive
CIA
ES-62
12b

Figure 4-13 Therapeutic and prophylactic treatments with 12b upregulate SOCS1 protein level in SF

A: DBA/1 mice were therapeutically treated with 12b or PBS as control as previously described in the Figure 3-6. SF from those mice were extracted, pooled by treatment group and expanded ex vivo. Total protein was extracted and SOCS1 was revealed by Western blot as described in the M&M section 2.8. Semi-quantification has been realised using the software ImageJ and data are represented as relative to total ERK protein level.

B: SF from the model previously displayed in Figure 3-7 were extracted from naïve mice, CIA mice (mean score 3.66 ± 1.5, n=6), CIA + IL-1β (mean score 6 ± 1.93, n=6) 12b mice (mean score 0.71 ± 0.36, n=7) and 12b + IL-1β mice (mean score 7.62 ± 1.67, n=8). Total protein was extracted and SOCS3 was revealed by Western blot as described in the M&M section 2.8. Semi-quantification has been realised using the software ImageJ and data are represented as relative to total ERK protein level.

A

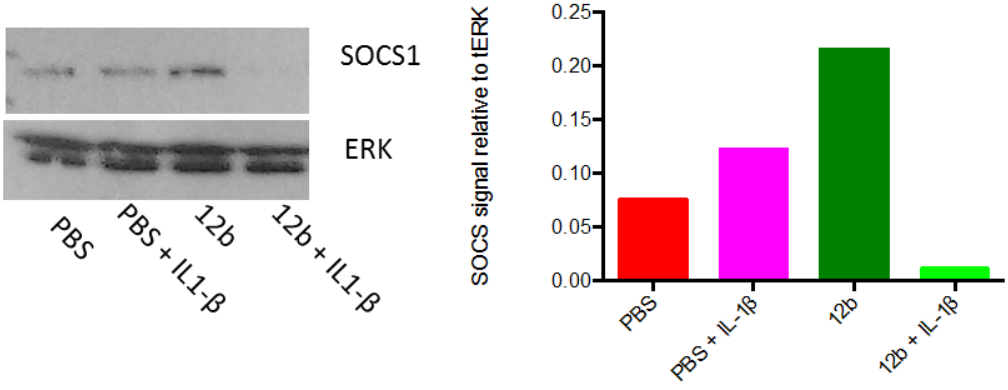
SOCS1
ERK
PBS
PBS + IL1-β
12b
12b + IL1-β
SOCS signal relative to tERK
0.25
0.20
0.15
0.10
0.05
0.00
PBS
PBS + IL-1β
12b
12b + IL-1β

B

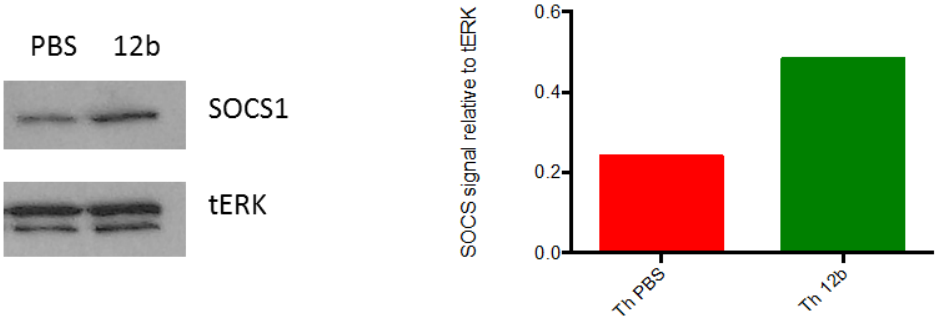
PBS
12b
SOCS1
tERK
SOCS signal relative to tERK
0.6
0.4
0.2
0.0
Th PBS
Th 12b

Figure 4-14 ES-62 regulation of SF downstream signaling, a summary

ES-62 makes SF less responsive to pro-inflammatory signals like IL-17 and IL-1ß, consequently reducing their subsequent production of IL-6, CCL2 or MMPs. It appears to achieve this by suppressing pathogenic ERK and STAT3 signal transduction. Moreover, ES-62 also appears to promote the induction of IFNß in response to IL-17-associated inflammation to to induce STAT1 activation. In addition to counter-acting STAT3 signalling, this provides the potential for a switch in IL-22 downstream signaling from STAT3 to STAT1 allowing conversion of pathogenic IL-22 signalling to that associated with inflammation-resolution. In addition, such pro-inflammatory signaling pathways can be regulated thanks to the SOCS 1 and 3 proteins respectively potent inhibitors of IFNɣ and STAT3 are found upregulated by ES-62 and 12b.

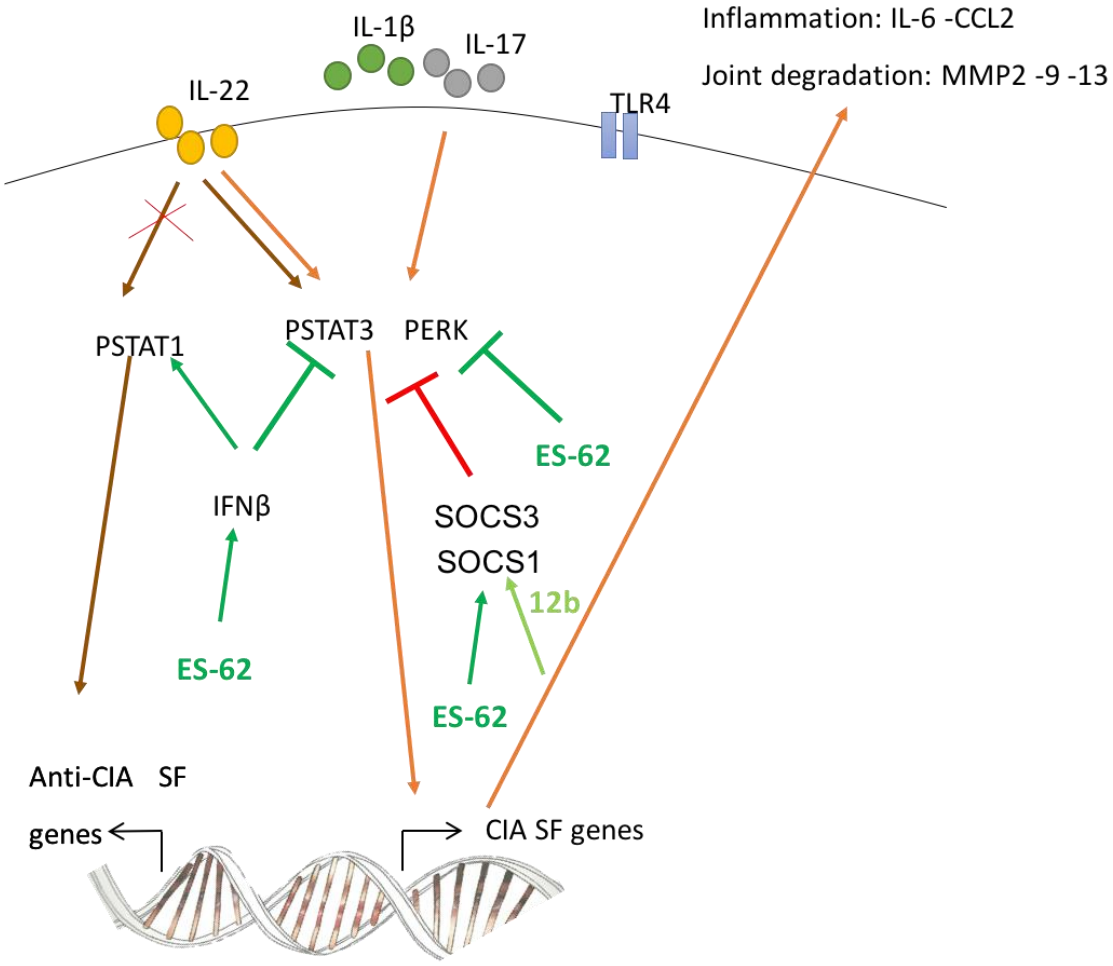
IL-1β
IL-17
IL-22
TLR4
Inflammation: IL-6 -CCL2
Joint degradation: MMP2 -9 -13
PSTAT1
PSTAT3
PERK
ES-62
IFNβ
SOCS3
SOCS1
12b
ES-62
ES-62
Anti-CIA SF genes
CIA SF genes

5. microRNAs as key modulators of signal integration

5.1 Introduction

The data presented above support the hypothesis that ES-62 can directly target SF during CIA to prevent them from producing pro-inflammatory and tissue destruction factors. It appears to be able to rewire these cells to modulate the panel of genes expressed at mRNA and protein levels as well as reducing their sensitivity to IL-17 and consequently re-setting control of the expression of IL-17 targeted genes. Thus, in the following studies (Chapters 5 & 6) the mechanisms by which ES-62 can control gene expression both directly at translation and transcription level are investigated, with focus here in this chapter, on modulation of gene translation by miRNAs during CIA.

MicroRNAs (miRNAs) are short non-coding RNAs (around 20 nucleotides in length) that regulate gene expression either by inducing targeted mRNA degradation or inhibiting mRNA translation. In particular, they target single strand mRNA via base-pairing with complementary sequences. The consequence of such pairing can be the cleavage of the mRNA, or alternatively its destabilization through shortening of its polyA tail or a reduction in translation efficiency, since the ribosome is no longer able to properly bind the mRNA. Whatever the mechanism, the end result is a strong reduction in target gene translation implicating miRNAs as key regulators of cell function: as a proof of their importance, miRNAs are extremely well conserved in eukaryotes, both in plants and animals[199]. In humans, the genome encodes for thousands of miRNAs which seem to be able to target approximately 60% of transcribed genes, allowing them to control a large network of target genes. Reflecting reports of their efficient control of cell differentiation status[200], their dysregulation has been implicated in enabling cell reprogramming, dedifferentiation and cell transformation in cancer [201].

Thus, as SF appear to be reprogrammed and display a "transformed" phenotype in CIA, it has been proposed that this may potentially reflect impairment of the microRNA network contributing to the acquisition of their aggressive features. Indeed, a number of studies investigating the expression of a wide range of miRNAs have lead to the discovery of both the selective upregulation and downregulation of their expression, as well associations of certain miRNA polymorphisms in RA (Table 5-1) and specifically, RASF when compared to the profile found in normal SF[202].

For example, miR-146a has been proposed to be crucial for the regulation of pathogenesis of RA as the rs2910164 polymorphism has been found to be associated with autoimmune disease susceptibility[203], whilst upregulation of miRs155 and 146a has been associated with the (dys)regulation of cytokine signalling. Both miR-155 and -146a are expressed at increased levels in SF from RA patients and animal models, as well as in a range of other tissues[204,205]. Consistent with its polymorphisms being a key susceptibility factor in RA, miR-146a is found to be further upregulated in RASF upon stimulation by IL-1ß and LPS and shown to negatively regulate TLR signalling by directly targeting IRAK-1 (interleukin-1 receptor-associated kinase) and TRAF-6 (TNF receptor associated factor) expression, suggesting that it normally acts to mediate protection against aberrant inflammation. This hypothesis is supported by the recent observations of Nakasa *et al*. showing the inhibitory effect of miR-146a on bone destruction in a mouse CIA model[206]. By contrast, miR-155 was highlighted as a potential key driver of RA when Blüml *et al*. showed a lack of development of CIA in miR-155 -/- mice[207] and miR-155 was found to be expressed at very elevated levels in RA patients[208].

MiRNA 155 is the most described miRNA in autoimmunity[204] and is known to target the anti-inflammatory inositol phosphatase SHIP1, the absence of which increases disease severity in the K/BxN serum transfer model of RA, and acute agouty arthritis[209]. Consistent with this, miR-155 is upregulated by TNF-α, IL-1ß and TLR ligands, and further enhances TNF-α production, yet perhaps surprisingly promotes the downregulation of MMP-1 and MMP-3. A

potential explanation for these apparently contradictory findings with respect to RA pathogenesis could be that miR-155 normally acts to initiate "safe" inflammation that at high levels homeostatically induces protective mechanisms to counterbalance its proinflammatory effect. However, in addition to promoting TLR4 signalling by upregulating MyD88, TAB2 and IKKε miR155 can also negatively target SOCS1, therefore inhibiting negative feedback loops and maintaining pro-inflammatory signals[210,211].

Thus, as ES-62, 11a and 12b enable CIA SF to recover or remain in a healthier phenotype, it was hypothesised that these molecules may mediate such modulation, at least in part, via control of miRNA expression. This idea is supported by the fact that TLR pathways, which are targeted by ES-62 and its SMAs, regulate the translation of some of these miRNAs, namely miR-155, miR-146 and miR-132 [212-214] [215]. Specifically, in this chapter the aims were to investigate whether:

- The potential candidate miRNAs implicated in regulating RA are expressed in SF and their expression modulated by pathogenic mediators
- Such miRNA expression can be modulated by ES-62 and/or its SMAs.
- Analyse the consequences of such miRNA regulation by ES-62 and SMAs on the pro-inflammatory phenotype of SF and identify potential targets.

5.2 Screening of candidate miRNA targets of ES-62 in SF

Thirteen candidate miRNAs were selected on the basis of their demonstrated activity as regulators of inflammation, and having being shown to deregulated in CIA mice and/or RA patient samples (Table 5-1). MicroRNAs 155 and 146a are the most studied microRNAs in RA: both are expressed at increased levels in RA patients and in a large range of cell types, but more specifically in SF, in animal models[205,208,216]. In addition, miR-125a is considered to be a potential RA biomarker because it is found at high levels in patients' serum, although it is not known whether it is expressed by SF[217]. Several miRNAs, such as the miR-19 family[218] miR-23b[219] and miR-125a[217], have been included for their ability to regulate the NF-κB pathway which is a therapeutic target in RA[217,219] and also modulated by ES-62 and its SMAs in CIA[104,132]. MiR-203 and miR-346 have also been implicated in the pathogenicity of inflammatory arthritis, being a regulator of MMP-1 and IL-6 expression[220] and targeting a TNFα inhibitor[221,222], respectively. MiR-34a has been, in addition selected as candidate for the study since its KO it resistant to CIA development (data not published yet), while miR-34a* has been described anti-inflammatory miRNA[223]. Only miR-24-1 has not been previously studied in inflammatory arthritis: however microarray analysis by the Harnett group revealed that a SMAs of ES-62, namely 12b upregulated expression of this miRNA in macrophages stimulated with LPS *in vitro*[132].

A major goal of this study was to identify whether microRNAs can be modulated by ES-62 (and its small molecule derivatives, 11a and 12b) in order to address their potential role in mediating the protection afforded against CIA by these immunomodulators. Thus, to establish optimal conditions for studying the expression of miRNAs in SF from naive and CIA DBA/1 mice, the transcriptional kinetics of 3 candidate miRNAs implicated in RA pathogenesis, relative to the constitutively expressed miRNA Hs-RNU6-2, were analysed in resting and LPS-stimulated SF derived by explant culture from normal BALB/c mice (Figure 5-1A). LPS was chosen as a model stimulus, not only as a

surrogate for TLR4-acting DAMPs generated by tissue damage in the joint, but also because it is well established that whilst the effects of ES-62 are TLR4 dependant, it acts to subvert such signalling. This analysis revealed differential expression kinetics of the miRNAs: thus, while miR-155 seems to progressively and strongly accumulate over 24 hours stimulation with the classical pro-inflammatory TLR4 ligand LPS, miR-146 was only weakly upregulated, peaking at 6h following LPS stimulation. By contrast, exposure to LPS does not modulate the high constitutive expression of miR-125a. Thus, for a screen of candidate miRNAs potentially modulated by ES-62 and its SMAs, it was proposed to identify which, if any, of these miRNA are expressed in SF derived from pooled naive (score 0) and CIA (mean score 4.7 ± 1.48, n=10) mice under steady state conditions (medium) and following 6 hours of LPS stimulation (Figure 5-1B). In terms of validation of significant miRNA induction, if their expression was detected within 31 cycles, corresponding to a relative level of expression of 0.1 when Hs-RNU6-2 expression was used as the reference standard, these data were considered to be above the threshold of "real" expression[122]. Amongst all the miRNAs tested, the following five were found highly expressed under steady-state conditions: miR-155, miR-125a, miR-34a, miR-19b-1 and miR-23b and generally at comparable but higher levels in CIA-SF, relative to naive-SF. However, exposure to LPS differentially regulated the levels of many of the individual miRNAs: thus whilst miR-24-1, miR-146 and miR-203 were only detected around the threshold level in SF from both naive and CIA mice, miR-146 and miR-203 could be induced somewhat by LPS stimulation in SF from both CIA and naïve mice. Interestingly, CIA SF maintain (with or without LPS-stimulation) a higher level of miRNA expression compared to the naïve SF for the following miRNAs: miR-23b-2, 24-1, 34a 125a, 146, 155 and 203. Furthermore, certain miRNAs were considered not to be expressed by SF at all as their levels were below the significance threshold: miR-19b-2, miR-124* and miR-346-2. Therefore, further analysis was only performed with the following candidates: miR-19b-1, miR-23b, miR-24-1, miR-34a, miR-125a, miR-146, miR-155 and miR-203.

5.3 miRNA-155 expression in response to the pro-inflammatory environment is reduced by the SMAs and ES-62.

As a first step, the potential modulatory effects of the SMAs 11a and 12b were tested on this panel of miRNAs *in vitro* in SF from CIA mice under conditions (6h) designed to mimic the steady-state "aggressive" phenotype (medium) and also following LPS stimulation or exposure to two pro-inflammatory mediators typically present in the arthritic joint (IL-1β and IL-17), that are known targets of the SMAs 12b and 11a, respectively[114,132]. Data showing miRNA expression level are presented (Figure 5-2) and summarised in Table 5-2). Firstly, this analysis showed that all miRNAs were upregulated in SF from CIA, relative to naive mice, whilst expression of miR-146 miR-155 and miR-203 was, as predicted by the literature, upregulated by LPS. However, perhaps rather surprisingly, given previous indications in the literature, no downregulation of miR-23b due to an overproduction of IL-17[219] was observed in SF from CIA. This lack of effect in CIA SF may reflect that this was a snapshot of miRNA expression at 6 h and also that this *in vitro* assay does not recapitulate the cocktail of pro and anti-inflammatory signals occurring in the joint *in vivo*. Nevertheless, it highlights that it is difficult to predict from such screens what is likely to happen *in vivo,* where cells interacting in structured microenvironments will integrate multiple signals to regulate miRNA expression. Clearly, the effects of *in vitro* exposure to 11a and 12b (relative to miRNA expression in SF from CIA mice under each condition) are dependent on the precise stimulation. For example, for miR-146, 155 and 203 that are upregulated by LPS stimulation, both 11a and 12b decrease their expression levels, but differential effects according to the stimuli can be observed. For instance, for miR-146 11a and 12b increase the miRNA level under IL-17 stimuli, while they decrease it under LPS or IL-1β stimuli.

Since the miRNAs are expressed under LPS stimulation we decided to investigate the effects of exposure to ES-62 and its SMAs, both *in vitro* and *in vivo*, on miRNA expression in CIA SF treated with LPS to mimic their

induction/maintenance during ongoing chronic inflammation in disease. Although, LPS-stimulation of SF from naive mice might similarly provide a surrogate for initiation of inflammation, where miRNAs where elevated (19b, 23b, 24-1, 125a, 146, 155) in CIA relative to naive SF under steady-state conditions treatment of CIA SF with either SMA generally reverted miRNA expression back to levels observed in naive SF, and so it was decided to focus on the ability of the SMAs to antagonise the ongoing inflammatory responses in established disease. This showed that pre-exposure to 11a and 12b induced a significant decrease in the LPS-stimulated miR-34a and 155 levels in CIA SF (Figure 5-3), whilst miR-23b was again decreased by 11a and elevated by 12b. However, the anti-inflammatory miR-146 does not seem to be affected at all by *in vitro* exposure to 11a and 12b under conditions of LPS stimulation. Interestingly, therefore, investigation of the *in vivo* effect of 12b on several of these miRNAs (Figure 5-4), using LPS-stimulated SF derived from indicated cohorts of mice, confirmed that exposure to 12b resulted in SF that displayed a lower level of miR-155 compared to SF from CIA mice. However, under these *in vivo* modulatory conditions, a significant increase in the two anti-inflammatory miRNAs miR-146 and miR-23b was also observed, perhaps indicating a role for the inflammatory microenvironment in promoting these negative feedback effects. Indeed since miR-146 is known to downregulate TLR/IL-1R pathway[224] maybe 12b downregulates IL-1ß production[114] by inducing miR-146.

Likewise, to determine whether these *in vivo* effects of 12b were mimicking the effects of ES-62, SF explanted from naïve, CIA or ES-62 treated mice treated *in vitro* with LPS were analysed for expression of the candidate miRNAs (miRs-19b, -23b, -34a, -146 and -155) of major interest. This again revealed that all of these miRNAs tended to be expressed at higher levels in LPS-stimulated SF from CIA relative to naive DBA/1 mice. However, of these, only miR-155 manifests a significant change in expression following exposure to ES-62 *in vivo*, with the levels in SF from CIA-ES-62 mice being brought back to levels found in SF from naïve mice (Figure 5-5). Unlike 12b however, exposure to ES-62 does not result in significant upregulation of miR-23b or miR-146. Nevertheless, this proved proof of principle that ES-62 may mediate

at least some of its effects on SF by modulating the miRNA network and importantly, by targeting miR-155 that has been shown to play a pivotal role in regulating pathogenesis[207].

5.4 miR-155 a potent regulator of SF signaling

To investigate whether downregulation of the activity of the pathogenic miR-155 provides a molecular mechanism for any of the hyporesponsiveness associated with SF from ES-62-treated mice with CIA, miRNA mimic 155 was transfected into naïve, CIA and ES-62 SF to determine whether it could overcome the suppression of LPS-induced secretion of IL-6 and CCL2 normally observed in SF from CIA mice treated with ES-62 in vivo (Figure 5-6). Under conditions of steady state, SF from all cohorts of mice transfected with miR-155 produced significantly more IL-6 and CCL2 than those treated with the negative control miRNA (siRNA). Although under these conditions, both the naive+miR-155-5p and the CIA-ES-62+miR-155-5p cohorts resemble the "aggressive" phenotype of the control CIA group, neither of these SF cohorts is converted to the hyper-aggressive status of CIA -miR-155-5p group. Consistent, with what is observed in untransfected cells (eg Figure 3-3). Thus, CIA SF produces significantly more IL-6 and CCL2 than the naïve and ES-62 SF when transfected with either control siRNA or miR-155-5p. Moreover, under these steady state conditions, the protection by ES-62 is conserved, and with respect to CCL2, even enhanced relative to SF from naive mice, when the cells are transfected with miR-155-5p.

Perhaps surprisingly, when these SF were stimulated with LPS and already producing miR-155, the addition of the miR-155 mimic resulted in hyperproduction of the cytokines relative to that obtained with the control siRNA. Intriguingly, under the conditions pertaining in the presence of miR-155-5p, the protective effects resulting from exposure to ES-62 *in vivo* were lost, and again, this was particularly pronounced with respect to CCL2. These data therefore appear to suggest that the levels and/or integration of miR-155 signalling with other pathogenic effects is crucial to the maintenance of

SF hyporesponsiveness following exposure to ES-62. Thus, in steady-state ES-62 SF, in the absence of additional proinflammatory signals generated by LPS, addition of the miR155 mimic is not sufficient to counter the ES-62-induced hyporesponsive state as exemplified by the reduced ERK and STAT3 signalling observed in these cells (Chapter 4). Likewise, in the siRNA condition, the levels of miR155-induced by LPS in ES-62 SF may not be sufficient or stable to fully integrate with other pathogenic signals resulting from this TLR ligand. However, LPS-coupled signalling in the context of the elevated levels of miR-155 provided by the mimic appears to provide a sufficient platform to break the ES-62-induced hyporesponsiveness.

Perhaps pertinent to this, miR-155 has previously been shown to be able to directly target SOCS1[225] and SOCS3[226] in some cells. As these have also been identified as potential targets of great interest to our study, the effects of the miRNA-155 mimic on SOCS1 and SOCS3 mRNA expression in SF from the various cohorts of mice were also determined (Figure 5-7). As suggested by our studies in Chapter 4, our control siRNA steady-state data indicate that whilst SOCS1 and SOCS3 are downregulated in SF from CIA relative to naive mice, this appears to be at least partially prevented by exposure to ES-62 *in vivo* and this profile is amplified in LPS-treated cells for SOCS1. However, this protection is not associated with accompanying inhibition of LPS-induction of IL-6 in these cells, despite reports of the role of SOCS1 in inhibiting LPS-stimulation IL-6 release in macrophages by targeting JAK2/STAT5/p50 signalling[227]. Interestingly, therefore in terms of the hypothesis that induction of miR-155 during CIA contributes to at least some of the downregulation of SOCS1, our data confirm that SOCS1 indeed appears to be a target of miR-155 in SF since under steady-state conditions the addition of the miRNA totally abrogated SOCS1 mRNA expression in SF from all cohorts of CIA mice and the high levels of SOCS1 pertaining in SF from naive and ES-62 SF following stimulation with LPS are significantly reduced, but only to a level comparable with control CIA-ES-62 SF. Collectively, these data further support the likelihood that ES-62-mediated protection in these cells is not SOCS1-mediated. Moreover, when the miR-155 cells are stimulated with LPS, CIA SF

no longer express SOCS1, presumably due to the high level of miR-155 and/or its integration with other TLR4 signals downregulating SOCS1.

Intriguingly, although, SOCS3 induction does not appear to be targeted by miR-155 in SF from naïve and CIA mice, transfection with the miRNA-155 mimic rather surprisingly strongly upregulated SOCS3 expression in SF from ES-62-CIA mice. Such an important rise could potentially be induced by the inhibition of miR-155 effects by ES-62 resulting in SOCS mRNA accumulation rather than its potential degradation.

In any case the ability of ES-62-conditioned SF to maintain or even elevate SOCS1 and SCOC3 levels in the presence of LPS + miR-155-5p is rather counter-intuitive to the loss of their hyporesponsive phenotype, however, at least in the case of SOCS3, it may provide another mechanism in terms of negative feedback inhibition of STAT3 signalling[228,229] by ES-62 (Chapter 4) to restrain the effects the hyper-Il-6 production by these cells[230].

In addition, it is known that miR-155 can deeply control a cell status by binding and regulating DNMT1 protein activity and therefore induce abherrant DNA methylation of the genome, at least in HEK293T and HCT116 cells[231]. Therefore, the impact of miR-155 in DNMT1 protein level has been analysed (Figure 5-8). The study reveals that miR-155 do not directly regulated DNMT1 mRNA, level but do affect DNMT1 protein level with specially a strong decrease of DNMT1 in CIA SF under stimulation with LPS. This could explain somehow why in CIA SF we observe such a low level of DNMT1 while miR-155 is found strongly upregulated, if miR-155 somehow drives DNMT1 suppression or degradation.

5.5 Discussion and Conclusions

Modulation of the miRNA network by ES-62 and the SMAs in SF is an efficient way to rewire and control cell aggressiveness and control its responses to the pro-inflammatory signal due to the proven ability of several miRNAs to regulate relevant downstream signaling as previously summarize for our

candidate miRNAs (Table 5-1). In particular, miRNA-155 the expression of which is induced by TLR4 signalling and efficiently reduced by both ES-62 and its SMAs is of potential relevance as a well-known target of miR155 is the suppressor of cytokine signaling SOCS1 which downregulates the IFNɣ signalling that is a pathogenic in RA/CIA [191,192,195] and a target of ES-62[141,232]. Indeed, SOCS1 inhibits IL-6-driven Th1 differentiation[233]. Interestingly, therefore, data in this thesis (chapter 4) suggest that ES-62 can upregulate SOCS1 and thus the finding that ES-62 reduces miR-155 levels suggests that this might provide a contributing mechanism to prevent the decrease in SOCS1 occurring during CIA and enabling SF resistance to IFNɣ signals (Figure 5.9). Likewise, the increased level of SOCS3 observed in presence of both miR-155 and ES-62 might also be caused by an accumulation of SOCS3 mRNA resulting from ES-62 suppression of miR-155 levels and if so, it could perhaps explain how ES-62 inhibits IL-6 and IL-17-STAT3 activity. Perhaps amplifying this, in T cells, miR-155 has been reported to have the ability to promote Th-17 differentiation and activity by targeting SOCS1[225,234]. Therefore, this could potentially bring another mechanism by which ES-62 inhibits Th17 differentiation.

In summary it appears that ES-62 can control SF responses to the pro-inflammatory environment by controlling the cell response at various levels. Thus, while in chapter 4 it is shown to control the signaling pathways directly downstream of IL-6/Il-17, here it is shown to control important regulators of such signaling pathways, the miRNAs. Thus, by demonstrating action via miRNAs at the feedback loop levels, this provides a molecular mechanism for inhibition of pathogenic STAT3 signalling: the final step is to investigate whether ES-62 regulates SF response to the pro-inflammatory environment by regulating targeted gene expression. In addition, since miR-155 is enable to regulate DNMT1 protein level within the cell, potentially by a direct binding to the protein[231], ES-62 and the SMAs could potentially act to another level of cell phenotype regulation by directly acting on the global DNA methylation.

Table 5-1 List of candidate miRNAs potentially expressed by SF in CIA and regulated by ES-62 and/or its SMAs

All miRNAs have been selected for being previously identified as being involved in inflammatory arthritis and miR-24-1 is found upregulated by 12b in macrophages.

miRNAs	Action on signaling pathways	Known targets	Up-down regulated in patients /CIA	Pro-anti inflammatory	Reference
miR-19b-1 **miR-19b-1*** **miR-19b-2**	Upregulate TLR2 Induce NFkB	A20/Tnfaip3 -Rnf11 Fbxl11/Kdm2a - Zbtb16	---	Pro	[218]
miR-23b	Induce NFkB pathway	TAB2 - TAB3- IKK-α	Downregulated in patients and CIA	Anti	[219]
miR-24-1	Upregulated by the SMA of ES-62 12b in vitro in macrophages stimulated with LPS	---	---	---	[114]
miR-34a	KO resistant to CIA + increased SOCS3	---	---	Pro	Not published yet
miR-34a*	Inhibition of induced apoptosis resistance	XIAP	Downregulated in patients and CIA	Anti	[223]
miR-124	Overexpression reduces MCP-1		Down-regulated in RASF	--	[220]
miR-125a	Induce NFkB pathway	TNFAIP3	Upregulated in patients plasma	---	[217]
miR-146	Downregulate TLR/IL1 pathway	IRAK-1 TRAF6	Upregulated in patients + CIA	Anti	[203,205,206]
miR-155	Enhance TNFα production	SOCS1 SHIP1	Upregulated in patients + CIA	Pro	[204, 208, 213, 215]
miR-203	Upregulate in MMP-1 and IL-6 expression	---	Upregulated in CIA	Pro	[220]
miR-346-2	Downregulate TNFα inhibitor Indirectly downregulate IL-18	Tristetrapolin	Upregulated by LPS	Pro	[221, 222]

Figure 5-1 Profile of miRNA expression in SF

A: SF were extracted from BALB/c mice and expanded *ex vivo* for 3 weeks. Cells were stimulated with LPS (1µg/ml) for up to 24 h as indicated: miR-155, miR-146 and miR-125a levels were quantified by qRT-PCR as described and data normalised relative to Hs-RNU6-2 expression levels.

B: SF were derived from groups of Naive (score of zero) or CIA (mean score 4.7 ± 1.48, n=10) mice and stimulated ± LPS (1 µg/ml) for 24 hours. The miRNA levels of candidate miRNAs (Table 5-1) were quantified by qRT-PCR and data normalised relative to Hs-RNU6-2 expression levels. All gene expression determined as ≤0.1 fold of Hs-RNU6-2 expression was considered to be background as described by Qiagen[122]

A

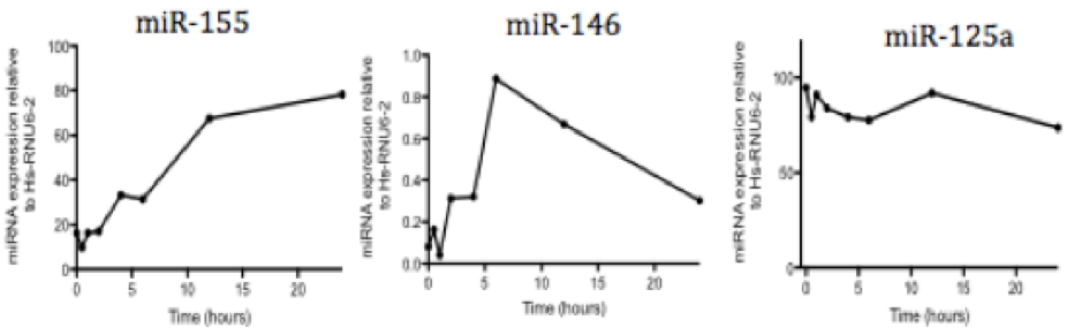
miR-155
miR-146
miR-125a
miRNA expression relative to Hs-RNU6-2
Time (hours)

B

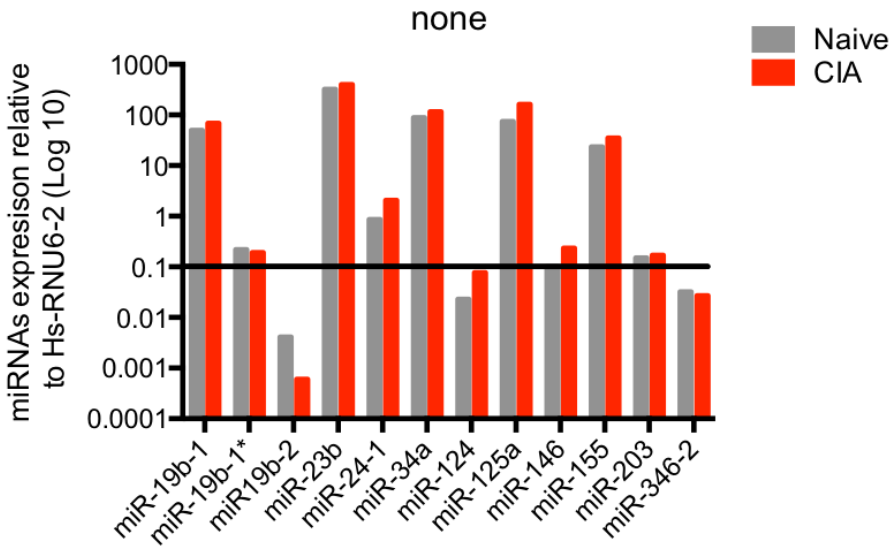
none
Naive
CIA
miRNAs expresison relative to Hs-RNU6-2 (Log 10)
1000
100
10
1
0.1
0.01
0.001
0.0001
miR-19b-1
miR-19b-1*
miR19b-2
miR-23b
miR-24-1
miR-34a
miR-124
miR-125a
miR-146
miR-155
miR-203
miR-346-2

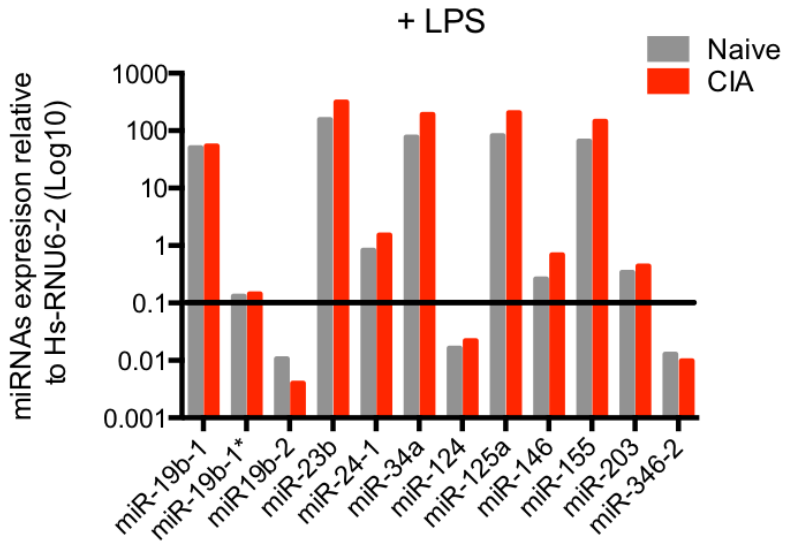
+ LPS
Naive
CIA
miRNAs expresison relative to Hs-RNU6-2 (Log10)
1000
100
10
1
0.1
0.01
0.001
miR-19b-1
miR-19b-1*
miR19b-2
miR-23b
miR-24-1
miR-34a
miR-124
miR-125a
miR-146
miR-155
miR-203
miR-346-2

Figure 5-2 Screening of potential miRNA targets of SMAs, 11a and 12b

SF extracted and expanded *ex vivo* from Naive or CIA (mean articular score 4.7 ± 1.48, n=10) mice to were pre-treated overnight *in vitro* with the SMAs 11a and 12b (both at 5 µg/ml) and then further stimulated for another 6 hours with IL-1ß (10 ng/ml), IL-17 (25 ng/ml) or LPS (1 µg/ml). Candidate miRNAs Table 5-1 were quantified by RT-qPCR (as described in the M&M 2-8) as indicated by fold change relative to the endogenous control Hs-RNU6-2 from a single experiment (n=1).

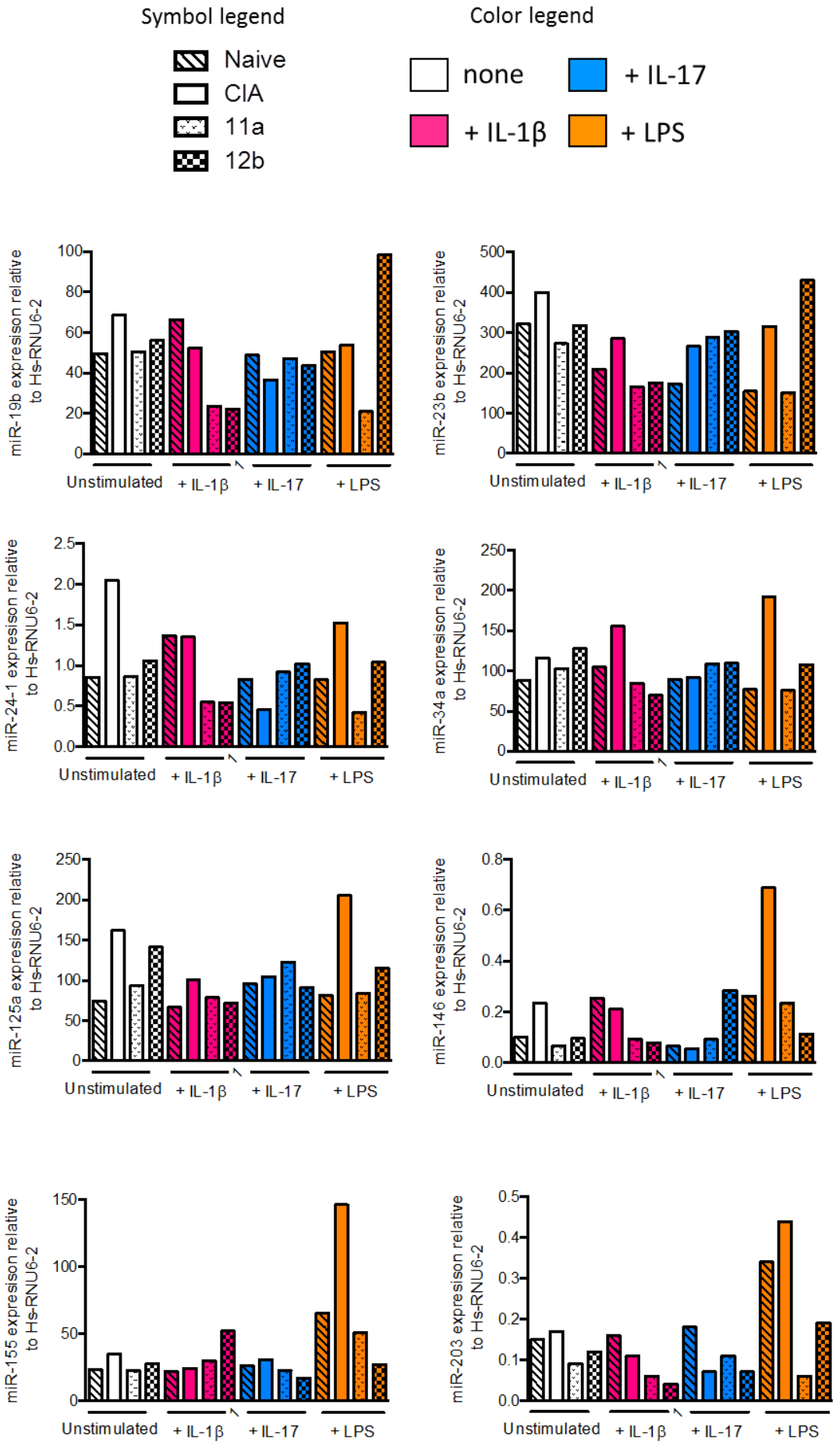
Symbol legend
Naive
CIA
11a
12b
Color legend
none
+ IL-17
+ IL-1β
+ LPS
miR-19b expresison relative to Hs-RNU6-2
miR-23b expresison relative to Hs-RNU6-2
miR-24-1 expresison relative to Hs-RNU6-2
miR-34a expresison relative to Hs-RNU6-2
miR-125a expresison relative to Hs-RNU6-2
miR-146 expresison relative to Hs-RNU6-2
miR-155 expresison relative to Hs-RNU6-2
miR-203 expresison relative to Hs-RNU6-2
Unstimulated
+ IL-1β
+ IL-17
+ LPS

Table 5-2 Summary of in vitro regulation of miRNAs by 12b and 11a

This table summarizes the data previously presented in figure 5-2. Red and green arrows represent respectively downregulation and upregulation of miRNA levels by the SMAs 11a and 12b in response to the various stimuli IL-1β, IL-17 or LPS.

	Unstimulated		+IL-1β		+ IL-17		+ LPS	
	11a	12b	11a	12b	11a	12b	11a	12b
miR-19b	↓	↓	↓	↓	↑	↑	↓	↑
miR-23b	↓	↓	↓	↓	↑	↑	↓	↑
miR-24-1	↓	↓	↓	↓	↑	↑	↓	↓
miR-34a	↓	↑	↓	↓	↑	↑	↓	↓
miR-125a	↓	↓	↓	↓	↑	↑	↓	↓
miR-146	↓	↓	↓	↓	↑	↑	↓	↓
miR-155	↓	↓	↑	↑	↓	↓	↓	↓
miR-203	↓	↓	↓	↓	↑	-	↓	↓

Figure 5-3 SMAs 12b and 11a decrease expression of miR-155 in SF from CIA mice, in vitro

SF from Naïve and CIA (mean score 4.7 ± 1.48, n=10). After being plated at a concentration of 0.3 10^6 cells per well as triplicate culture for each treatment group, cells were pre-treated overnight with the SMAs 11a and 12b (5 µg/ml for each molecule) and then further stimulated with LPS (1 µg/ml) for 6 hours, *in vitro*. miRNAs -19b, -23b, -34a, -146, -155, and -203* were quantified by RT-qPCR and normalised relative to the level of the endogenous control Hs-RNU6-2 as described in the M&M section 2.8. Data are from three independent cultures for each treatment group are represented as fold change relative to the CIA condition.

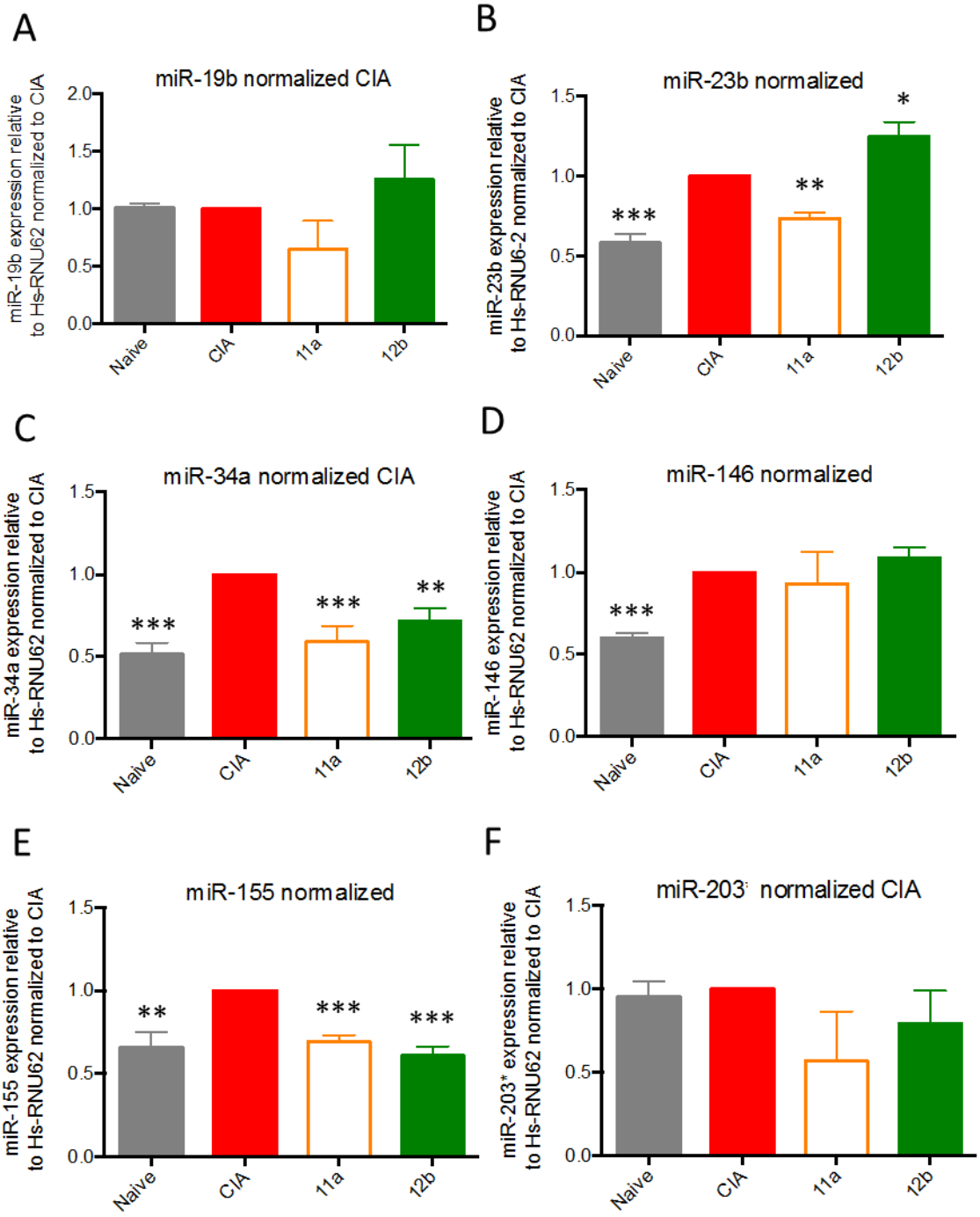
A
miR-19b normalized CIA
miR-19b expression relative to Hs-RNU62 normalized to CIA
2.0
1.5
1.0
0.5
0.0
Naive
CIA
11a
12b
B
miR-23b normalized
miR-23b expression relative to Hs-RNU6-2 normalized to CIA
1.5
1.0
0.5
0.0
***
**
*
Naive
CIA
11a
12b
C
miR-34a normalized CIA
miR-34a expression relative to Hs-RNU62 normalized to CIA
1.5
1.0
0.5
0.0
***
***
**
Naive
CIA
11a
12b
D
miR-146 normalized
miR-146 expression relative to Hs-RNU62 normalized to CIA
1.5
1.0
0.5
0.0
***
Naive
CIA
11a
12b
E
miR-155 normalized
miR-155 expression relative to Hs-RNU62 normalized to CIA
1.5
1.0
0.5
0.0
**
***
***
Naive
CIA
11a
12b
F
miR-203* normalized CIA
miR-203* expression relative to Hs-RNU62 normalized to CIA
1.5
1.0
0.5
0.0
Naive
CIA
11a
12b

Figure 5-4 Exposure to 12b *in vivo* upregulates expression of miRNAs 146 and 23b and downregulates expression of miR-155 in SF from mice undergoing CIA

SF were extracted pooled and expanded *ex vivo* from naïve mice or CIA mice treated *in vivo* with 12b (mean score 0.714 ± 0.360, n=7) or PBS (CIA, mean score 3.667 ± 1.5, n=6). Cells were plated at a concentration of 0.3 10^6 cells per well in a 6 wells-plate as triplicate culture for each group treatment. After stimulation for 6 hours with LPS (1 µg/ml) and levels of the miRNAs -19b, -23b, -34a, -146, -155, and -203* quantified by RT-qPCR relative to the level of the endogenous control Hs-RNU6-2 as described in the M&M section 2.8. Analysis by ANOVA followed by the Tukey multiple comparison test was performed and results are expressed as the mean ± SEM, where * $p < 0.05$; ** $p < 0.01$, *** $p<0.001$.

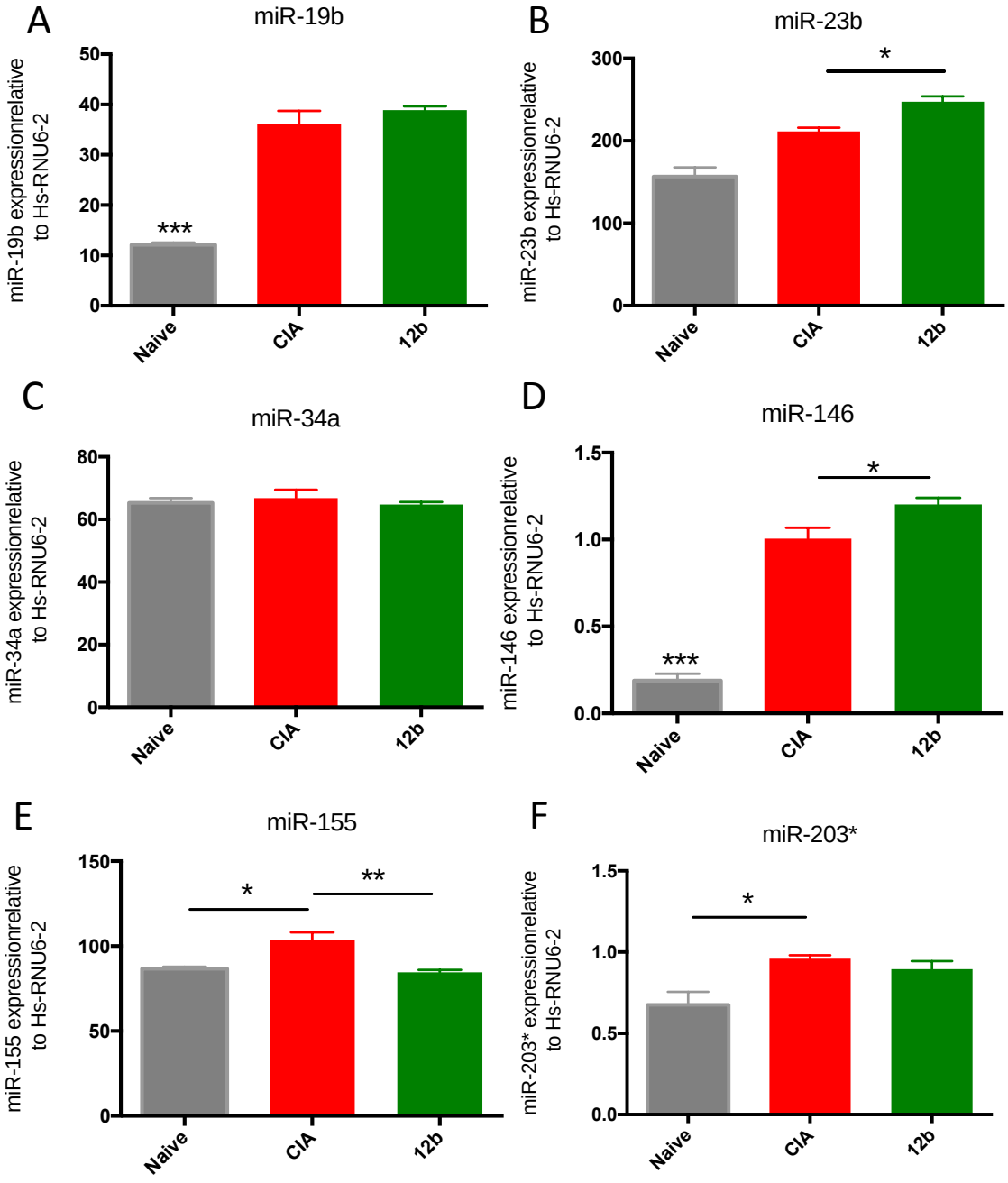
A
miR-19b
miR-19b expressionrelative to Hs-RNU6-2
50
40
30
20
10
0
***
Naive
CIA
12b
B
miR-23b
miR-23b expressionrelative to Hs-RNU6-2
300
200
100
0
*
Naive
CIA
12b
C
miR-34a
miR-34a expressionrelative to Hs-RNU6-2
80
60
40
20
0
Naive
CIA
12b
D
miR-146
miR-146 expressionrelative to Hs-RNU6-2
1.5
1.0
0.5
0.0
*
***
Naive
CIA
12b
E
miR-155
miR-155 expressionrelative to Hs-RNU6-2
150
100
50
0
*
**
Naive
CIA
12b
F
miR-203*
miR-203* expressionrelative to Hs-RNU6-2
1.5
1.0
0.5
0.0
*
Naive
CIA
12b

Figure 5-5 *in vivo* ES-62 decreases miR-155

SF were extracted pooled and expanded *ex vivo* from naïve mice or CIA mice treated *in vivo* with ES-62 (mean score 0.8 ± 0.8, n=6) or PBS (CIA, mean score 4.67 ± 2, n=6). Cells were plated at a concentration of 0.3 10^6 cells per well in a 6 wells-plate as triplicate culture for each group treatment. After stimulation for 6 hours with LPS (1 µg/ml) and levels of the miRNAs -19b, -23b, -34a, -146, -155, and -203* quantified by RT-qPCR relative to the level of the endogenous control Hs-RNU6-2 as described in the M&M section 2.8. Analysis by ANOVA followed by the Tukey multiple comparison test was performed and results are expressed as the mean ± SEM, where * $p < 0.05$; ** $p < 0.01$, *** $p<0.001$.

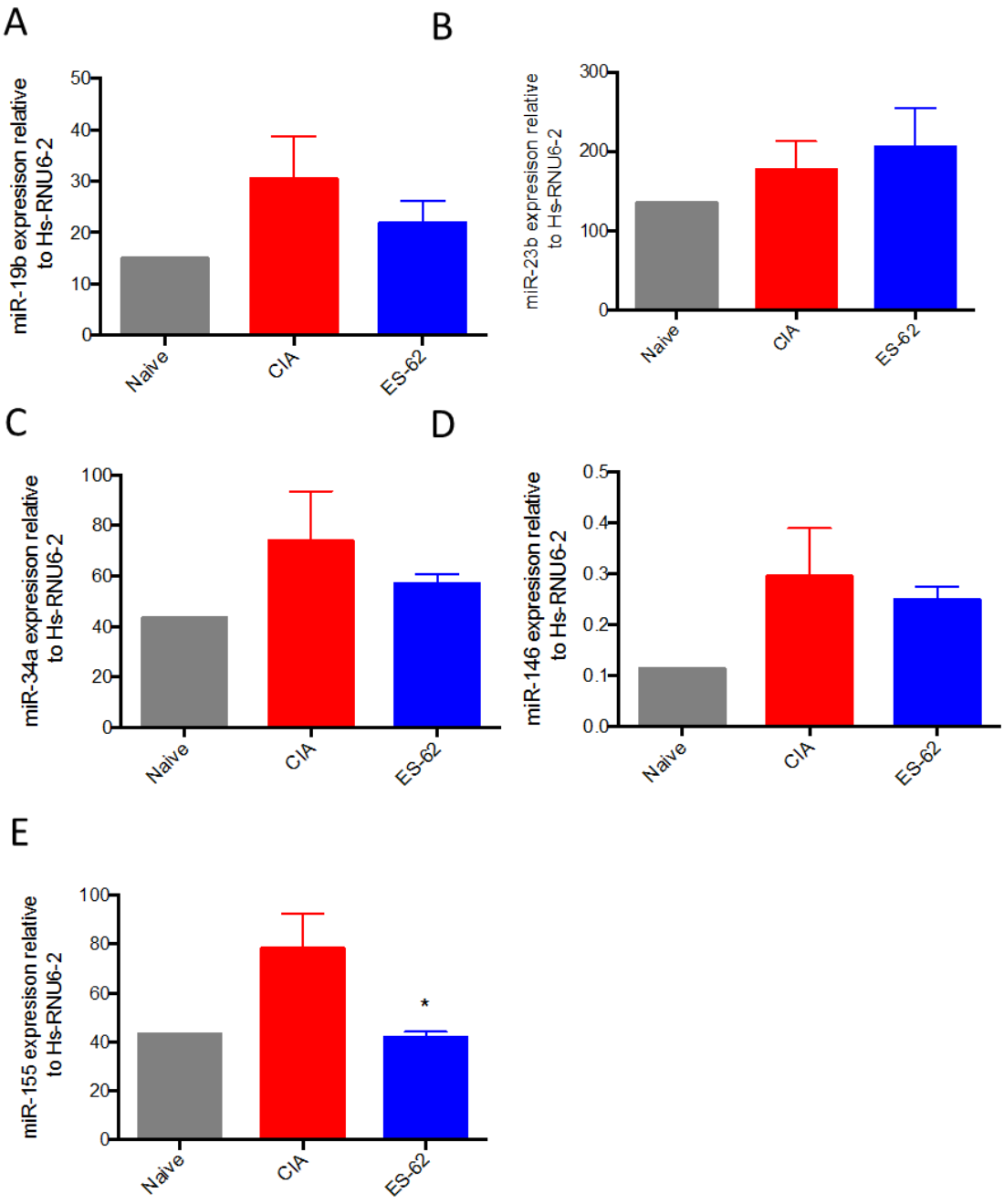
A
miR-19b expresison relative to Hs-RNU6-2
50
40
30
20
10
0
Naive
CIA
ES-62
B
miR-23b expresison relative to Hs-RNU6-2
300
200
100
0
Naive
CIA
ES-62
C
miR-34a expresison relative to Hs-RNU6-2
100
80
60
40
20
0
Naive
CIA
ES-62
D
miR-146 expresison relative to Hs-RNU6-2
0.5
0.4
0.3
0.2
0.1
0.0
Naive
CIA
ES-62
E
miR-155 expresison relative to Hs-RNU6-2
100
80
60
40
20
0
*
Naive
CIA
ES-62

Figure 5-6 A miR-155 mimic promotes SF aggressiveness

SF from Naïve mice, CIA mice (mean score 3.17 ± 1.37, n=6) and CIA mice treated *in vivo* with ES-62 (mean score 0.5 ± 0.22, n=6) were plated at a concentration of 0.3 10^6 cells per well as independent culture triplicate for each of the following treatments. Cells were transfected for 24 hours with miR-155-5p mimic (50 nM), whilst being stimulated or not with LPS (1 μg/ml). Cell supernatants were assessed for IL-6 and CCL2 production by ELISA as described in the M&M section 2.5. Data are expressed as the mean (of triplicate assays) ± SEM of three independent cultures and analysed by ANOVA followed by the Tukey multiple comparison test where * $p < 0.05$; ** $p < 0.01$, *** $p<0.001$. Such experiment has been successfully repeated independently using SF extracted from the same animal model.

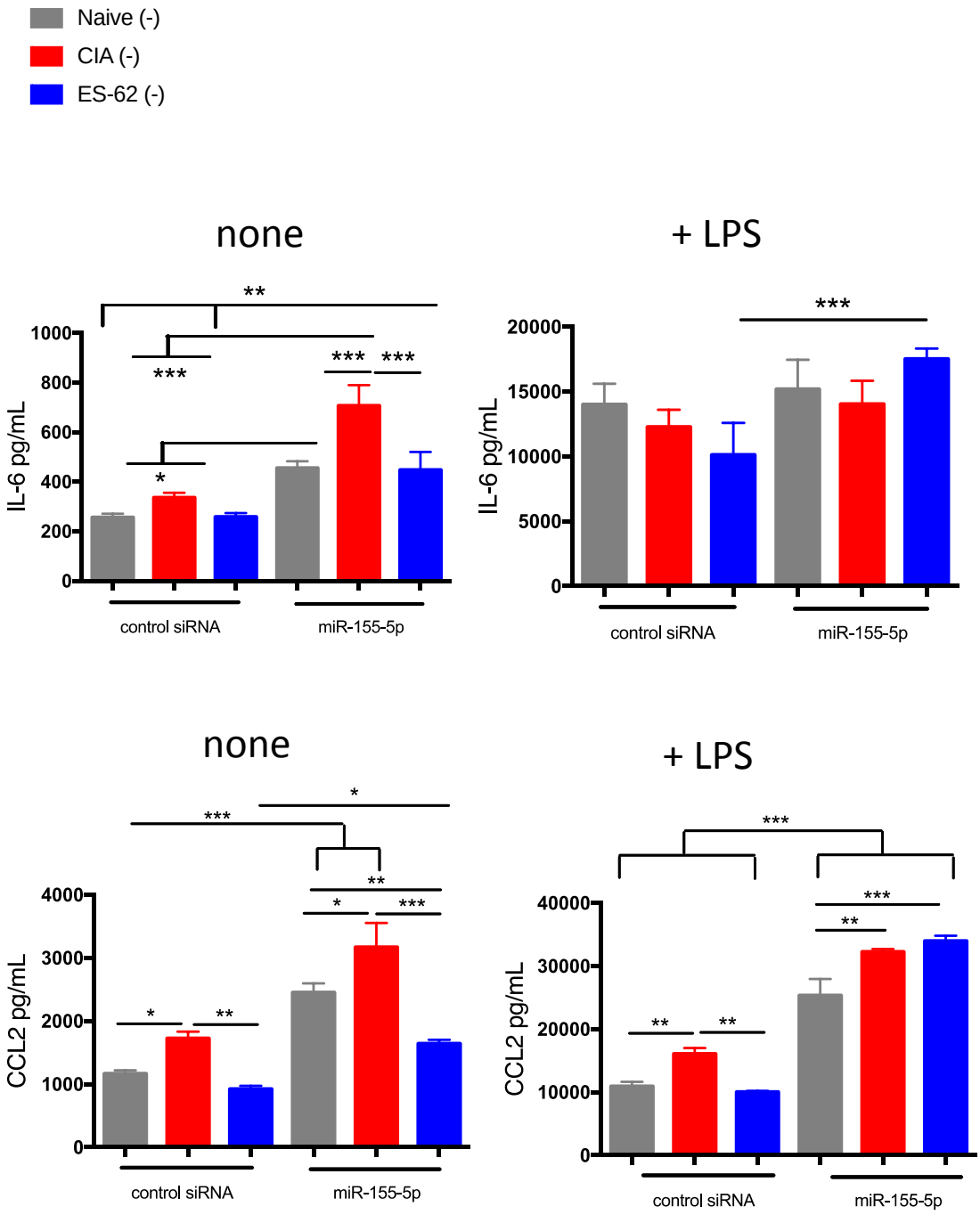
Naive (-)
CIA (-)
ES-62 (-)
none
+ LPS
IL-6 pg/mL
CCL2 pg/mL
control siRNA
miR-155-5p

Figure 5-7 A miR-155 mimic can regulate SOCS expression in SF

SF from naïve mice, CIA mice (mean score 3.17 ± 1.37, n=6) and CIA mice treated *in vivo* with ES-62 (mean score 0.5 ± 0.22, n=6) were plated at a concentration of 0.3 10^6 cells per well as independent culture triplicate for each of the following treatments. Cells were transfected with miR-155-5p mimic (50 nM) whilst being stimulated with LPS (1 µg/ml) for 6 hours. Total RNA was extracted mRNA levels of SOCS1 and SOCS3 assessed by qRT-PCR as described in the M&M section 2.8 with data presented as relative to the levels of the endogenous control, GAPDH. Data were analysed by ANOVA followed by the Tukey multiple comparison test and expressed as the mean ± SEM where n=3 independent cultures and * $p < 0.05$; ** $p < 0.01$, *** $p<0.001$. Only relevant statistics are displayed on the graph.

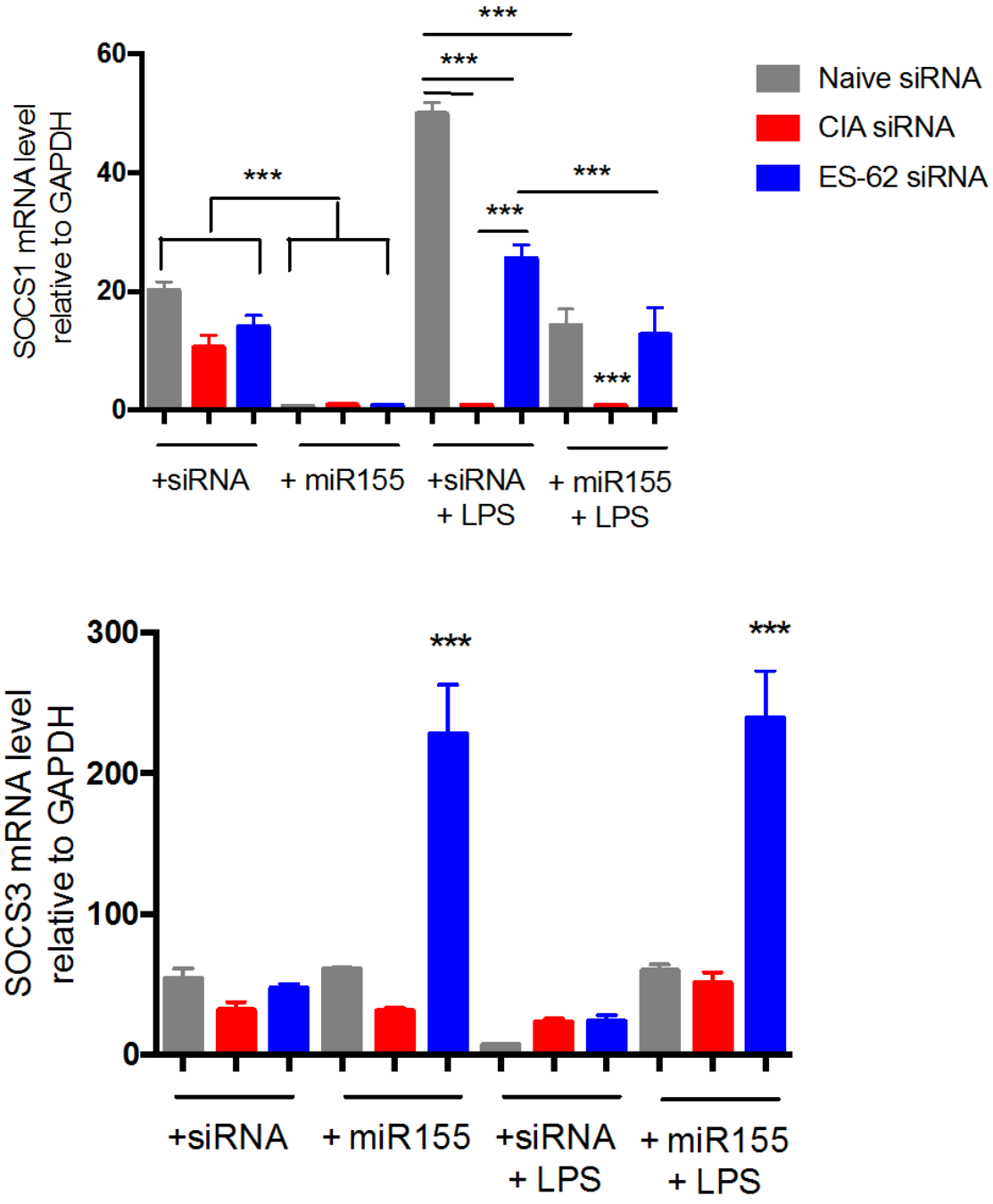
SOCS1 mRNA level
relative to GAPDH
60
40
20
0
***
***
***
***
***
Naive siRNA
CIA siRNA
ES-62 siRNA
+siRNA
+ miR155
+siRNA
+ LPS
+ miR155
+ LPS
SOCS3 mRNA level
relative to GAPDH
300
200
100
0
***
***
+siRNA
+ miR155
+siRNA
+ LPS
+ miR155
+ LPS

Figure 5-8 miR-155 regulates DNMT1 protein, but not mRNA level

A-B: SF used in Figure 5-6 from Naïve mice, CIA mice (mean score 3.17 ± 1.37, n=6) and CIA mice treated *in vivo* with ES-62 (mean score 0.5 ± 0.22, n=6) were plated at a concentration of 0.3 10^6 cells per well as independent culture triplicate for each of the following treatments. Cells were transfected for 24 hours with miR-155-5p mimic (50 nM) whilst being stimulated or not with LPS (1 µg/ml) as in Figure 5-6. Total protein was collected in order to reveal DNMT1 protein level by Western blot as described in the M&M method section 2.7. Semi-quantification of DNMT1 and GAPDH is done by ImageJ. Data are represented as relative to GAPDH protein level. Such experiment has been realised only once.

A

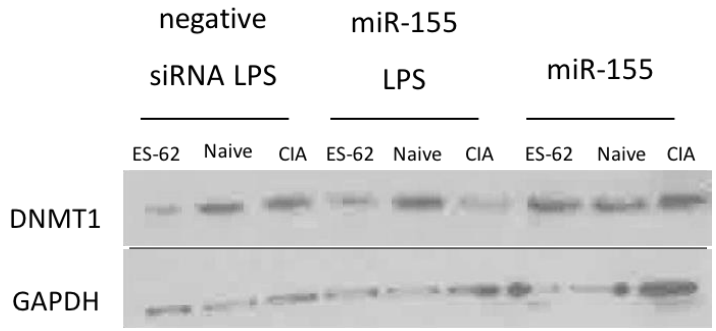
negative
siRNA LPS
miR-155
LPS
miR-155
ES-62
Naive
CIA
ES-62
Naive
CIA
ES-62
Naive
CIA
DNMT1
GAPDH

B

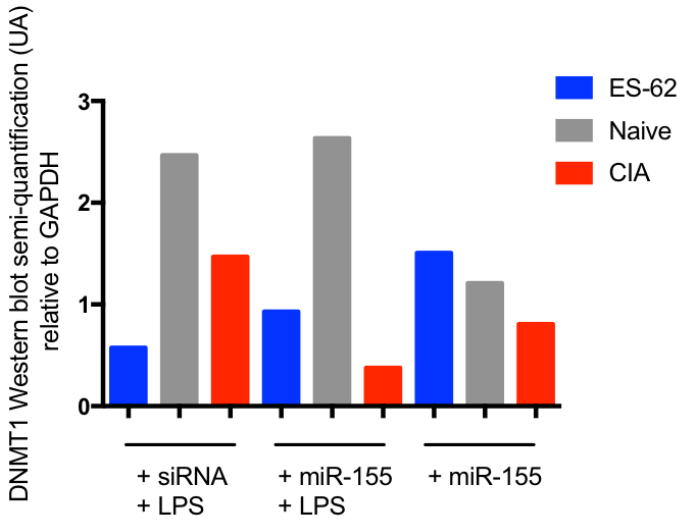
DNMT1 Western blot semi-quantification (UA)
relative to GAPDH
3
2
1
0
ES-62
Naive
CIA
+ siRNA
+ LPS
+ miR-155
+ LPS
+ miR-155

C

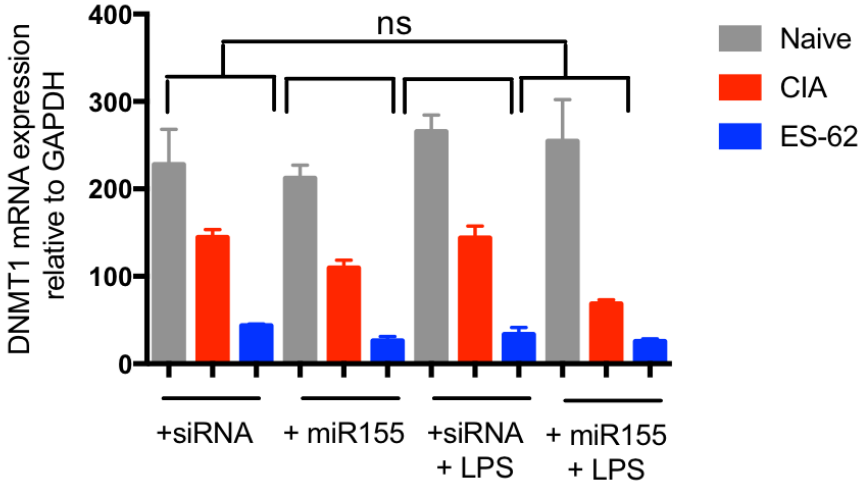
DNMT1 mRNA expression
relative to GAPDH
400
300
200
100
0
ns
Naive
CIA
ES-62
+siRNA
+ miR155
+siRNA
+ LPS
+ miR155
+ LPS

Figure 5-9 Model of the role of miR-155 in SF aggressiveness and its modulation by ES-62 and 12b

By reducing miR-155 expression, ES-62 and 12b prevent its downregulation of SOCS1 resulting in dampening of cytokine signaling. In addition, the elevated expression of miR-155 due to inflammation primes an ES-62-mediated increase in SOCS3 expression that can potentially act to inhibit STAT3 signals. As a consequence of this dampening of JAK/STAT signalling, there is a reduction in the production of pro-inflammatory mediators and MMPs reflecting a less aggressive phenotype of SF.

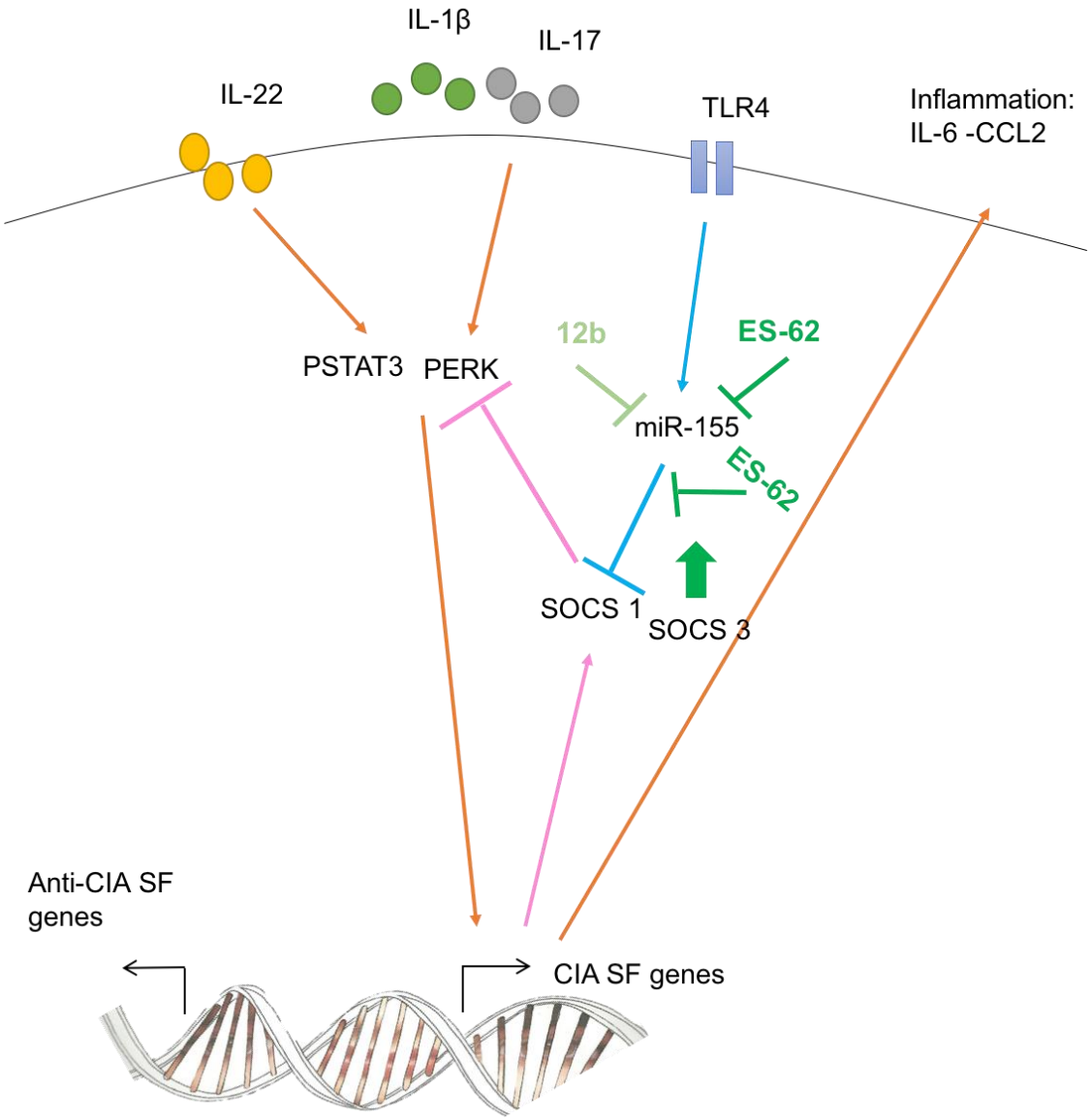
IL-1β
IL-17
IL-22
TLR4
Inflammation:
IL-6 -CCL2
PSTAT3
PERK
12b
ES-62
miR-155
ES-62
SOCS 1
SOCS 3
Anti-CIA SF
genes
CIA SF genes

6. SF activation during RA establishment: role of DNA methylation

6.1 Introduction

Acquisition of an aggressive phenotype by RASF or CIA SF is associated with the expression of new sets of genes, including those involved, for instance, in apoptosis resistance[235], matrix degradation and production of pro-inflammatory factors[134]. Moreover, such changes in their gene expression profile are conserved even after isolation from the pro-inflammatory environment *ex vivo*, highlighting that this is an intrinsic and permanent modification of the genomic expression profile. Such changes in gene expression or silencing are usually regulated by epigenetic processes involving modifications of histones (methylation and acetylation) and/or DNA (methylation). DNA methylation is by far the most studied and understood epigenetic process, usually being associated with stable gene silencing. Consistent both with this and the induction of pro-inflammatory genes in RA, previous studies have highlighted that cells from patients, and in particular their RASF, are globally hypomethylated[85]. Following on from this, a study on the DNA methylome of RASF has revealed that specifically, genes involved in migration, adhesion or matrix-degradation are amongst those hypomethylated[236]. It seems that this global hypomethylation reflects an increased polyamine metabolism in RASF that causes a decrease in S-adenosyl-L-methionine levels[86] as well as a decrease in DNMT1 activity[124].

Thus, the core aims of this chapter were to investigate whether:

- murine SF similarly undergo a decrease in global DNA methylation during CIA and if so, address identifying events that can trigger such a change in the epigenetic landscape.
- global DNA demethylation is sufficient and responsible for transformation of the responses of SF from naïve mice to the aggressive phenotype seen in CIA mice.

- the protection afforded against CIA by ES-62 (and its SMA 12b) that is associated with prevention and/or desensitisation of the aggressive SF phenotype reflects ES-62 and 12b counteracting the global DNA demethylation events that occur in SF during inflammation.

6.2 CIA SF are epigenetically modified cells

Previous studies revealed that RASF display a lower global level of DNA methylation than those from OA patients[85]. It was therefore hypothesised that the stably aggressive phenotype of SF from CIA, relative to those from naive mice[126], reflects that such SF have acquired a novel epigenetic landscape during initiation and progression of disease. This hypothesis is supported by our finding of a decrease in global DNA methylation in CIA SF, which display a 44% decrease in the levels of global methylation compared to naïve SF (Figure 6-1A). Various mechanisms are involved in regulating DNA methylation levels as it can be an active process mediated by DNA demethylases or, as proposed for proliferating tissue such as the pannus, this can occur passively with DNA hypomethylation resulting due to the lack of maintenance of DNA methylation[237]. In mammals, maintenance of DNA methylation during cell division is achieved by the DNA methylase, DNMT1 whilst DNMT3a/3b appear to be the major enzymes responsible for *de novo* methylation. Interestingly, therefore, a decrease in the protein levels of DNMT1 has been shown to correlate with the observed global demethylation of DNA in RASF[124]. Similarly, it is now shown here that whilst there is a significant decrease in the levels of DNMT1 mRNA, this is not the case for DNMT3a in SF from CIA, relative to those from naive mice (Figure 6-1B). Moreover, such downregulation of DNMT1 is translated to the protein level, where substantially lower levels of DNMT1 protein are observed in CIA SF compared to naïve SF (Figure 6-1C). Little or no DNMT3a protein, however was detected in resting SF from either naive or CIA mice by Western blot (data not shown). Collectively, therefore, these data are consistent with the human studies suggesting that SF undergo epigenetic landscape reprograming of (at least) their DNA methylation profile that could explain, at least in part, previous observations about the acquisition of an unusual aggressive phenotype during CIA.

6.3 Pro-inflammatory cytokines contribute to the epigenetic transformation of SF during CIA

Previous *in vitro* studies by Nakano *et al*[126] suggested that the cytokine, IL-1ß that is pathogenic in RA/CIA may be one of the pro-inflammatory factors that can drive global demethylation of DNA in RASF. It is known that an early first step in RA pathogenesis, that occurs before SF activation, is T cell infiltration within the synovial membrane[238]: this may suggest that by establishing a local pro-inflammatory environment, such T cell responses could contribute to SF transformation by inducing global demethylation of their DNA. To test this hypothesis, it was investigated whether chronic exposure to cytokines associated with pathogenic Th responses[126] can induce global DNA demethylation in SF from naive mice. Thus, the ability of IL-17, IL-22 and IL-1ß, the latter of which can promote both Th17/Th22 responses[239], to modulate the global status of DNA methylation of SF from naive mice was tested. All of these cytokines were able to induce global DNA demethylation relative to control untreated (Naive) cells, with IL-22 being the least effective with a 38 % decrease, whilst IL-17 induced a 46 % decrease that was not further enhanced by co-stimulation with IL-22. IL-1ß exhibited the strongest effect with a 60 % decrease (Figure 6-2A), mirroring the effects reported for human SF. To explain whether the decrease in DNA methylation reflected the changes in DNMT expression observed following induction of CIA *in vivo*, changes in the protein levels of DNMT1 and DNMT3 were also analysed. As expected IL-1ß, IL-17 and IL-17 plus IL-22 together decreased the levels of DNMT1 compared to those seen in untreated SF (Naïve). However, surprisingly, IL-22 actually upregulated DNMT1 expression. Moreover, IL-22, and to a lesser extent IL-17, also induced an increase in DNMT3a expression, whilst expression of this enzyme was not substantially modulated by treatment with IL-1ß or IL-17 plus IL-22 (Figure 6-2B and C). Therefore, these data suggested that chronic exposure to pro-inflammatory cytokines *in vivo* might indeed be able to modulate the DNA methylation landscape by virtue of regulating the expression levels of both DNMT1 and DNMT3a. Interestingly and perhaps reflecting that it induced the strongest global demethylation of DNA,

IL-1ß downregulated both DNMT1 and 3a. By contrast, whilst both IL-17 and IL-22 play important roles in initiating CIA[104,133], they appear to do so by distinct mechanisms. Thus consistent with the overall pattern associated with CIA *in vivo*, treatment with IL-17 or IL-17 plus IL-22 resulted in DNA hypomethylation predominantly via downregulation of DNMT1 and presumably consequently, induction of pro-inflammatory mediators: however, treatment with IL-22 alone increased expression of DNMT1 and 3a suggesting that it may act to silence anti-inflammatory factors, an activity that may be partially shared by IL-17 via its induction of DNMT3. However, this cannot be the full story as treatment with IL-22 results in global DNA demethylation suggesting that it either downregulates another DNMT, inactivates DNMT1/3 or induces active demethylase activities.

6.3.1 Global DNA demethylation resulting from chronic exposure to cytokines *in vitro* is associated with hyperproduction of IL-6

To address whether global DNA demethylation of naive SF induced by pro-inflammatory cytokine *in vitro* is sufficient to remodel such normal SF to an aggressive CIA-like SF, their IL-6 production was determined. The basal and pro-inflammatory (IL-1ß, IL-17 and LPS) mediator driven IL-6 production by such demethylated fibroblasts was indeed found to be significantly hyper-induced in IL-1ß-treated and, to a lesser extent, IL-17- and IL-17 plus IL-22-treated fibroblasts (Figure 6-3A). However surprisingly, given the DNA methylation data, IL-22-treated cells did not produce more IL-6 than the naïve fibroblasts, rather if anything, in the IL-1β and LPS-stimulated cultures, they exhibited hyporesponsive cytokine responses. Moreover, whilst the hyper-cytokine promoting mediators resulted in a reduction in the numbers of SF at the end the two weeks culture perhaps reflecting their terminal differentiation to the aggressive phenotype, IL-22 maintained cell survival/proliferation (Figure 6-3B). This may therefore suggest however, that in the initiating phase of CIA, IL-22 may act to promote SF hyperplasia,

invasion of the synovium and pannus formation, thereby promoting pathogenesis. Therefore, cell aggressiveness in terms of hyper-cytokine production generally seems to correlate with DNA demethylation as does the observed cell cycle arrest, a phenomenon often observed during cell reprogramming and dedifferentiation[240].

6.3.2 Is the global DNA demethylation observed in CIA dependent on ERK and/or STAT3 signalling?

As demonstrated earlier in this thesis (Figure 4-4 and Figure 4-8), ERK and STAT3 signalling appears to be constitutively activated in SF from CIA presumably because of the chronic IL-17 signalling in the joint during initiation and progression of CIA/RA. As chronic *in vitro* treatment of naive SF with IL-17 can induce similar levels of global DNA hypomethylation to that observed with CIA *in vivo* it was hypothesised that the constitutive activation of STAT3 and ERK could be important to the induction and maintenance of the global demethylated state of DNA associated with aggressive CIA SF. Certainly, it has been proposed that there is a close relationship amongst STAT3 and ERK signalling and DNA methylation. Indeed, STAT3 has been shown to directly bind to DNMT1 and HDAC1 and cause epigenetic remodelling[241,242]. Likewise, the ERK pathway has been implicated in the modulation of DNMT1 with consequent impact on DNA methylation[243]. Thus, for instance, inhibition of ERK signalling in CD4+ T cells by oxidative stress during lupus, results in suppression of DNMT1 thereby inducing global DNA demethylation[244]. Moreover, HDAC1-mediated regulation of DNMT1 has been shown to be ERK dependent[243]. To explore the potential importance of ERK and STAT3 signalling in driving the DNA demethylation associated with CIA, the effects of ERK- and STAT3-selective inhibitors on the *in vitro* induction of global DNA demethylation by IL-17 and IL-1ß were tested. Whilst the inhibitors were shown to selectively inhibit their projected targets (Figure 4-5 and **Figure 4-10**) they did not themselves affect global DNA methylation, presumably due to the low basal levels of STAT3 and ERK signalling in these

cells. However, the ERK pathway inhibitor Pd98059 significantly suppressed the DNA demethylating effects of both IL-17 and IL-1ß (Figure 6-4). Likewise, the STAT3 inhibitor appeared to impede the effects of IL-17, and to a lesser extent IL-1ß, albeit this did not reach significance perhaps reflecting that this inhibitor did not fully inhibit STAT3 activity. However, the data clearly show that the global DNA demethylation observed in SF exposed to either of the pro-inflammatory cytokines, IL-17 and IL-1ß, is ERK dependent as summarized in the Figure 6-5.

6.4 Is inhibition of DNMT1 sufficient to induce SF aggressiveness?

The above experiments dictated direct investigation of whether global DNA demethylation, and more specifically DNMT1 inhibition, is necessary and sufficient to reprogram naïve SF to an aggressive CIA-like phenotype. In order to investigate this hypothesis, the DNMT1 inhibitor, 5-azacytidine was used: 5-azacytidine is a nucleoside analogue that can be incorporated into DNA and inhibit DNA methylation by preventing DNMT1 from binding. Indeed, Karouzakis et al. [124] reported that the exposure of SF from a trauma patient to 5-azacytidine reproduced the aggressive phenotype of RASF. Consistent with this, SF from naïve DBA/1 mice treated for one week with 5-azacytidine exhibited levels of global DNA methylation that were reduced by approximately 50% (Figure 6-6A) and secreted higher levels of IL-6 spontaneously (Figure 6-6B). However, no difference could be detected in IL-6 production by naive or 5-aza cells stimulated with either IL-17 or IL-1β suggesting that whilst demethylation may be sufficient for some degree of hyperactivity, the actions of chronic cytokine signalling can further enhance this. Nevertheless, these data provided direct evidence that inhibition of DNMT1 by 5-azacytidine can induce a CIA SF like aggressive phenotype in naïve fibroblasts.

6.5 Does the protection against CIA afforded by ES-62 and 12b reflect effects on the epigenetic landscape?

6.5.1 Modulation of DNA methylcytosine levels by ES-62 and 12b

Collectively, the data presented above support the hypothesis that inhibition of DNMT1 and hence consequent global demethylation of DNA likely contributes to the acquisition of an aggressive SF phenotype in CIA. Since ES-62 and 12b are able to prevent and/or counteract development of this aggressive phenotype during CIA it was important to assess whether these immunomodulators could directly regulate DNMT1 expression and hence global DNA methylation in SF during CIA. Therefore, SF were extracted from mice undergoing CIA that had been treated *in vivo* with PBS, ES-62 or 12b: in addition, some of these mice were concurrently treated IL-1ß (Figure 6-7A and B) as this cytokine, which is pathogenic in RA/CIA[177], is not only the target of 12b (and to a lesser extent ES-62) in CIA[114], but also is the most effective mediator at inducing DNA hypomethylation *in vitro*. Indeed, exposure to IL-1ß *in vivo* abrogates protection by ES-62 and 12b and further increases the severity of CIA in PBS-treated mice. Consistent with this, the lower levels of global DNA methylation displayed by SF from PBS-CIA mice were further reduced by exposure to IL-1ß *in vivo*. Interestingly, therefore, whilst 12b acts to promote global methylation of DNA and hence presumably suppress inflammatory responses, somewhat counterintuitively, this is further promoted by co-administration of 12b and IL-1ß, possibly suggesting the triggering of homeostatic inflammation-resolution mechanisms in this latter group of mice that exhibit severe disease. However, more surprisingly, exposure to ES-62 induced an even stronger global DNA hypomethylation profile than that of PBS-CIA (± IL-1ß) although, and as seen with the 12b treatment, in this case exposure to IL-1ß appeared to counter-act ES-62-induced global DNA demethylation.

Consistent with its ability to induce global hypomethylation of DNA, *in vivo* exposure of mice undergoing CIA to ES-62, but not 12b, further downregulates the expression of DNMT1 and DNMT3a in SF to even below the levels seen in mice undergoing CIA at the mRNA level (Figure 6-7C and D). Although this further suppression did not translate to the protein level (Figure 6-7D and E), reflecting their hypomethylated status, these cells still exhibited reduced levels (comparable to those seen in SF from CIA mice) of DNMT1, whilst DNMT3a protein expression was not detected in SF from any of the groups (data not shown). By contrast, and as originally predicted based on its protective effects, treatment with 12b significantly increased the mRNA levels of DNMT1 and DNMT3a, compared to those in CIA SF, returning them to levels observed in naïve SF.

Although, the data obtained with ES-62 appear counterintuitive to the hypothesis that global DNA hypomethylation in SF is associated with the pathogenic phenotype, such global analysis does not inform on the genes regulated: hence these data may suggest that ES-62 induces expression of anti-inflammatory/tissue protective genes to counteract pathology in the joint rather than simply prevent/reverse the upregulation of pro-inflammatory genes, a hypothesis that supports the therapeutic potential of ES-62 in established joint disease.

6.5.2 ES-62 may also impact on the epigenetic landscape by upregulating HDAC1

The epigenetic landscape is shaped by many factors in addition to DNA methylation, such as various modifications of histones. Indeed, there are close interactions between histone modifications and DNA methylation, a good example being the correlation between histone acetylation (often associate with upregulated gene expression) and DNA methylation[245] (Figure 6-8). Moreover, as it has been reported that HDAC1 can directly bind DNMT1 and regulate its activity[246], it was of particular interest to investigate whether differential expression of HDAC1 by SF derived from CIA mice, treated with

PBS or ES-62, could potentially explain the diametrically opposite phenotypic results associated with strong global DNA demethylation under these conditions. Analysis of HDAC1 expression by ES-62- CIA- and Naïve SF revealed a strong upregulation of this enzyme by ES-62 (Figure 6-9), suggesting that in the context of global DNA hypomethylation this may have anti-arthritogenic effects, perhaps by silencing some pro-inflammatory genes or alternatively, by inducing some inflammation-resolving, tissue repair genes. Intriguingly, therefore, analysis of the effect of chronic cytokine treatment of SF *in vitro* revealed a correlation between the most demethylated and aggressive cells (IL-1ß and IL-17 plus IL-22) and least HDAC1 expression (Figure 6-10). Collectively therefore, these data support the hypothesis that upregulated HDAC1, at least in the context of severe DNA hypomethylation, might be associated with protection against the development/maintenance of the aggressive SF phenotype, and provide a mechanism to explain why SF with demethylated DNA from ES-62-treated mice display a protective phenotype.

6.5.3 Understanding the mechanisms underpinning ES-62 modulation of the epigenetic landscape – site dependent demethylation?

The data presented in this chapter clearly demonstrate that the genome of CIA SF is hypomethylated and to our surprise, is further globally demethylated in SF from CIA-mice exhibiting protection afforded by ES-62. Thus, it is important to understand which promoter sites are targeted for demethylation. Pertinently, therefore, a particular SF methylome signature has already been identified from RA patients that reveals the demethylation of specific sites such as STAT3, CASP1, IL-6 or CXCL12 known to be involved in SF aggressiveness[247-249]. To attempt to reveal genes targeted by DNA demethylation in RASF that are potentially regulated by ES-62, a cross array bioinformatics analysis was performed (Table 6-1). This analysis was based on the two previously published arrays, the DNA methylome signature published by Nakano *et al*[248] and the expression profile of RA synovial membranes

exposed *in vitro* to ES-62 by Harnett *et al*[99]. Genes identified in both arrays are summarised in Table 6-1 and provide a first hint of potential sites at which ES-62 can modulate the DNA methylation profile and include prediction of known targets of ES-62 action such as downregulation of IL-1β (via downregulation of caspase 1). Such genes therefore represent potential candidates for further investigation and they provide proof of concept that the hypomethylation of DNA in SF from ES-62-treated CIA mice may be regulating different promoter sites from those activated during CIA resulting in responses to counteract the pro-inflammatory expression profile induced in CIA SF.

6.6 Discussion and Conclusions

The data presented in this chapter confirm the hypothesis that SF extracted from CIA mice are indeed intrinsically epigenetically modified cells, exhibiting global hypomethylation of their DNA predominantly due to a decrease in DNMT1 expression. Such transformation of the epigenetic landscape of naive SF can be recapitulated *in vitro* by chronic exposure to several pro-inflammatory cytokines, implicated in RA pathogenesis, as evidenced by this driving DNA demethylation and associated hyper-production of IL-6. Perhaps surprisingly, this was not the case for IL-22, which has been shown to be critical to the initiation of CIA, with this mediator exhibiting differential effects on the levels of DNMT1 and DNMT3a, relative to the other pro-inflammatory cytokines tested. In addition, it is possible that IL-22 acts via a different mechanism, perhaps inducing DNA methylation to silence anti-inflammatory/tissue protective genes expression. Nevertheless, the data arising out of concomitant treatment with IL-17 plus IL-22 underlines that, i*n vivo,* integration of all signals during inflammation determines the resulting levels of DNA methylation. In particular, they highlight the importance of the local environment and its role in signal integration in remodelling the SF epigenetic landscape contributing to its pathogenic phenotype (Figure 6-11).

Global DNA demethylation therefore indeed provides a good explanation for the transformation of SF to an aggressive phenotype during the induction of CIA: however, the effects of ES-62 on DNA methylation raise the question as to whether global DNA demethylation of SF constitutes a good marker for SF aggressiveness as previously suggested, since exposure to ES-62 induces an even stronger global demethylation of DNA than that observed in SF from CIA mice. Thus, it is possible that whilst a certain level of demethylation may be pathogenic, more profound demethylation may result in the induction of homeostatic control mechanisms to effect resolution of inflammation and instigate tissue repair mechanisms. Indeed, such a mechanism may reflect the reports that in distinct types of cancers, DNA demethylation can result in dramatically opposite effects in different cell types[81,250]. This reinforces that it is crucial to identify the specific sites of demethylation rather than focusing on global effects. Indeed, even if cells are globally hypomethylated, certain promoters such as that of the death receptor 3 gene (DR3; a member of the pro-apoptotic Fas gene family) have been found to be hypermethylated in some RA patients[87]. Bisulfite sequencing could reveal which sites are differentially targeted in SF from CIA and CIA-ES-62-treated mice and predictions by the cross array analysis have already provided proof of concept that some genes expressed by DNA demethylation in RASF may be silenced by ES-62 and vice versa.

Finally, the disconnect in action between ES-62 and 12b is intriguing and may reflect that this SMA can only recapitulate certain of the properties of the parasite molecule. Nevertheless, the apparent hypermethylation induced by 12b might explain its protection against CIA in terms of its inhibition of IL-1ß production[114]. Indeed as Firestein and colleagues reported, and confirmed here with CIA SF, prolonged exposure of SF to IL-1β induces global demethylation of DNA by decreasing DNMT1 and 3a expression and activity[248], promoting the pathogenic phenotype of these key arthritogenic cells in the joint.

Figure 6-1 CIA SF display global DNA demethylation relative to SF from naive mice and this is associated with reduced expression of DNMT1

A: SF were isolated from naïve and CIA mice from 3 different animal models (mean score 3.6 ± 1.5, n = 6; mean score 4.5 ± 1.3, n=10 and mean score 2.5 ± 0.8, n=12). Genomic methyl cytosine levels were measured as described in the M&M section 2.9 with the OD values obtained, normalised to the value of untreated fibroblasts from naive mice (considered as 100% genomic methylation). This experiment represents three independent mouse model experiments which shows that SF from CIA mice exhibit in average 79.3% of methyl cytosine ± 11.6, n=3 relative to those from naive mice.

B and C: SF were isolated from naïve and CIA mice (mean score 3.6 ± SEM, n = 6). Cells were plated at a concentration of 0.3 10^6 cells per well in a 6 wells-plate as independent triplicate or duplicate cultures for each treatment condition (respectively for mRNA and protein extraction) for 24 hours. Total mRNA was extracted and DNMT1 and DNMT3a expression at the mRNA level were analysed by qRT-PCR as described in the M&M section 2.8. Triplicate estimations from each culture and the mean levels were normalised to GAPDH expression and expressed as a mean fold change ± SEM (n=3) (B). Expression of DNMT1 at the protein level from independent duplicate cultures was determined by Western blot (C) total ERK protein level is as well revealed as control for protein loading.

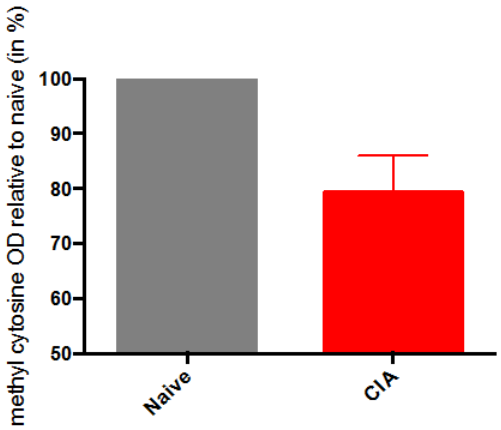
methyl cytosine OD relative to naive (in %)
100
90
80
70
60
50
Naive
CIA

B

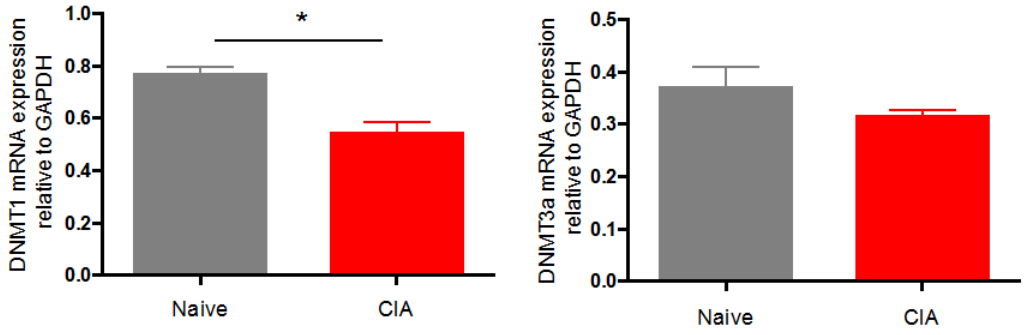
DNMT1 mRNA expression relative to GAPDH
1.0
0.8
0.6
0.4
0.2
0.0
*
Naive
CIA
DNMT3a mRNA expression relative to GAPDH
0.5
0.4
0.3
0.2
0.1
0.0
Naive
CIA

C

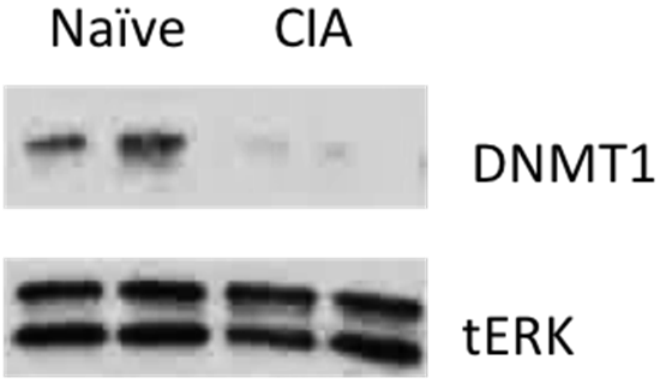
Naïve
CIA
DNMT1
tERK

Figure 6-2 Pro-inflammatory cytokines can modulate *in vitro* the global DNA methylation profile of SF from naive mice

Naïve SF were plated at 0.3 x 10^6 cells/ml and as individual culture for the different treatment groups. For 2 weeks cells were stimulated with daily addition of the indicated cytokines, IL-22, IL-17 or both together (2.5 ng/ml each) and IL-1ß (1 ng/ml). At the end of the treatment, genomic DNA and proteins were extracted for further analysis.

A: Genomic methyl cytosine level was measured and presented as the absolute OD value relative to the naïve OD value. Considering the untreated fibroblasts from naive mice (Naive) as 100% genomic methylation, the average methylation after the treatment is expressed as percentage on the figure. This experiment has been successfully repeated three time independently.

B: DNMT1 and DNMT3a protein expression was determined by Western blot analysis and the levels in the 3 independent cultures from the cell extracted from the same naïve mouse and levels relative, to GAPDH was quantified using the software ImageJ (C) and expressed as the mean values ± SEM. ANOVA tests followed by Tukey multiple comparison test were performed where * $p < 0.05$; ** $p < 0.01$, *** $p<0.001$. This experiment has been realised only once.

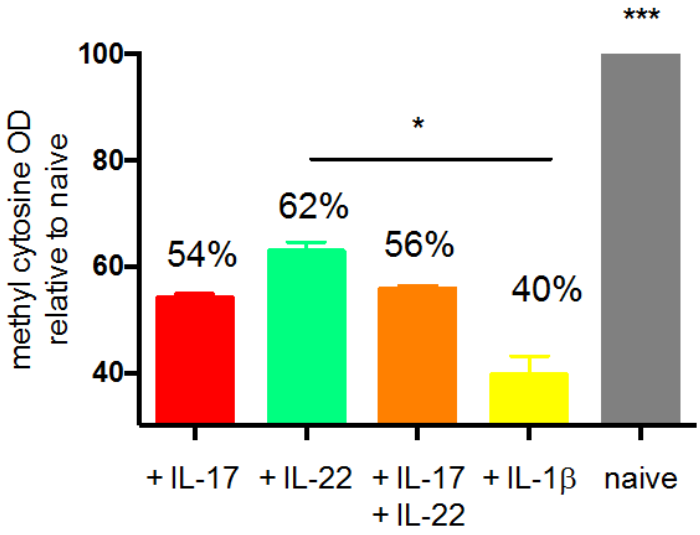
***
100
80
60
40
*
methyl cytosine OD
relative to naive
54%
62%
56%
40%
+ IL-17
+ IL-22
+ IL-17
+ IL-22
+ IL-1β
naive

B

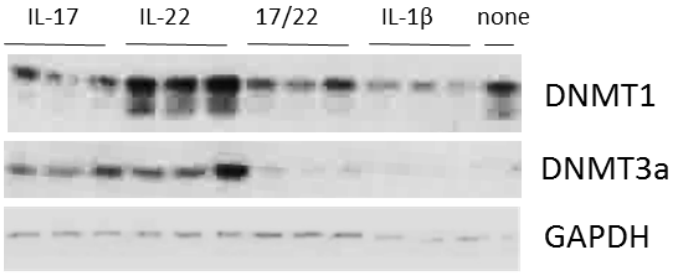
IL-17
IL-22
17/22
IL-1β
none
DNMT1
DNMT3a
GAPDH

C

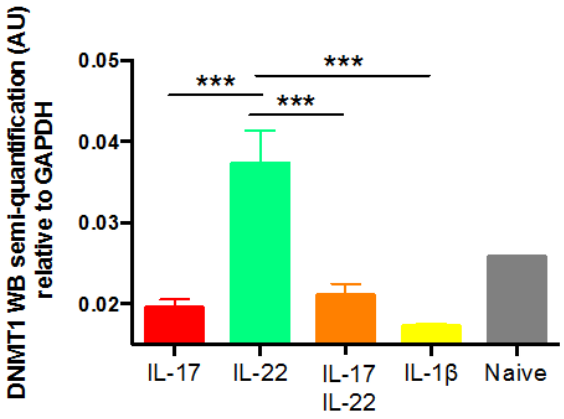
DNMT1 WB semi-quantification (AU)
relative to GAPDH
0.05
0.04
0.03
0.02
***
***
***
IL-17
IL-22
IL-17
IL-22
IL-1β
Naive

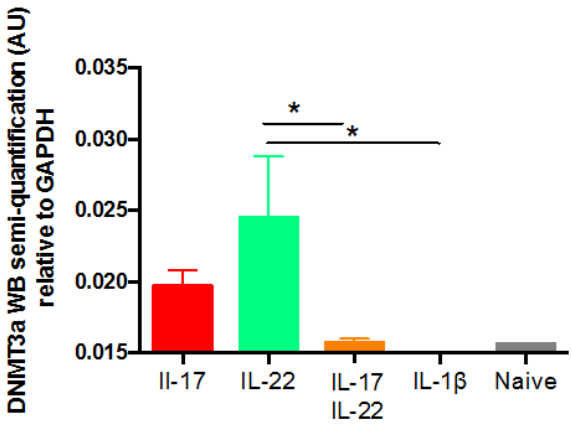
DNMT3a WB semi-quantification (AU)
relative to GAPDH
0.035
0.030
0.025
0.020
0.015
*
*
Il-17
IL-22
IL-17
IL-22
IL-1β
Naive

Figure 6-3 Global DNA demethylation induced by cytokines is associated with development of an aggressive SF phenotype

SF from Naïve mice treated *in vitro* with cytokines as described in Figure 6-2 were assessed for live cell concentration at the end of the chronic exposure experiment (A). Such cells were re-plated in triplicate cultures for each treatment group (10^4/well) and synchronised overnight in DMEM 1% FCS prior to stimulation for 24 h with IL-17 (25 ng/ml), IL-1ß (10 ng/ml), LPS (1 µg/ml) or medium alone in DMEM 10% FCS. Cell supernatants were collected and IL-6 release was measured by ELISA. Data are expressed as the mean (or means of triplicate estimations) ± SEM of n=3 independent cultures and analysed using one-way ANOVA and the Tukey multiple comparison post-test where * $p < 0.05$; ** $p < 0.01$, *** $p<0.001$ as compared to the untreated (naïve) condition. Data are from a single experiment.

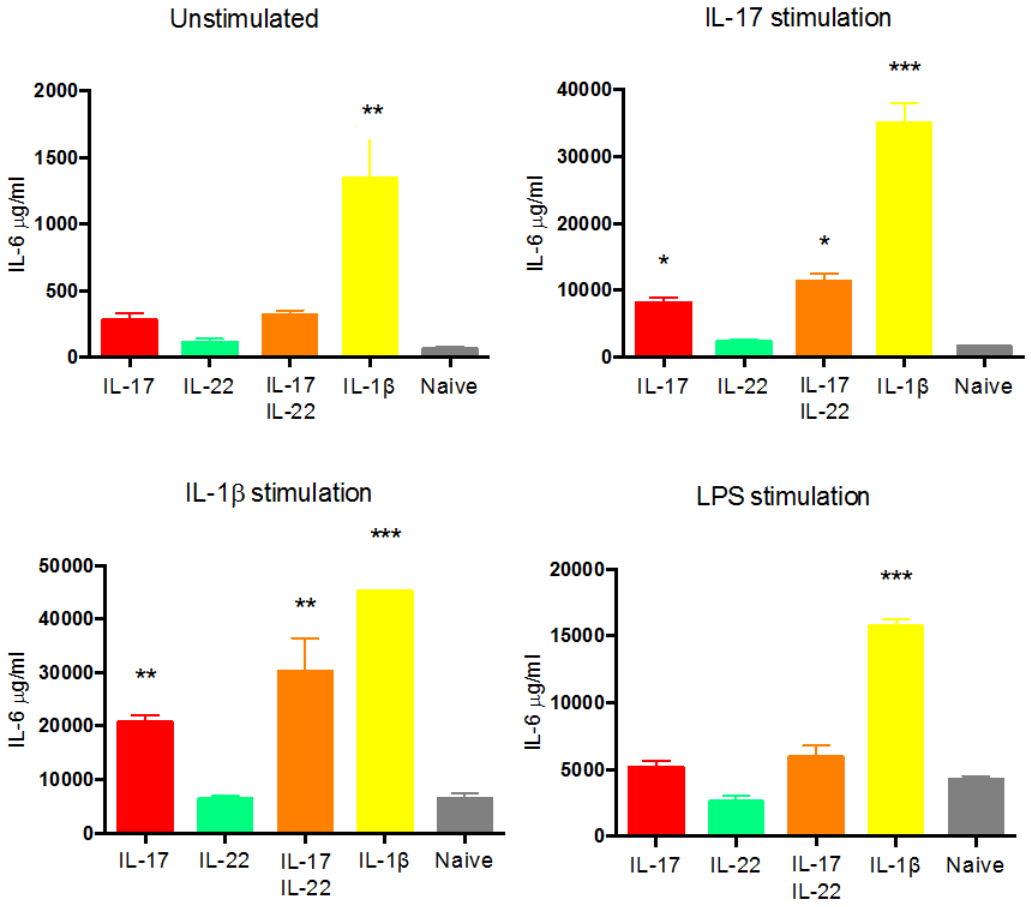
Unstimulated
IL-6 µg/ml
2000
1500
1000
500
0
**
IL-17
IL-22
IL-17 IL-22
IL-1β
Naive
IL-17 stimulation
40000
30000
20000
10000
0
*
*
***
IL-1β stimulation
50000
40000
30000
20000
10000
0
**
**
***
LPS stimulation
20000
15000
10000
5000
0
***

B

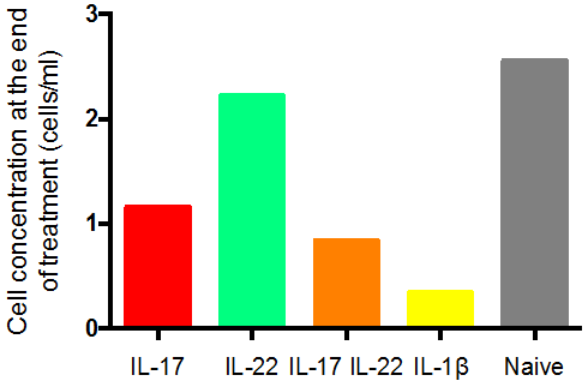
Cell concentration at the end of treatment (cells/ml)
3
2
1
0
IL-17
IL-22
IL-17 IL-22
IL-1β
Naive

Figure 6-4 IL-17- and IL-1ß-induction of global DNA demethylation is dependent on ERK and STAT3 signalling

SF from Naïve mice were treated for two weeks daily as in with IL-17 (2.5 ng/ml) and IL-1ß (1 ng/ml) as described in the figure 6-2, in the presence of the MEK (ERK pathway) inhibitor, PD98059 (25 µM) or the STAT3 inhibitor 5.15 DPP (50 µM) as previously used in Figure 4-5 and **Figure 4-10**. Genomic DNA was extracted from the treated cells and the levels of methyl cytosine determined and data presented as mean absolute OD values from 3 independent cultures. In addition, the relative percentage of global methylation when normalised to the "naïve" untreated cells (100% methylation) is shown on the figure. The data are expressed as mean values ± SEM, with ANOVA and Tukey multiple comparison tests performed, with * $p < 0.05$; ** $p < 0.01$, *** $p<0.001$ indicated for relevant statistics.

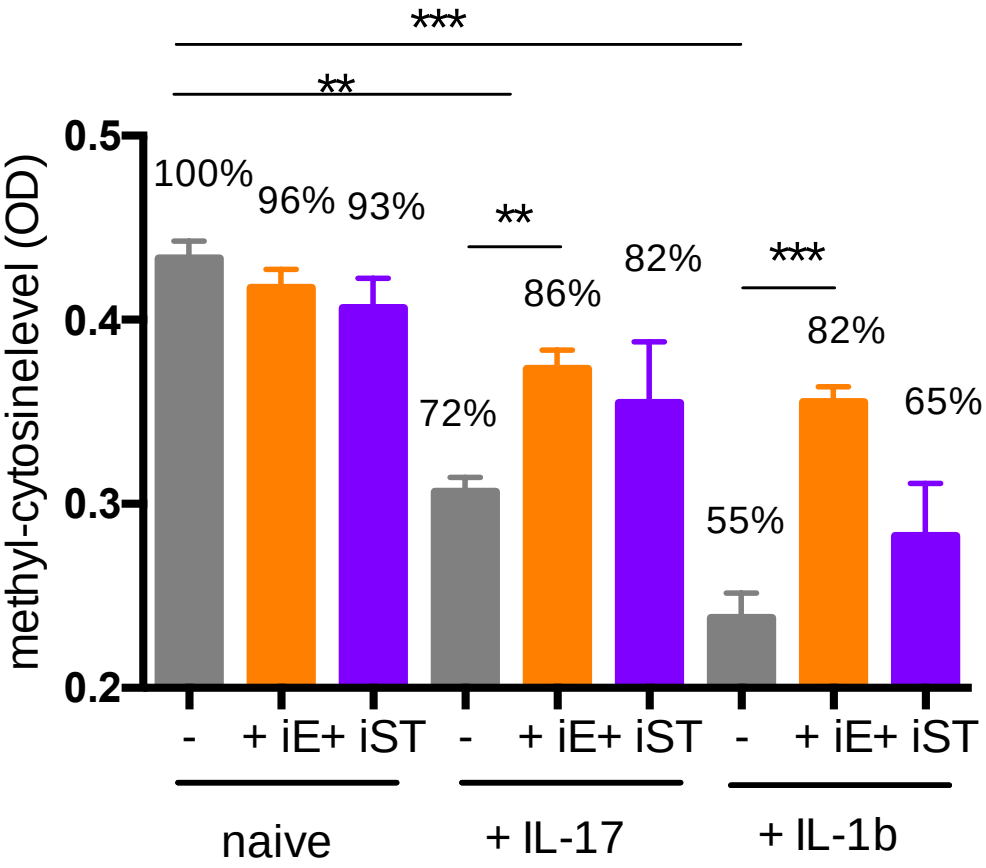
***
**
methyl-cytosinelevel (OD)
0.5
0.4
0.3
0.2
100%
96%
93%
**
72%
86%
82%
***
55%
82%
65%
- + iE+ iST - + iE+ iST - + iE+ iST
naive
+ IL-17
+ IL-1b

Figure 6-5 Hypothetical model of the events underpinning the global DNA demethylation occurring in SF during CIA

Proinflammatory and pleiotropic cytokines, such as IL-17, IL-22 and IL-1ß, are present in affected joints during CIA. By promoting ERK and STAT3 signalling, IL-17 and IL-1β modulate levels of DNMT1 and DNMT3a thereby inducing global changes in the epigenetic DNA methylation landscape. Such changes in global DNA methylation allow the expression of sets of genes promoting CIA. However, IL-22 does not appear to utilise these pathways and so for its pathogenic effects during disease initiation, IL-22 may act via as yet undefined signals to silence anti-CIA genes, providing an additional mechanism to explain the acquisition of an aggressive SF phenotype during CIA.

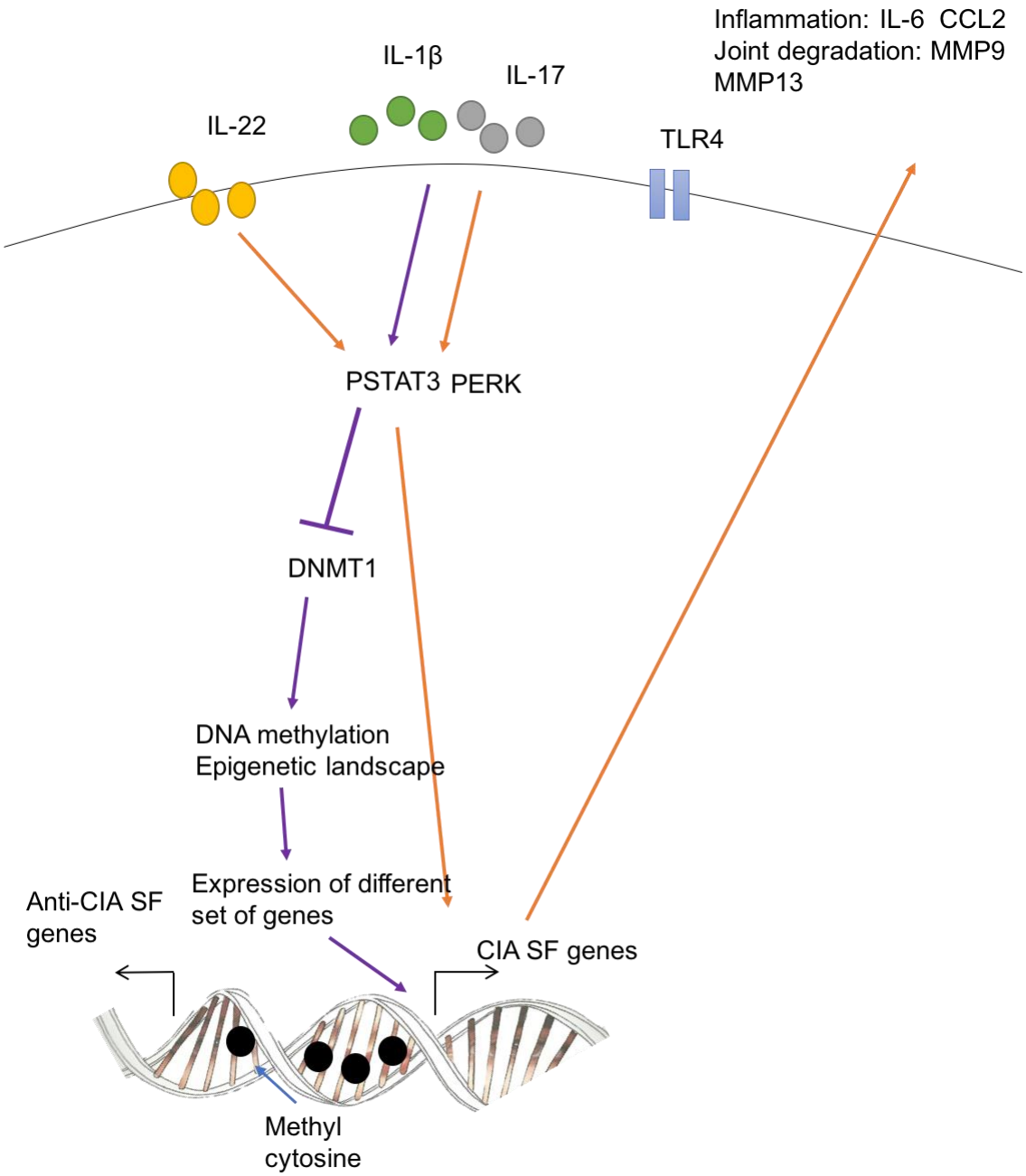
Inflammation: IL-6 CCL2
Joint degradation: MMP9
MMP13
IL-1β
IL-17
IL-22
TLR4
PSTAT3
PERK
DNMT1
DNA methylation
Epigenetic landscape
Expression of different
set of genes
Anti-CIA SF
genes
CIA SF genes
Methyl
cytosine

Figure 6-6 The DNMT1 inhibitor, 5-azacytidine induces global DNA hypomethylation and associated hyper-production of IL-6

Naïve SF were plated as independent triplicate cultures and treated daily for a week by the addition of the DNMT1 inhibitor 5-azacytidine (1 μM) dissolved in DMEM with 10% FCS.

A: Genomic DNA was assessed for methyl cytosine levels after treatment, with the data presented as the means of absolute OD values from 2 independent cultures. In addition, the relative percentage of global methylation normalised to the naïve untreated cells (100% methylation) is shown on the figure. This experiment has been successfully repeated independently three times.

B: From parallel cultures, such cells after treatment were plated (10^4/well and stimulated for 24 h with IL-17 (25 ng/ml), IL-1β (10 ng/ml) or DMEM 10% FCS as control. Supernatants from independent triplicate culture were collected and IL-6 concentration measured by ELISA. Data were expressed as the mean (of means of triplicate analyses) ± SEM and ANOVA followed by Tukey multiple comparison tests were performed where * $p < 0.05$; ** $p < 0.01$, *** $p<0.001$ for the relevant statistics. These sets of data are representative of two independent studies.

A

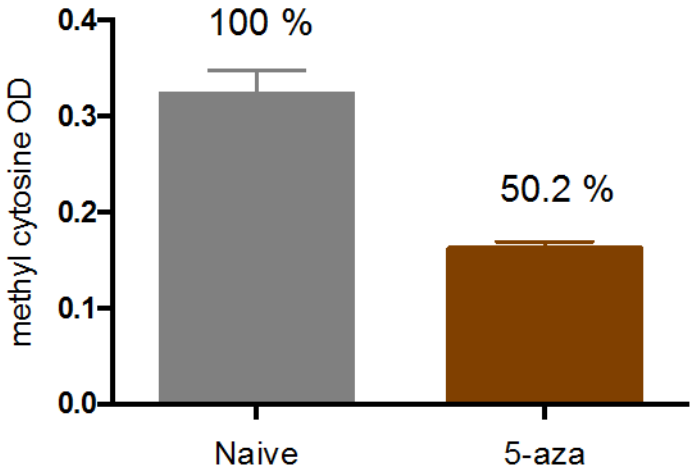
methyl cytosine OD
0.4
0.3
0.2
0.1
0.0
100 %
50.2 %
Naive
5-aza

B

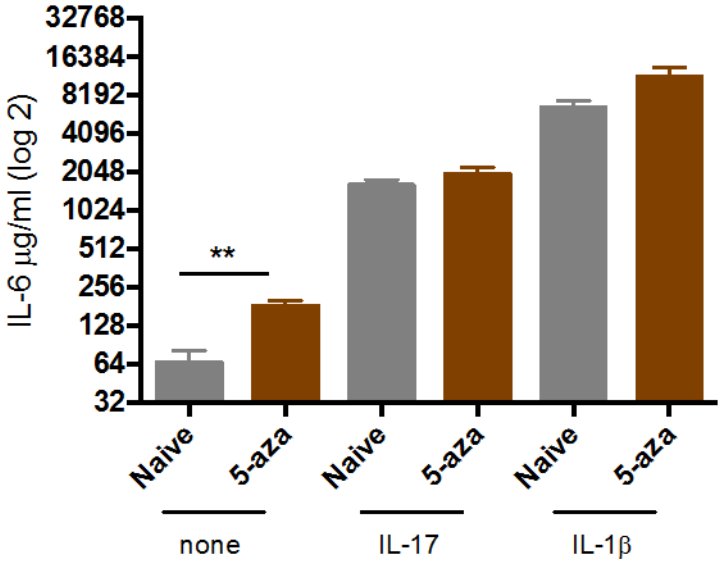
IL-6 µg/ml (log 2)
32768
16384
8192
4096
2048
1024
512
256
128
64
32
**
Naive
5-aza
Naive
5-aza
Naive
5-aza
none
IL-17
IL-1β

Figure 6-7 ES-62 and 12b differentially modulate the global DNA methylation status of SF from mice undergoing CIA

A: All SF used for the following experiments were isolated from the CIA mouse model experiment presented in figure 3-7 and represented again to facilitate awareness of the disease scores of the particular treatment groups.

B: SF were derived from the joints from mice undergoing CIA treated with PBS (CIA, mean score 3.66 ± 1.5, n=6), PBS + IL-1β (CIA+ IL-1β, mean score 6 ± 1.93, n=6), 12b (mean score 0.71 ± 0.36, n=7), 12b + IL-1β (mean score 7.62 ± 1.67, n=8), ES-62 (mean score 1.5 ± 1.15, n=6) or ES-62 + IL-1β (mean score 9 ± 1.93, n=6). Genomic methyl cytosine levels were measured as described in the M&M section and presented as normalised to level (100%) found in SF derived from naïve mice. Data are from a single CIA model.

C: SF derived from the CIA and naive mice treated in vivo as described above, namely, naïve untreated, or CIA mice exposed to PBS (CIA, mean score 3.66 ± 1.5, n=6), 12b (mean score 0.71 ± 0.36, n=7) or ES-62 (mean score 1.5 ± 1.15, n=6) plated as independent triplicate culture for each treatment group and were assessed for their levels of DNMT1 and DNMT3a mRNA by RT-qPCR as described in the M&M section (2.8). Levels were normalised to GAPDH and expressed as a fold change for the three independent cultures where data are expressed as mean± SEM, n=3 and statistical analysis was by ANOVA followed by the Tukey post-test where * $p < 0.1$ ** $p < 0.01$ and *** $p < 0.001$.

D: SF extracted from joints from naïve or CIA mice, the latter treated with PBS (CIA, mean score 3.66 ± 1.5, n=6) or ES-62 mice (mean score 1.5 ± 1.15, n=6) were analysed for DNMT1 protein levels by Western blot and the levels of expression relative to ERK were quantified using Image J software. Data were obtained from 3 independent cultures and were representative of two such independent studies. ANOVA tests followed by the Tukey multiple comparison test were performed and results were expressed as the mean ± SEM, n=3, where ** $p < 0.01$

A

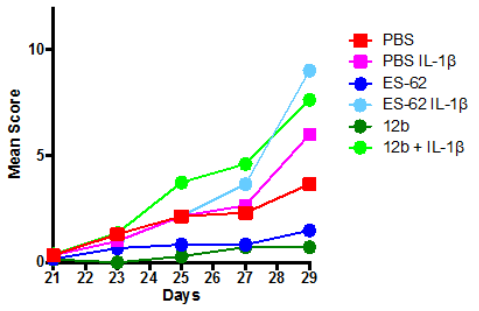
Mean Score
Days
PBS
PBS IL-1β
ES-62
ES-62 IL-1β
12b
12b + IL-1β

B

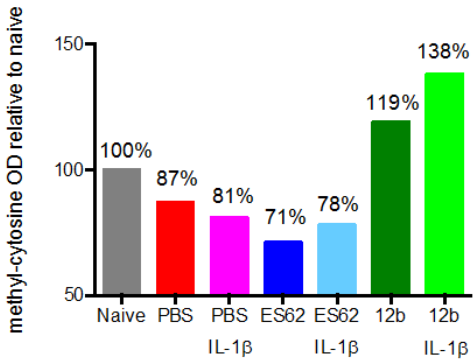
methyl-cytosine OD relative to naive
100%
87%
81%
71%
78%
119%
138%
Naive
PBS
PBS IL-1β
ES62
ES62 IL-1β
12b
12b IL-1β

C

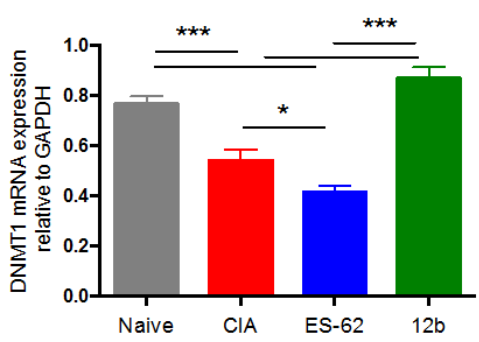
DNMT1 mRNA expression relative to GAPDH
Naive
CIA
ES-62
12b

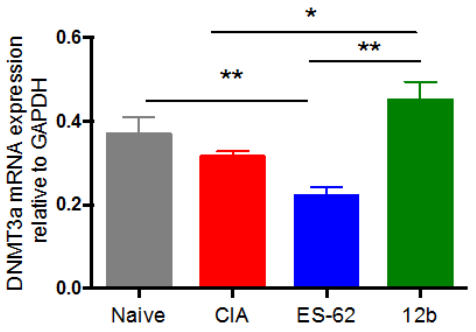
DNMT3a mRNA expression relative to GAPDH
Naive
CIA
ES-62
12b

D

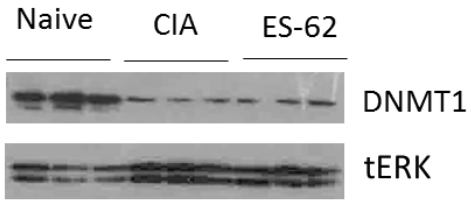
Naive
CIA
ES-62
DNMT1
tERK

E

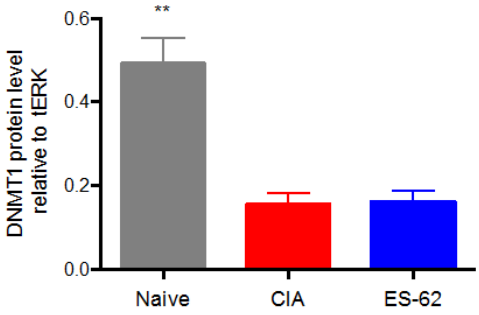
DNMT1 protein level relative to tERK
Naive
CIA
ES-62

Figure 6-8 Importance of the balance between DNA methylation and promoter acetylation to gene expression

The balance between the levels of DNA methylation and histone acetylation in a particular promoter region determines the potential accessibility of the promoter to transcription factors. Thus, a heavily DNA-methylated and poorly acetylated promoter will be in the heterochromatin state and will be permanently repressed, while the presence of highly acetylated histones and poorly methylated DNA in a promoter region results in euchromatin and constitutive gene expression. All states in between allow inducible gene expression.

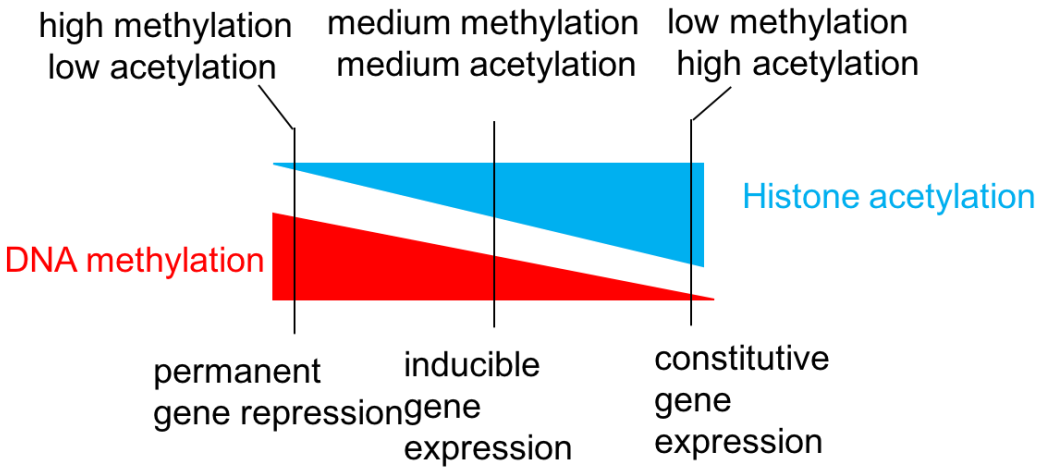
high methylation
low acetylation
medium methylation
medium acetylation
low methylation
high acetylation
Histone acetylation
DNA methylation
permanent
gene repression
inducible
gene
expression
constitutive
gene
expression

Figure 6-9 Exposure to ES-62 *in vivo* upregulates HDAC1 expression in SF from CIA mice

SF derived from ES-62-treated CIA mice (mean score 0.5 ± 0.22, n=6), CIA mice (mean score 3.17 ± 1.38, n=6). Such cells were pooled by treatment group and plated as independent triplicate culture and naïve mice were analysed for protein expression of HDAC1 by Western blot and the levels relative to GAPDH were quantified using Image J software. Data are shown from 3 independent cultures and represented by mean ± SEM, n=3 and ANOVA, followed by the Tukey multiple comparison test, was performed where ** $p < 0.01$

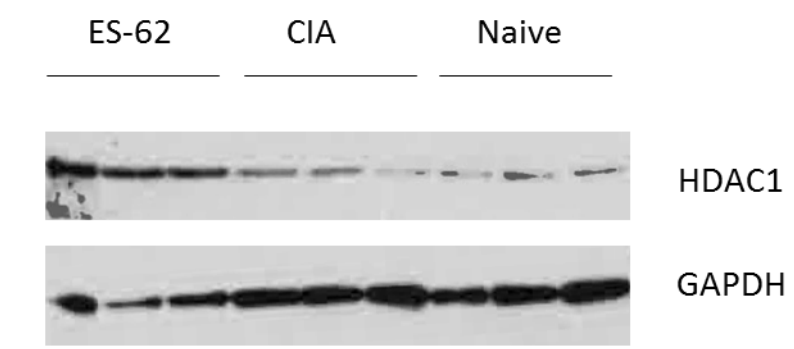
ES-62
CIA
Naive
HDAC1
GAPDH

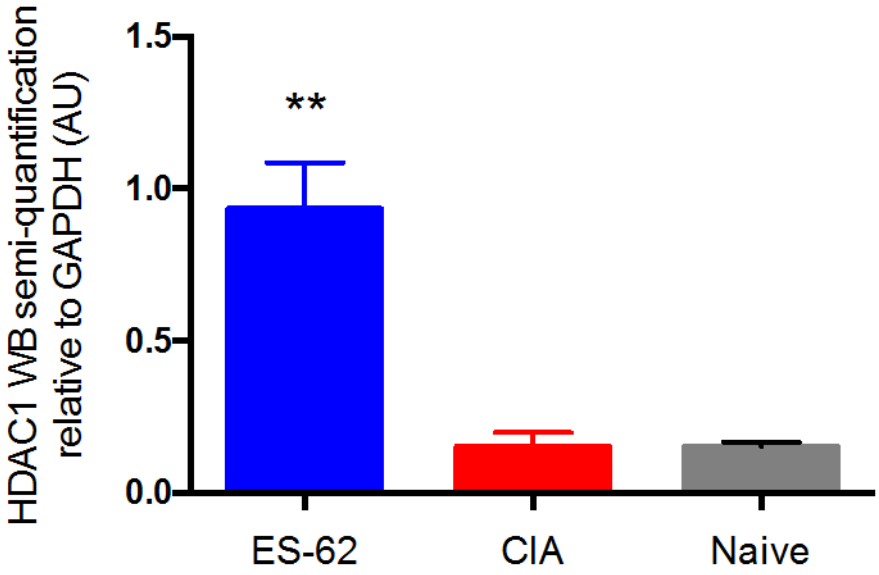
HDAC1 WB semi-quantification relative to GAPDH (AU)
1.5
1.0
0.5
0.0
**
ES-62
CIA
Naive

Figure 6-10 Induction of DNA demethylation following chronic exposure to cytokines *in vitro* is associated with modulation of HDAC1 expression

SF derived from naive mice were chronically exposed for two weeks to IL-17 (2.5 ng/ml), IL-22 (2.5 ng/ml), both cytokines, or IL-1ß (1 ng/ml) as described in figure 6-3. At the end of the treatment, total cellular protein was recovered and the levels of HDAC1 determined by Western blot analysis and quantified relative to GAPDH using Image J software. The data shown represents the levels found in three independent cultures and analysis by ANOVA followed by the Tukey multiple comparison test where results were expressed as the mean ± SEM and * $p < 0.1$.

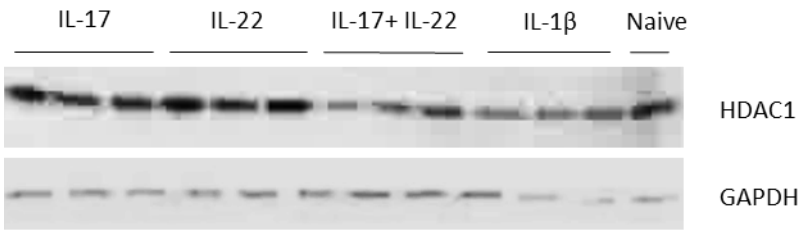
IL-17
IL-22
IL-17+ IL-22
IL-1β
Naive
HDAC1
GAPDH

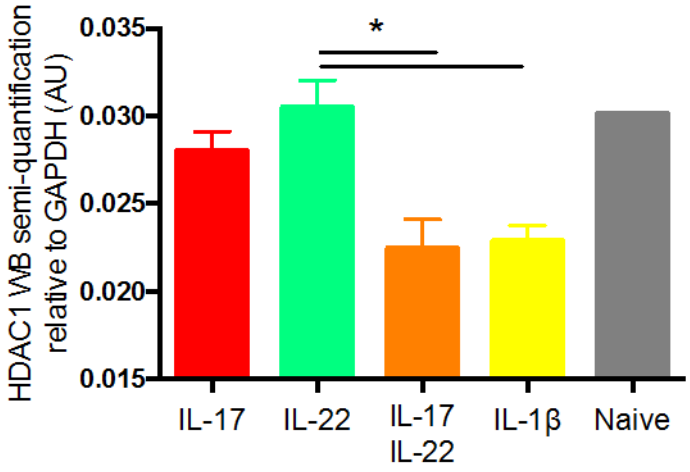
HDAC1 WB semi-quantification relative to GAPDH (AU)
0.035
0.030
0.025
0.020
0.015
*
IL-17
IL-22
IL-17 IL-22
IL-1β
Naive

Table 6-1 Cross-array referencing of genes modulated by ES-62 in Synovial Membranes from an RA patient with SF genes undergoing regulation via DNA methylation in RA

Previously published array data from Nakano *et al*[251] and Harnett *et al*[99] were cross-analysed to identify genes characteristic of the signature DNA methylome of RASF that are also modulated by ES-62 in the synovial membrane of an RA patient, *in vitro*. Such genes were classified in four categories: upregulated by ES-62 and hypermethylated in RASF, upregulated by ES-62 and demethylated in RASF, downregulated by ES-62 and hypermethylated in RASF and downregulated by ES-62 and demethylated in RASF.

Upregulated by ES-62 and hypermethylated in RASF

Gene name	Function
COLEC12	surface glycoprotein associated with host defence.
DAPK1	positive mediator of interferon gamma induced programmed cell death
EGF	growth factor important in cell growth, proliferation and differentiation
FCGRT	encodes the Fc region of monomeric immunoglobulin G
NCK1	adaptor protein transducing signal from receptor tyrosine kinase for pathways related to the immune system and GPCR
PDE4DIP	interacts with the phosphodiesterase 4 to anchor it to the Golgi.
SLC22A1	organic cation transporter
SLC29A1	Nucleoside transporter
STAT5B	another member of the STAT family, its transduction is triggered by IL-2, IL-4 cytokines.
TGFBR3	encodes a TGFβ receptor
TNF	pro-inflammatory cytokine known to be particularly involved in rheumatoid arthritis
TNXB	anti-adhesive effect, important in matrix maturation during would healing

Upregulated by ES-62 and hypomethylated in RASF

Gene name	Function
AMOTL2	Inhibitor of WNT/βcatenin pathway
CA12	Carbonic anhydrase, involved in calcification and bone resorption
CRYBB2	Crystalin beta B2 – Wnt pathway inhibitor
FUT4	Generate fucosylated carbohydrate structures
KCNMA1	Potassium-calcium channel
SQLE	Squalene epoxidase catalyzes the first oxygenation step in sterol biosynthesis
TRHDE	extracellular peptidase that specifically cleaves and inactivates the neuropeptide thyrotropin-releasing hormone

Downregulated by ES-62 and hypermethylated in RASF

Gene name	Function
APLP2	Interacts with major histocompatibility complex (MHC) class I molecules.
DUSP10	Dual specificity protein phosphatases inactivate their target kinases by dephosphorylating both the phosphoserine/threonine and phosphotyrosine residues. Negatively regulate MAP kinase superfamily
EPHA3	ephrin receptor subfamily of the protein-tyrosine kinase family
HAS1	Enzyme synthetizing hyluronan
ITGBL1	beta integrin subunit protein that is a member of the EGF-like protein family
SLC16A3	Monocarboxylate transporter

Downregulated by ES-62 and hypomethylated in RASF

Gene name	Function
CASP1	involved in cell apoptosis and as well has the ability to proteolytically cleave and activate the inactive precursor of interleukin-1
LPP	involved in cell-cell adhesion and cell motility and as may may promote tumor growth
MGMT	gene crucial for genome stability

Figure 6-11 Model of how ES-62 and 12b act to modulate the epigenetic landscape in SF.

ES-62 and 12b are able to regulate the levels (mRNA and protein) of DNMTs and therefore, the global DNA methylation profile of SF. Interestingly, whilst protection afforded by 12b induces an increase in global DNA methylation (potentially associated with silencing of pathogenic genes), that resulting from exposure to ES-62 is perhaps surprisingly associated with a decrease in it (potential induction of inflammation-resolving and tissue protective genes) However, the ES-62-mediated decrease in DNMT1 and DNA methylation is accompanied by an increase in HDAC1, that presumably contributes to the modification of the genetic landscape observed under conditions of CIA. Such changes in the epigenetic landscape presumably reflect the silencing of some pro-inflammatory genes and induction of anti-inflammatory genes.

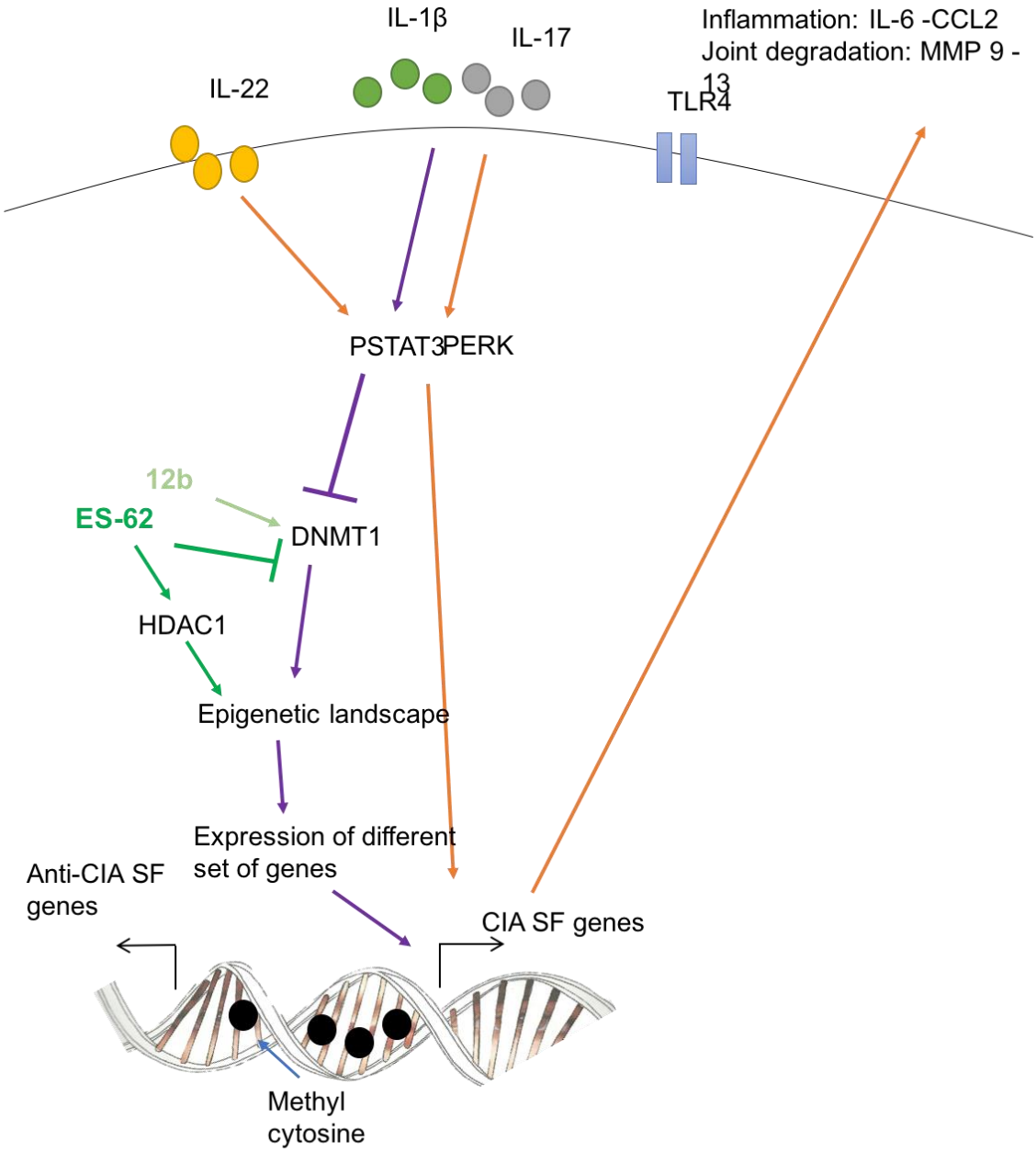
IL-1β
IL-17
IL-22
Inflammation: IL-6 -CCL2
Joint degradation: MMP 9 -13
TLR4
PSTAT3
PERK
12b
ES-62
DNMT1
HDAC1
Epigenetic landscape
Expression of different set of genes
Anti-CIA SF genes
CIA SF genes
Methyl cytosine

7. General discussion

7.1 Drug development from helminth-derived products

Parasitic worms are common infectious agents of humans in developing countries. Helminths have been infecting humans for a long time as evidenced by the discovery of eggs in mummified faeces that are thousands of years old[252], as well the testimonies of helminth infections related in ancient writings such as the Bible, the writings of Hippocrates or Egyptian papyri. They present a serious risk to health and indeed, it has been estimated, firstly in 1947 by Stoll and then confirmed by the CDC, that about 37% of the worldwide population is infected by parasitic worms[253,254]. Such parasites like the guineaworm, ascariasis or schistosomiasis are responsible for many disorders if left untreated whilst the best known effects of nematode infection are blindness and elephantiasis[255].

However, despite being a major health issue, infection with parasitic worms correlates with a low incidence rate of asthma and allergies as corroborated by the recent dramatic increase in these disorders in developed and dewormed countries[256,257]. These observations support the hygiene hypothesis, a theory suggesting that in the "too clean" environment found in Western countries the immune system will not mature properly and fail to react properly to contact with pathogens resulting in its overreaction to some environmental triggers causing asthma and allergies in children. Consistent with this, in animal models, helminth infection have been shown to be protective for a number of immunopathological diseases[90,91]. Such observations have led to increased interest in studying the effects of helminths in patients with immune disorders and this has identified increasing evidence that patients with multiple sclerosis display less severe symptoms when infected with helminths[258]. In addition, a recent study from Panda et al[259] revealed that in Odisha (India) RA patients were free of filarial infection in an area where helminth infection is considered as endemic. Indeed, collectively, such studies have driven the development of various helminth-

based clinical trials for Inflammatory bowel disease like Crohn's disease[92,93], coeliac disease[94] or ulcerative colitis[95] as well rhinitis[97].

One explanation for their protective effects against immune disorders is that as some helminth species, like tapeworm, are able to live for up to 30-40 years, they need to keep the host healthy and control the immune system in order to hide and survive. The study of patient's urine or serum revealed the presence of immunomodulatory excretory-secretory molecules in the helminth secretome[98]. One of the first and most studied immunomodulatory ES molecules is ES-62 isolated for the first time in 1989 by Harnett *et al*[110]. ES-62 is a 62 kDa protein and is the major ES product secreted by the filarial nematode *Acanthocheilonema viteae*. It is a PC-containing homotetrameric glycoprotein that exhibits therapeutic potential in various mouse models of inflammatory disorders[260] such as the OVA-induced airway hypersensitivity models of asthma[103] , MRL/lpr model of lupus[102] as well as the CIA model of RA[104]. In this thesis ES-62 has been confirmed to protect against CIA development and new information about its ability to act directly at the site of inflammation and joint damage by modifying the functional phenotype of SF, andthe molecular mechanisms involved, has been presented.

7.2 *In vivo* treatment with ES-62, or its SMAs 11a and 12b, reduces SF aggressiveness

As shown by Pineda *et al*[104,133], ES-62 prevents the development of CIA in mice by resetting the IL-17/IL-22 axis. Thus, ES-62 was first found to downregulate pathogenic IL-17 responses in CIA mice, by targeting an IL-17 producing cellular network comprising dendritic cells, γδ T cells and CD4+ T cells. Indeed, ES-62 suppresses the level of IL-17-producing CD4+ and γδ T cells by modulating DC-mediated priming and polarization of such T cell responses as well as also directly attenuating IL-1β-mediated maintenance of Th17 responses by reducing MyD88 expression in Th17 cells. However, while it reduces IL-17 production in the joint, ES-62 strongly increases IL-22 production, the latter a cytokine shown to be pathogenic in early disease

phase but able to promote resolution of inflammation in the late established phase of disease[261]. Exposure to ES-62 suppresses the early systemic pathogenic production of IL-22 and promotes that driving resolution in the joints. Such counter-regulatory control of the IL-17/22 axis by ES-62 seem to be a consistent mechanism of ES-62 action since it is also targeted in other contexts such as asthma and lupus. Thus, in the OVA induced airway hypersensitivity model, suppression of disease was due to the reduction of the pathogenic IL-17 response[101]. However, in the MRL/Lpr lupus model as well as in asthma, disease was reduced by ES-62 suppressing pathogenic IL-22 responses and increasing IL-17A production during established disease, demonstrating that as like IL-22 in RA, IL-17A appears able to play a dual role in both lupus and asthma, being pathogenic prior onset of disease whilst acting to promote resolution of inflammation once the disease is established[101-102].

In this thesis, the protective effect(s) of ES-62 on CIA mice was reaffirmed, with its actions on SF highlighted. Thus, it was demonstrated that SF extracted from ES-62-treated mice were less sensitive to pathogenic signals, such as TLR ligands, IL-17 or IL-1ß, than those from PBS-treated mice with CIA. Such modulated SF were less aggressive, both in terms of their ability to perpetuate inflammation and mediate bone destruction, due to their reduced production of the pro-inflammatory cytokine, IL-6 the chemokine, CCL2 and the MMPs, MMP9 and MMP13. IL-6 is well established as a pathogenic driver in RA, being found in high levels in patients' serum and synovial fluid[9]: IL-6 acts to promote neutrophil migration, osteoclast maturation, VEGF-stimulated pannus proliferation as well as the maturation of B cells and Th17 cells[158]. It has therefore been proposed to be a good therapeutic target and consistent with this, the anti-IL-6R antibody, Tocilizumab has given promising results in various phase III clinical trials in improving the physical condition of patients[262]. CCL2 (MCP-1) is likewise found abundantly in RA patient serum and synovial fluid and appears to be crucial for the attraction of pro-inflammatory leukocytes, particularly monocytes, to the joint[263]. MMP9 and MMP13 are respectively a gelatinase and a collagenase and both of these MMPs are found at elevated hyper-activated levels in RA synovial fluid: moreover,

there is a strong correlation between the levels of MMP9 and MMP13 and the disease severity of patients and thus, they are often used as potent clinical markers of disease activity in early RA[264].

Thus, the intracellular signalling driven by pro-inflammatory signals like IL-17 or IL-1ß resulting in the production of IL-6, CCL2 or MMPs was investigated in order to understand better how ES-62 may functionally reduce SF aggressiveness. The mechanisms unravelled in this thesis are developed below with the pathogenic mechanisms and their subversion by ES-62/12b summarized in, respectively.

7.3 ES-62 modulates pro-inflammatory cytokine signalling

To modulate functional responses resulting from the pro-inflammatory environment in the arthritic joint (Figure 7-1), ES-62 can potentially control various factors. For instance, ES-62 is well known to reduce MyD88 expression levels in a variety of cell types, such as mast cells[265], dendritic cells, macrophages[266], T cells[109] and kidney cells[102] in order to downregulate the inflammatory potential of TLR/IL-1R pathways and/or perhaps, switch to a MyD88-independent response. For example, with respect to the latter, the MyD88-dependent TLR4 pathway drives NFκB and consequently inflammatory gene transcription: however, when TLR4 signalling is MyD88 independent it is conducted through TRIF and IRF3[267] which induces IFNß gene transcription[268-270]. Usually such production of IFNß is observed after repeated stimulation of TLR3 and TLR4 receptors in order to attenuate NFκB activation. Here, ES-62-exposed SF were shown to express IFNß following stimulation with the pathogenic cytokine IL-17, a response that was absent in SF from naïve and CIA mice. Interestingly, therefore, increasing data suggest therapeutic potential for IFNß in RA in terms of its ability not only to downregulate driven production of the pro-inflammatory cytokines, IL-1ß and TNFα *in vitro* but also its capacity to reduce MMP1 and increase IL-10 and IL-1 receptor agonist

levels, *in vivo*[271,272]. Moreover a pilot study in 12 patients showed significant improvement after 3 months of treatment with IFNß[273-275].

Data further supporting a protective role for IFNβ were presented in this thesis as, in addition to confirming that IFNß signals through STAT1, it was shown to enhanced the expression of STAT1 protein and as well as its activation (phosphorylation) and STAT1 induced gene expression is usually associated with growth restraint and/or promotion of apoptosis[184,276,277], responses counter-regulatory to the pathogenic STAT3-mediated pro-survival/proliferative signalling observed in RASF[175]. Moreover, STAT3 is crucial for CCL2 production following IL-6 or IL-1ß stimulation[278,279] as well as being important for MMP9 and MMP13 production, the latter at least in chondrocytes[280,281]. Intriguingly, therefore, ES-62-exposed SF were also shown to display a higher level of STAT1 phosphorylation compared to SF from naïve and CIA mice, whilst such ES-62 SF also appeared to exhibit downregulated levels of pathogenic STAT3 signalling. Indeed, given that IL-22 can signal through both STAT3 and STAT1[193] and that it has been shown to be pro-inflammatory in early arthritis, potentially signaling through STAT3[171,175], yet inflammation-resolving in the joint in established disease[133], such a dual role of ES-62 in switching the balance from pathogenic STAT3 to potentially protective, pro-apoptotic STAT1 signalling in SF might provide a mechanism for ES-62-mediated rewiring IL-22 function towards resolution of inflammation[133]. Certainly, ES-62 only promotes IL-22 production and its resolution function in the joint during established disease (Figure 7-2).

Such a 'STAT switch' from STAT3 to STAT1 could therefore explain how SF become insensitive to the pathogenic actions of IL-22 and indeed to other pro-inflammatory signals liked IL-6 and IL-17 that also signal via STAT3 (Figure 7-1). This capacity of ES-62 to effect the STAT switch could potentially reflect its priming of induction of IFNß to not only promote STAT1 activation but also upregulate SOCS expression, which are key controllers of STAT pathways[189]. Consistent with this, exposure to ES-62 was found to increase SOCS1 and SOCS3 expression in SF from mice undergoing CIA (Figure 7-2). Of particular relevance, SOCS3 is known to be an inhibitor of STAT3 and its overexpression

was shown to block STAT3 signalling and result in a reduction of CIA severity, even more efficiently than expression of a STAT3 dominant negative construct[282]. Likewise, previous studies have shown that SOCS1 inhibits JAK activity by preferentially binds to such kinases through its SH2 domain to consequently inhibit JAK activity via interactions with its KIR domain leading to its degradation in a mechanism involving its SOCS box[189]. Such an action would decrease the JAK-STAT signalling of many cytokine receptors, such as IL-2, IL-4, IL-7, IL-12 or IL-15 and as well IFNα/β but its major target remains IFNɣ[283,284] which is pathogenic in RA[192]. In addition, SOCS1 also seems to be able to directly supress TLR signaling, as SOCS1 knock out cells are more sensitive to TLR ligands even in a IFNɣ-deficient background[285].

Such upregulation of SOCS1 by ES-62 can potentially be achieved both by direct induction of its expression, but also by reduction of the levels of miR-155, which can directly target its messenger RNA. Both the *in vivo* and *in vitro* ES-62 experiments presented here, revealed that exposure to ES-62 can significantly reduce miR-155 expression induced in response to LPS. Moreover, the ability of miR-155 to target and reduce SOCS1 mRNA levels in SF was confirmed, suggesting that by decreasing miR-155 levels ES-62 relieves the inhibition of SOCS1 mediated by miR-155. One consequence of the resulting elevated levels of SOCS1 could be the observed reduction in STAT3 activation since the ability of SOCS1 to target JAK kinases enables it, like SOCS3 to inhibit STAT3 signaling[286]. As a proof of concept, overexpression of miR-155 in human laryngeal squamous cell carcinoma induced not only a reduction in SOCS1 levels but also an elevation of STAT3 expression and activation[234]. Moreover, STAT3 activation has been shown, via a positive feedback loop, to induce miR-155 for instance in Th17 cells to promote autoimmune uveitis[287]. Therefore, such downregulation of miR-155 by ES-62 could explain, at least in part, the STAT3 inhibition observed in ES-62 SF.

Modulation of the miRNA network by ES-62 is potentially important due to its ability to rewire the intracellular signaling network of SF since a single miRNA can regulate thousands of genes and therefore control multiple pathways[214]. Pertinently, miRNA-155 appears to be particularly involved in the

pathogenesis of RA[207] (Figure 7-1), being implicated in the control of cell proliferation, inflammation and resistance to apoptosis[207,213]. Interestingly, given the observed suppression of ERK signalling in SF by ES-62, amongst all the cell signaling pathways controlled by miR-155, ERK signalling seems to be a key miR155 target in many cell types[288-290]: thus, the efficient inhibition of ERK activation by ES-62, may in part reflect its ability to suppress miR-155 and consequently, upregulation of ERK activation. Downregulation of ERK activation has the potential to strongly reduce SF aggressiveness as it is crucial for production of IL-6 production[291], MMP9 induced by CCL2[292] as well as that of MMP13[293]. Interestingly, therefore, the inflammation-resolving actions of IL-22, administered to the paws of mice once inflammation was established[133], were also associated with the ability of this treatment to recapitulate ES-62-mediated inhibition of ERK signalling in SF derived from CIA mice (Figure 7-2).

7.4 ES-62 prevents SF acquiring a "mesenchymal-fibrotic" phenotype

In the 1980s, Fassbender hypothesised that the pannus-mediated destruction of cartilage could be caused by the invasion of 'tumor-like' immature mesenchymal cells generated by dedifferentiation of fibroblasts and that such mesenchymal cells redifferentiated once cartilage destruction was accomplished[294]. This hypothesis of a tumor-like phenotype of pathogenic RASF is supported by many of their characteristics such as their STAT3 addiction and resistance to apoptosis[175,235,295,296], acquisition of motility[135] and mosaic chromosomal aberration[297]. Moreover, these characteristics of RA/CIA SF are conserved even following their isolation and culture *ex vivo*, supporting the idea of an intrinsic cell modification during inflammation. Although these cells are not tumor cells per se, as for instance, they do not metastasise, they appear to undergo a similar process to that of tumor cell transformation. For example, one of the processes that is similar to that occurring in RA synovial membranes is the epithelial mesenchymal transition (ECM), a process that

drives multiple changes in a polarized epithelial cell that allows it to assume the functional phenotype of a mesenchymal cell, such as cell migration, tissue invasion and resistance to apoptosis[298]. Fibroblasts are prototypical mesenchymal cells[299] and thus distinguishing them from a mesenchymal stem cell is still problematic[300,301] especially as they seem to be closer in phenotype than previously recognized[302]. Therefore, "transformation" (activation) of SF during RA is believed to process through a mechanism similar to EMT resulting in them gaining a mesenchymal/fibrotic phenotype[303,304]. Reflecting this, the data presented in this thesis support the hypothesis that CIA SF and naïve SF display functionally distinct phenotypes, even following isolation from the pro-inflammatory joint and culture for several weeks *ex vivo*. Thus, CIA SF are cells that appear to be more sensitive to pro-inflammatory cytokines, exhibit an altered miRNA network and display constitutive activation of ERK and STAT3. ERK and STAT3 signaling pathways are necessary for EMT induction[305] and indeed, blockade of STAT3 suppresses EMT in pancreatic cancer cells[306]. Therefore, suppression of ERK and STAT3 signaling by ES-62 may reduce the activation/transformation of SF and prevent their acquisition of the pathogenic aggressive "mesenchymal-fibrotic" phenotype.

Interestingly, a key signaling pathway in EMT, and more generally in cell differentiation, is the Wnt cascade: although Wnt activity was not measured in this study, ES-62 SF were found to exhibit high protein expression levels of HDAC1, a well-known inhibitor of the Wnt/ß-catenin pathway[307]. Indeed, inhibition of HDAC1 has been found to be important for cell dedifferentiation as this results in induction of Wnt signaling[308]. Perhaps of relevance therefore, microarray analysis of gene expression of RA synovial membranes revealed that *in vitro* treatment of these cells with ES-62 strongly induced, (approximately 4-fold compared to the control samples) Wnt inhibitory factor 1 (WIF1), as well as AMOTL2 and CRYBB2[99] which are respectively Angiomotin Like 2 and Crystallin Beta B2 known to be efficient wnt inhibitors[309]. Collectively, these data suggest that potentially, by inhibiting Wnt signaling ES-62 suppresses SF activation/transformation by targeting the known pathogenic effects of Wnt signaling in inducing MMPs, RANKL, and cytokines such as IL-6, IL-8 and IL-15[310,311].

7.5 ES-62 impacts on gene expression by modulating the epigenetic landscape

Usually, in tumor cell transformation, cell differentiation or EMT, the epigenetic landscape is remodelled, driving the acquisition of new features and a 'dedifferentiated' cell state. Many events can induce changes in the epigenetic landscape, including cell reprogramming induced by chronic inflammation, as described for instance for melanoma cells[312]. Reprogramming induced by chronic inflammation following infiltration of the joint with e.g. pathogenic T cells has been proposed to provide a potential explanation for the acquisition of the aggressive phenotype of CIA-SF developing in early RA or CIA[313]. Amongst the various epigenetic modifications possible, changes in the DNA methylation profile have been implicated as a driving force in the regulation of cell differentiation status, and is usually involved in cell transformation[314,315]. Therefore, in this thesis the impact of pro-inflammatory cytokine signalling and its modulation by ES-62 on global DNA methylation of SF during CIA was analysed. As proposed previously[124,248] and confirmed in this thesis, CIA SF exhibit global DNA hypomethylation and display lower expression levels of DNMT1 than naïve SF. Such global DNA demethylation appears associated with disease, and indeed, gene array analysis of the effects of the DNMT1 inhibitor 5-azacytidine indicated that such treatment enabled human OA SF to acquire a RA-like aggressive phenotype[124]. However, the data presented here show that whilst 5-azacytidine treatment is sufficient to drive a more aggressive phenotype in terms of elevated basal levels of IL-6 release by SF from naive mice, acute stimulation with cytokines can further enhance this, at least *in vitro*. Moreover, the finding that SF from CIA treated with ES-62 *in vivo* display the highest levels of hypomethylation shows that global DNA demethylation is not always associated with acquisition of aggressiveness. Indeed, *in vivo* treatment with ES-62 resulted in SF that exhibit even less DNMT1 mRNA expression than CIA SF and consistent with this, display further DNA demethylation.

This suggests that *in vivo* exposure to ES-62 does not simply prevent SF transformation, but actually induces differential rewiring of the epigenetic landscape presumably in order to allow expression of genes driving the resolution of inflammation or cell apoptosis. ES-62 is not the only reagent to induce DNA demethylation and DNMT1 inhibition, while protecting SF from developing an aggressive phenotype: a good example of a similar effect is daphnetin[316], a compound derived from Chinese medicine, (7, 8-dihydroxycoumarin) extracted from Daphne odora Var. Marginata, has been shown to downregulate DNMT1, DNMT3a and DNMT3b expression in rat CIA SF resulting in the protective expression of the pro-apoptotic genes DR3, PDCD5, FasL and p53.

Thus, global DNA methylation might not always be a sign of SF aggressiveness, although the DNA methylation signature may be of use in distinguishing early and longstanding arthritis patients[317] and their specific pathogenic processes[318]. However, the new data presented here underline that it is important to focus on the specific sites of methylation, as potential anti-inflammatory therapeutics such as ES-62 are likely to induce methylation profiles distinct from the SF disease signature since the cells will respond differently to the modulated inflammatory environment. For example, ES-62 reduces the effect of IL-17 and IL-1β by suppressing ERK and STAT3 activation, signals which are necessary for induction of global DNA demethylation observed for these two cytokines, *in vitro*. Such suppression of ERK and STAT3 signalling by ES-62 could possibly enable a modification of the methylome profile as STAT3 and ERK act together with DNMT1 in order to regulate specific gene expression[241-243] (Figure 7-2). Indeed, STAT3 has been reported to directly bind to DNMT1 and regulate its activity, for instance to allow PTPN6 promoter silencing[241] and the epigenetic silencing of SHP-1, a tumor suppressor in malignant T lymphocytes[242]. Moreover, in lupus T cells, ERK dependent modulation of DNMT1 expression contributes to the regulation of CD11a and CD70 expression[319], resulting in T cell proliferation and activation contributing the development of autoimmunity. Importantly, HDAC regulation of DNMT1 activity appears to be ERK dependent[243] and HDAC1 can form a complex with DNMT1, Rb and E2F in order to regulate specific promoters

important for cell proliferation and resistance to apoptosis[320,321]. Since *in vivo* exposure to ES-62 results in higher expression of HDAC1 in SF than that observed in CIA fibroblasts, the combination of modulating both DNMT1 and HDAC1 rather than just DNMT1, STAT3 or other potential co-factors might, whilst maintaining a low level of global DNA methylation, enable a new protective epigenetic profile.

The role of HDAC1 in RA is however very complex: although this study suggests it to be protective since it is induced by ES-62 and could potentially regulate Wnt activity in SF, some studies have revealed the use of HDAC inhibitors to be protective in CIA models[322] as evidenced by them having various anti-inflammatory effects such as reducing IL-6 production[323]. Moreover, HDAC1 has been shown to support cell proliferation and survival although it has (perhaps consistent with the ES-62 effects) ben shown to be associated with reducing MMP-1 production[324]. In addition, alteration of the histone modification profile appears to be a key event in establishment of RA, especially in terms of SF activation[323] and their production of IL-6[325]. Thus, it is important to keep in mind that regulators like HDAC1 have a multitude of co-factors that impact on their activity depending on the context of local environment[320,321], as exemplified by the ability of IL-22 to both induce inflammation and contribute to its resolution in CIA.

7.6 Developing efficient clinical drugs from ES-62

Studying the actions of parasitic worm-derived immunomodulators in order to potentially develop safer therapies for inflammatory disorders is currently of particular interest: this focus has arisen since such molecules have emerged as the result of millennia of evolution allowing generation of 'safe' immunomodulators that benefit both host and parasite. By contrast, conventional anti-inflammatory therapies are usually strongly immunosuppressive with numerous and, potentially serious, side effects. Thus, information gained from parasitic immunomodulatory mechanisms, such as those exploited by ES-62, is very useful to our understanding of the

pathogenicity of inflammatory disorders and may reveal novel safe and effective therapeutic targets. For instance whilst protection by ES-62 confirmed the importance of IL-17 in CIA pathogenicity[104] it revealed the bi-phasic effect of IL-22 in driving both pathogenesis and inflammation resolution[133].

However, since ES-62 is a large and potentially immunogenic molecule it cannot be used directly as therapeutics. This is the reason why SMAs based on the active moiety of ES-62, PC, were designed and screened for their immunomodulatory properties. Two SMAs, 11a and 12b, were chosen, on the basis of their anti-inflammatory properties *in vitro*, for testing of their ability to supress CIA. Confirming and extending previous findings of their therapeutic potential in RA[114,132], data in this thesis revealed that both SMAs are very efficient in reducing CIA both prophylactically and therapeutically. It is unlikely that the SMAs will mimic ES-62 perfectly since their interactions at the surface or within the cell may well be different to that of ES-62. However, it has been previously shown that whilst both SMAs 11a and 12b can downregulate MyD88 expression[113,114], they differentially mimic certain features of ES-62 action, namely that 11a acts through inhibiting IL-17 production[132] and 12b suppresses IL-1ß production by regulating the inflammasome in an NRF2-dependent manner[114]. Thus, the potential for these SMAs to mimic the actions of ES-62 on SF was investigated in this thesis. This revealed that SF treated with either 11a and 12b *in vitro* displayed reduced cytokine production that was associated with lower levels of expression of the pro-inflammatory miRNA, miR-155 and induction of SOCS expression, actions reminiscent of those of ES-62. However, it is not yet clear whether these effects are achieved by the same mechanism: indeed, SF derived from CIA mice exposed to a prophylactic regime of 12b treatment *in vivo* display a distinct epigenetic landscape to that of SF from CIA mice treated with ES-62. Thus 12b appears to act to increase DNMT1 expression and global DNA methylation presumably to drive the silencing of many pro-inflammatory genes and/or anti-apoptotic genes otherwise induced during CIA suggesting that it acts to prevent or reverse the hypomethylation associated with pathogenesis. By contrast, although both 12b and ES-62 effect protection, ES-

62 does not simply appear to prevent the epigenetic remodelling, but rather to induce a distinct landscape associated with inflammation resolution and tissue repair that could be exploited for treatment of established disease.

Thus, to apply such research for clinical purposes, more deep investigation using the SMAs 11a and 12b is required, as although they mimic certain of its effects, they appear to potentially act through (additional) different mechanisms to ES-62. In particular, it would be interesting to see the effects of 11a and 12b on the epigenetic landscape of SF when the SMAs are administered therapeutically to determine whether they mimic ES-62's effects under this inflammatory context. Nevertheless, such SMAs provide excellent starting points for the further development of parasitic worm-based drugs for clinical trials especially since preliminary data suggests that they display low toxicity and good tolerability profile (unpublished data, Harnett, Harnett and Suckling).

Figure 7-1 Model of the signalling network underpinning SF aggressiveness in CIA

Production of proinflammatory factors such as IL-6 and CCL2 and mediators of bone destruction, including MMP9 and MMP13 are induced in SF in response to signalling by pathogenic mediators, such as IL-17, IL-1ß and TLR ligands. Signalling via their receptors induces activation of a variety of downstream elements converging on the STAT3 and ERK pathways to regulate the miRNA network, rewire the epigenetic landscape and induce pathogenic gene expression. Interestingly, IL-22 plays a dual role being pro-inflammatory during pathogenesis and resolving inflammation during established disease: for example, under the later conditions, when IFNß is also produced in the joint, IL-22 can potentially induce STAT1 activation to promote expression of anti-inflammatory genes.

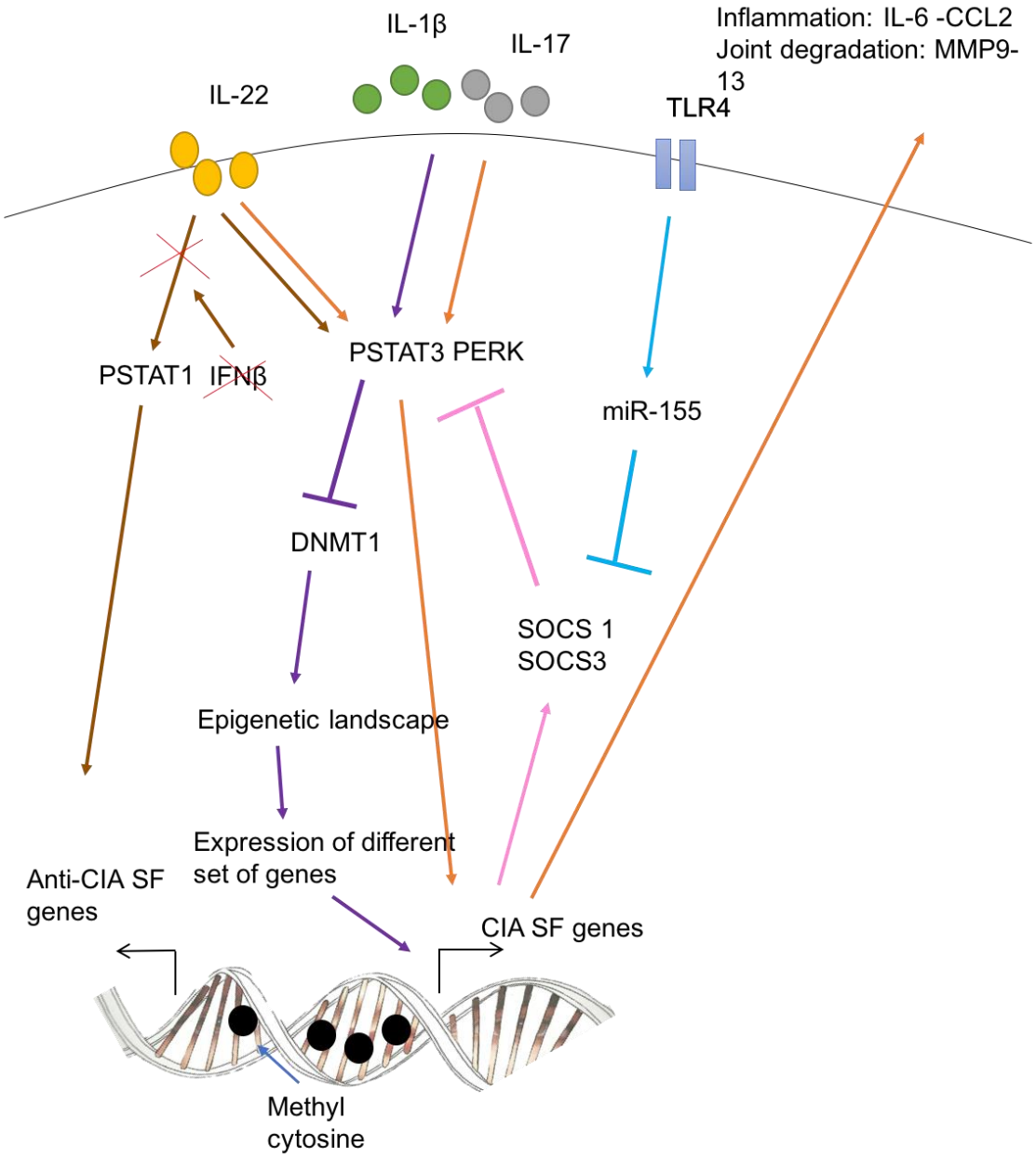
IL-1β
IL-17
IL-22
Inflammation: IL-6 -CCL2
Joint degradation: MMP9-13
TLR4
PSTAT1
IFNβ
PSTAT3 PERK
miR-155
DNMT1
SOCS 1
SOCS3
Epigenetic landscape
Expression of different set of genes
Anti-CIA SF genes
CIA SF genes
Methyl cytosine

Figure 7-2 Model of the molecular mechanisms by which ES-62 and 12b reduce CIA SF aggressiveness

ES-62 and 12b can directly target SF to reduce the production of the pro-inflammatory molecules IL-6 and CCL2, as well as the mediators of bone destruction, MMP9 and MMP13. This is achieved by their ability to modulate the activation of various signalling elements resulting from the pro-inflammatory environment of the joint. For example, ES-62 modulates STAT3 and ERK signalling downstream of the IL-17A receptor as well as controlling the miRNA landscape in order to induce a nugatory feedback loop orchestrated by SOCS molecules. Moreover, ES-62 promotes IFNß production when the cells are exposed to IL-17. Therefore, IFNß stimulates STAT1 phosphorylation and potentially enables IL-22 to switch its downstream signaling towards STAT1 and induces the expression of genes promoting resolution of inflammation. Likewise, the suppression of STAT3 signalling reduces the ability of proinflammatory cytokines to signal via this pathway. Integration of signals results in regulation of DNMT and HDAC1 expression enabling ES-6 to rewire the epigenetic landscape and induce expression of a protective set of genes. Whilst sharing some of the actions of ES-62, 12b is differentially found to reduce SF sensitivity to pro-inflammatory mediators by regulating miR-155 and SOCS expression in the context of increasing DNMT1 levels and consequently, the global DNA methylation associated with silencing of pathogenic genes.

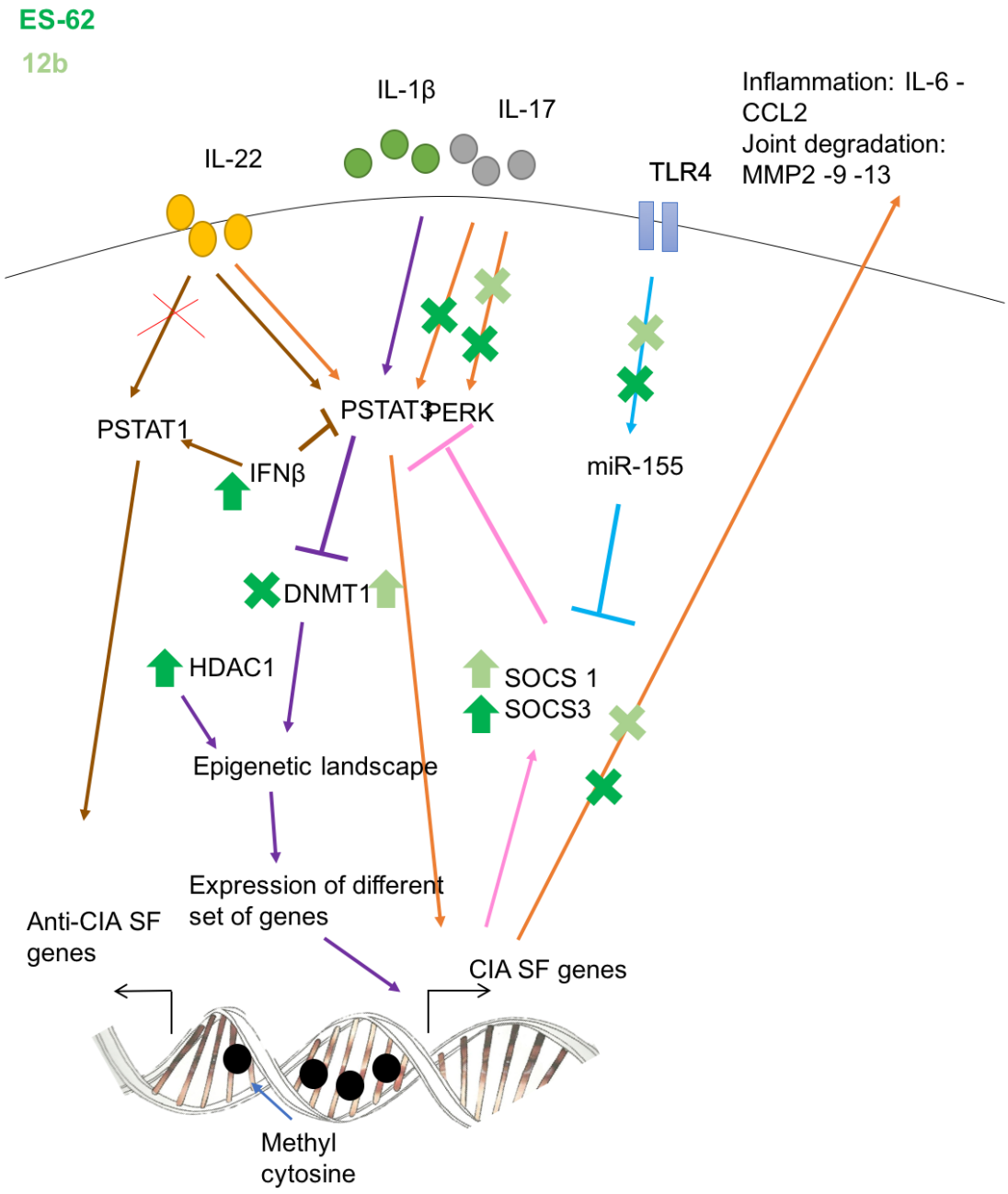
ES-62
12b
IL-1β
IL-17
IL-22
Inflammation: IL-6 -
CCL2
Joint degradation:
MMP2 -9 -13
TLR4
PSTAT1
PSTAT3
PERK
IFNβ
miR-155
DNMT1
HDAC1
SOCS 1
SOCS3
Epigenetic landscape
Expression of different
set of genes
Anti-CIA SF
genes
CIA SF genes
Methyl
cytosine

1 Calabrò, A. *et al*. One year in review 2016: novelties in the treatment of rheumatoid arthritis. *Clin Exp Rheumatol* **34**, 357-372 (2016).

2 Ishchenko, A. & Lories, R. J. Safety and Efficacy of Biological Disease-Modifying Antirheumatic Drugs in Older Rheumatoid Arthritis Patients: Staying the Distance. *Drugs Aging* **33**, 387-398 (2016).

3 Filer, A. The fibroblast as a therapeutic target in rheumatoid arthritis. *Curr Opin Pharmacol* **13**, 413-419 (2013).

4 Edwards, C. J. & Cooper, C. Early environmental factors and rheumatoid arthritis. *Clin Exp Immunol* **143**, 1-5 (2006).

5 Deane, K. D. Rheumatoid arthritis: Autoantibodies, citrullinated histones and initiation of synovitis. *Nat. Rev. Immunol.* **11**, 688–689 (2015).

6 M Kurowska-Stolarska, O. D., W Rudnicka, J Distler, RE Gay, W Maslinski, S Gay. IL-15 and its role in rheumatoid arthritis. *Arthritis Research & Therapy* (2003).

7 Roeleveld, D. M. & Koenders, M. I. The role of the Th17 cytokines IL-17 and IL-22 in Rheumatoid Arthritis pathogenesis and developments in cytokine immunotherapy. *Cytokine* **74**, 101-107 (2015).

8 Zhang, L. *et al*. Elevated Th22 cells correlated with Th17 cells in patients with rheumatoid arthritis. *J Clin Immunol* **31**, 606-614 (2011).

9 Cicuttini, F. M. *et al*. Serum IL-4, IL-10 and IL-6 levels in inflammatory arthritis. *Rheumatol Int* **14**, 201-206 (1995).

10 Kyburz, D., Carson, D. A. & Corr, M. The role of CD40 ligand and tumor necrosis factor alpha signaling in the transgenic K/BxN mouse model of rheumatoid arthritis. *Arthritis Rheum* **43**, 2571-2577 (2000).

11 Lai, N. S., Lan, J. L., Yu, C. L. & Lin, R. H. Role of tumor necrosis factor-alpha in the regulation of activated synovial T cell growth: down-regulation of synovial T cells in rheumatoid arthritis patients. *Eur J Immunol* **25**, 3243-3248 (1995).

12 Ohmura, K., Nguyen, L. T., Locksley, R. M., Mathis, D. & Benoist, C. Interleukin-4 can be a key positive regulator of inflammatory arthritis. *Arthritis Rheum* **52**, 1866-1875 (2005).

13 Kay, J. & Calabrese, L. The role of interleukin-1 in the pathogenesis of rheumatoid arthritis. *Rheumatology (Oxford)* **43 Suppl 3**, iii2-iii9 (2004).

14 Lubberts, E. & van den Berg, W. B. Cytokines in the pathogenesis of rheumatoid arthritis and collagen-induced arthritis. *Adv Exp Med Biol* **520**, 194-202 (2003).

15 Moffett, B. C. The morphogenesis of joints. (1965).

16 Bartok, B.F. Fibroblast-like synoviocytes: key effector cells in rheumatoid arthritis. *Immunological Reviews* **233**, 233-255 (2010).

17 Smith, M. D. The normal synovium. *The open rheumatology journal* **5**, 100-106 (2011).

18 Barland, P., Novikoff, A. B. & Hamerman, D. Electron microscopy of human synovial membrane. . *Journal of Cell Biology* **14**, 207 (1962).

19 Edwards, J. C. W. W., D. A. Demonstration of bone marrow derived cells in synovial lining by means of giant intracellular granules as genetic markers. *Annals of the Rheumatic Diseases* **41**, 177-182, (1982).

20 Firestein, G. S. Invasive fibroblast-like synoviocytes in rheumatoid arthritis - Passive responders or transformed aggressors? *Arthritis Rheum* **39**, 1781-1790 (1996).
21 Smith, M. D. e. a. Microarchitecture and protective mechanisms in synovial tissue from clinically and arthroscopically normal knee joints. *Annals of the Rheumatic Diseases*, 303-307 (2003).
22 Edwards, J. C. W. Synovial intimal fibroblasts. *Annals of the Rheumatic Diseases* **54**, 395-397 (1995).
23 Connolly, M., Veale, D. J. & Fearon, U. Acute serum amyloid A regulates cytoskeletal rearrangement, cell matrix interactions and promotes cell migration in rheumatoid arthritis. *Annals of the Rheumatic Diseases* **70**, 1296-1303 (2011).
24 Takemura, S. Lymphoid neogenesis in rheumatoid synovitis. *ournal of Immunology* **167**, 1072-1080 (2001).
25 Strand, V., Kimberly, R. & Isaacs, J. D. Biologic therapies in rheumatology: lessons learned, future directions. *Nature Reviews Drug Discovery* **6**, 75-92 (2007).
26 Vasanthi P, Role of tumor necrosis factor-alpha in rheumatoid arthritis: a review. *APLAR Journal of Rheumatology* **10**, 270-274 (2007).
27 Ziolkowska N. High levels of IL-17 in rheumatoid arthritis patients: IL-15 triggers in vitro IL-17 production via cyclosporin A-sensitive mechanism. *Journal of Immunology* **164**, 2832-2838 (2000).
28 Nakae, S., Nambu, A., Sudo, K. & Iwakura, Y. Suppression of immune induction of collagen-induced arthritis in IL-17-deficient mice. *Journal of Immunology* **171**, 6173-6177 (2003).
29 Koenders, M. I. e. a. Induction of Cartilage Damage by Overexpression of T Cell Interleukin-17A in Experimental Arthritis in Mice Deficient in Interleukin-1. *Arthritis and Rheumatism* **52**, 975-983 (2005).
30 Sato, K. e. a. Th17 functions as an osteoclastogenic helper T cell subset that links T cell activation and bone destruction. *Journal of Experimental Medicine* **203**, 2673-2682 (2006).
31 Benderdour, M. Interleukin 17 (IL-17) induces collagenase-3 production in human osteoarthritic chondrocytes via AP-1 dependent activation: Differential activation of AP-1 members by IL-17 and IL-1 beta. *Journal of Rheumatology* **29**, 1262-1272 (2002).
32 Koshy, P. J. e. a. Interleukin 17 induces cartilage collagen breakdown: novel synergistic effects in combination with proinflammatory cytokines. *Annals of the Rheumatic Diseases* **61**, 704-713 (2002).
33 Kay J, C. L. The role of interleukin-1 in the pathogenesis of rheumatoid arthritis. *Rheumatology (Oxford)* **43**, S3:2-9 (2004).
34 Choy, S. S. a. D. E. H. The Role of Interleukin 6 in the Pathophysiology of Rheumatoid Arthritis. *Ther Adv Musculoskelet Dis* **2**, 247–256 (2010).
35 Furuzawa-Carballeda J, Cabral AR. Osteoarthritis and rheumatoid arthritis pannus have similar qualitative metabolic characteristics and pro-inflammatory cytokine response. *Clin Exp Rheumatol*. **26**, 554-560 (2008).
36 G.-H Yuan, M. T., K Masuko-Hongo, A Shibakawa, T Kato, K Nishioka, H Nakamura. Characterization of cells from pannus-like tissue over

articular cartilage of advanced osteoarthritis. *Osteoarthritis and Cartilage* **12**, 38-45 (2004).

37 Gravallese EM, M. C., Tsay A, Naito A, Pan C, Amento E, Goldring SR. Synovial tissue in rheumatoid arthritis is a source of osteoclast differentiation factor. *Arthritis Rheum* **43**, 250-258 (2000).

38 Lefevre, S. *et al*. Synovial fibroblasts spread rheumatoid arthritis to unaffected joints. *Nature Medicine* **15** (2009).

39 Qu, Z. H. *et al*. Local proliferation of fibroblast-like synoviocytes conributes to synovial hyperplasia - results of proliferation cell nuclear antigen/cyclin, c-myc, and nucleolar organizer region staining. *Arthritis Rheum* **37**, 212-220 (1994).

40 Pap, T. *et al*. Activation of synovial fibroblasts in rheumatoid arthritis: lack of expression of the tumour suppressor PTEN at sites of invasive growth and destruction. *Arthritis Research* **2**, 59-64 (2000).

41 Keyszer, G. M., Heer, A. H. & Gay, S. Cytokines and oncogenes in cellular interactions of rheumatoid arthritis. *Stem Cells* **12**, 75-86 (1994).

42 Fassbender, H. G. & Simmlingannefeld, M. The potential aggressiveness of synovial tisue in rheumatoid arthritis. *Journal of Pathology* **139**, 399-406 (1983).

43 Bottini, N. & Firestein, G. S. Duality of fibroblast-like synoviocytes in RA: passive responders and imprinted aggressors. *Nat Rev Rheumatol* **9**, 24-33 (2013).

44 Rinaldi, N., Barth, T., Henne, C., Mechtersheimer, G. & Moller, P. Synoviocytes in chronic synovitis in-situ and cytokine stimulated synovial cells in vitro neo express alpha-1, alpha-3 and alpha-5 chains of beta-1 integrins. *Virchows Archiv-an International Journal of Pathology* **425**, 171-180 (1994).

45 Ahmed, S. *et al*. Largazole, a class I histone deacetylase inhibitor, enhances TNF-alpha-induced ICAM-1 and VCAM-1 expression in rheumatoid arthritis synovial fibroblasts. *Toxicology and Applied Pharmacology* **270**, 87-96 (2013).

46 Pirila, L. & Heino, J. Altered integrin expression in rheumatoid synovial lining type B cells: In vitro cytokine regulation of alpha 1 beta 1, alpha 6 beta 1, and alpha v beta 5 integrins. *Journal of Rheumatology* **23**, 1691-1698 (1996).

47 Yang, C.-M. *et al*. Interleukin-1 beta Induces ICAM-1 Expression Enhancing Leukocyte Adhesion in Human Rheumatoid Arthritis Synovial Fibroblasts: Involvement of ERK, JNK, AP-1, and NF-kappa B. *Journal of Cellular Physiology* **224**, 516-526 (2010).

48 Werb, Z., Tremble, P. M., Behrendtsen, O., Crowley, E. & Damsky, C. H. Signal transduction through the fibronectin receptor induces collagenase and stromelysin gene expression. *Journal of Cell Biology* **109**, 877-889 (1989).

49 Kiener, H. P. *et al*. Cadherin 11 Promotes Invasive Behavior of Fibroblast-like Synoviocytes. *Arthritis and Rheumatism* **60**, 1305-1310 (2009).

50 Chang, S. K. *et al*. Cadherin-11 regulates fibroblast inflammation. *Proceedings of the National Academy of Sciences of the United States of America* **108**, 8402-8407 (2011).

51 MullerLadner, U. *et al*. Synovial fibroblasts of patients with rheumatoid arthritis attach to and invade normal human cartilage when engrafted into SCID mice. *American Journal of Pathology* **149**, 1607-1615 (1996).

52 Pap, T. *et al*. Differential expression pattern of membrane-type matrix metalloproteinases in rheumatoid arthritis. *Arthritis Rheum* **43**, 1226-1232 (2000).

53 Burger, D. *et al*. Imbalance between interstitial collagenase and tissue inhibitor of metalloproteinases 1 in synoviocytes and fibroblasts upon direct contact with stimulated T lymphocytes - Involvement of membrane-associated cytokines. *Arthritis and Rheumatism* **41**, 1748-1759 (1998).

54 Danks L, K. N., Guerrini MM, Sawa S, Armaka M, Kollias G, Nakashima T, Takayanagi H. RANKL expressed on synovial fibroblasts is primarily responsible for bone erosion during joint inflammation. *Ann Rheum Dis* (2014).

55 Szekanecz Z, B. T., Paragh G and Koch AE. Angiogenesis in rheumatoid arthritis. *Autoimmunity* **42**, 563-573 (2009).

56 Ben-Av P, C. L., Wilder RL, Hla T. Induction of vascular endothelial growth factor expression in synovial fibroblasts by prostaglandin E and interleukin-1: a potent mechanism for inflammatory angiogenesis. *FEBS Letter* **372**, 83-87 (1995).

57 C, R. Fibroblast biology effector signals released by the synovial fibroblast in arthritis. *Arthritis Research and Therapy* **2**, 356 (2000).

58 Szekanecz, Z., Vegvari, A., Szabo, Z. & Koch, A. E. Chemokines and chemokine receptors in arthritis. *Front Biosci (Schol Ed)* **2**, 153-167 (2010).

59 Cornish, A. L., Campbell, I. K., McKenzie, B. S., Chatfield, S. & Wicks, I. P. G-CSF and GM-CSF as therapeutic targets in rheumatoid arthritis. *Nat Rev Rheumatol* **5**, 554-559 (2009).

60 Tak, P. P., Zvaifler, N. J., Green, D. R. & Firestein, G. S. Rheumatoid arthritis and p53: how oxidative stress might alter the course of inflammatory diseases. *Immunology Today* **21**, 78-82 (2000).

61 Firestein, G. S., Echeverri, F., Yeo, M., Zvaifler, N. J. & Green, D. R. Somatic mutations in the p53 tumor suppressor gene in rheumatoid arthritis synovium. *Proceedings of the National Academy of Sciences of the United States of America* **94** (1997).

62 Inazuka, M. *et al*. Analysis of p53 tumour suppressor gene somatic mutations in rheumatoid arthritis synovium. *Rheumatology* **39**, 262-266 (2000).

63 Roivainen, A. *et al*. H-ras oncogene point mutations in arthritic synovium. *Arthritis Rheum* **40**, 1636-1643 (1997).

64 Cannons, J. L., Karsh, J., Birnboim, H. C. & Goldstein, R. HPRT- mutant T cells in the peripheral blood and synovial tissue of patients with rheumatoid arthritis. *Arthritis Rheum* **41**, 1772-1782 (1998).

65 Kullmann, F. *et al*. Microsatellite analysis in rheumatoid arthritis synovial fibroblasts. *Annals of the Rheumatic Diseases* **59**, 386-389 (2000).
66 Da Sylva, T. R., Connor, A., Mburu, Y., Keystone, E. & Wu, G. E. Somatic mutations in the mitochondria of rheumatoid arthritis synoviocytes. *Arthritis Research & Therapy* **7**, R844-R851 (2005).
67 Maeshima, K. & Eltsov, M. Packaging the genome: the structure of mitotic chromosomes. *J Biochem* **143**, 145-153 (2008).
68 Halusková, J. Epigenetic studies in human diseases. *Folia Biol (Praha)* **56**, 83-96 (2010).
69 Hussain, N. Epigenetic influences that modulate infant growth, development, and disease. *Antioxid Redox Signal* **17**, 224-236 (2012).
70 Cantley, M. D. & Haynes, D. R. Epigenetic regulation of inflammation: progressing from broad acting histone deacetylase (HDAC) inhibitors to targeting specific HDACs. *Inflammopharmacology* **21**, 301-307 (2013).
71 Hawtree, S., Muthana, M. & Wilson, A. G. The role of histone deacetylases in rheumatoid arthritis fibroblast-like synoviocytes. *Biochemical Society Transactions* **41**, 783-788 (2013).
72 Li, M. *et al*. Therapeutic Effects of NK-HDAC-1, a Novel Histone Deacetylase Inhibitor, on Collagen-Induced Arthritis Through the Induction of Apoptosis of Fibroblast-Like Synoviocytes. *Inflammation* **36**, 888-896 (2013).
73 Horiuchi, M. *et al*. Expression and Function of Histone Deacetylases in Rheumatoid Arthritis Synovial Fibroblasts. *Journal of Rheumatology* **36**, 1580-1589 (2009).
74 Kawabata, T. *et al*. Increased activity and expression of histone deacetylase 1 in relation to tumor necrosis factor-alpha in synovial tissue of rheumatoid arthritis. *Arthritis Research & Therapy* **12**, R133-R133 (2010).
75 Maciejewska-Rodrigues, H. *et al*. Epigenetics and rheumatoid arthritis: The role of SENP1 in the regulation of MMP-1 expression. *Journal of Autoimmunity* **35**, 15-22 (2010).
76 Nishida, K. *et al*. Histone deacetylase inhibitor suppression of auto antibody-mediated arthritis in mice via regulation of p16(INK4a) and p21(WAF1/Cip1) expression. *Arthritis Rheum* **50**, 3365-3376 (2004).
77 Trenkmann, M. *et al*. Expression and function of EZH2 in synovial fibroblasts: epigenetic repression of the Wnt inhibitor SFRP1 in rheumatoid arthritis. *Annals of the Rheumatic Diseases* **70**, 1482-1488 (2011).
78 Ehrlich M, G.-S. M., Huang LH, Midgett RM, Kuo KC, McCune RA, Gehrke C. Amount and distribution of 5-methylcytosine in human DNA from different types oftissues of cells. *Nucleic Acids Res.* **10**, 2709-2721 (1982).
79 Newell-Price J, C. A., King P. DNA methylation and silencing of gene expression. *Trends Endocrinol Metab.* **11**, 142-148 (2000).
80 TH, B. The DNA methyltransferases of mammals. *Human Molecular Genetics* **13**, 26-34 (2000).
81 Kulis, M. & Esteller, M. DNA methylation and cancer. *Adv Genet* **70**, 27-56 (2010).

82 Robertson, K. D. DNA methylation and human disease. *Nat Rev Genet* **6**, 597-610 (2005).
83 Khavari DA, S. G., Rinn JL. DNA methylatino and epigenetic control of cellular differentiation. *Cell Cycle* **9**, 3880-3883 (2010).
84 Smith, Z. D. & Meissner, A. DNA methylation: roles in mammalian development. *Nat Rev Genet* **14**, 204-220 (2013).
85 Karouzakis, E., Gay, R. E., Michel, B. A., Gay, S. & Neidhart, M. DNA Hypomethylation in Rheumatoid Arthritis Synovial Fibroblasts. *Arthritis Rheum* **60**, 3613-3622 (2009).
86 Karouzakis, E., Gay, R. E., Gay, S. & Neidhart, M. Increased recycling of polyamines is associated with global DNA hypomethylation in rheumatoid arthritis synovial fibroblasts. *Arthritis Rheum* **64**, 1809-1817 (2012).
87 Takami, N. *et al*. Hypermethylated promoter region of DR3, the death receptor 3 gene, in rheumatoid arthritis synovial cells. *Arthritis Rheum* **54**, 779-787 (2006).
88 DP, S. Hay fever, hygiene, and household size. *BMJ* **299**, 1259-1960 (1989).
89 Jouvin, M.-H. & Kinet, J.-P. Trichuris suis ova: Testing a helminth-based therapy as an extension of the hygiene hypothesis. *Journal of Allergy and Clinical Immunology* **130**, 3-12 (2012).
90 Maizels, R. M., Pearce, E. J., Artis, D., Yazdanbakhsh, M. & Wynn, T. A. Regulation of pathogenesis and immunity in helminth infections. *J Exp Med* **206**, 2059-2066 (2009).
91 McSorley, H. J. & Maizels, R. M. Helminth infections and host immune regulation. *Clin Microbiol Rev* **25**, 585-608 (2012).
92 Lashner, B. A. & Loftus, E. V. True or false? The hygiene hypothesis for Crohn's disease. *Am J Gastroenterol* **101**, 1003-1004 (2006).
93 Summers, R. W., Elliott, D. E., Urban, J. F., Thompson, R. & Weinstock, J. V. Trichuris suis therapy in Crohn's disease. *Gut* **54**, 87-90 (2005).
94 McSorley, H. J. *et al*. Suppression of inflammatory immune responses in celiac disease by experimental hookworm infection. *PLoS One* **6**, e24092 (2011).
95 Summers, R. W., Elliott, D. E., Urban, J. F., Thompson, R. A. & Weinstock, J. V. Trichuris suis therapy for active ulcerative colitis: a randomized controlled trial. *Gastroenterology* **128**, 825-832 (2005).
96 Helmby, H. Human helminth therapy to treat inflammatory disorders - where do we stand? *BMC Immunol* **16**, 12 (2015).
97 Feary, J. *et al*. Safety of hookworm infection in individuals with measurable airway responsiveness: a randomized placebo-controlled feasibility study. *Clin Exp Allergy* **39**, 1060-1068 (2009).
98 Harnett, W. Secretory products of helminth parasites as immunomodulators. *Mol Biochem Parasitol* **195**, 130-136 (2014).
99 Harnett, M. M., Melendez, A. J. & Harnett, W. The therapeutic potential of the filarial nematode-derived immunodulator, ES-62 in inflammatory disease. *Clin Exp Immunol* **159**, 256-267 (2010).

100 Harnett, W. & Harnett, M. M. Helminth-derived immunomodulators: can understanding the worm produce the pill? *Nat Rev Immunol* **10**, 278-284 (2010).
101 Rzepecka, J. *et al*. The helminth product, ES-62, protects against airway inflammation by resetting the Th cell phenotype. *Int J Parasitol* **43**, 211-223 (2013).
102 Rodgers, D. T. *et al*. The parasitic worm product ES-62 targets myeloid differentiation factor 88-dependent effector mechanisms to suppress antinuclear antibody production and proteinuria in MRL/lpr mice. *Arthritis Rheumatol* **67**, 1023-1035 (2015).
103 Coltherd, J. C. *et al*. The parasitic worm-derived immunomodulator, ES-62 and its drug-like small molecule analogues exhibit therapeutic potential in a model of chronic asthma. *Sci Rep* **6**, 19224 (2016).
104 Pineda, M. A. *et al*. The parasitic helminth product ES-62 suppresses pathogenesis in collagen-induced arthritis by targeting the interleukin-17-producing cellular network at multiple sites. *Arthritis Rheum* **64**, 3168-3178 (2012).
105 van den Berg, W. B. & Miossec, P. IL-17 as a future therapeutic target for rheumatoid arthritis. *Nat Rev Rheumatol* **5**, 549-553 (2009).
106 Kellner, H. Targeting interleukin-17 in patients with active rheumatoid arthritis: rationale and clinical potential. *Ther Adv Musculoskelet Dis* **5**, 141-152 (2013).
107 Connor, V. Anti-TNF therapies: a comprehensive analysis of adverse effects associated with immunosuppression. *Rheumatol Int* **31**, 327-337 (2011).
108 Han, X. *et al*. Interleukin-17 enhances immunosuppression by mesenchymal stem cells. *Cell Death Differ* **21**, 1758-1768 (2014).
109 Pineda, M. A., Eason, R. J., Harnett, M. M. & Harnett, W. From the worm to the pill, the parasitic worm product ES-62 raises new horizons in the treatment of rheumatoid arthritis. *Lupus* **24**, 400-411 (2015).
110 Harnett, W., Worms, M. J., Kapil, A., Grainger, M. & Parkhouse, R. M. Origin, kinetics of circulation and fate in vivo of the major excretory-secretory product of Acanthocheilonema viteae. *Parasitology* **99 Pt 2**, 229-239 (1989).
111 Al-Riyami, L. *et al*. Designing anti-inflammatory drugs from parasitic worms: a synthetic small molecule analogue of the Acanthocheilonema viteae product ES-62 prevents development of collagen-induced arthritis. *Journal of medicinal chemistry* **56**, 9982-10002 (2013).
112 Guglani, L. & Khader, S. A. Th17 cytokines in mucosal immunity and inflammation. *Curr Opin HIV AIDS* **5**, 120-127 (2010).
113 Rodgers, D. T., Pineda, M. A., Suckling, C. J., Harnett, W. & Harnett, M. M. Drug-like analogues of the parasitic worm-derived immunomodulator ES-62 are therapeutic in the MRL/Lpr model of systemic lupus erythematosus. *Lupus* **24**, 1437-1442 (2015).
114 Rzepecka, J. *et al*. Prophylactic and therapeutic treatment with a synthetic analogue of a parasitic worm product prevents experimental arthritis and inhibits IL-1ß production via NRF2-mediated counter-regulation of the inflammasome. *J Autoimmun* **60**, 59-73 (2015).

115 Wruck, C. J. *et al*. Role of oxidative stress in rheumatoid arthritis: insights from the Nrf2-knockout mice. *Ann Rheum Dis* **70**, 844-850 (2011).
116 Moffett, B. C. *The morphogenesis of joints*. (1965).
117 McInnes, I. B. *et al*. A Novel Therapeutic Approach Targeting Articular Inflammation Using the Filarial Nematode-Derived Phosphorylcholine-Containing Glycoprotein ES-62. *The Journal of Immunology* **171**, 2127-2133 (2003).
118 Gelse, K. *et al*. Role of hypoxia-inducible factor 1 alpha in the integrity of articular cartilage in murine knee joints. *Arthritis Res Ther* **10**, R111 (2008).
119 Radu, M. & Chernoff, J. An in vivo assay to test blood vessel permeability. *J Vis Exp*, e50065 (2013).
120 Maria Armaka, V. G., Dimitris Kontoyiannis & George Kollias. A standardized protocol for the isolation and culture of normal and arthritogenic murine synovial fibroblasts. *Protocol exchange* **102** (2009).
121 Versteeg, H. H. *et al*. A new phosphospecific cell-based ELISA for p42/p44 mitogen-activated protein kinase (MAPK), p38 MAPK, protein kinase B and cAMP-response-element-binding protein (vol 350, pg 717, 2000). *Biochemical Journal* **355**, 879-879 (2001).
122 Marzi, M. J. a. N., F. Flexible, efficient miRNA detection using the miScript PCR System. *qiagen*.
123 Christman, J. K. 5-Azacytidine and 5-aza-2'-deoxycytidine as inhibitors of DNA methylation: mechanistic studies and their implications for cancer therapy. *Oncogene* **21**, 5483-5495 (2002).
124 Karouzakis, E., Gay, R. E., Michel, B. A., Gay, S. & Neidhart, M. DNA hypomethylation in rheumatoid arthritis synovial fibroblasts. *Arthritis Rheum* **60**, 3613-3622 (2009).
125 Stanczyk, J. *et al*. Altered expression of microRNA-203 in rheumatoid arthritis synovial fibroblasts and its role in fibroblast activation. *Arthritis Rheum* **63**, 373-381 (2011).
126 Nakano, K., Boyle, D. L. & Firestein, G. S. Regulation of DNA methylation in rheumatoid arthritis synoviocytes. *J Immunol* **190**, 1297-1303 (2013).
127 Harnett, W. & Harnett, M. M. Therapeutic immunomodulators from nematode parasites. *Expert Rev Mol Med* **10**, e18 (2008).
128 Harnett, W. & Harnett, M. M. Helminth-derived immunomodulators: can understanding the worm produce the pill? *Nat Rev Immunol* **10**, 278-284 (2010).
129 Rosman, Z., Shoenfeld, Y. & Zandman-Goddard, G. Biologic therapy for autoimmune diseases: an update. *BMC Med* **11**, 88 (2013).
130 Al-Riyami, L. *et al*. Protective effect of small molecule analogues of the Acanthocheilonema viteae secreted product ES-62 on oxazolone-induced ear inflammation. *Exp Parasitol* **158**, 18-22 (2015).
131 Rzepecka, J. *et al*. Small molecule analogues of the immunomodulatory parasitic helminth product ES-62 have anti-allergy properties. *Int J Parasitol* **44**, 669-674 (2014).

132 Al-Riyami, L. *et al*. Designing anti-inflammatory drugs from parasitic worms: a synthetic small molecule analogue of the Acanthocheilonema viteae product ES-62 prevents development of collagen-induced arthritis. *J Med Chem* **56**, 9982-10002 (2013).

133 Pineda, M. A., Rodgers, D. T., Al-Riyami, L., Harnett, W. & Harnett, M. M. ES-62 protects against collagen-induced arthritis by resetting interleukin-22 toward resolution of inflammation in the joints. *Arthritis Rheumatol* **66**, 1492-1503 (2014).

134 Huber, L. C. *et al*. Synovial fibroblasts: key players in rheumatoid arthritis. *Rheumatology (Oxford)* **45**, 669-675 (2006).

135 Lefèvre, S. *et al*. Synovial fibroblasts spread rheumatoid arthritis to unaffected joints. *Nat Med* **15**, 1414-1420 (2009).

136 Asquith DL, M. A., McInnes IB, Liew FY. Animal models of rheumatoid arthritis. *Eur J Immunol*. **38**, 2040-2044 (2009).

137 Anna-Karin B Lindqvistemail, R. B., Åsa C.M Johansson, Kutty S Nandakumar, Martina Johannesson, Rikard Holmdahl. Mouse models for rheumatoid arthritis. *Trends in Genetics* **18**, pS7-S13 (2002).

138 RO, W. Collagen-induced arthritis as a model for rheumatoid arthritis. *Methods Mol Med*. **98**, 207-216 (2004).

139 David D Brand, K. A. L., & Edward F Rosloniec. Collagen-induced arthritis. *Nature Protocols* **2**, 1269-1275 (2007).

140 Harnett, W., McInnes, I. B. & Harnett, M. M. ES-62, a filarial nematode-derived immunomodulator with anti-inflammatory potential. *Immunol Lett* **94**, 27-33 (2004).

141 Marshall, F. A., Grierson, A. M., Garside, P., Harnett, W. & Harnett, M. M. ES-62, an immunomodulator secreted by filarial nematodes, suppresses clonal expansion and modifies effector function of heterologous antigen-specific T cells in vivo. *J Immunol* **175**, 5817-5826 (2005).

142 Pineda, M. A., Rodgers, D. T., Al-Riyami, L., Harnett, W. & Harnett, M. M. ES-62 protects against collagen-induced arthritis by resetting interleukin-22 toward resolution of inflammation in the joints. *Arthritis & rheumatology (Hoboken, N.J.)* **66**, 1492-1503 (2014).

143 Celia María Quiñonez-Flores, S. A. G.-C., and César Pacheco-Tena. Hypoxia and its implications in rheumatoid arthritis. *J Biomed Sci* **23**, 62 (2016).

144 Harnett, M. M., Harnett, W. & Pineda, M. A. The parasitic worm product ES-62 up-regulates IL-22 production by γδ T cells in the murine model of Collagen-Induced Arthritis. *Inflamm Cell Signal* **1** (2014).

145 Miranda-Carus, M. E., Balsa, A., Benito-Miguel, M., de Ayala, C. P. & Martin-Mola, E. IL-15 and the initiation of cell contact-dependent synovial fibroblast-T lymphocyte cross-talk in rheumatoid arthritis: Effect of methotrexate. *Journal of Immunology* **173**, 1463-1476 (2004).

146 Liu, X. Z., B. ;Zhang, J. ;Li, W. ;Mou, F. ;Wang, H. ;Zou, Q. ;Zhong, B. ;Wu, L. ;Wei, H. ;Fang, Y. . Role of the Gut Microbiome in Modulating Arthritis Progression in Mice. *Sci Rep* **6**, 30594 (2016).

147 Rosser, E. C. O., K. ;Tonon, S. ;Doyle, R. ;Bosma, A. ;Carter, N. A. ;Harris, K. A. ;Jones, S. A. ;Klein, N. ;Mauri, C. Regulatory B cells are

induced by gut microbiota-driven interleukin-1β and interleukin-6 production. *Nat Med* **20**, 1334-1339 (2014).

148 Assi, L. K. W., S. H. ;Ludwig, A. ;Raza, K. ;Gordon, C. ;Salmon, M. ;Lord, J. M. ;Scheel-Toellner, D. . Tumor necrosis factor alpha activates release of B lymphocyte stimulator by neutrophils infiltrating the rheumatoid joint. *Arthritis Rheum* **56**, 1776-1786 (2007).

149 Tak, P.;Daha, M. R. ;Kluin, P. M. ;Meijers, K. A. ;Brand, R. ;Meinders, A. E. ;Breedveld, F. C. Analysis of the synovial cell infiltrate in early rheumatoid synovial tissue in relation to local disease activity. *Arthritis Rheum* **40**, 217-225 (1997).

150 Hu, F. *et al*. Toll-like receptors expressed by synovial fibroblasts perpetuate Th1 and th17 cell responses in rheumatoid arthritis. *PLoS One* **9**, e100266 (2014).

151 Bottini, N. & Firestein, G. S. Duality of fibroblast-like synoviocytes in RA: passive responders and imprinted aggressors. *Nature Reviews Rheumatology* **9**, 24-33 (2013).

152 Gelderman, K. A. *et al*. Rheumatoid arthritis: the role of reactive oxygen species in disease development and therapeutic strategies. *Antioxid Redox Signal* **9**, 1541-1567 (2007).

153 Konisti, S., Kiriakidis, S. & Paleolog, E. M. Hypoxia-a key regulator of angiogenesis and inflammation in rheumatoid arthritis. *Nature Reviews Rheumatology* **8**, 153-162 (2012).

154 Juarez, M., Filer, A. & Buckley, C. D. Fibroblasts as therapeutic targets in rheumatoid arthritis and cancer. *Swiss medical weekly* **142**, w13529-w13529 (2012).

155 Mario Mellado, L. M.-M., Graciela Cascio, Pilar Lucas, José L. Pablos, and José Miguel Rodríguez-Frade. T Cell Migration in Rheumatoid Arthritis. *Front Immunol*. **6**, 384 (2015).

156 Huber, L. C. *et al*. Synovial fibroblasts: key players in rheumatoid arthritis. *Rheumatology* **45**, 669-675 (2006).

157 A, H., M, O., K, M. & M., M. STAT3, but not ERKs, mediates the IL-6-induced proliferation of renal cancer cells, ACHN and 769P. *Kidney Int*. **61**, 926-938 (2002).

158 Deon, D. *et al*. Cross-talk between IL-1 and IL-6 signaling pathways in rheumatoid arthritis synovial fibroblasts. *J Immunol* **167**, 5395-5403 (2001).

159 Chang, F. *et al*. Signal transduction mediated by the Ras/Raf/MEK/ERK pathway from cytokine receptors to transcription factors: potential targeting for therapeutic intervention. *Leukemia* **17**, 1263-1293 (2003).

160 Broom, O. J., Widjaya, B., Troelsen, J., Olsen, J. & Nielsen, O. H. Mitogen activated protein kinases: a role in inflammatory bowel disease? *Clin Exp Immunol* **158**, 272-280 (2009).

161 Thalhamer, T., McGrath, M. A. & Harnett, M. M. MAPKs and their relevance to arthritis and inflammation. *Rheumatology (Oxford)* **47**, 409-414 (2008).

162 Schett, G. *et al*. Activation, differential localization, and regulation of the stress-activated protein kinases, extracellular signal-regulated kinase, c-JUN N-terminal kinase, and p38 mitogen-activated protein

kinase, in synovial tissue and cells in rheumatoid arthritis. *Arthritis Rheum* **43**, 2501-2512 (2000).
163 Sebolt-Leopold, J. S. *et al*. Blockade of the MAP kinase pathway suppresses growth of colon tumors in vivo. *Nat Med* **5**, 810-816 (1999).
164 Thiel, M. J. *et al*. Central role of the MEK/ERK MAP kinase pathway in a mouse model of rheumatoid arthritis: Potential proinflammatory mechanisms. *Arthritis & Rheumatism* **56**, 3347-3357 (2007).
165 Yang CM, L. S., Hsieh HL, Lin CC, Wu CC, Hsiao LD. Interleukin-1 beta induces ICAM-1 expression enhancing leukocyte adhesion in human rheumatoid arthritis synovial fibroblasts: involvement of ERK, JNK, AP-1 and NFkappaB. *J Cell Physiol*. **224**, 516-526 (2010).
166 Brauchle, M., Glück, D., Di Padova, F., Han, J. & Gram, H. Independent role of p38 and ERK1/2 mitogen-activated kinases in the upregulation of matrix metalloproteinase-1. *Exp Cell Res* **258**, 135-144 (2000).
167 Thiel, M. J. *et al*. Central role of the MEK/ERK MAP kinase pathway in a mouse model of rheumatoid arthritis: potential proinflammatory mechanisms. *Arthritis Rheum* **56**, 3347-3357 (2007).
168 PJ, M. The JAK-STAT signaling pathway: input and output integration. *The Journal of Immunology* **34**, 177-187 (2007).
169 E, M. C. a. P. Targeting JAK/STAT Signaling Pathway in Inflammatory Diseases. *Current Signal Transduction Therapy* **4**, 201-202 (2008).
170 Dutta P, L. W. Role of the JAK-STAT Signalling Pathway in Cancer. *eLS* (2013).
171 Walker, J. G. & Smith, M. D. The Jak-STAT pathway in rheumatoid arthritis. *J Rheumatol* **32**, 1650-1653 (2005).
172 M, K. V. a. G. Novel Small Molecule Therapeutics in Rheumatoid Arthritis. *Rheumatoilogy* **52**, 1155-1162 (2013).
173 Kasperkovitz P, V. N., Smeets T, JG Van Rietschoten, Kraan M and Verweij C. Activation of the STAT1 pathway in rheumatoid arthritis. *Ann Rheum Dis* **63**, 233-239 (2004).
174 Walker JG, A. M., ..., and MD Smith. Expression of Jak3, STAT1, STAT4 and STAT6 in inflammatory arthritis: unique Jak3 and STAT4 expresion in dendritic cells in seropositive rheumatoid arthritis. *Ann Rheum Dis* **65**, 149-156 (2006).
175 Krause, A., Scaletta, N., Ji, J. D. & Ivashkiv, L. B. Rheumatoid arthritis synoviocyte survival is dependent on Stat3. *J Immunol* **169**, 6610-6616 (2002).
176 Ray, S. *et al*. The IL-6 Trans-Signaling-STAT3 Pathway Mediates ECM and Cellular Proliferation in Fibroblasts from Hypertrophic Scar. *J Invest Dermatol* (2013).
177 Mori T, M. T., Yoshida H, Asakawa M, Kawasumi M, Kobayashi T, Morioka H, Chiba K, Toyama Y and Yoshimura A. IL-1b and TNFa-initiated IL-6-STAT3 pathway is critical in mediating inflammatory cytokines and RANKL expression in inflammatory arthritis. *International Immunology* **11**, 1-12 (2011).
178 Goodridge, H. S. *et al*. Immunomodulation via novel use of TLR4 by the filarial nematode phosphorylcholine-containing secreted product, ES-62. *Journal of Immunology* **174**, 284-293 (2005).

179 Puneet, P. *et al*. The helminth product ES-62 protects against septic shock via Toll-like receptor 4-dependent autophagosomal degradation of the adaptor MyD88. *Nat Immunol* **12**, 344-351 (2011).
180 Lin, X., Kong, J., Wu, Q., Yang, Y. & Ji, P. Effect of TLR4/MyD88 signaling pathway on expression of IL-1ß and TNF-α in synovial fibroblasts from temporomandibular joint exposed to lipopolysaccharide. *Mediators Inflamm* **2015**, 329405 (2015).
181 Marotte H, A. S., Ruth JH and AE Koch. Blocking ERK-1/2 reduces tumor necrosis factor a-induced interleukin-18 bioactivity in rheumatoid arthritis synovial fibroblasts by induction of interleukin-18 binding protein a *Arthritis and Rheumatism* **62**, 722-731 (2010).
182 Yu, C. R., Young, H. A. & Ortaldo, J. R. Characterization of cytokine differential induction of STAT complexes in primary human T and NK cells. *J Leukoc Biol* **64**, 245-258 (1998).
183 Schindler, C., Levy, D. E. & Decker, T. JAK-STAT signaling: from interferons to cytokines. *J Biol Chem* **282**, 20059-20063 (2007).
184 Kumar, A., Commane, M., Flickinger, T. W., Horvath, C. M. & Stark, G. R. Defective TNF-alpha-induced apoptosis in STAT1-null cells due to low constitutive levels of caspases. *Science* **278**, 1630-1632 (1997).
185 Xie, Q., Huang, C. & Li, J. Interleukin-22 and rheumatoid arthritis: emerging role in pathogenesis and therapy. *Autoimmunity* **48**, 69-72 (2015).
186 Verma, R. *et al*. A network map of Interleukin-10 signaling pathway. *J Cell Commun Signal* **10**, 61-67 (2016).
187 Gordon RA1, G. G., Lee A, Kalliolias GD, Ivashkiv LB. The interferon signature and STAT1 expression in rheumatoid arthritis synovial fluid macrophages are induced by tumor necrosis factor α and counter-regulated by the synovial fluid microenvironment. *Arthritis Rheum* **64**, 3119-3128 (2012).
188 van Holten, J. *et al*. Treatment with recombinant interferon-beta reduces inflammation and slows cartilage destruction in the collagen-induced arthritis model of rheumatoid arthritis. *Arthritis Res Ther* **6**, R239-249 (2004).
189 Liang, Y., Xu, W. D., Peng, H., Pan, H. F. & Ye, D. Q. SOCS signaling in autoimmune diseases: molecular mechanisms and therapeutic implications. *Eur J Immunol* **44**, 1265-1275 (2014).
190 Starr, R. *et al*. A family of cytokine-inducible inhibitors of signalling. *Nature* **387**, 917-921 (1997).
191 Dolhain, R. J. *et al*. Increased expression of interferon (IFN)-gamma together with IFN-gamma receptor in the rheumatoid synovial membrane compared with synovium of patients with osteoarthritis. *Br J Rheumatol* **35**, 24-32 (1996).
192 T Karonitsch, K. D., R Byrne, B Niedereiter, E Cetin, A Wanivenhaus, C Scheinecker, J S Smolen, H P Kiener. IFN-gamma promotes fibroblast-like synoviocytes motility. *Ann Rheum Dis* **69** (2010).
193 Sabat, R., Ouyang, W. & Wolk, K. Therapeutic opportunities of the IL-22-IL-22R1 system. *Nat Rev Drug Discov* **13**, 21-38 (2014).
194 Treschow, A. P., Teige, I., Nandakumar, K. S., Holmdahl, R. & Issazadeh-Navikas, S. Stromal cells and osteoclasts are responsible for

exacerbated collagen-induced arthritis in interferon-beta-deficient mice. *Arthritis Rheum* **52**, 3739-3748 (2005).

195 Alexander, W. S. *et al.* SOCS1 is a critical inhibitor of interferon gamma signaling and prevents the potentially fatal neonatal actions of this cytokine. *Cell* **98**, 597-608 (1999).

196 Casar, B., Pinto, A. & Crespo, P. ERK dimers and scaffold proteins: unexpected partners for a forgotten (cytoplasmic) task. *Cell Cycle* **8**, 1007-1013 (2009).

197 Cerioni, L., Palomba, L. & Cantoni, O. The Raf/MEK inhibitor PD98059 enhances ERK1/2 phosphorylation mediated by peroxynitrite via enforced mitochondrial formation of reactive oxygen species. *FEBS Letter* **547**, 92-96 (2003).

198 Uehara, Y., Mochizuki, M., Matsuno, K., Haino, T. & Asai, A. Novel high-throughput screening system for identifying STAT3-SH2 antagonists. *Biochem Biophys Res Commun* **380**, 627-631 (2009).

199 Berezikov, E. Evolution of microRNA diversity and regulation in animals. *NAt Rev Genet* **12**, 846-860 (2011).

200 Ivey KN, S. D. MicroRNAs as Regulators of Differentiation and Cell Fate Decisions. *Cell Stem Cell* **7**, 36-41 (2010).

201 Yang Z. The involvement of microRNAs in malignant transformation. *Histology and histopathology* **10**, 1263-1270 (2012).

202 Stanczyk, J. *et al.* Altered expression of MicroRNA in synovial fibroblasts and synovial tissue in rheumatoid arthritis. *Arthritis and Rheumatism* **58**, 1001-1009 (2008).

203 Chen, H. F. e. a. Association between miR-146a rs2910164 polymorphism and autoimmune diseases susceptibility: A meta-analysis,. *Genes* **521** (2013).

204 Kurowska-Stolarska, M. e. a. MicroRNA-155 as a proinflammatory regulator in clinical and experimental arthritis. *Proceedings of the National Academy of Sciences of the United States of America* **108**, 11193-11198 (2011).

205 Pauley, K. M. & Cha, S. miRNA-146a in rheumatoid arthritis: a new therapeutic strategy. *Immunotherapy* **3**, 829-831 (2011).

206 Nakasa, T. *et al.* Expression of MicroRNA-146 in rheumatoid arthritis synovial tissue. *Arthritis and Rheumatism* **58**, 1284-1292 (2008).

207 Blueml, S. e. a. Essential Role of MicroRNA-155 in the Pathogenesis of Autoimmune Arthritis in Mice. *Arthritis and Rheumatism* **63** (2011).

208 Long, L. *et al.* Upregulated microRNA-155 expression in peripheral blood mononuclear cells and fibroblast-like synoviocytes in rheumatoid arthritis. *Clinical & developmental immunology* **2013**, 296139 (2013).

209 Jin, H. M. *et al.* MicroRNA-155 as a proinflammatory regulator via SHIP-1 down-regulation in acute gouty arthritis. *Arthritis Res Ther* **16**, R88 (2014).

210 Tang, B. *et al.* Identification of MyD88 as a novel target of miR-155, involved in negative regulation of Helicobacter pylori-induced inflammation. *FEBS Letters* **584**, 1481-1486 (2010).

211 O'Connell, R. M., Chaudhuri, A. A., Rao, D. S. & Baltimore, D. Inositol phosphatase SHIP1 is a primary target of miR-155. *Proceedings of the National Academy of Sciences* **106**, 7113-7118 (2009).

212 Virtue, A., Wang, H. & Yang, X.-f. F. MicroRNAs and toll-like receptor/interleukin-1 receptor signaling. *Journal of hematology & oncology* **5**, 66 (2012).
213 O'Connell, R. M. *et al*. MicroRNA-155 Promotes Autoimmune Inflammation by Enhancing Inflammatory T Cell Development. *Immunity* **33**, 607-619 (2010)
214 Leng, R.-X., Pan, H.-F., Qin, W.-Z., Chen, G.-M. & Ye, D.-Q. Role of microRNA-155 in autoimmunity. *Cytokine & Growth Factor Reviews* **22**, 141-147 (2011).
215 Taganov, K. D., Boldin, M. P., Chang, K.-J. J. & Baltimore, D. NF-kappaB-dependent induction of microRNA miR-146, an inhibitor targeted to signaling proteins of innate immune responses. *Proceedings of the National Academy of Sciences of the United States of America* **103**, 12481-12486 (2006).
216 Stanczyk, J. *et al*. Altered expression of MicroRNA in synovial fibroblasts and synovial tissue in rheumatoid arthritis. *Arthritis & Rheumatism* **58**, 1001-1009 (2008).
217 Kim, S.-W. *et al*. MicroRNAs miR-125a and miR-125b constitutively activate the NF-κB pathway by targeting the tumor necrosis factor alpha-induced protein 3 (TNFAIP3, A20). *Proceedings of the National Academy of Sciences* **109**, 7865-7870 (2012).
218 Gantier, M. P. *et al*. A miR-19 regulon that controls NF-κB signaling. *Nucleic acids research* **40**, 8048-8058 (2012).
219 Zhu, S. *et al*. The microRNA miR-23b suppresses IL-17-associated autoimmune inflammation by targeting TAB2, TAB3 and IKK-α. *Nature Medicine* **18**, 1077-1086 (2012).
220 Stanczyk, J. *et al*. Altered expression of microRNA-203 in rheumatoid arthritis synovial fibroblasts and its role in fibroblast activation. *Arthritis and Rheumatism* **63**, 373-381 (2011).
221 Alsaleh, G. *et al*. Bruton's Tyrosine Kinase Is Involved in miR-346-Related Regulation of IL-18 Release by Lipopolysaccharide-Activated Rheumatoid Fibroblast-Like Synoviocytes. *Journal of Immunology* **182**, 5088-5097 (2009).
222 Semaan, N. *et al*. miR-346 Controls Release of TNF-alpha Protein and Stability of Its mRNA in Rheumatoid Arthritis via Tristetraprolin Stabilization. *Plos One* **6** (2011).
223 Niederer, F. *et al*. Down-regulation of microRNA-34a* in rheumatoid arthritis synovial fibroblasts promotes apoptosis resistance. *Arthritis Rheum* **64**, 1771-1779 (2012).
224 Nakasa, T., Shibuya, H., Nagata, Y., Niimoto, T. & Ochi, M. The Inhibitory Effect of MicroRNA-146a Expression on Bone Destruction in Collagen-Induced Arthritis. *Arthritis and Rheumatism* **63**, 1582-1590 (2011).
225 Lu, L.-F. *et al*. Foxp3-Dependent MicroRNA155 Confers Competitive Fitness to Regulatory T Cells by Targeting SOCS1 Protein. *Immunity* **30**, 80-91 (2008)
226 Zhai, A. *et al*. Borna disease virus encoded phosphoprotein inhibits host innate immunity by regulating miR-155. *Antiviral Res* **98**, 66-75 (2013).

227 Kimura A *et al*. Suppressor of cytokine signaling-1 selectively inhibits LPS-induced IL-6 production by regulating JAK-STAT. *Proc Natl Acad Sci U S A* **102**, 17089-17094 (2005).
228 Wormald S, Z. J., Krebs DL, Mielke LA, Silver J, Alexander WS, Speed TP, Nicola NA, Hilton DJ. The comparative roles of suppressor of cytokine signaling-1 and -3 in the inhibition and desensitization of cytokine signaling. *J Biol Chem.* **281**, 11135-11143 (2006).
229 Jeffrey J. Babon, L. N. V., and Nicos A. Nicola. Inhibition of IL-6 family cytokines by SOCS3. *Semin Immunol*. **26**, 13-19 (2014).
230 Bode JG, N. A., Schmitz J, Schaper F, Schmitt M, Frisch W, Häussinger D, Heinrich PC, Graeve L. LPS and TNFalpha induce SOCS3 mRNA and inhibit IL-6-induced activation of STAT3 in macrophages. *FEBS Lett* **463**, 365-370 (1999).
231 Guoqiang Zhang, P.-O. E. v., Hang Gyeong Chin, Jolyon Terragni, Nan Dai, Ivan R. Correa Jr and Sriharsa Pradhan. Small RNA-mediated DNA (cytosine-5) methyltransferase 1 inhibition leads to aberrant DNA methylation. *Nucleic Acids Res.* **43**, 6112-6124 (2015).
232 Goodridge, H. S. *et al*. Modulation of macrophage cytokine production by ES-62, a secreted product of the filarial nematode Acanthocheilonema viteae. *J Immunol* **167**, 940-945 (2001).
233 Diehl S, A. J., Hoffmeyer A, Zapton T, Ihle JN, Fikrig E, Rincón M. Inhibition of Th1 differentiation by IL-6 is mediated by SOCS1. *Immunity* **13**, 805-815 (2000).
234 Zhao, X. D., Zhang, W., Liang, H. J. & Ji, W. Y. Overexpression of miR - 155 promotes proliferation and invasion of human laryngeal squamous cell carcinoma via targeting SOCS1 and STAT3. *PLoS One* **8**, e56395 (2013).
235 Pap, T. [Regulation of apoptosis in aggressive fibroblasts]. *Z Rheumatol* **66**, 239-240 (2007).
236 Frank-Bertoncelj, M. & Gay, S. The epigenome of synovial fibroblasts: an underestimated therapeutic target in rheumatoid arthritis. *Arthritis Res Ther* **16**, 117 (2014).
237 Carey, N., Marques, C. J. & Reik, W. DNA demethylases: a new epigenetic frontier in drug discovery. *Drug discovery today* **16**, 683-690 (2011).
238 Raza, K. *et al*. Early rheumatoid arthritis is characterized by a distinct and transient synovial fluid cytokine profile of T cell and stromal cell origin. *Arthritis Res Ther* **7**, R784-795 (2005).
239 Anuradha, R. *et al*. Interleukin 1 (IL-1)- and IL-23-mediated expansion of filarial antigen-specific Th17 and Th22 cells in filarial lymphedema. *Clin Vaccine Immunol* **21**, 960-965 (2014).
240 Cai, S., Fu, X. & Sheng, Z. Dedifferentiation: A New Approach in Stem Cell Research. *BioScience* **57**, 655-662 (2007).
241 Thomas, N. S. The STAT3-DNMT1 connection. *JAKSTAT* **1**, 257-260 (2012).
242 Zhang, Q. *et al*. STAT3- and DNA methyltransferase 1-mediated epigenetic silencing of SHP-1 tyrosine phosphatase tumor suppressor gene in malignant T lymphocytes. *Proc Natl Acad Sci U S A* **102**, 6948-6953 (2005).

243 Sarkar, S. *et al*. Histone deacetylase inhibitors reverse CpG methylation by regulating DNMT1 through ERK signaling. *Anticancer Res* **31**, 2723-2732 (2011).
244 Li, Y., Gorelik, G., Strickland, F. M. & Richardson, B. C. Oxidative stress, T cell DNA methylation, and lupus. *Arthritis Rheumatol* **66**, 1574-1582 (2014).
245 Cedar, H. & Bergman, Y. Linking DNA methylation and histone modification: patterns and paradigms. *Nat Rev Genet* **10**, 295-304 (2009).
246 Fuks, F., Burgers, W. A., Brehm, A., Hughes-Davies, L. & Kouzarides, T. DNA methyltransferase Dnmt1 associates with histone deacetylase activity. *Nat Genet* **24**, 88-91 (2000).
247 Karouzakis, E. *et al*. DNA methylation regulates the expression of CXCL12 in rheumatoid arthritis synovial fibroblasts. *Genes Immun* **12**, 643-652 (2011).
248 Nakano, K., Whitaker, J. W., Boyle, D. L., Wang, W. & Firestein, G. S. DNA methylome signature in rheumatoid arthritis. *Ann Rheum Dis* **72**, 110-117 (2013).
249 Nile, C. J., Read, R. C., Akil, M., Duff, G. W. & Wilson, A. G. Methylation status of a single CpG site in the IL6 promoter is related to IL6 messenger RNA levels and rheumatoid arthritis. *Arthritis Rheum* **58**, 2686-2693 (2008).
250 Ehrlich, M. DNA methylation in cancer: too much, but also too little. *Oncogene* **21**, 5400-5413 (2002).
251 Nakano, K., Whitaker, J. W., Boyle, D. L., Wang, W. & Firestein, G. S. DNA methylome signature in rheumatoid arthritis. *Annals of the Rheumatic Diseases* **72**, 110-117 (2013).
252 Cox, F. E. History of human parasitology. *Clin Microbiol Rev* **15**, 595-612 (2002).
253 de Silva, N. R. *et al*. Soil-transmitted helminth infections: updating the global picture. *Trends Parasitol* **19**, 547-551 (2003).
254 Stoll, N. R. This wormy world. 1947. *J Parasitol* **85**, 392-396 (1999).
255 Hotez, P. J. *et al*. Helminth infections: the great neglected tropical diseases. *J Clin Invest* **118**, 1311-1321 (2008).
256 Maizels, R. M. Infections and allergy - helminths, hygiene and host immune regulation. *Curr Opin Immunol* **17**, 656-661 (2005).
257 Yazdanbakhsh, M., Kremsner, P. G. & van Ree, R. Allergy, parasites, and the hygiene hypothesis. *Science* **296**, 490-494 (2002).
258 Rosche, B., Wernecke, K. D., Ohlraun, S., Dörr, J. M. & Paul, F. Trichuris suis ova in relapsing-remitting multiple sclerosis and clinically isolated syndrome (TRIOMS): study protocol for a randomized controlled trial. *Trials* **14**, 112 (2013).
259 Panda AK, R. B., Das BK. Rheumatoid arthritis patients are free of filarial infection in an area where filariasis is endemic: comment on the article by Pineda et al. . *Arthritis Rheum*. **65**, 1402-1403 (2013).
260 Harnett, W., Frame, M. J., Nor, Z. M., MacDonald, M. & Houston, K. M. Some preliminary data on the nature/structure of the PC-glycan of the major excretory-secretory product of Acanthocheilonema viteae (ES-62). *Parasite* **1**, 179-181 (1994).

261 Pineda, M. A., Rodgers, D. T., Al-Riyami, L., Harnett, W. & Harnett, M. ES-62 protects against collagen-induced arthritis by resetting IL-22 towards resolution of inflammation in the joints. *Arthritis & rheumatology (Hoboken, N.J.)* (2014).
262 Srirangan, S. & Choy, E. H. The role of interleukin 6 in the pathophysiology of rheumatoid arthritis. *Ther Adv Musculoskelet Dis* **2**, 247-256 (2010).
263 Zhang, L. *et al*. Chemokine Signaling Pathway Involved in CCL2 Expression in Patients with Rheumatoid Arthritis. *Yonsei Med J* **56**, 1134-1142 (2015).
264 Fiedorczyk, M., Klimiuk, P. A., Sierakowski, S., Domysławska, I. & Chwiećko, J. [Correlations between serum matrix metalloproteinase (MMP-1, MMP-3, MMP-9, MMP-13) concentrations and markers of disease activity in early rheumatoid arthritis]. *Przegl Lek* **62**, 1321-1324 (2005).
265 Ball, D. H. *et al*. Mast Cell Subsets and Their Functional Modulation by the Acanthocheilonema viteae Product ES-62. *J Parasitol Res* **2013**, 961268 (2013).
266 Goodridge, H. S. *et al*. Immunomodulation via novel use of TLR4 by the filarial nematode phosphorylcholine-containing secreted product, ES-62. *J Immunol* **174**, 284-293 (2005).
267 Bagchi, A. *et al*. MyD88-dependent and MyD88-independent pathways in synergy, priming, and tolerance between TLR agonists. *J Immunol* **178**, 1164-1171 (2007).
268 Oshiumi, H., Matsumoto, M., Funami, K., Akazawa, T. & Seya, T. TICAM-1, an adaptor molecule that participates in Toll-like receptor 3-mediated interferon-beta induction. *Nat Immunol* **4**, 161-167 (2003).
269 Yamamoto, M. *et al*. Cutting edge: a novel Toll/IL-1 receptor domain-containing adapter that preferentially activates the IFN-beta promoter in the Toll-like receptor signaling. *J Immunol* **169**, 6668-6672 (2002).
270 Broad, A., Kirby, J. A., Jones, D. E. & Group, A. I. a. T. R. Toll-like receptor interactions: tolerance of MyD88-dependent cytokines but enhancement of MyD88-independent interferon-beta production. *Immunology* **120**, 103-111 (2007).
271 Sheikh, F., Dickensheets, H., Gamero, A. M., Vogel, S. N. & Donnelly, R. P. An essential role for IFN-β in the induction of IFN-stimulated gene expression by LPS in macrophages. *J Leukoc Biol* **96**, 591-600 (2014).
272 Toshchakov, V. *et al*. TLR4, but not TLR2, mediates IFN-beta-induced STAT1alpha/beta-dependent gene expression in macrophages. *Nat Immunol* **3**, 392-398 (2002).
273 Palmer, G. *et al*. Interferon beta stimulates interleukin 1 receptor antagonist production in human articular chondrocytes and synovial fibroblasts. *Ann Rheum Dis* **63**, 43-49 (2004).
274 Smeets, T. J. *et al*. The effects of interferon-beta treatment of synovial inflammation and expression of metalloproteinases in patients with rheumatoid arthritis. *Arthritis Rheum* **43**, 270-274 (2000).
275 van Holten, J., Plater-Zyberk, C. & Tak, P. P. Interferon-beta for treatment of rheumatoid arthritis? *Arthritis Res* **4**, 346-352 (2002).

276 Chin, Y. E., Kitagawa, M., Kuida, K., Flavell, R. A. & Fu, X. Y. Activation of the STAT signaling pathway can cause expression of caspase 1 and apoptosis. *Mol Cell Biol* **17**, 5328-5337 (1997).
277 Lee, K. Y., Anderson, E., Madani, K. & Rosen, G. D. Loss of STAT1 expression confers resistance to IFN-gamma-induced apoptosis in ME180 cells. *FEBS Lett* **459**, 323-326 (1999).
278 Chen, W., Gao, Q., Han, S., Pan, F. & Fan, W. The CCL2/CCR2 axis enhances IL-6-induced epithelial-mesenchymal transition by cooperatively activating STAT3-Twist signaling. *Tumour Biol* **36**, 973-981 (2015).
279 Sarközi, R. *et al*. Synergistic induction of CCL2/MCP-1 expression driven by oncostatin M and IL-1β in human proximal tubular cells depends on STAT3 and p65 NFκB/RelA. *Physiol Rep* **3** (2015).
280 Orgaz, J. L. *et al*. Diverse matrix metalloproteinase functions regulate cancer amoeboid migration. *Nat Commun* **5**, 425 (2014).
281 S. Hayashi, T. N., S. Hashimoto, T. Fujishiro, N. Kanzaki, K. Iwasa, S. Sakata, N. Chinzei, R. Kuroda, M. Kurosaka. P21 regulates MMP-13 expression through STAT3 signaling in chondrocytes. *Osteoarthritis and cartilage* **21**, S46-S47 (2013).
282 Shouda, T. *et al*. Induction of the cytokine signal regulator SOCS3/CIS3 as a therapeutic strategy for treating inflammatory arthritis. *J Clin Invest* **108**, 1781-1788 (2001).
283 Fujimoto, M. & Naka, T. Regulation of cytokine signaling by SOCS family molecules. *Trends Immunol* **24**, 659-666 (2003).
284 Yoshimura, A., Naka, T. & Kubo, M. SOCS proteins, cytokine signalling and immune regulation. *Nat Rev Immunol* **7**, 454-465 (2007).
285 Kinjyo, I. *et al*. SOCS1/JAB is a negative regulator of LPS-induced macrophage activation. *Immunity* **17**, 583-591 (2002).
286 Souma, Y. *et al*. Antiproliferative effect of SOCS-1 through the suppression of STAT3 and p38 MAPK activation in gastric cancer cells. *Int J Cancer* **131**, 1287-1296 (2012).
287 Escobar, T., Yu, C. R., Muljo, S. A. & Egwuagu, C. E. STAT3 activates miR-155 in Th17 cells and acts in concert to promote experimental autoimmune uveitis. *Invest Ophthalmol Vis Sci* **54**, 4017-4025 (2013).
288 Lv, L., An, X., Li, H. & Ma, L. Effect of miR-155 knockdown on the reversal of doxorubicin resistance in human lung cancer A549/dox cells. *Oncol Lett* **11**, 1161-1166 (2016).
289 Martin, E. C. *et al*. miR-155 induced transcriptome changes in the MCF-7 breast cancer cell line leads to enhanced mitogen activated protein kinase signaling. *Genes Cancer* **5**, 353-364 (2014).
290 Trotta, R. *et al*. Overexpression of miR-155 causes expansion, arrest in terminal differentiation and functional activation of mouse natural killer cells. *Blood* **121**, 3126-3134 (2013).
291 Ohori, M. ERK inhibitors as a potential new therapy for rheumatoid arthritis. *Drug News Perspect* **21**, 245-250 (2008).
292 Yang, C. Q. *et al*. MCP-1 stimulates MMP-9 expression via ERK 1/2 and p38 MAPK signaling pathways in human aortic smooth muscle cells. *Cell Physiol Biochem* **34**, 266-276 (2014).

293 Raggatt, L. J. *et al.* Matrix metalloproteinase-13 influences ERK signalling in articular rabbit chondrocytes. *Osteoarthritis Cartilage* **14**, 680-689 (2006).
294 Mitrovic, D. The mechanism of cartilage destruction in rheumatoid arthritis. *Arthritis Rheum* **28**, 1192-1195 (1985).
295 Demaria, M. *et al.* A STAT3-mediated metabolic switch is involved in tumour transformation and STAT3 addiction. *Aging (Albany NY)* **2**, 823-842 (2010).
296 Liu, H. & Pope, R. M. The role of apoptosis in rheumatoid arthritis. *Curr Opin Pharmacol* **3**, 317-322 (2003).
297 Kinne, R. W. *et al.* Mosaic chromosomal aberrations in synovial fibroblasts of patients with rheumatoid arthritis, osteoarthritis, and other inflammatory joint diseases. *Arthritis Res* **3**, 319-330 (2001).
298 Kalluri, R. & Weinberg, R. A. The basics of epithelial-mesenchymal transition. *J Clin Invest* **119**, 1420-1428 (2009).
299 Kalluri, R. & Zeisberg, M. Fibroblasts in cancer. *Nat Rev Cancer* **6**, 392-401 (2006).
300 Alt, E. *et al.* Fibroblasts share mesenchymal phenotypes with stem cells, but lack their differentiation and colony-forming potential. *Biol Cell* **103**, 197-208 (2011).
301 Brohem, C. A. *et al.* Comparison between fibroblasts and mesenchymal stem cells derived from dermal and adipose tissue. *Int J Cosmet Sci* **35**, 448-457 (2013).
302 Haniffa, M. A., Collin, M. P., Buckley, C. D. & Dazzi, F. Mesenchymal stem cells: the fibroblasts' new clothes? *Haematologica* **94**, 258-263 (2009).
303 Steenvoorden, M. M. *et al.* Transition of healthy to diseased synovial tissue in rheumatoid arthritis is associated with gain of mesenchymal/fibrotic characteristics. *Arthritis Res Ther* **8**, R165 (2006).
304 Zvaifler, N. J. Relevance of the stroma and epithelial-mesenchymal transition (EMT) for the rheumatic diseases. *Arthritis Res Ther* **8**, 210 (2006).
305 Lamouille, S., Xu, J. & Derynck, R. Molecular mechanisms of epithelial-mesenchymal transition. *Nat Rev Mol Cell Biol* **15**, 178-196 (2014).
306 Huang, C. *et al.* The effects and mechanisms of blockage of STAT3 signaling pathway on IL-6 inducing EMT in human pancreatic cancer cells in vitro. *Neoplasma* **58**, 396-405 (2011).
307 Kim, W., Kim, M. & Jho, E. H. Wnt/β-catenin signalling: from plasma membrane to nucleus. *Biochem J* **450**, 9-21 (2013).
308 Debeb, B. G. *et al.* Histone deacetylase inhibitors stimulate dedifferentiation of human breast cancer cells through WNT/β-catenin signaling. *Stem Cells* **30**, 2366-2377 (2012).
309 Zhiqiang Li, Y. W., and Anming Meng. The Amotl2 Gene Inhibits Wnt/β-Catenin Signaling and Regulates Embryonic Development in Zebrafish. *J. Biol. Chem.* **287**, 13005-13015 (2012).
310 Miao, C. G. *et al.* Wnt signaling pathway in rheumatoid arthritis, with special emphasis on the different roles in synovial inflammation and bone remodeling. *Cell Signal* **25**, 2069-2078 (2013).

311 Sen, M. Wnt signalling in rheumatoid arthritis. *Rheumatology (Oxford)* **44**, 708-713 (2005).
312 Landsberg, J. *et al*. Melanomas resist T-cell therapy through inflammation-induced reversible dedifferentiation. *Nature* **490**, 412-416 (2012).
313 Williams, R. O. Collagen-induced arthritis as a model for rheumatoid arthritis. *Methods Mol Med* **98**, 207-216 (2004).
314 Bock, C. *et al*. DNA methylation dynamics during in vivo differentiation of blood and skin stem cells. *Mol Cell* **47**, 633-647 (2012).
315 Szyf, M. & Detich, N. Regulation of the DNA methylation machinery and its role in cellular transformation. *Prog Nucleic Acid Res Mol Biol* **69**, 47-79 (2001).
316 Shu, K. *et al*. Therapeutic effect of daphnetin on the autoimmune arthritis through demethylation of proapoptotic genes in synovial cells. *J Transl Med* **12**, 287 (2014).
317 Ai, R. *et al*. DNA Methylome Signature in Synoviocytes From Patients With Early Rheumatoid Arthritis Compared to Synoviocytes From Patients With Longstanding Rheumatoid Arthritis. *Arthritis Rheumatol* **67**, 1978-1980 (2015).
318 Ai, R. *et al*. Joint-specific DNA methylation and transcriptome signatures in rheumatoid arthritis identify distinct pathogenic processes. *Nat Commun* **7**, 11849 (2016).
319 Sawalha, A. H. *et al*. Defective T-cell ERK signaling induces interferon-regulated gene expression and overexpression of methylation-sensitive genes similar to lupus patients. *Genes Immun* **9**, 368-378 (2008).
320 Cacan, E., Ali, M. W., Boyd, N. H., Hooks, S. B. & Greer, S. F. Inhibition of HDAC1 and DNMT1 modulate RGS10 expression and decrease ovarian cancer chemoresistance. *PLoS One* **9**, e87455 (2014).
321 Robertson, K. D. *et al*. DNMT1 forms a complex with Rb, E2F1 and HDAC1 and represses transcription from E2F-responsive promoters. *Nat Genet* **25**, 338-342 (2000).
322 Lin, H. S. *et al*. Anti-rheumatic activities of histone deacetylase (HDAC) inhibitors in vivo in collagen-induced arthritis in rodents. *Br J Pharmacol* **150**, 862-872 (2007).
323 Grabiec, A. M., Korchynskyi, O., Tak, P. P. & Reedquist, K. A. Histone deacetylase inhibitors suppress rheumatoid arthritis fibroblast-like synoviocyte and macrophage IL-6 production by accelerating mRNA decay. *Ann Rheum Dis* **71**, 424-431 (2012).
324 Horiuchi, M. *et al*. Expression and function of histone deacetylases in rheumatoid arthritis synovial fibroblasts. *J Rheumatol* **36**, 1580-1589 (2009).
325 Wada, T. T. *et al*. Aberrant histone acetylation contributes to elevated interleukin-6 production in rheumatoid arthritis synovial fibroblasts. *Biochem Biophys Res Commun* **444**, 682-686 (2014).